# THE EFFECTS OF RESIDUAL CONCENTRATION AND MOISTURE CONTENT ON POLLUTANT REMOVAL AND CARBON RECOVERY IN A SOIL BIOFILTER

---

A thesis

submitted in partial fulfilment

of the requirements for the Degree of

**DOCTOR OF PHILOSOPHY IN CHEMICAL AND PROCESS ENGINEERING**

at

UNIVERSITY OF CANTERBURY

by

Quang Anh Dang

---

2019

Abstract of a thesis submitted in partial fulfilment of the requirements

for the Degree of Doctor of Philosophy in Chemical and Process Engineering.

# The effects of residual concentration and moisture content on pollutant removal and carbon recovery in a soil biofilter

by

Quang Anh Dang

This study quantitatively determined the importance and potential interaction between operating conditions – combination of residual pollutant concentration and water potential and soil type on $\%CO_2$ recovery and biofilter performance (elimination capacity - EC). A 2 x 3 factorial design was adopted, which included two levels of operating conditions: (1) low residual pollutant concentrations and wetter conditions and (2) high residual pollutant concentrations; and drier conditions. This experimental design was done for three types of soil (Soil 1, Soil 2, Soil 3).

A continuous lab-scale differential biofilter was used as a research tool to control the environmental conditions. The biofilter was operated without supplemental nutrient addition to remove a variety of pollutants (toluene and methane) in an air stream. The carbon flux was rigorously tracked through the biofiltration system. Over the range of operation, the carbon

balance closure for 37 experiments was 96.1 ± 5.3%. The carbon fraction found in the liquid phase was less than 5% of the degraded carbon. Majority of the biodegraded carbon (> 90%) ends up in the form of either $CO_2$ or active biomass/EPS.

In general, operating the toluene biofilters at low residual concentrations (5 ppm to 49 ppm) and wetter condition (-10 $cm_{H_2O}$) resulted in a 20% higher EC and a 20% higher $CO_2$ than operating at high residual concentrations (115 ppm to 146 ppm) and drier condition (-100 $cm_{H_2O}$). Conversely, operating the methane biofilters at low residual concentrations (1709 ppm to 1942 ppm) and wetter condition (-10 $cm_{H_2O}$) resulted in a 35% lower EC and a 45% higher $CO_2$ than operating at high residual concentrations (8590 ppm to 9054 ppm) and drier condition (-100 $cm_{H_2O}$).

Soil type had a strong effect on the EC and $\%CO_2$ recovery in methane biofilters and on the EC in toluene biofilters. Among three soil types, Soil 2 had the lowest EC. The interaction between soil type and operating condition was not significant. Preliminary microbial analysis suggested the differences in the community structure was mainly attributed to the soil type rather than the operating conditions, type of substrate during acclimation.

A feedback control system was developed to maintain the residual toluene to the desired value. The impact of residual toluene concentration on biofilter performance packed with Soil 2 was investigated. Substrate inhibition occurred when the residual toluene concentration exceeded 250 ppm. Start-up concentration studies showed that starting the reactor at a lower residual concentration (20 ppm) then increasing it to higher value (65 ppm) increased the EC by 22% compared to starting the reactor at a high residual concentration (65 ppm).

**Key words:** Soil biofilter, toluene, methane, carbon balance, feedback control system.

# Acknowledgements

I am grateful to people who helped me during my thesis research. I especially would like to thank to my senior supervisor, Dr. Peter Gostomski, for guiding me through every obstacle I met during my research work. His creativity and tireless afford in researching sustainable development make me learn a great deal.

I would like to thank my associate supervisor Ms. Kim Baronian for her valuable guidance, comments and suggestions throughout this project. Further, I would like to express my thanks to Dr. Katheryn Wigley in CAPE (University of Canterbury, New Zealand) for helping me with the microbiological part and Dr. Tung Nguyen (University of Nottingham, United Kingdom) for helping me with the programming in LabView.

Special thanks are also given to the technicians in CAPE: Mr. Leigh Richardson, Mr. Stephen Beuzenberg, Dr. Michael Sandrige, Mr. Graham Furniss and Mr. Glenn Wilson for their continual support and help with the purchasing, experiment set-up, sampling and data analysis. I thank my research group members Roger, Josh, Mimi, Emmanuel and Sunday for their kind support.

Finally, I express my love and gratitude to my parents and my sister for their love and support throughout my life.

# Table of Contents

# List of Tables

# List of Figures

# Chapter 1: Introduction

## 1.1 Overview of air pollution

Air pollution occurs at all geographical and temporal scales, causing human health concerns, inducing acidification, haze and forest dieback for over 100 years. In the future, air pollution could alter the conditions for people and nature around the world. Because air pollution has severe effects on human health, eco-systems and especially the Earth's climate, it is arguable that air pollution and climate change are closely connected. It is well known that climate change and air pollution are recognized as one of the greatest challenges of the 21$^{st}$ Century. On December 2015, 195 countries met in Paris for the 21$^{st}$ Conference of Parties (COP21) and signed a historic agreement to lower greenhouse gas emissions that cause global warming. Conventional air pollutants such as ozone and particulates have a direct impact on climate change whilst volatile organic compounds (VOCs) have an indirect effect through a number of chemical reactions. In 2007, the World Meteorological Organization launched a worldwide programme called "Global Atmosphere Watch" to measure the VOCs released into the atmosphere (WMO, 2007). Considering the hazards posed by air pollution, one of the challenges for environmental scientists and engineers is to improve existing air pollution control technologies and develop novel and more efficient ones.

## 1.2 Emission of Volatile Organic Compounds

Volatile organic compounds (VOCs) are a major source of air pollution which pose problems for human health and ecosystems (Mudliar et al., 2000). The definition of VOCs depends on the country or region. In the United States (US), VOCs are defined as any volatile organic carbon compound, excluding carbon monoxide, carbon dioxide ($CO_2$), carbonic acid, metallic carbides and carbonates, and ammonium carbonate (Kennes and Veiga, 2002). The European

Commission's "Directive 2004/42/EC" has recently proposed another definition which defines a VOC as an organic compound having an initial boiling point lower than or equal to 250 $^{o}$C 101.3 kPa (EC, 2004). Similarly, the European Eco-Labelling scheme (2002/739/EC) for "Indoor paints and Varnishes" defines a VOC as an organic compound with an initial boiling point lower than or equal to 250 $^{o}$C (EC, 2002).

In the US, according to a study performed by the EPA (2014) (Environmental Protection Agency) the overall emissions of VOCs increased from 1900 to 1970 and peaked in the early 1970s. A steady decrease in VOC emissions was observed until 1992, and since then levels have remained relatively constant. The majority of the emissions in the early 1900s were attributed to uncontrolled fuel combustion sources. However, between 1940 and 1970, emissions due transportation became the primary source of VOC emissions. By the 1990s, vehicle emissions were significantly reduced through technological advances in combustion and exhaust control and the implementation of stringent vehicle inspection and maintenance programs.

Nowadays, emissions from industrial sources have replaced mobile sources as the main issue for VOC control (Walter, 2010). In the US, based on an air quality report made by the EPA (2014), in 2011, there were 7.1 million tons of VOC emissions from industrial processes released to environment whereas the release from on-road vehicles was 2.41 million tons. Industrial emission sources pose a difficult challenge for VOC control with respect to both regulatory and technological considerations. This is primarily because of the release of a wide range of quantities and types of VOCs, including aldehydes, alcohols, aromatics, and aliphatics (Hunter and Oyama, 2000).

In New Zealand, some regional councils were developing emission inventories for their regions. Based on an ambient air quality and pollution levels report made by Ministry of Transport and Ministry of Environment in 1998, Auckland Council estimated the total quantity of VOCs was approximately 200 tonnes/day with major source (~68%) from motor vehicles. At the similar report, the total of VOCs in summer in Christchurch was 45 tonnes/day and the motor vehicles accounted for 64% of the total VOC emissions (MfE, 1998). This report on the total VOCs in New Zealand has not been updated yet.

### 1.3 Existing VOC Control Technologies

There are various existing technologies for the treatment of VOC emissions. Economical and ecological constraints dictate the choice of technologies, based on the nature, the flow and the mode of emission of the gaseous waste stream. The most commonly used techniques are listed below.

**Incineration**

The polluted gas streams can be incinerated thermally or catalytically. The heat generated by incineration processes can be recovered. Thermal oxidation of VOCs requires a huge amount of energy because nominal combustion temperatures ranges from 650 $^{o}$C to 850 $^{o}$C (Ruddy and Carroll, 1993). This temperature range cannot be sustained by the usual amount of VOCs in air due to their inadequate oxidation energy. This means that the combustion process requires a large quantity of auxiliary fuel even with the presence of heat recovery equipment. The operating temperature of catalytic oxidation is normally between 250 $^{o}$C and 500 $^{o}$C. Precious or base metals such as Pt, Pd, Rh are usually used as catalysts to lower the activation energy for oxidation, thus reducing the fuel cost associated with thermal incinerators (Kamal et al., 2016). The selection of catalysts depends on the nature of the gaseous pollutants

present and the processing operating characteristics. The contaminants in the air can interfere with the catalysis through mechanisms such as poisoning, masking and fouling. These catalyst deactivators typically involve heavy metals, phosphorus, sulfur, and most halogens, although more advanced designs of catalyst beds and catalysts can somewhat mitigate the deactivation processes (Walter, 2010).

**Condensation**

This technology uses liquid nitrogen or other cryogenic fluids to condense organic compounds in the exhaust stream. Pollutants can be partially recovered by simultaneous cooling and compressing gaseous effluents (Davis and Zeiss, 2002). This technology is only cost effective for high pollutant concentrations (> 5000 ppm) but is very expensive at low concentrations (Khan and Ghoshal, 2000). It is usually combined with another technology to reach required emission levels.

**Adsorption**

VOCs from the gas stream can be removed by physical adsorption and chemisorption based on the interaction between adsorbate and adsorbent (i.e. activated carbon or zeolite). Adsorption achieves high removal efficiencies while eliminating low gaseous phase pollutant concentrations. For carbon adsorption, periodic replacement or regeneration of spent carbon is required once it is saturated. The regeneration process may be accomplished on site by steam desorption or vacuum desorption, but both of these solutions can be costly due to high energy requirements (Walter, 2010).

**Absorption**

Absorption consists of transferring contaminants from the gas phase to the liquid phase followed by treating the VOC in the liquid phase. Absorption uses a scrubbing phase, frequently using water but also other solvents such as silicon oils (Darracq et al., 2010). Recovery of the pollutants from solvents is possible. Washing towers or packed bed scrubbing are used to increase the contact area which is necessary for efficient gas-liquid phase mass transfer. The advantage of this technology is its capability of handling large range of flow rates with concentrations from 500 to 5000 ppm (Khan and Ghoshal, 2000). However, this technology often has high investment and high operating costs.

**Photocatalysis**

In photolytic and photocatalytic technologies, VOC degradation occurs on the surface of a semiconductor photocatalyst under light irradiation at ambient temperature (Lim et al., 2009, Kabir and Kim, 2012). Titanium dioxide ($TiO_2$) is a traditional photocatalyst with superior photocatalytic oxidation ability, high photocorrosion resistance and non-toxic properties, however it can only respond to UV irradiation (Schneider et al., 2014). Literature shows that photocatalysts are cost effective and work well with low concentration gas streams (Zou et al., 2006, Rezaee et al., 2014). The main drawback of this technology is the intermediates formed on the catalyst surface during degradation, resulting in the suppression or termination of the reaction kinetics. Hence there is a need to investigate reactivation and regeneration of the catalyst during long-term operation.

**Biological methods**

Biological treatment techniques use the ability of specific bacteria, fungi or mixed microbial consortia to degrade the contaminants. The contaminants diffuse from the gas phase to the aqueous phase prior to biodegradation. Biological waste air treatment is an effective, economical and relatively green technology for removing low concentrations of contaminants (up to 5,000 $mg \cdot m^{-3}$ depending on the specific contaminant) in large quantities of air (1,000 – 150,000 $m^3 \cdot h^{-1}$) . There are three main types of biological systems for treating contaminated air: bioscrubbers, biofilters and biotrickling filters.

- Bioscrubbers are reactors in which the gaseous pollutants are first absorbed in a free liquid phase prior to biodegradation by either suspended or immobilized microorganisms. The wastewater from bioscrubbers then needs to be treated by conventional techniques.
- Biofilters are packed bed reactors with a biofilm containing microorganisms which consume the gaseous contaminant of interest. The biofilter processes differ from scrubbing techniques in that the transfer of the contaminant to the liquid phase and biodegradation take place in the same packed bed reactor, therefore little waste water is produced. Details of this process are presented in Chapter 2.
- A biotrickling filter is a combination of a bioscrubber and a biofilter. It is governed by many of the same phenomena as biofilters, except that the water phase is continuously flowing through the packed bed, as opposed to a limited or slow moving water phase in biofilters. By recirculating liquid, the pH of the filter bed can be easily monitored and controlled by addition of base or acid along with the addition of nutrients.

## 1.4 Definition of research scope and need

In a biofilter, the contaminant enters the bed medium, is degraded and then transformed to $CO_2$, water, biomass and other metabolites (Deshusses et al., 1996). Therefore, the amount of carbon from the contaminant entering the biofilter should equal the amount accumulating plus the amount leaving. Hence, for studies interested in a carbon balance or carbon recovery, the carbon must be quantified in all streams exiting or accumulating in the system. Studying the carbon balance is useful for determining the stability of a biofilter according to Aho et al. (2007). When the system is at steady state, most of the carbon should be in the outlet streams. However, in reality, the carbon in the outlet streams in biofilters never achieve 100% carbon recovery (Bordoloi and Gostomski, 2019).

Many authors have made rigorous attempts to close the carbon balance but very few of them have achieved 100% closure. $CO_2$ is normally identified as a major fraction of the carbon released from the system, which accounts for 60% to 80% of the recovered carbon. However, approximately 10% - 50% of the carbon is often missing (Deshusses, 1997, Fürer and Deshusses, 2000, Grove et al., 2009, Delhoménie et al., 2005). Many authors assume the missing carbon is associated with biomass growth without directly measuring the mass of carbon accumulated in the packed bed (Li et al., 2002, Elmrini et al., 2004). However, if the missing carbon only accumulates as new active biomass, the beds would rapidly clog which is not seen in systems operated in nutrient-limited conditions (Singh et al., 2006, Grove et al., 2009). Weber and Hartmans (1996) and Girard et al. (2011) state that the production of exopolymeric substances and internal storage polymers (e.g. polyhydroxyalkanoate (PHA), glycogen) are other products containing carbon. In some exceptional cases, some compounds may not be fully degraded during treatment (Martinez, 2001), or are merely transformed into

intermediate compounds (Morales et al., 1998) which possibly adsorb to the packed bed medium.

Besides the products retained in the biofilter, the carbon released from biofilter can be found in different compounds. $CO_2$ and undegraded VOCs are commonly released from the biofilter in the exit gas. Other potential carbon end-points include dissolved $CO_2$ (Pratt et al., 2003), soluble microbial products – SMP (Meng et al., 2009) and soluble metabolites (Díaz et al., 2008) in the aqueous phase.

Based on the literature, it is vital to understand the fate of the contaminants and where the carbon is going in biofiltration. Knowledge of how much carbon is associated with solids accumulation in the bed can be used to predict clogging of the bed medium and the associated increased pressure drop which is an important operational problem in biofiltration.

### 1.5 Aim, objectives and justification of the research

The interest for this research began with the work of Bordoloi (2016) and Bordoloi et al. (2019). These investigations were undertaken at the University of Canterbury using a differential bioreactor system. This reactor allows continous gas flow, rigorous control of environmental parameters, uniform gas/liquid concentration exposure to the entire biofilm (details are presented in Section 3.1). In their study, carbon was found in three phases: $CO_2$ and residual volatile organic compound leaving the reactor, dissolved $CO_2$ and dissolved pollutants/soluble microbial products in the liquid and the carbon deposited in the packing. Toluene was selected as the VOC due to its wide range of applications in industry and it is also a common model compound used in biofiltration research giving a wider range of results for comparison (Qasim and Shareefdeen, 2013). Soil was used as a biofiltration medium as it is commonly used in industrial biofiltration and has a large indigenous microbial population

(Devinny et al., 1999). Over the range of operating conditions tested, the carbon balance closure for all of their experiments was approximately 90.5 ± 5% at a 95% confidence interval, however this approached 100% with increased experimental run times improving the uncertainty of some of the analysis.

According to Bordoloi et al. (2019), the distribution between $CO_2$ and the non-$CO_2$ fraction (total amount of carbon in solid and liquid phases) was a function of temperature, matric potential and residual toluene concentration. They found that matric potential and residual concentration had strong impact on the %$CO_2$ recovery while temperature had minor impact. On the other-hand, temperature strongly increased the non-$CO_2$ production rate whereas matric potential and residual concentration had less influence. At an operating temperature of 40 $^oC$, a higher %$CO_2$ recovery and a lower non-$CO_2$ production rate was observed with the combination of wetter conditions (-10 $cm_{H_2O}$) and lower residual toluene concentrations (20 – 70 ppm) than at drier conditions (-20 $cm_{H_2O}$; -100 $cm_{H_2O}$) and higher residual concentrations (70 – 180 ppm). However, these conclusions were derived from one type of pollutant (toluene) and one soil type.

The primary objective of this research is to track the carbon flux through a biofiltration system and determine the influence of environmental parameters (matric potential and residual concentration) on the %$CO_2$ recovery and biofilter performance for a multipleof pollutants and soil types beyond those investigated by Bordoloi et al. (2019). The differential reactor continued to be used as a research-tool in this study. Three soil types with different physico-chemical characteristics (details are presented in Section 5.3.1) was collected from Parkhouse Garden Supplies in Canterbury, New Zealand. Methane and toluene are selected as model substrates since they are of interest to many systems (Wang et al., 2007, Menard et al., 2014). Methane in particular is a potent greenhouse gas (GHG) many times more damaging than

carbon dioxide, and highly relevant to New Zealand's GHG emissions accounting (42% of the total GHG in 2017) (Basset-Mens et al., 2009, Syed, 2016, MfE, 2019). Each substrate has a unique degradation pathway hence the form the carbon takes in the process might be different. Therefore, looking at interactions between diverse contaminants and media would expand the specific results determined by Bordoloi et al. (2019).

The next goal is to determine the impact of residual concentration on biofiltration performance. Generally, the residual concentration is variable in biofiltration systems. In biofilters, residual concentration is a crucial factor to assess the elimination capacity (EC) which represents the biofilter performance under fixed conditions. The impact of residual concentration on EC was indicated in Bordoloi and Gostomski (2019) study. However, it was assessed under variable residual concentrations hence this evaluation was not explicit. Controlling the residual concentration could help in determining the influence on biofilter performance. A feedback control system will be implemented on the differential biofilter that uses an on-line GC measurement to manipulate the inlet concentration to maintain the residual pollutant concentration at the desired value.

**References**

AHO, T., KIVINEN, V., KOSKINEN, P., PUHAKKA, J. & YLI-HARJA, O. Exploring the interrelationship between bioreactor stability and carbon balance. Proceedings of the Fifth IEEE International Workshop on Genomic Signal Processing and Statistics, GENSIPS'07, Tuusula, Finland, 10-12 June 2007, 2007.

BASSET-MENS, C., KELLIHER, F. M., LEDGARD, S. & COX, N. 2009. Uncertainty of global warming potential for milk production on a New Zealand farm and implications for decision making. *The International Journal of Life Cycle Assessment,* 14**,** 630-638.

BORDOLOI, A. 2016. *Toluene degradation by an unsaturated biofilm: The impact of environmental parameters on the carbon end-points in biofiltration.* Doctor of Philosophy, University of Canterbury.

BORDOLOI, A., GAPES, D. J. & GOSTOMSKI, P. A. 2019. The impact of environmental parameters on the conversion of toluene to CO2 and extracellular polymeric substances in a differential soil biofilter. *Chemosphere,* 232**,** 304-314.

BORDOLOI, A. & GOSTOMSKI, P. A. 2019. Carbon recovery and the impact of start-up conditions on the performance of an unsaturated *Pseudomonas putida* biofilm compared with soil under controlled environmental parameters in a differential biofilter. *Journal of Chemical Technology and Biotechnology,* 94**,** 600-610.

DARRACQ, G., COUVERT, A., COURIOL, C., AMRANE, A., THOMAS, D., DUMONT, E., ANDRES, Y. & LE CLOIREC, P. 2010. Silicone oil: An effective absorbent for the removal of hydrophobic volatile organic compounds. *Journal of Chemical Technology and Biotechnology,* 85**,** 309-313.

DAVIS, R. J. & ZEISS, R. F. 2002. Cryogenic condensation: A cost-effective technology for controlling VOC emissions. *Environmental Progress,* 21**,** 111-115.

DELHOMÉNIE, M. C., BIBEAU, L. & HEITZ, M. 2005. A study of the biofiltration of high-loads of toluene in air: Carbon and water balances, temperature changes and nitrogen effect. *Canadian Journal of Chemical Engineering,* 83**,** 153-160.

DESHUSSES, M. A. 1997. Transient behavior of biofilters: Start-up, carbon balances, and interactions between pollutants. *Journal of Environmental Engineering-Asce,* 123**,** 563-568.

DESHUSSES, M. A., HAMER, G. & DUNN, I. J. 1996. Transient-state behavior of a biofilter removing mixtures of vapors of MEK and MIBK from air. *Biotechnology and Bioengineering,* 49**,** 587-598.

DEVINNY, J. S., DESHUSSES, M. A. & WEBSTER, T. S. 1999. *Biofiltration for air pollution control,* United States of America, CRC press.

DÍAZ, L. F., MUÑOZ, R., BORDEL, S. & VILLAVERDE, S. 2008. Toluene biodegradation by *Pseudomonas putida* F1: targeting culture stability in long-term operation. *Biodegradation,* 19**,** 197-208.

EC 2002. Community eco-label to certain products. *In:* COMMISSION, E. (ed.) *2002/747/EC*

EC 2004. Paint directive. *In:* COMMISSION, E. (ed.) *2004/42/EC.*

ELMRINI, H., BREDIN, N., SHAREEFDEEN, Z. & HEITZ, M. 2004. Biofiltration of xylene emissions: bioreactor response to variations in the pollutant inlet concentration and gas flow rate. *Chemical Engineering Journal,* 100**,** 149-158.

EPA. 2014. *Volatile organic compounds emissions* [Online]. United States: U.S. Environmental Protection Agency. Available: https://cfpub.epa.gov/roe/indicator.cfm?i=23 [Accessed 26th May 2016].

FÜRER, C. & DESHUSSES, M. A. Biodegradation in biofilters: Did the microbe inhale the VOC. Proceedings of the Annual Meeting & Exhibition of the Air & Waste Management Association, 2000. 18-22.

GIRARD, M., RAMIREZ, A. A., BUELNA, G. & HEITZ, M. 2011. Biofiltration of methane at low concentrations representative of the piggery industry-Influence of the methane and nitrogen concentrations. *Chemical Engineering Journal,* 168**,** 151-158.

GROVE, J. A., ZHANG, H., ANDERSON, W. A. & MOO-YOUNG, M. 2009. Estimation of carbon recovery and biomass yield in the biofiltration of octane. *Environmental Engineering Science,* 26**,** 1497-1502.

HUNTER, P. & OYAMA, S. T. 2000. *Control of volatile organic compound emissions: Convential and emerging technologies,* New York, John Wiley&Son.

KABIR, E. & KIM, K.-H. 2012. A Review of Some Representative Techniques for Controlling the Indoor Volatile Organic Compounds. *Asian Journal of Atmospheric Environment,* 6**,** 137-146.

KAMAL, M. S., RAZZAK, S. A. & HOSSAIN, M. M. 2016. Catalytic oxidation of volatile organic compounds (VOCs) - A review. *Atmospheric Environment,* 140**,** 117-134.

KENNES, C. & VEIGA, M. C. 2002. *Bioreactors for waste gas treatment,* Dorddrecht, Netherlands, Kluwer Academic

KHAN, F. I. & GHOSHAL, A. K. 2000. Removal of Volatile Organic Compounds from polluted air. *Journal of Loss Prevention in the Process Industries,* 13**,** 527-545.

LESON, G. & WINER, A. M. 1991. Biofiltration - an innovative air-pollution control technology for VOC emissions. *Journal of the Air & Waste Management Association,* 41**,** 1045-1054.

LI, G. W., HU, H. Y., HAO, J. M. & FUJIE, K. 2002. Use of biological activated carbon to treat mixed gas of toluene and benzene in biofilter. *Environmental Technology,* 23**,** 467-477.

LIM, M., ZHOU, Y., WANG, L. Z., RUDOLPH, V. & LU, G. Q. 2009. Development and potential of new generation photocatalytic systems for air pollution abatement: an overview. *Asia-Pacific Journal of Chemical Engineering,* 4**,** 387-402.

MARTINEZ, F. A. 2001. *Polyurethane foam based packing media for biofilters removing volatile organic compounds from contaminated air.* Master of Science, Universidad del Valle.

MENARD, C., RAMIREZ, A. A. & HEITZ, M. 2014. Kinetics of simultaneous methane and toluene biofiltration in an inert packed bed. *Journal of Chemical Technology and Biotechnology,* 89**,** 597-602.

MENG, F. G., CHAE, S. R., DREWS, A., KRAUME, M., SHIN, H. S. & YANG, F. L. 2009. Recent advances in membrane bioreactors (MBRs): Membrane fouling and membrane material. *Water Research,* 43**,** 1489-1512.

MFE 1998. Aimbient air quality and pollution levels in New Zealand; targets for vehicle emissions control. *Air quality technical report* New Zealand.

MFE 2019. New Zealand's greenhouse gas inventory 1990–2017.

MORALES, M., REVAH, S. & AURIA, R. 1998. Start-up and the effect of gaseous ammonia additions on a biofilter for the elimination of toluene vapors. *Biotechnology and Bioengineering,* 60**,** 483-491.

MUDLIAR, S., GIRI, B., PADOLEY, K., SATPUTE, D., DIXIT, R., BHATT, P., PANDEY, R., JUWARKAR, A. & VAIDYA, A. 2000. Bioreactors for treatment of VOCs and odours - A review. *Environmental Management,* 91**,** 1039-1054.

PRATT, S., YUAN, Z. G., GAPES, D., DORIGO, M., ZENG, R. J. & KELLER, J. 2003. Development of a novel titration and off-gas analysis (TOGA) sensor for study of biological processes in wastewater treatment systems. *Biotechnology and Bioengineering,* 81**,** 482-495.

QASIM, M. & SHAREEFDEEN, Z. 2013. Analysis of a recent biofilter model for toluene biodegradation. *Advances in Chemical Engineering and Science,* Vol.03 No.01**,** 10.

REZAEE, A., RANGKOOY, H., KHAVANIN, A. & JAFARI, A. J. 2014. High photocatalytic decomposition of the air pollutant formaldehyde using nano-ZnO on bone char. *Environmental Chemistry Letters,* 12**,** 353-357.

RUDDY, E. N. & CARROLL, L. A. 1993. Select the best VOC control strategy. *Chemical Engineering Progress;(United States),* 89.

SCHNEIDER, J., MATSUOKA, M., TAKEUCHI, M., ZHANG, J. L., HORIUCHI, Y., ANPO, M. & BAHNEMANN, D. W. 2014. Understanding Tio2 photocatalysis: mechanisms and materials. *Chemical Reviews,* 114**,** 9919-9986.

SINGH, R. S., RAI, B. N. & UPADHYAY, S. N. 2006. Performance evaluation of an agro waste based biofilter treating toluene vapours. *Environmental Technology,* 27**,** 349-357.

SYED, R. A. 2016. *Understanding methanotroph ecology in a biofilter for efficiently mitigating methane emissions : a thesis presented in fulfilment of the requirements for the degree of Doctor of Philosophy in Soil Science (Biotechnology) at Massey University, Palmerston North, New Zealand.* Doctor of Philosophy (PhD) Doctoral, Massey University.

WALTER, D. 2010. *Biofiltration: Modeling and applications,* Germany, VDM Verlag Dr.Muller Gmbh & Co.KG.

WANG, S. B., ANG, H. M. & TADE, M. O. 2007. Volatile organic compounds in indoor environment and photocatalytic oxidation: State of the art. *Environment International,* 33**,** 694-705.

WEBER, F. J. & HARTMANS, S. 1996. Prevention of clogging in a biological trickle-bed reactor removing toluene from contaminated air. *Biotechnology and Bioengineering,* 50**,** 91-97.

WMO, G. A. W. Report No 171: A WMO. GAW Expert Workshop on Global Long-Term Measurement of Volatile Organic Compounds (VOCs), 2007.

ZOU, L., LUO, Y. G., HOOPER, M. & HU, E. 2006. Removal of VOCs by photocatalysis process using adsorption enhanced TiO2-SiO(2)catalyst. *Chemical Engineering and Processing,* 45**,** 959-964.

# Chapter 2: Literature review

## 2.1 Overview of biofiltration

### 2.1.1 History of biofiltration

Biofiltration is an energy-efficient technology for the control of VOC emissions. It was initially developed in Europe along with some examples in the U.S. According to Leson and Winer (1991), the first publication related to biological air treatment was made by Bach (1923) in a German journal. He discussed a concept of using a biologically active biofilter to control the hydrogen sulfide ($H_2S$) emitted from a waste water treatment plant. In 1955, applications of this concept were published in the U.S. and in West Germany. Soil beds were successfully installed in California, U.S. and Nuremberg, West Germany in 1957 and around 1959 respectively (Pomeroy, 1963, Leson and Winer, 1991). During the 1980s and 1990s, biofiltration progressed rapidly in Europe and slowly in U.S. (Devinny et al., 1999). Leson and Winer (1991) stated that there were more than 500 active biofilters operating in Germany and the Netherlands. Van Groenestijn (2005) estimated the number of biological filters systems used for gas treatment was at least 15,000 world-wide.

In recent years biofiltration has received increasing attention as a viable technology for air emissions control in municipal, industrial manufacturing and remediation facilities (Table 2.1). An increasing number of systems are being installed in the U.S. and Japan, and numerous research studies are being conducted to characterize biofiltration's suitability for a wide variety of air emissions control (Walter, 2010).

Table 2.1: Examples of industrial applications using biofiltration for VOC control.

| Industry | Major VOCs | References |
|---|---|---|
| Paint and Coating | Ethanol, toluene, propane, isobutene, n-butane, styrene, acetone, methyl ethyl ketone (MEK) | Kiared et al. (1996)<br>Li et al. (2012) |
| Printing Processes | Universal 30, n-propanol-1, Alcohol 2A | Rothenbuhler et al. (1995) |
| Soil Vapor Extraction | Toluene, total petroleum hydrocarbons | Amin et al. (2014)<br>Namkoong et al. (2004) |
| Furniture Manufacturing | Aromatic hydrocarbons (toluene, xylene, isomers, ethylbenzene, styrene) and oxygenated hydrocarbons (acetone, methylpropyl ether and butyl acetate) | Martinez-Soria et al. (2009) |
| Petrochemical | Benzene, toluene, ethylbenzene and xylenes (BTEX) | Zhao et al. (2014) |

### 2.1.2 Applicability of biofiltration technology for non-VOC treatment

Biofiltration is also frequently applied as an advanced odor control method. Most of malodorous substances results from the anaerobic decomposition of organic matter containing nitrogen and sulfur. Hydrogen sulfide ($H_2S$) is the common emission product from industrial processes, such as petroleum refining, wastewater treatment plants and food processing (Hughes et al., 2009, Janssen et al., 2009). It has been identified as the most potent of inorganic malodorants due to its low odor threshold (0.00004 – 0.001 ppm)(Murnane et al., 2013). Many rigorous attempts have been made to develop biofiltration systems capable

of eliminating $H_2S$. In 1986, Van Langenhove et al. successfully designed a biofilter packed with wood bark to eliminate approximately 10 ppm of $H_2S$. The results showed that more than 95% of the $H_2S$ was biologically oxidized to sulfate. Since then, many researchers have succeeded in using biofilters for treating sulfur-containing compounds (Ho et al., 2008, Li and Liu, 2009, Li et al., 2011, Morales et al., 2011, Zhang et al., 2015, Myung Cha et al., 1999). Myung Cha et al. (1999) conducted an experiment using immobilized microorganisms which were isolated from sewage to remove sulfur containing compounds. The removal efficiencies of $H_2S$, methanethiol ($CH_4S$), dimethyl disulphide ($C_2H_6S_2$) and dimethyl sulphide ($C_2H_6S$) were 100, 100, 87 and 73%, respectively at the inlet concentration of 30 ppm of the mixture after 4 days of operation. *Thiobacillus sp.* and *Pseudomonas sp.* are the most common bacteria used to metabolize sulfurous pollutants in biofiltration systems (Li et al., 2015).

Nitrogen containing compounds may also contribute to the odor problems from publicly owned treatment works and various industries. Ammonia is one of the typical nitrogen compounds usually treated through biofilters. Ammonia removal is mainly due to the nitrification process, which ammonia is eventually oxidized into nitrate. Hartikainen et al. (1996) state that air streams contain ammonia concentration exceeding 60 ppm strongly affect the biofilter removal efficiency. Some studies report the elimination capacity of ammonia is lower than 10 $g \cdot m^{-3} \cdot h^{-1}$ at inlet concentrations between 10 to 50 ppm (Joshi et al., 2000, Yang et al., 2014). Generally, unless a long acclimation period for the nitrifying bacteria is allowed, or a synergetic mechanism is provided, partial oxidation of ammonia frequently observed (Kanagawa et al., 2004, Baquerizo et al., 2005, Cai et al., 2015).

In addition, biofiltration is one of the promising technologies for reducing greenhouse gases such as methane ($CH_4$) (Massié, 2006). Over the past decade, methane biofiltration has been widely used for the treatment of effluent gases generated during landfill, coal mine ventilation

and animal husbandry operations (Nikiema et al., 2005, Girard et al., 2011, Limbri et al., 2013). The highest EC for methane reported among these studies is 29.2 $g \cdot m^{-3} \cdot h^{-1}$ at an inlet load of 65 $g \cdot m^{-3} \cdot h^{-1}$ (Nikiema et al., 2005) as most of the biofiltration technology for this pollutant could only offer partial elimination. The low water solubility of $CH_4$ limits the transfer of the gas to the biofilm, hence increasing the empty bed residence time required for its complete removal.

## 2.2 Biofilter

Three configurations are possible for biological reactors for air pollution control: biofilters, biotrickling filters and bioscrubbers. The basic removal mechanisms are similar in each reactor type, as described in Section 2.1. The key difference between these three bioreactors is their design and operating procedures. Additional factors are presented in Table 2.2.

Table 2.2: The classification of bioreactors for waste gas purification (Delhoménie and Heitz, 2005).

| Reactor type | Microorganisms | Liquid phase | Biodegradation step |
|---|---|---|---|
| Biofilter | Immobilized on the filter material | Limited and slow moving | In the filter bed biofilm |
| Biotrickling filter | Immobilized on the filter material and suspended in recirculated water | Continuous | In the filter bed biofilm and recirculated water |
| Bioscrubber | Suspended in the aqueous growth medium | Continuous | VOC/air separation within the absorption column,<br>VOC oxidation in the bioreactor |

A biofilter can be built as either an open or an enclosed system. The open system design involves the placement of the packing medium on a supporting structure, which includes an air distribution system, with the upper part of the reactor open to the environment. They are the most prevalent configuration in use especially in New Zealand (Cudmore and Gostomski, 2005). Although an open system might present some relative advantage due to the natural supply of water by precipitation, they are much more unstable than closed systems. The enclosed system usually operates slightly above atmosphere pressure with the contaminated gas being pumped into the reactor. These systems are advantageous over open systems, because enclosed systems require less space and allows for better control of operational parameters such as water content, temperature, pH (Kennes and Veiga, 2002).

Often a biofilter needs to have a pretreatment step. Filtration is the most typical pretreatment. It removes particles and dust which would be likely to stick to the packing medium leading to clogging problems (Togna et al., 1997). A humidification step is also common in order to saturate the air with water, which prevents the medium from drying to maintain optimal biodegradation activity. Contaminated air then enters either in an upflow or a downflow mode to the packed column containing a porous solid support medium. The microorganisms immobilized on the particles form a biofilm. As the gaseous waste stream passes through the medium and the contaminants sorb into the biofilm where the microorganisms degrade them. Further post treatment such as adsorption columns may be installed to remove residual contaminants (Devinny et al., 1999).

### 2.3 The biofilm

In microbial ecosystems, microorganisms often organize themselves into films at the surfaces of solids. Some microorganisms can detach from the surface and others attach permanently within a few minutes of their first contact (Devinny et al., 1999). Communities of

microorganisms that are accumulated at the surface make up a “biofilm”. Singh et al. (2006) states that water represents 97% of the biofilm matrix, which is bound to the capsules of microbial cells. Besides water and microbial cells, the biofilm matrix is a complex of polymers (extracellular polymeric substance, internal storage polymers) (Weber and Hartmans, 1996, Girard et al., 2011), absorbed nutrients, metabolites and intermediate compounds (Morales et al., 1998, Martinez, 2001). The diffusion rate in the biofilm which can influence the rate of treatment in biofiltration is dependent on the water binding capacity and mobility of the biofilm. Kinney et al. (1996) states that when a thick biofilm existed, the total surface area is reduced leading to a gas-transfer limitation. The same conclusion is given by Alonso et al. (1997) after they model the rate at which a growing biofilm fills the crevices near the point of contact between two support particles. A significant reduction in surface area occurs as these are filled. Therefore, in order to optimize biofilter performance, the biofilm component of the system need to characterize and its activity, composition and population dynamics has to be estimated and well controlled.

## 2.4 Mechanisms of biofiltration

The basic process of a biofiltration system consists of passing contaminated air through a filter bed. The filter bed contains a medium that supports microbial growth. The organic contaminants diffuse from the gas phase to the aqueous phase where microbial degradation occurs. Through oxidative and occasionally reductive reactions, the contaminants are converted into typical biological oxidation end products: carbon dioxide, water vapor and organic biomass (Devinny et al., 1999).

The treatment begins with the movement of the contaminant from the air to the water phase. At equilibrium, the partition between the air and water is usually described by Henry’s law:

$$C_L = \frac{C_G}{H} \qquad \text{(Equation 2.1)}$$

Where:

$C_G$ is the concentration of contaminant in the air phase ($g \cdot l^{-1}$)

$C_L$ is the concentration of contaminant in the water phase ($g \cdot l^{-1}$)

H is the dimensionless Henry's law coefficient for the compound

H is a function of the solution, temperature and pressure. Henry's law coefficients are normally below 1, meaning that for any volume within a biofilter, more contaminant is in the water than in the air (Devinny et al., 1999). Chemical compounds having Henry's law coefficient values over 0.01 are considered volatile. The influence of Henry's law coefficient on biodegradation of pollutants in biofilters has been described in several studies (Deshusses and Johnson, 2000, Zhu et al., 2004). They concluded that the difficulty in removing the contaminant increases with its Henry's law coefficients.

The next step in the biofiltration process is the transfer of pollutant to the biofilm, which is a thin layer created by microorganisms on the surface of the solid. Pollutants, oxygen, carbon dioxide and possibly volatile by-products in equilibrium at the interface diffuse into the biofilm according to Fick's first law:

$$J_z = -D\left(\frac{dC}{dZ}\right) \qquad \text{(Equation 2.2)}$$

Where:

D is the diffusion coefficient for a given compound in the biofilm ($m^2 \cdot s^{-1}$)

dC/dZ is the gradient at point z ($kg \cdot m^{-4}$)

$J_z$ is the corresponding flux at the z point ($kg \cdot m^{-2} \cdot s^{-1}$)

The diffusion coefficient of the pollutant in the biofilm is often replaced by an effective diffusion coefficient, which is much smaller than in water due to the presence of microbial cells, extracellular polymers or gas bubbles that are trapped in the biofilm. However, the calculation of an effective diffusion coefficient is very complex, thus they are generally described by empirical correlations (Stewart, 1998, Stewart, 2003).

## 2.5 Parameters affecting biofilter performance

### 2.5.1 Microbial aspects for biofiltration

The community of microorganisms present in the biofilter is a key factor of the biological processes. The species which are present, their population densities, the structure of the microbial community and their interactions with the environment and each other are fundamental to biofilter operation (Devinny et al., 1999). Isolation is a common method to characterize the species with relevant metabolic pathways (Lipski and Altendorf, 1997, Juteau et al., 1999, Muranyi et al., 2016). In a natural carrier, the biofiltration communities usually have high diversity levels as shown with studies of a full-scale biofilter used for waste gas treatment in an animal rendering plant (Friedrich et al., 2002). The same group, in 2003, related microbial diversity to environmental parameters such as biocompatibility of waste gas compounds, water content, partition coefficients and inhibitory effects, have an impact to the microbial communities and their activities (Friedrich et al., 2003).

Recalcitrant pollutants may require inoculation with pure or mixed cultures to achieve a shorter acclimation period (Kennes and Veiga, 2013). Leson and Smith (1997) stated that inoculation can speed acclimation but will not affect the ultimate removal efficiency. However, the combination of different groups of species give the biofilter more stability and robustness (Cabrol and Malhautier, 2011).

Several groups of microorganisms which are predominately heterotrophic organisms such as bacteria, fungi, yeasts and algae are involved in the biodegradation of organic compounds. Among these, bacteria and fungi are certainly the dominant microorganisms in biofilters. Most biofilms will contain substantial numbers of both, but their relative abundances can vary widely. Bacteria are capable of rapidly absorbing the substrate leading to their rapid growth. On the other hand, fungi generally grow more slowly but they are able to consume a wider variety of contaminants and can cope with hasher environments (Devinny et al., 1999).

The combination of Quantitative-PCR (qPCR) and high-throughput sequencing are useful techniques used to investigate the microbial community structure in biofilters (Bacchetti De Gregoris et al., 2011, Philippot et al., 2009, Hoefman et al., 2012). These techniques unravel the relationship of the microbial communities with different environmental variables in bioreactors such as fed sources (Ziganshin et al., 2013), temperature (Lee et al., 2016). Understanding the relationship of the microbial communities in the system with operating parameters is a key aspect for optimizing the biofilter performance.

### 2.5.2 Environmental parameters

**Temperature**

Operating temperature is a crucial factor that influences the biofilter performance. The temperature variations affect both the physical and biological features of the biofilter. The increase in temperature leads to the increase in reaction rate. Over a limited range of temperature, a 10 $^{o}$C temperature increase roughly doubles the microbial degradation rates (Devinny et al., 1999, McKinney, 2004). For temperature increases of about 20 - 30 $^{o}$C above the optimal, some microbial species may no longer be effective. If it continues to increase, at a certain point all cells are killed by the high temperatures. The same phenomena happens

when the temperature declines. Near the freezing point of water, most microorganisms become dormant and may die as necessary functions cease (Devinny et al., 1999). Wani et al. (1997) suggested keeping system temperature relatively constant to achieve successfully operation. There are numerous successful biofiltration systems which operate over the temperature range from 15 to 50 $^{o}$C in natural carriers (Mohammad et al., 2007, Ryu et al., 2009, Wang et al., 2012). In other words, most biofiltration studies have been carried out under mesophilic and thermophilic conditions.

**Water content**

The moisture content of the filter bed is an important parameter for an effective biofilter. Delhoménie and Heitz (2005) report that around 75% of problems with operating biofilters are related to poor humidity control. Microorganisms immobilized on the filter bed need water for survival and activity. Too little water content leads to bed desiccation which affects the microorganisms. As a result, the biological activity is significantly reduced or even stopped completely. Also, as the bed material contracts, it creates fissures causing channelling and short circuiting which in turn decreases the retention time and eventually reduces the removal efficiency. Conversely, excess water inhibits the transfer of oxygen to the biofilm, thereby promoting the development of anaerobic zones within the bed and limiting the reaction rate. Due to the development of these anaerobic zones there can be emission of foul smelling compounds. Increasing back pressure, due to reduced void volume and channelling of the gas within the bed is also attributed to the presence of too much water (Mudliar et al., 2000).

**Nutrients and Oxygen**

Macronutrients (e.g. carbon, nitrogen) and micronutrients (e.g. potassium, magnesium and so on) are indispensable for the majority of microorganisms to remain active, to maintain

membrane transport and especially to degrade pollutants in the bioprocess. In some specific cases, a few species might need special compounds such as vitamins or trace elements. The availability of these nutrients is partially fulfilled in natural media such as soil and compost that are used in biofiltration. However, they might not be present in a balanced concentration. Besides carbon (~50%), nitrogen is the second most common element in the microbial cell, and represents up to 15% of the dry cell weight (Soni, 2007). Solid nitrogen fertilizers can be directly supplied to the medium (Gribbins and Loehr, 1998). However, addition of nitrogen as mineral salts dissolved in aqueous phases is preferred. Whether as liquid or solid, nitrogen is provided to the microbes in inorganic forms: ammonium ($NH_4^+$) from ammonium chloride, ammonium sulfate, nitrate ($NO_3^-$) or nitrite ($NO_2^-$) from sodium nitrate and potassium nitrate (Nikiema et al., 2007).

Microorganisms used in biofiltration are predominantly aerobic and oxygen is essential for them to metabolize organic constituents and oxidize pollutants from the gas stream. Wani et al. (1997) stated the heterotrophic bacteria need at least 5 – 15% oxygen from the inlet gas stream to survive. Studies have demonstrated that oxygen limitation can affect biofilter performance (Shareefdeen and Baltzis, 1994, Zarook et al., 1997) hence biofiltration needs to avoid operating in anaerobic conditions.

**Filter bed**

The filter bed medium is a solid phase which provides the support for microbial growth. The nature and characteristics of packing materials hold a vital role for attaining high pollutant removal rate and to maintain the performance over a prolonged period of time. The properties of the support medium that are critical to its proper function include porosity, air permeability, water retention capability and adsorptive capacity (Dorado et al., 2010). Sakuma

et al. (2009) also argued that the effectiveness of a packing material is also influenced by its specific surface area, surface properties, absorption capacity and its nutrient-releasing ability. In addition, the presence of a dense and diverse microbial consortia is another important criteria. Filter beds are classified into two major groups: natural carriers and synthetic (inert) carriers (Kennes and Veiga, 2002).

In natural carriers, such as compost, peat and soil, microorganisms are distributed on the particles. Most biofilters use a natural medium and its characteristics are decided by the nature of the materials involved. Generally, they are easily obtained and are inexpensive. These materials have the advantage of containing a high initial microbial load and natural presence of nutrients needed for biomass growth and synthesis. However, the limitation of nutrients in the natural media can lead to the loss of activity and structure over time. Hence, the medium needs to be replaced after long-term operation (3 to 7 years) (Devinny et al., 1999) to prevent the filter bed clogging due to an increase in biomass and to replenish the mineral nutrients in the bed in order to avoid nutrient depletion (Ortiz et al., 2003).

On the other hand, synthetic carriers are normally biologically inactive. Materials such as vermiculate (Ortiz et al., 1998, Pineda et al., 2000), ceramics (Aizpuru et al., 2005), activated carbon (Paredes et al., 2016) and pelletized synthetics (Serial et al., 1995) have been used as media in number of studies. Their chemical compositions have been identified and are quite stable overtime, which reduces compression and gives easier airflow circulation (Ortiz et al., 2003). However, the initial absence of nutrients and microorganisms increase the start-up cost. It is the main drawback to using these carriers (Kennes and Veiga, 2002).

**Medium pH**

A similar effect on biofilter success is observed for pH as for temperature. Each species of microorganism thrives at different range of pH and will be inhibited or killed if conditions go outside this range. Some species work well at high pH but the species tolerant of moderate pH are more common. There are a few species able to grow under low pH conditions, for example *Thiobacillus thiooxidans* is able to grow under highly acidic conditions (1.0 to 2.0), which is advantageously used in biofiltration of hydrogen sulfide (Rattanapan et al., 2009). A sudden change in pH causes damage to most species resulting in reduction of pollutant removal efficiencies. Because of the pH-sensitivity of biofilters, it is useful to maintain constant pH values. However, the pH in a biofilter may also change during operation. For instance, the degradation of contaminants in biofilters produces acidifying products or the pH of the new medium does not meet the desired value (Devinny et al., 1999). Thus, "buffering agents", such as limestone or $Ca(OH)_2$, are often used as additives for pH regulation.

**Contaminant load**

Contaminant load, expressed as mass of the pollutant fed to the biofilter per unit time and volume ($g \cdot m^{-3} \cdot h^{-1}$), is a major factor affecting the operation of a biofilter. The physical footprint of the biofilter is dependent on the amount of contaminants to be eliminated, i.e. higher contaminant load means a larger biofilter footprint and higher capital investment. With the growth of biomass during the operation, bigger biofilters require more costly operation and maintenance activities like cleaning, and replacement of packing and nutrient media. This increased cost may offset the advantage of biofilter over other technologies. On the contrary, low loads allows biofilters to reach steady state with respect to biomass growth and nutrient

supply, hence rendering the system efficient. Ideal contaminant load is in the range of 1 - 100 $g \cdot m^{-3} \cdot h^{-1}$ (Devinny et al., 1999).

**Flow rate**

Gas flow rate, along with the bed volume, is a critical aspect in the design of a biofilter because it determines the empty bed residence time (EBRT) as given by equation EBRT = V/Q; where Q is air flow rate ($m^3 \cdot min^{-1}$) and V is the volume of bed material ($m^3$). According to the studies made by Picioreanu et al. (1999), the pollutants diffusion (10 – 1000 s) is slower than the biological reactions (0.001 – 10 s). Thus, in order to achieve high removal efficiency, long EBRT is required, which means low operating air flow rate and larger filter bed volumes. However, biofilters with larger volumes are more expensive. The recommended EBRT value ranges from 10 s to several minutes (Delhoménie and Heitz, 2005).

**References**

AIZPURU, A., DUNAT, B., CHRISTEN, P., AURIA, R., GARCIA-PENA, I. & REVAH, S. 2005. Fungal biofiltration of toluene on ceramic rings. *Journal of Environmental Engineering-Asce,* 131**,** 396-402.

ALONSO, C., SUIDAN, M. T., SORIAL, G. A., SMITH, F. L., BISWAS, P., SMITH, P. J. & BRENNER, R. C. 1997. Gas treatment in trickle-bed biofilters: Biomass, how much is enough? *Biotechnology and Bioengineering,* 54**,** 583-594.

AMIN, M. M., HATAMIPOUR, M. S., MOMENBEIK, F., NOURMORADI, H., FARHADKHANI, M. & MOHAMMADI-MOGHADAM, F. 2014. Toluene removal from sandy soils via in situ technologies with an emphasis on factors influencing soil vapor extraction. *The Scientific World Journal,* 2014.

BACCHETTI DE GREGORIS, T., ALDRED, N., CLARE, A. S. & BURGESS, J. G. 2011. Improvement of phylum- and class-specific primers for real-time PCR quantification of bacterial taxa. *Journal of Microbiological Methods,* 86**,** 351-356.

BAQUERIZO, G., MAESTRE, J. P., SAKUMA, T., DESHUSSES, M. A., GAMISANS, X., GABRIEL, D. & LAFUENTE, F. J. 2005. A detailed model of a biofilter for ammonia removal: Model parameters analysis and model validation. *Chemical and Engineering Journal,* 113**,** 205-214.

CABROL, L. & MALHAUTIER, L. 2011. Integrating microbial ecology in bioprocess understanding: the case of gas biofiltration. *Microbiol Biotechnol,* 90**,** 837-849.

CAI, Y. A., LI, D., LIANG, Y., LUO, Y., ZENG, H. & ZHANG, J. 2015. Effective start-up biofiltration method for Fe, Mn, and ammonia removal and bacterial community analysis. *Bioresource Technology,* 176**,** 149-155.

CUDMORE, R. & GOSTOMSKI, P. 2005. Biofilter Design and Operation for Odor Control — The New Zealand Experience. *In:* SHAREEFDEEN, Z. & SINGH, A. (eds.) *Biotechnology for Odor and Air Pollution Control.* Berlin, Heidelberg: Springer Berlin Heidelberg.

DELHOMÉNIE, M. C. & HEITZ, M. 2005. Biofiltration of air: A review. *Critical Reviews in Biotechnology,* 25**,** 53-72.

DESHUSSES, M. A. & JOHNSON, C. T. 2000. Development and validation of a simple protocol to rapidly determine the performance of biofilters for VOC treatment. *Environmental Science & Technology,* 34**,** 461-467.

DEVINNY, J. S., DESHUSSES, M. A. & WEBSTER, T. S. 1999. *Biofiltration for air pollution control,* United States of America, CRC press.

DORADO, A. D., LAFUENTE, F. J., GABRIEL, D. & GAMISANS, X. 2010. A comparative study based on physical characteristics of suitable packing materials in biofiltration. *Environ. Technol.,* 31**,** 193-204.

FRIEDRICH, U., LANGENHOVE, H. V., ALTENDORF, K. & LIPSKI, A. 2003. Microbial community and physicochemical analysis of an industrial waste gas biofilter and design of 16S rRNA-targeting oligonucleotide probes. *Environmental Microbiology,* 5**,** 183-201.

FRIEDRICH, U., PRIOR, K., ALTENDORF, K. & LIPSKI, A. 2002. High bacteria diversity of a waste gas-degrading community in an industrial biofilter as shown by a 16S rDNA clone library. *Environmental Microbiology,* 4**,** 721-734.

GIRARD, M., RAMIREZ, A. A., BUELNA, G. & HEITZ, M. 2011. Biofiltration of methane at low concentrations representative of the piggery industry-Influence of the methane and nitrogen concentrations. *Chemical Engineering Journal,* 168**,** 151-158.

GRIBBINS, M. J. & LOEHR, R. C. 1998. Effect of media nitrogen concentration on biofilter performance. *Journal of the Air & Waste Management Association,* 48**,** 216-226.

HARTIKAINEN, T., RUUSKANEN, J., VANHATALO, M. & MARTIKAINEN, P. J. 1996. Removal of ammonia from air by a peat biofilter. *Environmental Technology,* 17**,** 45-53.

HO, K. L., CHUNG, Y. C., LIN, Y. H. & TSENG, C. P. 2008. Microbial populations analysis and field application of biofilter for the removal of volatile-sulfur compounds from swine wastewater treatment system. *Journal of Hazardous Materials,* 152**,** 580-588.

HOEFMAN, S., VAN DER HA, D., DE VOS, P., BOON, N. & HEYLEN, K. 2012. Miniaturized extinction culturing is the preferred strategy for rapid isolation of fast-growing methane-oxidizing bacteria. *Microbial Biotechnology,* 5**,** 368-378.

HUGHES, M. N., CENTELLES, M. N. & MOORE, K. P. 2009. Making and working with hydrogen sulfide. The chemistry and generation of hydrogen sulfide in vitro and its measurement in vivo: A review. *Free Radical Biology and Medicine,* 47**,** 1346-1353.

JANSSEN, A. J. H., LENS, P. N. L., STAMS, A. J. M., PLUGGE, C. M., SOROKIN, D. Y., MUYZER, G., DIJKMAN, H., VAN ZESSEN, E., LUIMES, P. & BUISMAN, C. J. N. 2009. Application of bacteria involved in the biological sulfur cycle for paper mill effluent purification. *Science of the Total Environment,* 407**,** 1333-1343.

JOSHI, J. A., HOGAN, J. A., COWAN, R. M., STROM, P. F. & FINSTEIN, M. S. 2000. Biological removal of gaseous ammonia in biofilters: Space travel and earth-based applications. *Journal of the Air & Waste Management Association,* 50**,** 1647-1654.

JUTEAU, P., LAROCQUE, R., RHO, D. & LEDUY, A. 1999. Analysis of the relative abundance of different types of bacteria capable of toluene degradation in a compost biofilter. *Applied Microbiology and Biotechnology,* 52**,** 863-868.

KANAGAWA, T., QI, H. W., OKUBO, T. & TOKURA, M. 2004. Biological treatment of ammonia gas at high loading. *Water Science and Technology,* 50**,** 283-290.

KENNES, C. & VEIGA, M. C. 2002. *Bioreactors for waste gas treatment,* Dorddrecht, Netherlands, Kluwer Academic

KENNES, C. & VEIGA, M. C. (eds.) 2013. *Bioreactors for air pollution control,* United Kingdom: Wiley & Sons Inc.

KIARED, K., BIBEAU, L., BREZEZINSKI, R., VIEL, G. & HEITZ, M. 1996. Biological elimination of VOCs in biofilter. *Environmental Progress,* 15**,** 148-152.

KINNEY, K., DU PLESSIS, C., SCHROEDER, E. D., CHANG, D. P. Y. & SCOW, K. M. Optimizing microbial activity in a directionally switching biofilter. *In:* REYNOLDS, F. E., ed. Proceedings of the 1996 Conference on Biofiltration (an Air Pollution Control Technology), 1996 California, United States. The Reynolds Group, 150.

LEE, D. E., LEE, J., KIM, Y. M., MYEONG, J. I. & KIM, K. H. 2016. Uncultured bacterial diversity in a seawater recirculating aquaculture system revealed by 16S rRNA gene amplicon sequencing. *Journal of Microbiology,* 54**,** 296-304.

LESON, G. & SMITH, B. J. 1997. Petroleum environmental research forum field study on biofilters for control of volatile hydrocarbons. *Journal of Environmental Engineering-Asce,* 123**,** 556-562.

LESON, G. & WINER, A. M. 1991. Biofiltration - an innovative air-pollution control technology for VOC emissions. *Journal of the Air & Waste Management Association,* 41**,** 1045-1054.

LI, J. J., YE, G. Y., SUN, D. F., AN, T. C., SUN, G. P. & LIANG, S. Z. 2012. Performance of a biotrickling filter in the removal of waste gases containing low concentrations of mixed VOCs from a paint and coating plant. *Biodegradation,* 23**,** 177-187.

LI, L. & LIU, J. X. 2009. Identification and characteristic analysis of microorganisms in an integrated bioreactor for odours treatment. *International Journal of Environment and Pollution,* 37**,** 216-234.

LI, L., YANG, C., HE, Y. Q., QIAO, C. L. & LIU, J. X. 2011. Simultaneous removal of parathion and methyl parathion by genetically engineered *Escherichia coli* in a biofilter treating polluted air. *International Journal of Environment and Pollution,* 45**,** 3-14.

LI, L., ZHANG, J. Y., LIN, J. & LIU, J. X. 2015. Biological technologies for the removal of sulfur containing compounds from waste streams: bioreactors and microbial characteristics. *World Journal of Microbiology & Biotechnology,* 31**,** 1501-1515.

LIMBRI, H., GUNAWAN, C., ROSCHE, B. & SCOTT, J. 2013. Challenges to developing methane biofiltration for coal mine ventilation air: A review. *Water Air and Soil Pollution,* 224.

LIPSKI, A. & ALTENDORF, K. 1997. Identification of heterotrophic bacteria isolated from ammonia-supplied experimental biofilters. *Systematic and Applied Microbiology,* 20**,** 448-457.

MARTINEZ-SORIA, V., GABALDON, C., PENYA-ROJA, J. M., PALAUJ, J., ALVAREZ-HORNOS, F. J., SEMPERE, F. & SORIANO, C. 2009. Performance of a pilot-scale biotrickling filter in controlling the volatile organic compound emissions in a furniture manufacturing facility. *Journal of the Air & Waste Management Association,* 59**,** 998-1006.

MARTINEZ, F. A. 2001. *Polyurethane foam based packing media for biofilters removing volatile organic compounds from contaminated air.* Master of Science, Universidad del Valle.

MASSIÉ, D. 2006. Final report of greenhouse gas mitigation program demonstration and communication project. Ottawa, Canada: Canadian Pork Council.

MCKINNEY, R. E. 2004. *Environmental pollution control microbiology,* United States, CRC Press.

MOHAMMAD, B. T., VEIGA, M. C. & KENNES, C. 2007. Mesophilic and thermophilic biotreatment of BTEX-polluted air in reactors. *Biotechnology and Bioengineering,* 97**,** 1423-1438.

MORALES, M., ARANCIBIA, J., LEMUS, M., SILVA, J., GENTINA, J. C. & AROCA, G. 2011. Bio-oxidation of H2S by *Sulfolobus metallicus*. *Biotechnology Letters,* 33**,** 2141-2145.

MORALES, M., REVAH, S. & AURIA, R. 1998. Start-up and the effect of gaseous ammonia additions on a biofilter for the elimination of toluene vapors. *Biotechnology and Bioengineering,* 60**,** 483-491.

MUDLIAR, S., GIRI, B., PADOLEY, K., SATPUTE, D., DIXIT, R., BHATT, P., PANDEY, R., JUWARKAR, A. & VAIDYA, A. 2000. Bioreactors for treatment of VOCs and odours - A review. *Environmental Management,* 91**,** 1039-1054.

MURANYI, I. S., VOLKE, D., HOFFMANN, R., EISNER, P., HERFELLNER, T., BRUNNBAUER, M., KOEHLER, P. & SCHWEIGGERT-WEISZ, U. 2016. Protein distribution in lupin protein isolates from *Lupinus angustifolius* L. prepared by various isolation techniques. *Food Chemistry,* 207**,** 6-15.

MURNANE, S. S., LEHOCKY, A. H. & OWENS, P. D. 2013. *Odor thresholds for chemicals with established health standards,* Fairfax, Virgina, American Industrial Hygiene Association.

MYUNG CHA, J., SUK CHA, W. & LEE, J.-H. 1999. Removal of organo-sulphur odour compounds by *Thiobacillus novellus* SRM, sulphur-oxidizing microorganisms. *Process Biochemistry,* 34**,** 659-665.

NAMKOONG, W., PARK, J.-S. & VANDERGHEYNST, J. S. 2004. Effect of gas velocity and influent concentration on biofiltration of gasoline off-gas from soil vapor extraction. *Chemosphere,* 57**,** 721-730.

NIKIEMA, J., BIBEAU, L., LAVOIE, J., BRZEZINSKI, R., VIGNEUX, J. & HEITZ, M. 2005. Biofiltration of methane: An experimental study. *Chemical Engineering Journal,* 113**,** 111-117.

NIKIEMA, J., BRZEZINSKI, R. & HEITZ, M. 2007. Elimination of methane generated from landfills by biofiltration: a review. *Reviews in Environmental Science and Bio/Technology,* 6**,** 261-284.

ORTIZ, I., MORALES, M., GOBBEE, C., GUERRERO, V., AURIA, R. & REVAH, S. Biofiltration of gasoline VOCs with different support media. Proceedings of the 91st annual meeting and exhibition of the air and waste management association, 1998 Pittsburgh, United States. Air and Waste Management Association 247.

ORTIZ, I., REVAH, S. & AURIA, R. 2003. Effects of packing material on the biofiltration of benzene, toluene and xylene vapours. *Environmental Technology,* 24**,** 265-275.

PAREDES, L., FERNANDEZ-FONTAINA, E., LEMA, J. M., OMIL, F. & CARBALLA, M. 2016. Understanding the fate of organic micropollutants in sand and granular activated carbon biofiltration systems. *Science of The Total Environment,* 551–552**,** 640-648.

PHILIPPOT, L., ČUHEL, J., SABY, N. P. A., CHÈNEBY, D., CHROŇÁKOVÁ, A., BRU, D., ARROUAYS, D., MARTIN-LAURENT, F. & ŠIMEK, M. 2009. Mapping field-scale spatial patterns of size and activity of the denitrifier community. *Environmental Microbiology,* 11**,** 1518-1526.

PICIOREANU, C., VAN LOOSDRECHT, M. C. M. & HEIJNEN, J. J. 1999. Discrete-differential modelling of biofilm structure. *Water Science and Technology,* 39**,** 115-122.

PINEDA, J., AURIA, R., PEREZ-GUEVARA, F. & REVAH, S. 2000. Biofiltration of toluene vapors using a model support. *Bioprocess Engineering,* 23**,** 479-486.

POMEROY, R. D. 1963. Controlling sewage plant odors. *Consulting Engineer,* 20**,** 101.

RATTANAPAN, C., BOONSAWANG, P. & KANTACHOTE, D. 2009. Removal of H2S in down-flow GAC biofiltration using sulfide oxidizing bacteria from concentrated latex wastewater. *Bioresource Technology,* 100**,** 125-130.

ROTHENBUHLER, M., HEITZ, M., BEERLI, M. & MARCOS, B. 1995. Biofiltration of volatile organic emissions in reference to flexographic printing processes. *Water Air & Soil Pollution,* 83**,** 37-50.

RYU, H. W., YOO, S. K., CHOI, J. M., CHO, K. S. & CHA, D. K. 2009. Thermophilic biofiltration of $H_2S$ and isolation of a thermophilic and heterotrophic $H_2S$-degrading bacterium, *Bacillus* sp.TSO3. *Journal of Hazardous Materials,* 168**,** 501-506.

SAKUMA, T., HATTORI, T. & DESHUSSES, M. A. 2009. The effects of a lower irrigation system on pollutant removal and on the microflora of a biofilter. *Environmental Technology,* 30**,** 621-627.

SERIAL, G. A., SMITH, F. L., SUIDAN, M. T., BISWAS, P. & BRENNER, R. C. 1995. Evaluation of trickle bed biofilter media for toluene removal. *Journal of the Air & Waste Management Association,* 45**,** 801-810.

SHAREEFDEEN, Z. & BALTZIS, B. C. 1994. Biofiltration of toluene vapor under steady-state and transient conditions - theory and experimental results. *Chemical Engineering Science,* 49**,** 4347-4360.

SINGH, R., PAUL, D. & JAIN, R. K. 2006. Biofilms: implications in bioremediation. *Trends in microbiology,* 14**,** 389-397.

SONI, S. 2007. *Microbes: a source of energy for 21st century*, New India Publishing.

STEWART, P. S. 1998. A review of experimental measurements of effective diffusive permeabilities and effective diffusion coefficients in biofilms. *Biotechnology and Bioengineering,* 59**,** 261-272.

STEWART, P. S. 2003. Diffusion in Biofilms. *Journal of Bacteriology,* 185**,** 1485-1491.

TOGNA, A. P., FUCICH, W. J., LOUDON, R. E., DEL VECCHIO, M., BARSHTER, D. W. & NADEAU, A. J. Treatment of odorous toxic pollutants from a hardwood panel board manufacturing facility using biofiltration. Proceedings of the 90th Annual meeting and exhibition of the air and waste management association, 1997 Pittsburgh, United States.

VAN GROENESTIJN, J. W. Biotechniques for air pollution control: Past, present and future trends. Proceedings of the Biotechniques for Air Pollution Control, 2005 Spain. University of La Coruña Publisher, 3-12.

WALTER, D. 2010. *Biofiltration: Modeling and applications,* Germany, VDM Verlag Dr.Muller Gmbh & Co.KG.

WANG, C., KONG, X. & ZHANG, X. Y. 2012. Mesophilic and thermophilic biofiltration of gaseous toluene in a long-term operation: performance evaluation, biomass accumulation, mass balance analysis and isolation identification. *Journal of Hazard Mater,* 229-230**,** 94-9.

WANI, A. H., BRANION, R. M. R. & LAU, A. K. 1997. Biofiltration: A promising and cost-effective control technology for odors, VOCs and air toxics. *Journal of Environmental Science and Health Part a-Toxic/Hazardous Substances & Environmental Engineering,* 32**,** 2027-2055.

WEBER, F. J. & HARTMANS, S. 1996. Prevention of clogging in a biological trickle-bed reactor removing toluene from contaminated air. *Biotechnology and Bioengineering,* 50**,** 91-97.

YANG, L. C., KENT, A. D., WANG, X. L., FUNK, T. L., GATES, R. S. & ZHANG, Y. H. 2014. Moisture effects on gas-phase biofilter ammonia removal efficiency, nitrous oxide generation, and microbial communities. *Journal of Hazardous Materials,* 271**,** 292-301.

ZAROOK, S. M., SHAIKH, A. A. & ANSAR, Z. 1997. Development, experimental validation and dynamic analysis of a general transient biofilter model. *Chemical Engineering Science,* 52**,** 759-773.

ZHANG, J. Y., LI, L. & LIU, J. X. 2015. Thermophilic biofilter for SO2 removal: Performance and microbial characteristics. *Bioresource Technology,* 180**,** 106-111.

ZHAO, L., HUANG, S. B. & WEI, Z. M. 2014. A demonstration of biofiltration for VOC removal in petrochemical industries. *Environmental Science-Processes & Impacts,* 16**,** 1001-1007.

ZHU, X. Q., SUIDAN, M. T., PRUDEN, A., YANG, C. P., ALONSO, C., KIM, B. J. & KIM, B. R. 2004. Effect of substrate Henry's constant on biofilter performance. *Journal of the Air & Waste Management Association,* 54**,** 409-418.

ZIGANSHIN, A. M., LIEBETRAU, J., PRÖTER, J. & KLEINSTEUBER, S. 2013. Microbial community structure and dynamics during anaerobic digestion of various agricultural waste materials. *Applied Microbiology and Biotechnology,* 97**,** 5161-5174.

# Chapter 3: Materials and methods

## 3.1 Soil collection and preparation

Three soil types were used as biofilter medium in the study (Soil 1, Soil 2 and Soil 3). They were commercially available soils supplied by Parkhouse Garden Supplies in Canterbury, New Zealand. Soil 1 was firstly used in Detchanamurthy (2013) and then Bordoloi (2016) studies as a biofilter medium for toluene degradation. Soil 2 was used as a packing medium in the column reactor for toluene degradation(unpublished work). Soil 3 was used as a source for enrichment a mix methane oxidizing culture in Gallaher (2017) study. Soil samples were sieved to < 2 mm in diameter, using mesh number 10 to remove coarse materials.

## 3.2 Differential biofilter reactor

The differential biofilter reactor used in this project was first used by Beuger (2008) and modified by Detchanamurthy (2013) through the addition of an online monitoring system for inlet and outlet toluene and carbon dioxide concentration. This improvement allowed continuous uniform gas flow to the biofilm. It also provided control over the saturation of the biofilm, enabled measurement and control of the liquid phase and enhanced access to the biofilm for carbon analysis (Detchanamurthy and Gostomski, 2015, Bordoloi, 2016).

### 3.2.1 Introduction

Differential reactors are primarily used for catalytic studies. This type of reactor is helpful in determining the rate of reaction as a function of either concentration or partial pressure (Fogler, 2014). It has been employed in biofiltration since it allows easy control of experimental parameters such as contaminant concentration, temperature, water content and nutrients (Beuger, 2008, Detchanamurthy, 2013, Bordoloi, 2016). A reactor is considered a differential type if the single pass conversion of the reactants is extremely small (typically

below 5%) (Matar et al., 1988). In other words, a differential reactor should approach a gradient-less environment and a uniform reaction in the bed.

### 3.2.2 Components and configuration of the differential biofiltration reactor

The reactor is divided into two separate cylindrical chambers separated by a hydrophilic membrane: the top chamber for the gas phase and the bottom chamber for the liquid phase (

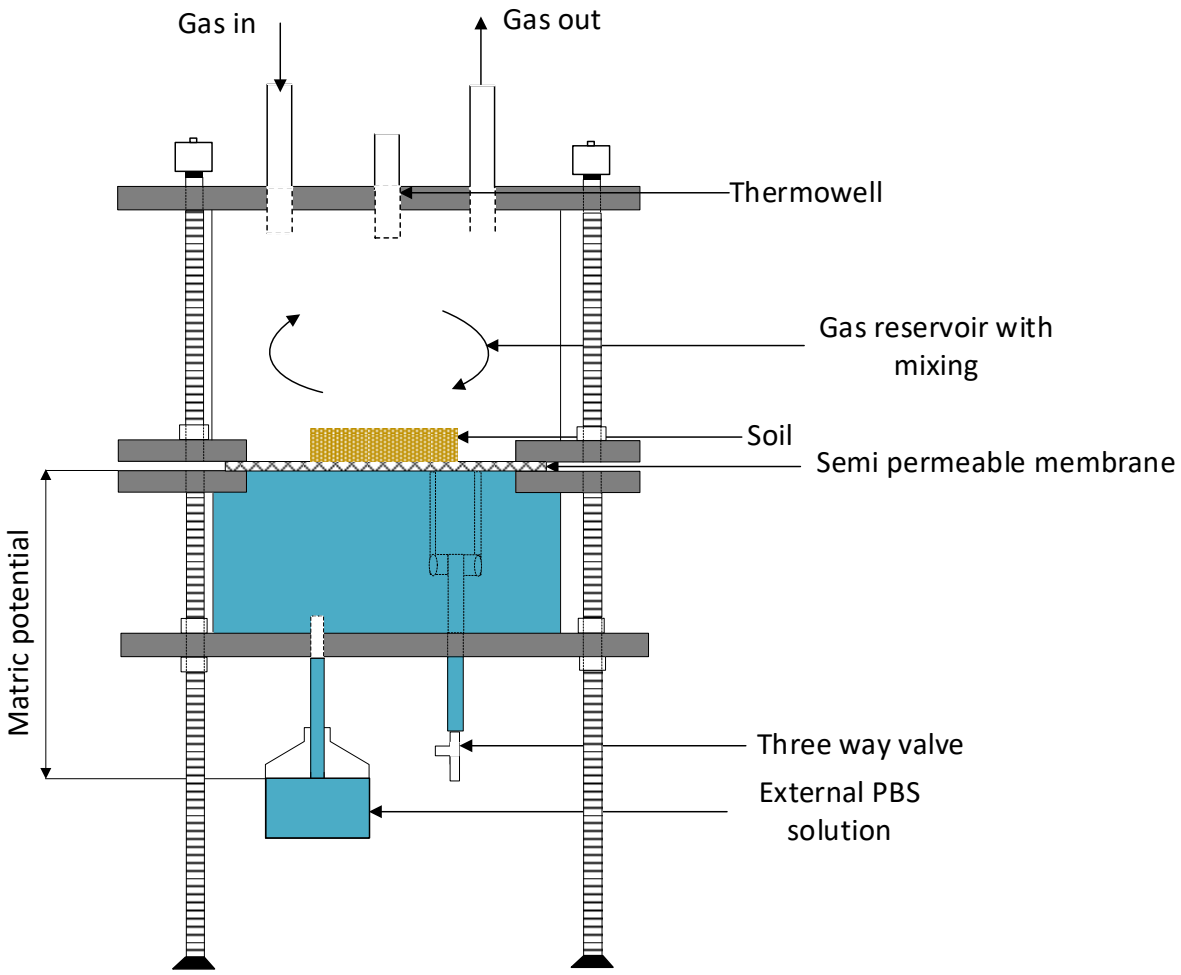


Figure 3.1). The chambers are made of glass tube with an OD of 100 mm and wall thickness of 5 mm. The gas chamber and liquid chamber are 100 mm and 50 mm in height respectively. Stainless steel plates seal the top and the bottom chambers via Viton O-Rings (Dotmar Engineering Plastics Ltd). These plates are configured with the requisite ports for the gas flow, thermowell and liquid drains.

The head-plate has three ports: Two 1/4'' ports for inlet and outlet gas and one 1/4'' port for the temperature probe which is connected to the temperature controller. The hydrophilic membrane is supported on a metal-mesh, situated between two chambers. The biofilter bed medium is placed on this membrane. To avoid leakage and abrasive grinding between the glass section and the membrane, a Viton O-ring is placed on top of the membrane.

Two 1/8” stainless steel tubes are welded to the bottom plate. One of the tubes is connected to the external PBS solution through Tygon tubing (Cole-Parmer) while the second one is intended to remove air bubbles that can accumulate under the membrane, especially at higher matric potentials. Air bubbles disturb the conductivity of the water through the membrane. In removing air bubbles entrapped underneath the membrane, the top portion of the second tube is connected to a 1/8” Viton tubing with a Y-connector that connects it to the bottom of the membrane.

Four external threaded stainless steel rods hold the reactor together. Tightening and loosening the nuts on the threaded rods allow assembly and disassembly of the reactor set-up.

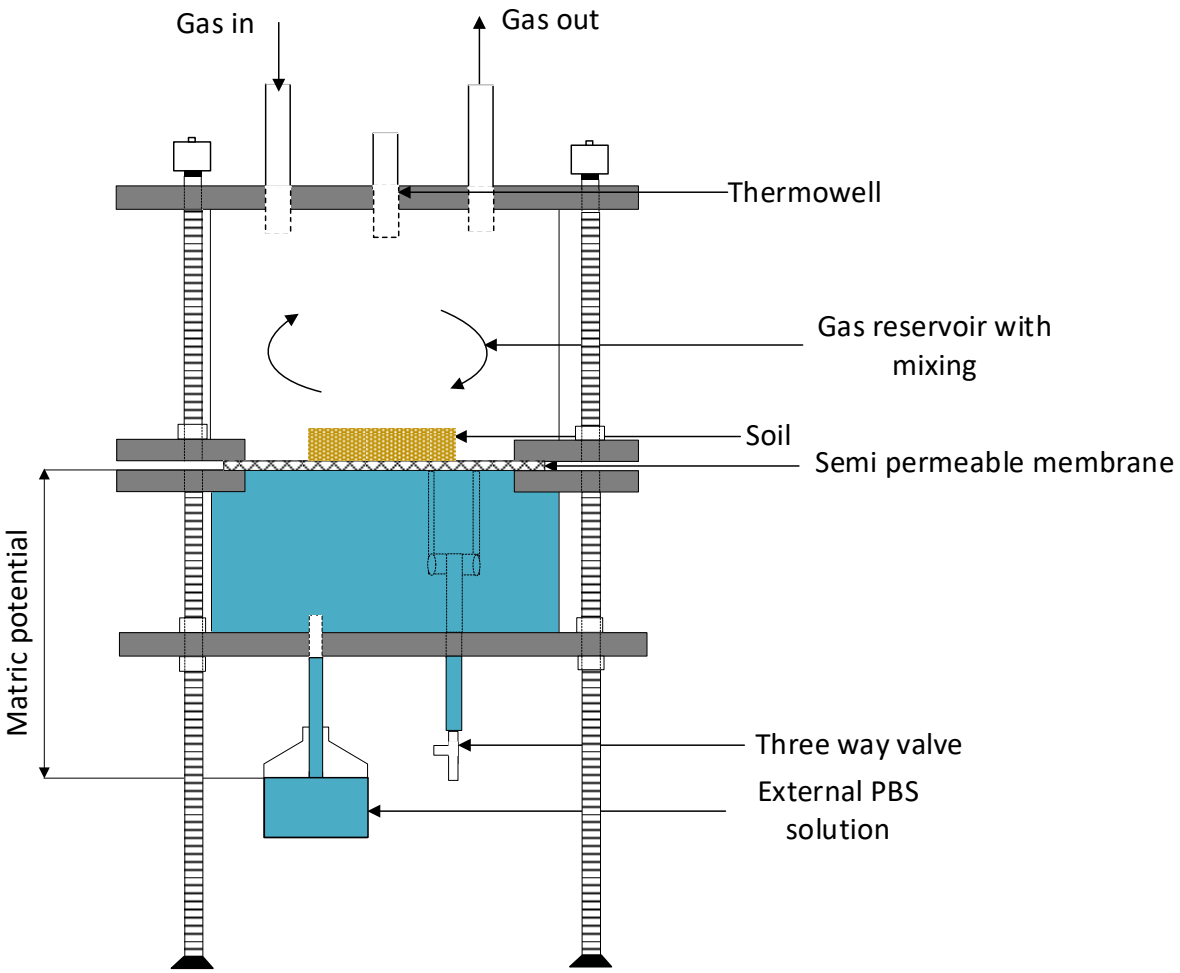


Figure 3.1: A set-up of a differential reactor with water content control.

Figure 3.2: The differential reactor inside a polyethylene foam box.

### 3.2.3 Procedure of the differential biofiltration reactor

The gases flowing into the reactor are well mixed in the head space of the reactor. The hydrophilic membrane is permeable to water but is impermeable to gas. A syringe is used to suck the air from the liquid chamber through the Tygon tubing which is connected with stainless steel tubing and to fill the liquid chamber with PBS solution. After the chamber is full of water, the syringe is removed and the tubing is capped. Hence, the liquid chamber is placed under vacuum when all of the air is removed, whereas the gas reservoir pressure is determined by the inlet gas flow. The magnitude of the vacuum is set by the relative heights of the free surface of the external PBS solution and the membrane. Because of the hydraulic link across the membrane, the vacuum controls the matric potential in the soil and thus the physical amount of water in the soil at equilibrium.

### 3.2.4 Biofilter assembling and loading

The reactor is loaded and assembled carefully to prevent liquid leaks and glass crack/breakage. Firstly, all the reactor parts including O-rings and tubing are washed in Virkon solution to disinfect surfaces and avoid contamination. Thereafter, they are autoclaved for 30 minutes at 121 $^{o}$C. The reactor assembly is conducted inside a biological safety cabinet. The ultraviolet lamp is turned on for 15 minutes prior to assembly to ensure sterility in biological cabinet.

A 10 mM phosphate buffered saline (PBS) is prepared in the laboratory at different pH values. It is used for the liquid phase and is autoclaved at 121 $^{o}$C for 30 minutes to eliminate contamination.

The reactor is fitted with four threaded stainless steel rods in order to support and seal the reactor. The water reservoir chamber is placed on the bottom plate. Other plate is placed on top of the water reservoir. The membrane is wetted with PBS solution and placed on the metallic mesh located in the middle of the plate. Approximately 8 g of sieved soil is wetted with PBS solution to make the soil homogeneous and have good contact with the membrane. A stainless steel ring (52 mm inner diameter, 3 mm height) is used to form a circular shape for loading the soil on to the membrane. The height of the filter bed and radius of the stainless steel ring is then measured for calculating the overall bed volume.

Once the soil is loaded, the metal ring is removed followed by placing the upper chamber on top of the O-ring on the central plate. The upper chamber is sealed with another O-ring placed in between the glass chamber and the upper stainless steel plate. To complete the assembly, the nuts on the stainless steel rods are tightened, first by hand and then lightly with a wrench.

A 30 ml syringe is used to fill the liquid chamber with water. The air bubble underneath the membrane can be removed by slightly tilting the reactor. The desired matric potential is set by lowering the height of the liquid level in the external PBS solution compared to the membrane until it reaches the desired height. The external PBS solution is closed with a rubber bung. Two ¼" stainless steel tube passes through the stopper: one is connected to the inlet line to eliminate back pressure modification to matric potential, one is connected with the liquid chamber.

### 3.2.5 Leak testing

In order to check leakage in the gas chamber, a $CO_2$–free air is fed to one of the ports with the flowrate controlled by a mass flow controller. The remaining port is connected to a bubble O-meter for flow measurement. Difference in the outlet and inlet flow indicates leakage. When a leak is suspected, a Snoop solution (Agilent, New Zealand) is applied at different connection points (i.e. glass-gasket-metal surfaces) to locate the leak.

## 3.3 Substrate-laden air stream generation

### 3.3.1 Methane

The methane is supplied from a cylinder of $CH_4$ (99.995% V/V purity) (Southern Gas Services, New Zealand). The dilution of the $CH_4$ is performed by mixing the pure $CH_4$ with the $CO_2$-free air supplied from dry air cylinder (79% $N_2$, 21% $O_2$) (BOC, New Zealand). By adjusting the flowrate of the dry air through the mass flow controller (Alicat or MKS), different methane concentrations are achieved. The methane concentration that can be generated ranges from 400 to 20,000 ppm by adjusting methane flow rate of 0.01 to 0.5 $ml \cdot min^{-1}$ and gas flow rate of 20 to 50 $ml \cdot min^{-1}$ (Appendix A.1).

### 3.3.2 Toluene

A diffusion method has been used to create a dilute toluene concentration in the feed air stream, as it produces a low but wide range of concentration of the volatile contaminant (Gautrois and Koppmann, 1999). The diffusion system was used in previous studies (Detchanamurthy, 2013, Bordoloi, 2016) and it will be used in the current research for generating a continuous and steady toluene concentration to the reactor system (Appendix B).

Pure liquid toluene (high performance liquid chromatography grade, Sigma-Aldrich) is added to a 10 ml diffusion flask (tube length = 0.05 m and inner diameter = 0.0035 m) which is inside a 1000 ml reagent bottle (Figure 3.3). The bottle is sealed with a rubber bung and has two ¼" stainless steel tubes passing through the stopper for inlet and outlet air flow. The whole system is held inside a temperature-controlled water bath (GD100, Grant Instruments). Carbon dioxide free air flows through the inlet tube creating a toluene-laden air stream and then exits via the outlet tube. The toluene concentration that can be generated from the diffusion system ranges from 100 to 940 ppm at 25 $ml \cdot min^{-1}$ air flow rate and water bath temperature of 20 to 60 $^{o}C$ (Appendix A.2).

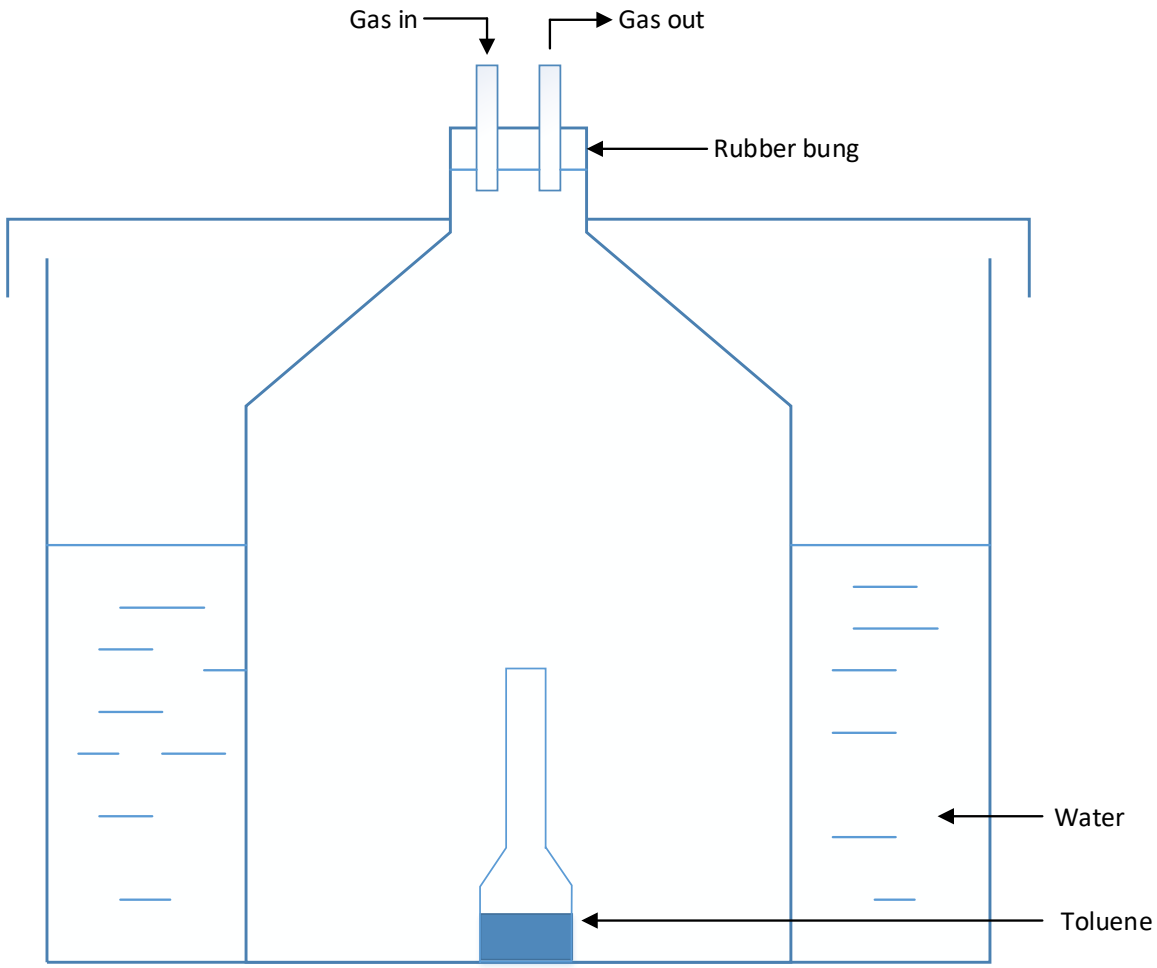


Figure 3.3: Schematic diagram of the diffusion system.

### 3.4 Humidifier

To add moisture to the inlet air, a shell and tube humidifier based on a Nafion membrane (Perma Pure LLC) is used (Figure 3.4). The dry gas to be humidified flows through the internal tubing (shaded portion) while the water is in the shell (outer tubing). Water molecules are absorbed into the tube walls and vaporize into the dry gas stream. A 50–ml glass burette with deionized water is connected to the humidifier to replace water evaporated during the humidification process. The vapour transfer is driven by the difference in partial water vapour pressure on opposing sides of the Nafion membrane in the humidifier. The humidifier is kept

inside the insulated box at the same temperature as the reactor; therefore no extra heating is required as the air achieves 100% relative humidity.

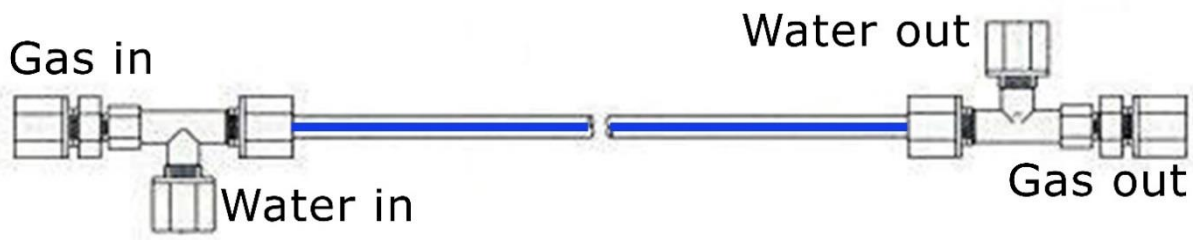


Figure 3.4: The schematic representation of the monotube humidifier used to humidify the feed air.

### 3.5 Development of the water retention apparatus

The ceramic plate (350 mm diameter) with the acrylic base is specifically designed for the use in the water retention experiment. The surface and base are separated by the filter paper (300 mm diameter). Two small holes are drilled down the acrylic base: one is connected with the suction tube (1/8'' Viton tubing), one is connected with the external water reservoir though a 1/8'' Viton tubing.

A syringe is used to suck the air from the acrylic base through the Tygon tubing and fill the base with DI water. The level of water in the external water reservoir with the open top at atmospheric pressure is adjusted to match the same height with the filter. This is done to ensure that the plate is saturated.

30 g of sieved soil sample (< 2 mm in diameter, using mess number 10) is placed on the centre ceramic plate and distributed in a thin layer (5 mm thick and 250 mm diameter) to ensure the water distribution is more uniform. The top surface of the ceramic plate is covered with the food wrap to prevent water loss to the air. The level of water in the reservoir is regularly adjusted to maintain the same height relative to the filter. The water content of the soil

sample is regularly checked by oven drying at 105 $^{o}$C (Section 3.7.7) to ensure the soil sample achieves equilibrium.

The water reservoir is lowered or/and the ceramic plate is raised so that the difference in levels between water in the reservoir and the filter is at the desired height. The applied suction generated by having the ceramic plate higher than the reservoir, drains water out of the sample. This technique is referred to as a hanging water column method of desaturating soil (Figure 3.5). The water retention curve is determined by recording the equivalent equilibrium moisture content of the soil sample at each height values between -10 and -100 $cm_{H_2O}$ (Figure 5.1).

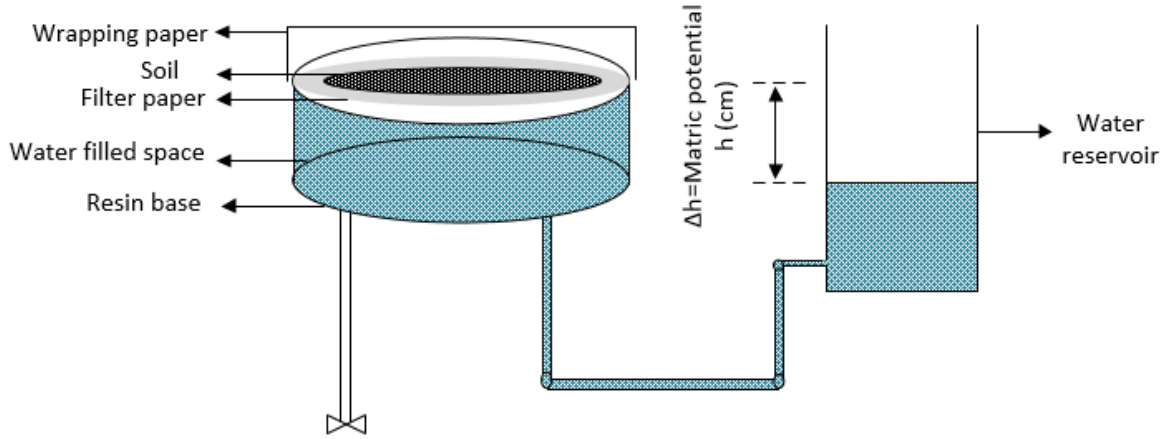


Figure 3.5: The schematic representation of the ceramic plate with hanging water column.

### 3.6 Process description

The methane- or toluene- contaminated air stream passes through a shell and tube humifier prior to entering the reactor (Figure 3.6 and Figure 3.7). The pollutant is transferred from the gas phase to the biofilm and then is partially degraded by the microorganisms. The reactor

and humidifier are in a polyethylene foam box to maintain constant temperature (Figure 3.2). The temperature in the box is controlled by a temperature controller combined with a heat source and a fan. There is a refrigeration unit with a thermostat which provides the necessary cooling load for the temperature controller to maintain temperature slightly above or below ambient as desired. The outlet tubing from the reactor is heat traced above 50 $^{o}$C in order to prevent condensation of water. The output is bubbled through a water column to maintain backpressure during GC sampling.

The inlet and outlet concentrations of pollutant are measured using a SRI gas chromatograph connected to a computer and controlled by software. Helium is the carrier gas. The SRI GC system uses a flame ionization detector (FID) for detection and analysis. Air and hydrogen are supplied to the FID. The $CO_2$ sensor is integrated online and connected at the GC sample loop purge port to measure the concentration of $CO_2$ at the inlet and outlet streams of the reactor (Appendix C).

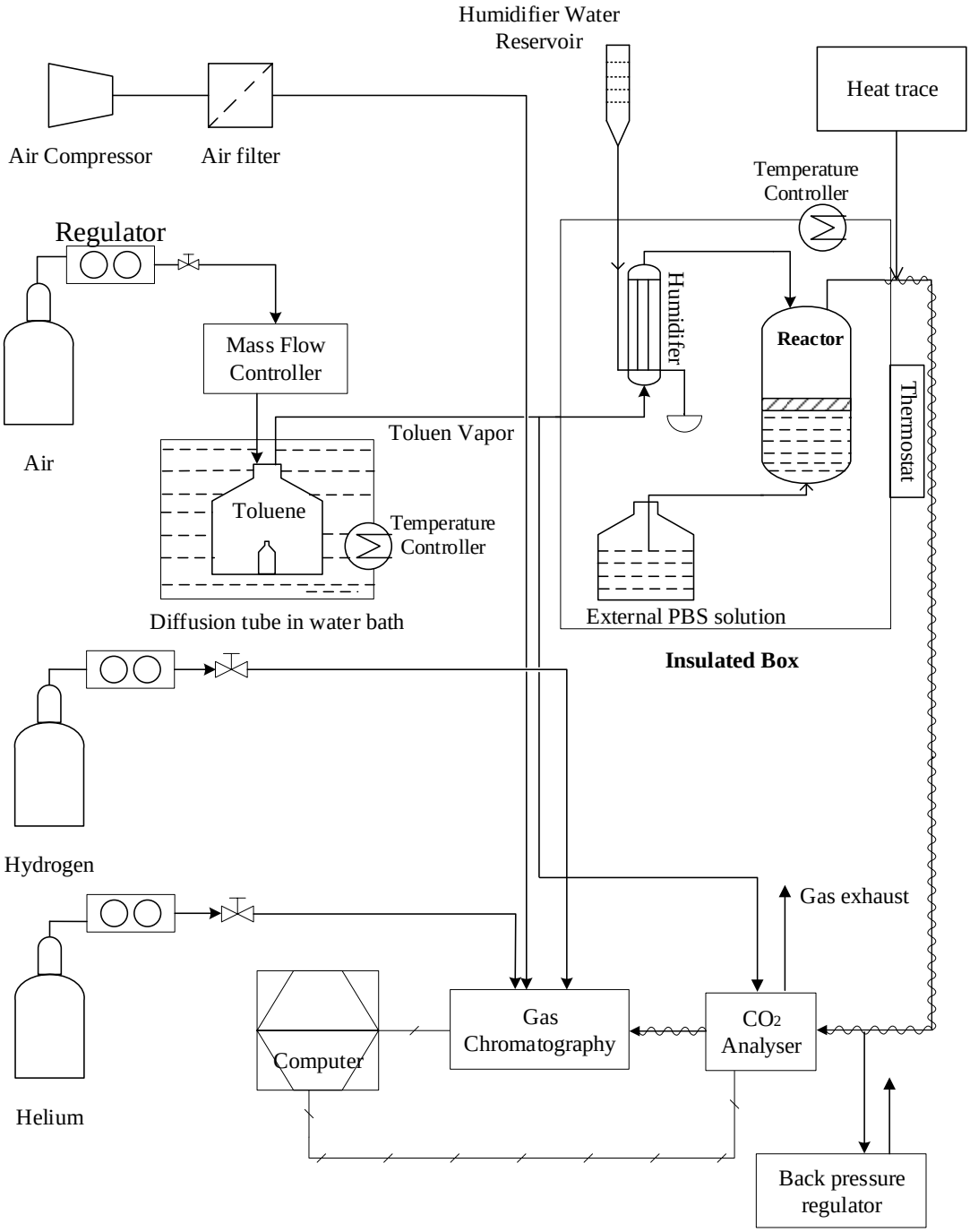


Figure 3.6: Process flow diagram of the lab scale biofilter setup for toluene biodegradation.

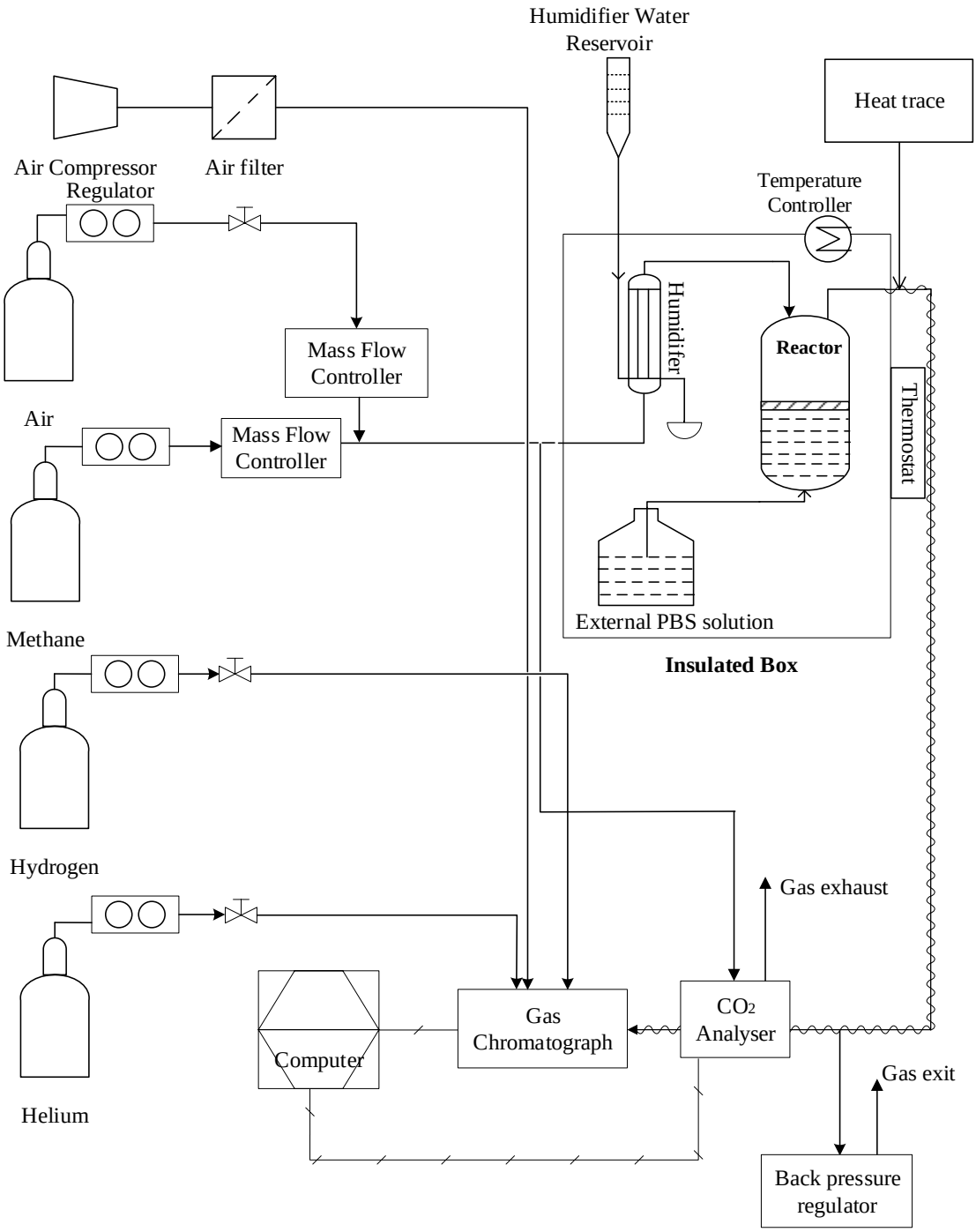


Figure 3.7: Process flow diagram of the lab scale biofilter setup for methane.

## 3.7 Analytical methods

### 3.7.1 Determination of pollutants concentration

The inlet and outlet air streams are measured at 90-minute intervals by a gas chromatograph (8610C, SRI instruments) equipped with a flame ionization detector (FID) and a MXT–1.5 ml capillary column (Restek Corporation). Sample lines from the reactor systems are selected using a ten port sample valve (Valco) integrated with a 1–ml sampling loop for automatic injection to measure the pollutant content. Helium is the carrier gas (5 psig, 10 ml·min$^{-1}$) while air (5 psig, 250 ml·min$^{-1}$) and hydrogen (20 psig, 25 ml·min$^{-1}$) are supplied to the FID. The temperature of the injector, column oven and detector temperature are maintained at 120 $^{o}$C, 150 $^{o}$C and 180 $^{o}$C respectively. The GC is connected to a computer through a USB cable. Peak Simple software version 4.35 is used for data acquisition and processing. Online monitoring for continuous operations is achieved by programming the auto sampler section in Peak Simple software.

### 3.7.2 Determination of carbon dioxide

The $CO_2$ concentration is measured using a carbon dioxide probe (GMP343, Vaisala Inc) attached to the purge port of the GC sample loop. The measurement is based on the principle of infra-red (IR) absorption. $CO_2$ concentration is proportional with the ratio between absorption at the measurement wavelength of $CO_2$ and the reference band (no absorption). It takes 1 second to measure and calculate one reading. A MI70 display (Vaisala Inc) is used as a display, communication and data logging device for the probe. MI70 link software is used to record the $CO_2$ concentration.

### 3.7.3 Determination of carbon monoxide

To find the presence of carbon monoxide, the inlet and outlet gas samples are collected in a Tedlar bag (2L, Restek). An aliquot of sample is withdrawn from the bag using a gas tight syringe and subsequently injected into a GC (SRI–8610C, SRI Instruments) equipped with FID – methanizer detector and confirmed with a HID detector.

### 3.7.4 Determination of total organic carbon

A TOC analyzer measures the quantity of the soluble organic carbon in the liquid phase and the total organic carbon in the solid phase. The biofilter soil is homogenized using a mortar and pestle. 0.3 – 0.8 g of soil from each sample is used for the analysis using the Shimadzu SSM–5000A solid analyser. The combustion catalytic oxidation method heats the samples up to 900 $^{o}$C (for total carbon) and 200 $^{o}$C (for inorganic carbon) and the $CO_2$ generated is then detected by the nondispersive infra-red sensor (NDIR). The total organic carbon (TOC) is calculated by subtracting the IC from the TC.

$$TOC = TC - IC \qquad \text{(Equation 3.1)}$$

- TOC: Total organic carbon in samples ($mg \cdot g_{soil}^{-1}$ with soil sample on a dry weight basis; $mg \cdot l^{-1}$ with liquid sample)
- TC: Total carbon in samples ($mg \cdot g_{soil}^{-1}$ with soil sample on a dry weight basis; $mg \cdot l^{-1}$ with liquid sample)
- IC: Inorganic carbon in samples ($mg \cdot g_{soil}^{-1}$ with soil sample on a dry weight basis; $mg \cdot l^{-1}$ with liquid sample)

The sample in the liquid chamber is analysed using the TOC analyser (TOC–$L_{CSH/CPH}$, Shimadzu). By heating the sample at 680 $^{o}$C in the combustion tube with an oxidation catalyst, the total carbon component is converted to $CO_2$. The total inorganic carbon components are

determined by measuring the $CO_2$ production after adding a small amount of HCl. The carbon dioxide generated in both cases is detected by the NDIR.

The Autosampler (ASI–L, Shimadzu) is used in combination with the TOC analyser allowing automatic analysis up to 100 samples per run. The advantages of using a fully automatic system were: minimized sample preparation steps; short analysis time, usually 3 – 5 minutes per sample and especially more precision than manual analysis (Schumacher, 2002).

### 3.7.5 Determination of total nitrogen

Samples are sent to Hill Laboratories, New Zealand for total nitrogen analysis. Total Nitrogen in soil samples is analysed using the Elemental Analyser equipped with Thermal Conductivity Detector. Total Kjeldahl nitrogen in liquid samples is analysed using the Discrete Analyser.

### 3.7.6 Determination of pH

The pH is determined using a SevenEasy pH meter. The pH meter is calibrated regularly with pH buffer (7.00; 4.00; 10.01).

The measurement of soil pH is performed by placing the pH meter in a mixture of soil and deionized water (1 : 2 volume ratio of soil to deionized) (Burt, 2014).

### 3.7.7 Determination of moisture content

The moisture content of soil material is measured using the gravimetric method. A measured quantity of sample is dried in an oven (8100, Contherm Scientific) for approximately 24 h at 105 $^{o}$C. Once the drying period is completed, the soil samples are placed in a desiccator until cooled to prevent the materials from absorbing moisture while cooling. The ratio of weight loss to final weight is recorded as the moisture content and reported on dry weight basis.

### 3.8 Molecular analysis

**Soil preparation**

The fresh soil samples were sieved (< 2 mm in diameter) and kept at ambient temperature (20 – 30 $^{o}$C). The bioreactor soil samples were stored -20 $^{o}$C before DNA extraction. Approximately 0.25 – 0.5 g of soil for each sample was used for the DNA extraction.

**DNA extraction and polymerase chain reaction (PCR)**

DNA was extracted from soil using the DNeasy PowerSoil Kit (Quiagen, USA) following the manufacturer's instructions. The 16S library preparation was undertaken by Auckland Genomics (Auckland, New Zealand). For microbial community analysis, the V3 and V4 region of the 16S rRNA gene of each sample was sequenced with primers 515f (GTGYCAGCMGCCGCGGTAA) and 806rB (GGACTACNVGGGTWTCTAAT) with overhang adapter sequence tails added (Lear et al., 2018). Each 25 µl of PCR contained 12.5 µl of 2 x Kapa Hifi HotStart ReadyMix (KapaBiosystems, South Africa), 0.2 µM of each primer and 12.5 ng of genomic DNA. Amplifications were performed using the following temperature program: 3 minutes at 95 $^{o}$C, 25 cycles of 30 seconds at 95 $^{o}$C, 30 seconds at 55 $^{o}$C and 30 seconds at 72 $^{o}$C, followed by a final extension for 5 minutes at 72 $^{o}$C. The PCR products were run on a Bioanalyzer DNA chip to verify the size. Using the primers 515f and 806rB, the expected size after the PCR amplicon step was ~300 bp.

**High-throughput amplicon sequencing (Illumina MiSeq)**

Amplicons were cleaned using AMPure XP beads (Beckman Coulter, USA) according to manufacturer's instructions. Unique dual index barcodes with Illumina sequencing adapters were attached to the cleaned PCR products using the Nextera XT Index kit (Illumina, Netherlands) according to manufacturer's instructions. The final library was cleaned using

AMPure XP beads (Beckman Coulter, USA) according to manufacturer's instructions. The size of amplicons was verified again and the library was quantified using QuBit (ThermoFisher, New Zealand). The uniquely indexed 16s amplicon libraries were normalised and sequenced (paired-end 250 bp sequencing) on the Illumina MiSeq 2500 platform (Auckland Genomics, New Zealand).

Adapters were trimmed from sequences using Cutadapt v1.16 (Martin, 2011) and QCed using fastqc v0.11.7 and multiqc v1.7 (Ewels et al., 2016). Sequences with less than 150 reads were discarded. Remaining sequences were processed with Dada2 (Callahan et al., 2016) and SILVA 132 reference database (Quast et al., 2013) was used to assign taxonomic identity to the amplicon sequence variants (ASVs). The amplicon sequence variant (ASV) nomenclature was chosen over the well-known Operational Taxonomic Unit (OTU) appellation to enable sequences between different studies to be compared (Callahan et al., 2017).

Relative abundance of genera for each of the samples was calculated in R v3.5.0 (R Core Team, 2015). Genera that had a relative abundance of 1% or less were removed. Unassigned genera that did not match anything in the database were labelled "unassigned" and included in the analysis.

Shannon Entropy (H') and Simpson diversity (D) indices were used to measure the diversity of communities (Schloss et al., 2009). The Shannon Entropy diversity index considers species richness more than species evenness while the Simson diversity index places a greater weight on species evenness in its measurement (Schloss and Handelsman, 2006, Schloss et al., 2009). Shannon Entropy (H') and Simpson diversity (D) indices were calculated using R v.3.5.0 using following equations (Kim et al., 2017):

$$H' = - \sum_{i=1}^{s} (p_i \times \ln p_i) \qquad \text{(Equation 3.2)}$$

$$D = 1 - \sum_{i=1}^{s} p_i^2 \qquad \text{(Equation 3.3)}$$

Where:

s – the total number of ASVs from the soil sample

$p_i$ – the proportion of the community represented by $ASV_i$

**References**


BEUGER, A. L. 2008. *The impact of water content and other environmental parameters on toluene removal from air in a differential biofiltration reactor.* Doctor of Philosophy University of Canterbury

BORDOLOI, A. 2016. *Toluene degradation by an unsaturated biofilm: The impact of environmental parameters on the carbon end-points in biofiltration.* Doctor of Philosophy, University of Canterbury.

BURT, R. 2014. *Kellogg soil survey laboratory methods manual*, United States Department of Agriculture, Natural Resources Conservation ….

CALLAHAN, B. J., MCMURDIE, P. J. & HOLMES, S. P. 2017. Exact sequence variants should replace operational taxonomic units in marker-gene data analysis. *Isme Journal,* 11**,** 2639-2643.

CALLAHAN, B. J., MCMURDIE, P. J., ROSEN, M. J., HAN, A. W., JOHNSON, A. J. A. & HOLMES, S. P. 2016. DADA2: High-resolution sample inference from Illumina amplicon data. *Nature Methods,* 13**,** 581-+.

DETCHANAMURTHY, S. 2013. *Impact of different metabolic uncouplers on the specific degradation rate of toluene in a differential biofiltration reactor.* Doctor of Philosophy, University of Canterbury.

DETCHANAMURTHY, S. & GOSTOMSKI, P. A. 2015. Studies on the influence of different metabolic uncouplers on the biodegradation of toluene in a differential biofilter reactor. *Biotechnology and Bioprocess Engineering,* 20**,** 915-923.

EWELS, P., MAGNUSSON, M., LUNDIN, S. & KALLER, M. 2016. MultiQC: summarize analysis results for multiple tools and samples in a single report. *Bioinformatics,* 32**,** 3047-3048.

FOGLER, H. S. 2014. Elements of chemical reaction engineering. 4th ed. New Jersey, United States of America: Prentice Hall.

GALLAHER, J. 2017. *The feasibility of methane as a feed-source for a microbial fuel cell.* Master of Engineering, University of Canterbury.

GAUTROIS, M. & KOPPMANN, R. 1999. Diffusion technique for the production of gas standards for atmospheric measurements. *Chromatography A,* 848**,** 239-249.

KIM, B. R., SHIN, J., GUEVARRA, R. B., LEE, J. H., KIM, D. W., SEOL, K. H., LEE, J. H., KIM, H. B. & ISAACSON, R. E. 2017. Deciphering Diversity Indices for a Better Understanding of Microbial Communities. *Journal of Microbiology and Biotechnology,* 27**,** 2089-2093.

LEAR, G., DICKIE, I., BANKS, J., BOYER, S., BUCKLEY, H. L., BUCKLEY, T. R., CRUICKSHANK, R., DOPHEIDE, A., HANDLEY, K. M., HERMANS, S., KAMKE, J., LEE, C. K., MACDIARMID, R., MORALES, S. E., ORLOVICH, D. A., SMISSEN, R., WOOD, J. & HOLDAWAY, R. 2018. Methods for the extraction, storage, amplification and sequencing of DNA from environmental samples. *New Zealand Journal of Ecology,* 42**,** 10-+.

MARTIN, M. 2011. Cutadapt removes adapter sequences from high-throughput sequencing reads. *EMBnet. journal,* 17**,** 10-12.

MATAR, M., MIRBACH, M. J. & TAYIM, H. A. 1988. *Catalysis in petrochemical processes*, Springer Science & Business Media.

QUAST, C., PRUESSE, E., YILMAZ, P., GERKEN, J., SCHWEER, T., YARZA, P., PEPLIES, J. & GLOCKNER, F. O. 2013. The SILVA ribosomal RNA gene database project: improved data processing and web-based tools. *Nucleic Acids Research,* 41**,** D590-D596.

SCHLOSS, P. D. & HANDELSMAN, J. 2006. Introducing SONS, a tool for operational taxonomic unit-based comparisons of microbial community memberships and structures. *Applied and Environmental Microbiology,* 72**,** 6773-6779.

SCHLOSS, P. D., WESTCOTT, S. L., RYABIN, T., HALL, J. R., HARTMANN, M., HOLLISTER, E. B., LESNIEWSKI, R. A., OAKLEY, B. B., PARKS, D. H., ROBINSON, C. J., SAHL, J. W., STRES, B., THALLINGER, G. G., VAN HORN, D. J. & WEBER, C. F. 2009. Introducing mothur: Open-source, platform-independent, community-supported software for describing and comparing microbial communities. *Applied and Environmental Microbiology,* 75**,** 7537-7541.

SCHUMACHER, B. A. 2002. Methods for the determination of total organic carbon (TOC) in soils and sediments. *Ecological Risk Assessment Support Center,* 2002**,** 1-23.

# Chapter 4: The fate of organic compounds in the biofiltration system

## 4.1 Introduction

In the treatment of hazardous organic compounds, it is important to understand the fate of the compounds and their degradation products. In biofiltration, the fate of the compounds depends on many factors such as design parameters, environmental conditions and their properties. Ideally, compounds should be fully mineralized to $CO_2$, water and salts by microbial oxidation. However, some compounds may not be fully degraded during treatment, or could be merely transformed into another compound, or used for biomass growth. It is difficult to track the fate of these organic compounds due to the complexity of their transformations and transport processes.

Conducting a carbon balance is one of the most effective methods to establish the fate of a specific contaminant. The aim of the carbon balance is to account for all the carbon contained in the target chemical. When the contaminant enters the biofilter, it may be degraded and transformed to various compounds but as an element, carbon (C) can neither be generated nor consumed. Therefore, tracking the carbon flux will help to identify the fate of compounds in biofilter systems.

Many authors have made rigorous attempts to measure all the carbon endpoints and close the carbon balance but very few of them have achieved 100% closure (Bester et al., 2011, Hu et al., 2015). Previous experiment with the current apparatus closed the carbon balance to 90.5 ± 5% at a 95% confidence interval (Bordoloi and Gostomski, 2019). They also found the carbon balance approached 100% with increased experimental run times improving the uncertainty of some of the analysis. Their experiments were conducted with the use of Soil 1 as a packing medium and toluene as a pollutant.

This study expands the carbon balance to multiple bed materials (Soil 1, Soil 2 and Soil 3) and pollutants (toluene and methane) using similar analytical methods with Bordoloi and Gostomski (2019). The results will improve the fundamental understanding of the carbon fraction distribution in a system and provide the basis for future work on the influence of the system inputs to the product ratios of the different carbon end-points. Thus, providing insight into the effects of operating parameters on the stability (i.e. minimization of clogging) and efficacy of biofilters.

## 4.2 Carbon balance background

Biofilters are a viable treatment technology for the emissions of organic compounds including many hazardous air pollutants (HAPs) (Devinny et al., 1999). They can effectively degrade a wide variety of organic compounds including: aromatic compounds (Torkian et al., 2003), aliphatic compounds (Wieczorek, 2005), chlorinated compounds (Devinny et al., 1999); sulphur and nitrogen containing compounds (Hwang et al., 1994). This study is focused on organic compounds that contain only carbon and hydrogen classified in two groups: aromatic compounds and aliphatic compounds.

In biofiltration, oxidative microbial processes degrade the organic compounds to $CO_2$, water, biomass and other metabolites (Deshusses, 1997a). When all the nutrients for growth are present, the stoichiometry is as followings:

$$\text{Pollutant} + O_2 \rightarrow CO_2 + H_2O + \text{Metabolites} + \text{Heat} + \text{Active biomass} \quad \text{(Equation 4.1)}$$

In non-growth systems, where the active microbial biomass within the medium is expected to stay constant over time, the reaction can be written as:

$$\text{Pollutant} + O_2 \rightarrow CO_2 + H_2O + \text{Metabolites} + \text{Heat} \quad \text{(Equation 4.2)}$$

The carbon-containing substrate ($m_{C\text{-}in}$) fed to biofilter system is distributed between the carbon-containing product(s) exiting the system ($m_{C\text{-}out}$) and carbon-containing compounds accumulating ($m_{C\text{-}acc}$) in the system.

$$m_{C\text{-}in} = m_{C\text{-}out} + m_{C\text{-}acc} \quad \text{(Equation 4.3)}$$

The carbon recovery, given by Equation 4.4, is defined as the percentage ratio of the $m_{C\text{-}in}$ transformed into the $m_{C\text{-}out}$:

$$\text{Carbon recovery} = \frac{m_{C\text{-}out}}{m_{C\text{-}in}} \quad \text{(Equation 4.4)}$$

Where:

$m_{C\text{-}out}$ represents the mass of the carbon exiting the system (g)

$m_{C\text{-}in}$ represents the mass of the carbon entering the system (g)

If nothing accumulates in the system ($m_{C\text{-}acc} = 0$), the carbon consumption is equal to the amount of carbon produced which means that a carbon recovery value is 1. If this value is lower than 1 ($m_{C\text{-}acc} > 0$), some of the carbon from the pollutant is incorporated into other molecular or macromolecular entities. It is also possible that some carbon is retained in the biofilter through adsorption or absorption of the pollutant.

Therefore, a systematic framework is proposed to complete the carbon balance in the biofilm soil differential biofilter. It consists of a robust analysis of the gas and liquid phase and a quantification of carbon which was being deposited in the biofilm layers. Under the experimental error expected from the overall analysis, a mass balance closure to ± 5% will be considered adequate.

### 4.3 Carbon balance across biofilter

The influent carbon into the biofiltration system is partitioned into three distinct phases: gas phase, liquid phase and solid phase. The carbon exiting the reactor includes the gaseous $CO_2$,

undegraded pollutants, possibly other carbon containing gases and also any liquid leachate that may contain carbon dissolved within it. Table 4.1 lists the possible end-products from the degradation of pollutants in a biofilter.

The carbon remaining in the system can accumulate in the soil, termed the solid phase, even though it contains a considerable amount of water. Equation 4.3 can be re-written to display the carbon found in the three phases:

$$m_{C\text{-}in} = m_{C\text{-}liquid} + m_{C\text{-}solid} + m_{C\text{-}out} \quad \text{(Equation 4.5)}$$

Where:

$m_{C\text{-}in}$ represents the mass of C into the reactor (g)

$m_{C\text{-}out}$ represents the mass of C in the gas phase exiting the reactor (g)

$m_{C\text{-}liquid}$ represents the mass of C in the liquid phase (g)

$m_{C\text{-}solid}$ represents the mass of C in the solid phase (g)

Table 4.1: The possible end-products of degradation of pollutants in a biofilter.

| **Gas phase** | **Reference** |
|---|---|
| CO | Haarstad et al. (2006)<br>Hellebrand and Schade (2008) |
| $CO_2$ | |
| Undegraded pollutant(s) | |
| **Liquid phase** | |
| Dissolved $CO_2$ | Summerfelt and Sharrer (2004) |
| Intermediate products | Garcia-Pena et al. (2005) |
| Dissolved pollutants | de Silva and Rittmann (2000) |
| Soluble microbial products | de Silva and Rittmann (2000) |
| **Solid phase** | |

| | |
|---|---|
| Active biomass | Fürer and Deshusses (2000) |
| EPS | Wakelin et al. (2010) |

### 4.3.1 Gas phase

The common gases exiting a biofilter are carbon dioxide ($CO_2$) and undegraded pollutants. The $CO_2$ recoveries from previous studies vary from 40% to 90% (Table 4.2), depending on the mode of operation and operational parameters. $CO_2$ evolution can be used to determine the microbial activity and substrate biodegradation (Aho et al., 2007). Metris et al. (2001) stated that $CO_2$ production is a good indicator of "not too stressful" operating conditions at steady and transient conditions. Using $^{14}C$ toluene, Fürer and Deshusses (2000) measured the fraction of $^{14}C$ incorporated within the biomass and a correlation between the dynamics of $CO_2$ production and the performance of the biofilter. Similar trends between the $^{14}CO_2$ production and the elimination capacity were observed over time. Maximum EC and $CO_2$ production values were achieved during the first days of operation and then slowly decreased to reach steady state after three months operation. Kolling et al. (2013) concluded $CO_2$ production provides reliable information the allocation of assimilated carbon in the systems.

Carbon monoxide is a potential product found in the off-gas stream. It can be attributed to the presence of carbon monoxide in the feed source or due to production during organic compound degradation (Haarstad et al., 2006, Hellebrand and Schade, 2008). Although few studies observed carbon monoxide generation during VOCs degradations, the need for an investigation is still required in order to track all of the carbon end-points.

#### 4.3.1.1 Gas analysis

There are many gas analysis techniques available in the literature. One of the common is gas chromatography (GC) with various detectors (thermal conductivity detector (TCD), helium

ionization detector (HID), flame ionization detector (FID) and electron capture detector (ECD)). Among of these detectors, FID is one of the most common detectors. It is able to detect virtually all organic carbon compounds containing pollutants over a wide range of concentrations with the exception of some halogenated hydrocarbons due to theirs high chemical stability (Milne and Morrow, 2009). Notably, a FID equipped with a methanizer (packed with a nickel catalyst) is capable of detecting $CO_2$ and CO at low levels which is critical for a carbon balance (Stangeland et al., 2017). When the target compounds are not known in advance, the GC can be combined with a mass spectrometry, to attempt to identify unknown compounds (Luo and Agnew, 2001, Defoer et al., 2002).

Nondispersive infra-red spectrometer (NDIR) is another detector used to monitor the concentration of carbon oxides at the respective ends of biofilter. By shining an infra-red beam through a sample cell, the concentration of target gases is measured electro-optically based on its absorption at a specific wavelength.

Table 4.2: Examples of carbon balance in biofilters treating organic compounds (toluene, methane) in a gaseous stream.

| **Pollutant** | **Type of Biofilter and Operation (*)** | **Packing material** | **Carbon balance (gC)** | **Reference** |
|---|---|---|---|---|
| Toluene | Biofilter: Growth | Peat enriched with nutrients | C – $CO_2$: 44.5%<br>Carbonates: 14.3%<br>Polymers: 32%<br>Biomass: 9.2% | Morales et al. (1998) |
| Toluene | Biotrickling filter: Growth | Pall rings with *P. Corrugata* + Protozoan | C – $CO_2$: 69%<br>Biomass: 13%<br>Liquid: 8%<br>Unaccounted: 10% | Cox et al. (1998) |

| | | | | |
|---|---|---|---|---|
| Toluene | Biotricking filter: Growth | Pall rings with *P. Corrugata* + Protozoan | C – $CO_2$: 69%<br>Biomass: 21%<br>Liquid: 8%<br>Unaccounted: 2% | Cox and Deshusses (1999) |
| Toluene | Biofilter: Non - growth | Compost, bark and lava rocks | C – $CO_2$: 70%<br>Unaccounted: 30% | Fürer and Deshusses (2000) |
| Toluene | Vapour phase bioreactor: Growth | Porous silicate pellets | C – $CO_2$: 60%<br>Biomass: 40%<br>Liquid: < 1% | Song and Kinney (2000) |
| Toluene, Benzene | Biofilter: Non - Growth | Cylindrical activated carbon | Toluene – $CO_2$: 64%<br>Benzene – $CO_2$: 51% | Li et al. (2002) |
| Toluene, Acetone | Biotricking filter: Growth | Coal particles | C – $CO_2$: 90%<br>Unaccounted: 10% | Chang and Lu (2003) |
| Toluene | Biotricking filter: Growth | Inorganic | C – $CO_2$: 63.2%<br>Liquid: 15.5%<br>Unaccounted: 21.3% | Kim et al. (2005a) |
| Toluene, styrene, methyl ethyl ketone and methyl isobutyl ketone | Biotricking filter: Growth | Pelletized diatomaceous earth | C – $CO_2$: 63.2%<br>Liquid: 20%<br>Unaccounted: 16.8% | Kim et al. (2005b) |
| Toluene | Biofilter: Growth | Wood chips, propylene spheres inoculated with activated sludge | C - $CO_2$: 83%<br>Unaccounted: 17% | Xi et al. (2006) |
| Toluene | Biofilter: Non - growth | Coir pith | C - $CO_2$: 60%<br>Unaccounted: 40% | Krishnakumar et al. (2007) |

| | | | | |
|---|---|---|---|---|
| Methane | Biofilter: Growth | Rock and clay particles | C – $CO_2$: 66 – 71%<br>Unaccounted: 34% | Nikiema and Heitz (2010) |
| Methane | Biofilter: Growth | Gravel | C – $CO_2$: 9 – 60% | Girard et al. (2011) |
| Toluene and p-xylene | Biofilter: Growth | Inert material | p-xylene: 74% $gCO_2/gC$<br>Toluene: 72% $gCO_2/gC$ | Gallastegui et al. (2011) |
| Toluene | Biotrickling filter: Growth | Granular activated carbon (GAC) | C – $CO_2$: 69%<br>Biomass: 30.5% | Wang et al. (2012) |
| Methane | Biofilter: Growth | Mupice and granular activated carbon | C – $CO_2$: 39%<br>Unaccounted: 61% | Kim et al. (2013) |
| Methane, toluene | Biofilter: Growth | Inorganic material | C – $CO_2$: 82%<br>Unaccounted: 18% | Menard et al. (2014) |
| Methane | Biotrickling filter: Growth | Polyurethane foam (PUF) | C – $CO_2$: 89% | Estrada et al. (2014) |
| Methane | Biofilter: Growth | Coal | C – $CO_2$: 27 – 62%<br>Biomass: 28 – 63% | Limbri et al. (2014) |
| Methane | Biofilter: Growth | Pumice soil | C – $CO_2$: 32%<br>Unaccounted: 68% | Syed et al. (2016) |
| Toluene | Biofilter: Growth | Perlite inoculated with activated sludge | C – $CO_2$: 85.9%<br>Biomass: 6.6%<br>Liquid: 5.6%<br>Unaccounted: 1.8% | Xi et al. (2016) |
| Toluene | Biofilter: Growth | Compost, cement, perlite, $CaCO_3$, plant fiber | C – $CO_2$: 43.2%<br>Unaccounted: 56.8% | Zhu et al. (2016) |
| Methane, methanol | Biofilter: Growth | Compost | C – $CO_2$: 78.3% | Lebrero et al. (2016) |

| | | | | |
|---|---|---|---|---|
| | | | Unaccounted: 21.7% | |
| Toluene | Biofilter: Growth | Perlite inoculated with activated sludge | C – $CO_2$: 77.0%<br>Biomass: 8.9%<br>Liquid: 1.0%<br>Unaccounted: 14% | Jimenez et al. (2016) |
| Benzene, toluene, ethylbenzene, xylene | Biofilter: Growth | Compost inoculated with wastewater | C – $CO_2$: 52.4%<br>Biomass: 41.0%<br>Liquid: 4.7%<br>Unaccounted: 1.9% | Leili et al. (2017) |
| Toluene | Biofilter: Non - growth | *Pseudomonas putida* (KT2440) | C – $CO_2$: 72.0%<br>Biofilm: 16%<br>Liquid: 12% | Bordoloi and Gostomski (2019) |

* Growth: supplemental nutrient addition; Non-growth: no nutrient addition

### 4.3.2 Liquid phase

The presence of dissolved carbon within the liquid purge can be derived from the dissolved $CO_2$ (Summerfelt and Sharrer, 2004), intermediate products (Garcia-Pena et al., 2005), dissolved pollutants and soluble microbial products (de Silva and Rittmann, 2000). These studies revealed the portion of these dissolved carbons is variable, from less than 1% to over 40% of the inflowing carbon. Studies conducted in the growth systems often recorded a higher portion of dissolved carbon (>10% of the consumed carbon) (Morales et al., 1998, Kim et al., 2005b, Bester et al., 2011). The majority of papers operating nutrient limited systems find that the leachate stream contains less than <3% of the consumed carbon (Cox and Deshusses, 1999, Chou and Wu, 1999, Kim et al., 2001).

#### 4.3.2.1 Liquid analysis

The total organic carbon in the liquid phase can be measured by oxidizing the organic compounds to $CO_2$ which then can be quantified. Two commonly techniques are often used

to quantify the organic carbon in water. The first technique is wet chemical oxidation, where carbon compounds in the sample are oxidized to $CO_2$ by a persulfate solution and irradiated with ultraviolet light. The resulting $CO_2$ is either detected via an NDIR detector or using a conductivity detector. However, this technique is reported to have a low oxidation efficiency compared to other methods especially with colloidal material such as complex polysaccharides (Chen and Wangersky, 1993) and algal exudate (Chen and Wangersky, 1996), particulate matter and some sulphur- and nitrogen- containing organic compounds.

The second technique is catalytic combustion. The sample is heated in an oxygen- rich environment (600 – 900 $^oC$) to ensure all the carbon containing compounds are converted to $CO_2$. A NDIR detector is used to measure the resulting $CO_2$.

### 4.3.3 Solid phase

The main assumption in earlier research was any carbon not released in the gas phase or discharged in leachate was incorporated into cell growth (Deshusses, 1997b, Jorio et al., 2000, Li et al., 2002, Elmrini et al., 2004, Xi et al., 2006). If all missing carbon was going to biomass growth, then the increasing amount would eventually clog up the biofilter. This was common in the growth systems due to rapid biomass formation (Ozis et al., 2007, Dorado et al., 2012, Wang et al., 2012). However, rapid biomass formation was not typically reported in nutrient-limited biofilter systems (Deshusses, 1997b, Xi et al., 2006, Bordoloi, 2016) potentially indicating that not all of the unaccounted carbon ended up in the bed. This was supported by Fürer and Deshusses (2000) who also worked with a non-growth system and did not find any missing radiolabelled $^{14}C$-toluene incorporated into biomass in their study, thereby indicating that unaccounted carbon may not have necessarily end up in the biofilter bed. Therefore, the assumption that carbon not detected in the gas and liquid phase was entirely used for cell growth could be incorrect.

Extracellular polymeric substances (EPS), which was a major structural component in biofilms, might be another carbon- containing product (Hilger et al., 2000). Flemming (2000) stated that EPS can account for 50 to 90% of the total biofilm organic carbon, depending on the species and environmental conditions. In some studies, EPS itself could be a source of carbon for the microorganisms (Sutherland, 2001, Gientka et al., 2016). Along with active biomass, EPS was one of the contributors to biofilter failure. Mauclaire et al. (2004) found that the clogging of the biofilter was largely caused by EPS when they dissected the pore spaces in a biological sand filter. In the highly clogged filter layer, they found the EPS to cell volume ratios were 100:1, where bacterial cells and total EPS were occupied 0.1% and 10% (V/V) of the pore space respectively. Wakelin et al. (2010) demonstrated that the layer where clogging often accrues had similar amounts of polysaccharide regardless of the bed media (granular activated carbon (GAC), anthracite and sand columns).

In summary, the accepted carbon end-points in the solid phase were biomass and EPS. However, determining the distribution of carbon in each product was beyond the scope of this study. Techniques used to measure the carbon being deposited in the solid phase are discussed in section below.

#### 4.3.3.1 Solid analysis

Total organic carbon measurements can be performed by a solid sample combustion unit. The sample is placed into a furnace for combustion. The furnace operates at temperatures as high as 900 $^{o}$C to ensure complete carbon destruction. The resulting combustion gases are swept by a carrier gas stream from the furnace directly into a detector for measurement of $CO_2$ and calculation of the carbon content. This approach limits the sample mass that can be efficiently combusted due to uneven distribution of the sample carbon content.

### 4.4 Carbon balance of the current system

Literature revealed that the endogenous respiration of bacterial in the soil and/or compost was one of the sources causing inaccuracies when closing the carbon balance (Fürer and Deshusses, 2000, Fierer and Schimel, 2003). To find the endogenous respiration, a "control" experiment was performed. The soil was held at a specific water content and temperature throughout the study. $CO_2$-free air was fed through the system. The endogenous $CO_2$ production was determined after achieving a steady $CO_2$ concentration.

The carbon flux through the biofilter system was examined under two different stages (Figure 4.1). The first stage ($t_1$) was when steady endogenous $CO_2$ concentration was achieved. Following this stage, a feed of pollutant was started. The second stage was when the system reached a steady state condition ($t_f$) and a stable elimination capacity.

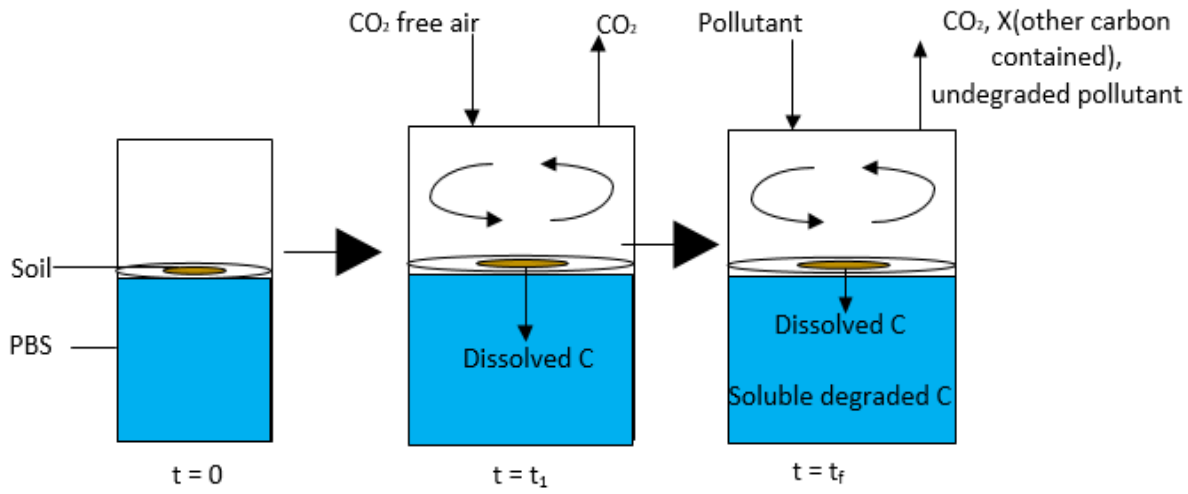


Figure 4.1: Fate of the carbon flux through biofiltration system from t = 0 to the final time $t = t_f$.

At t = 0, a thin soil layer was loaded on to the hydrophilic membrane above the liquid chamber. A PBS solution was added to the liquid chamber. The total volume of PBS used include both in

the liquid chamber and the PBS external reservoir. The carbon content in the gas, liquid ($m_{C\text{-}liquid}$) and soil ($m_{C\text{-}solid}$) at t = 0 was:

$$m_{C\text{-}gas\ out} = 0 \quad \text{(Equation 4.6)}$$

$$m_{C\text{-}liquid} + m_{C\text{-}solid} = m_{initial-liquid} + m_{initial-soil} \quad \text{(Equation 4.7)}$$

$$= (V_{external\ reservoir} + V_{liquid\ chamber})C_{initial\text{-}PBS} + mC_{initial\text{-}soil} \quad \text{(Equation 4.8)}$$

Where:

$m_{C\text{-}gas\ out}$ - the amount of carbon present in the gas phase exiting the reactor at t = 0 (g)

$m_{initial-liquid}$ - the amount of carbon present in the PBS solution at t = 0 (g)

$m_{initial-soil}$ - the carbon content of the soil sample at t = 0 (g)

$V_{external\ reservoir}$ and $V_{liquid\ chamber}$ - the volume of the external reservoir and the liquid chamber, respectively (l)

$C_{initial\text{-}PBS}$ - the concentration of the carbon present in the liquid phase at the beginning (t = 0) of experiment ($g \cdot l^{-1}$)

$C_{initial\text{-}soi}$ - the initial carbon content of the soil ($g \cdot g_{soil}^{-1}$)

m - the amount of soil in the system (g)

After the soil and the PBS solution were added, the synthetic air (a blend of oxygen and nitrogen) was fed to the system. It was employed to carry the endogenous $CO_2$ derived from the soil to the $CO_2$ analyser. Thus, the $CO_2$ concentration in the gas chamber could be determined at different time intervals. Time (t) = $t_1$ was when a steady endogenous $CO_2$ concentration was achieved ($C_{CO2\text{-}res}$).

Next, polluted air was continuously fed into the reactor, where it was biologically oxidized to end-products, mainly carbon dioxide and water. The $CO_2$ concentration during pollutant degradation was recorded. Assuming the $CO_2$ endogenous concentration ($C_{CO2\text{-}res}$) did not

change throughout the period, the $CO_2$ produced from the pollutant(s) degradation was determined by subtracting the endogenous $CO_2$ concentration from the $CO_2$ concentration during pollutant degradation. Other volatile carbon containing compounds might have been produced during the degradation process (e.g. toluene/methane intermediates, CO). The mass balance of the carbon entering and the carbon exiting in the gas phase in the biofilter system was:

$$\frac{dm_{C\text{-}acc}}{dt} = \dot{m}_{in} - \dot{m}_{out} \qquad \text{(Equation 4.9)}$$

Where:

$m_{C\text{-}acc}$ - mass of the carbon accumulating in the biofiltration system (g)

$\dot{m}_{in}$; $\dot{m}_{out}$ - mass flow rate of the carbon in and out of the biofiltration system, respectively ($g \cdot h^{-1}$)

Integrating Equation 4.9 with respect to time from $t = t_1$ to $t = t_f$:

$$\int_{t1}^{tf} \frac{dm_{C\text{-}acc}}{dt} = \int_{t1}^{tf} \dot{m}_{in} - \int_{t1}^{tf} \dot{m}_{out} \qquad \text{(Equation 4.10)}$$

Equation 4.11 can be re-written to display the carbon recovery in percentage:

$$\text{Carbon recovery (\%)} = \frac{(\int_{t1}^{tf} \dot{m}_{out} dt + m_{C\text{-}acc})}{\int_{t1}^{tf} \dot{m}_{in} dt} 100\% \qquad \text{(Equation 4.11)}$$

Expanding the term $\int_{t1}^{tf} \dot{m}_{in} dt$ in Equation 4.11 gives:

$$\int_{t1}^{tf} \dot{m}_{in} dt = Q \int_{t1}^{tf} C_{in}\, dt \qquad \text{(Equation 4.12)}$$

$$= Q \sum_{t1}^{tf} C_{pollutant\text{-}in} \Delta t_{in} \qquad \text{(Equation 4.13)}$$

Where:

Q - the flow rate in and out of the biofiltration system ($m^3 \cdot h^{-1}$)

$C_{in}$ - the concentration of the total carbon in the biofiltration system ($g \cdot m^{-3}$)

$C_{pollutant\text{-}in}$ - the concentration of carbon in the pollutant (methane or toluene) in the biofiltration system ($g \cdot m^{-3}$)

$\Delta t_{in}$ - the time between measurements of $C_{pollutant\text{-}in}$, ~ 12 hours

Expanding the $\int_{t1}^{tf} \dot{m}_{out} dt$ in Equation 4.11 gives:

$$\int_{t1}^{tf} \dot{m}_{out}\, dt = Q \int_{t1}^{tf} C_{out}\, dt \qquad \text{(Equation 4.14)}$$

$$= Q \int_{t1}^{tf} (C_{pollutant\text{-}out} + C_{CO2\text{-}out} + C_{CO2\text{-}res} + C_X)\, dt \qquad \text{(Equation 4.15)}$$

$$= Q[ \sum_{t1}^{tf} (C_{pollutant\text{-}out} + C_X + C_{CO2\text{-}out})\Delta t_{out} + C_{CO2\text{-}res}\, (t_f - t_1)] \qquad \text{(Equation 4.16)}$$

Where:

$C_{out}$ - the concentration of carbon exiting the biofiltration system in the gas phase ($g \cdot m^{-3}$)

$C_{pollutant\text{-}out}$ - the concentration of carbon in the pollutant (methane or toluene) out of the biofiltration system ($g \cdot m^{-3}$)

$C_x$ - the concentration of carbon containing products in the gas phase excluding the main pollutant (toluene/ methane) and $CO_2$ ($g \cdot m^{-3}$)

$\Delta t_{out}$ - the time between measurements of $C_{pollutant\text{-}out}$; $C_x$ and $C_{CO2\text{-}out}$, ~ 4 – 6 hours

$C_{CO2-out}$ - the concentration of carbon in the $CO_2$ exiting the biofiltration system ($g \cdot m^{-3}$)

$C_{CO2\text{-}res}$ - the endogenous $CO_2$ concentration exiting the biofiltration system due to the soil respiration ($g \cdot m^{-3}$)

The carbon content in the solid and liquid phase increased over time due to more carbon deposited in the system (i.e. EPS, biomass). At time $t = t_f$, the total carbon content in the solid and liquid was:

$$m_{C\text{-}liquid} + m_{c\text{-}solid} = m_{final-liquid} + m_{final-soil}$$

$$= (V_{external\ reservoir} C_{final\text{-}external\ PBS\ solution} + V_{liquid\ chamber} C_{final\text{-}liquid\ chamber}) + mC_{final\text{-}soil}$$

(Equation 4.17)

Where:

$m_{final-liquid}$ was the amount of carbon present in the liquid chamber at $t = t_f$ (g)

$m_{final-soil}$ was the carbon content of the soil sample at $t = t_f$ (g)

$C_{final\text{ - }liquid\ chamber}$ - the carbon present in the liquid chamber at $t = t_f$ ($g \cdot l^{-1}$)

$C_{final\text{ - }external\ PBS\ solution}$ - the carbon present in the external PBS solution at $t = t_f$ ($g \cdot l^{-1}$)

$C_{final\text{-}soil}$ - the final carbon content of the soil at $t = t_f$ ($g \cdot g_{soil}^{-1}$)

The total carbon accumulated in the solid and liquid was calculated by subtracting the total carbon before the experiment ($t = t_1$) to the total carbon after the experiment ($t = t_f$).

$$m_{C\text{-}acc} = (m_{final-liquid} + m_{final-soil}) - (m_{initial-liquid} + m_{initial-soil})$$

$$= [(V_{external\ reservoir} C_{final\text{-}external\ PBS\ solution} + V_{liquid\ chamber} C_{final\text{-}liquid\ chamber}) - (V_{external\ reservoir} + V_{liquid\ chamber}) C_{initial\text{-}PBS}] + m(C_{final\text{-}\ soil} - C_{initial\text{-}soil})$$

(Equation 4.18)

Combining the Equation 4.13 and Equation 4.16 and placing to Equation 4.11:

$$\text{Carbon recovery (\%)} = \left[\frac{Q[\sum_{t1}^{tf}(C_{pollutant\text{-}out} + C_X + C_{CO2\text{-}out})\Delta t_{out} + C_{CO2\text{-}res}(t_f - t_1)] + m_{C\text{-}acc}}{Q\sum_{t1}^{tf} C_{pollutant\text{-}in}\Delta t_{in}}\right]100\%$$

(Equation 4.19)

Equation 4.18 and Equation 4.19 can be solved numerically. Quantified carbon represents the total degraded carbon from the pollutant and tracked in the various phases by quantification of the components were used to solve these equations.

## 4.5 Results

### 4.5.1 Quantifying carbon end-points in the gas phase

The GC with a FID detector showed a single peak at the same retention time as toluene or methane as appropriate throughout the analysis (data not shown). The presence of carbon monoxide was explored using a methanizer combined with a FID and cross-checked with a HID detector. Carbon monoxide and other toluene/methane intermediates were not found in the outlet of the reactor at the detection limit of ~ 0.1 ppm in the exiting gas stream in 37 runs, therefore in Equation 4.15 $C_X$= 0 g·m$^{-3}$.

#### 4.5.1.1 Pollutant and carbon dioxide quantification

The gas concentration profiles (pollutant and $CO_2$) were tracked over the entire operation period for each experiment. Figure 4.2, Figure 4.3 and Figure 4.4 are representative concentration profiles from three experiments. The $CO_2$ released from a biofilter came from two sources: the biodegradation of organic material in the soil (endogenous respiration) and pollutant degradation (Section 4.3.1). In order to determine the endogenous respiration for each experiment, the $CO_2$-free air was passed through the reactor until achieving a steady state endogenous $CO_2$ concentration at the chosen set of conditions and soil type. Once steady state was achieved the pollutant feed was started.

The total $CO_2$ released from a biofilter was determined at the end of the experiment. The net $CO_2$ produced at any point in time was determined by subtracting the endogenous $CO_2$ concentration from the total $CO_2$ concentration. Determining the net $CO_2$ concentration and

tracking the inlet and residual concentration were required quantify the carbon recovery as $CO_2$. In addition, continuously tracking the carbon fractions in the gas phase provided data on the performance of the biofilters when treating a pollutant at a chosen set of conditions.

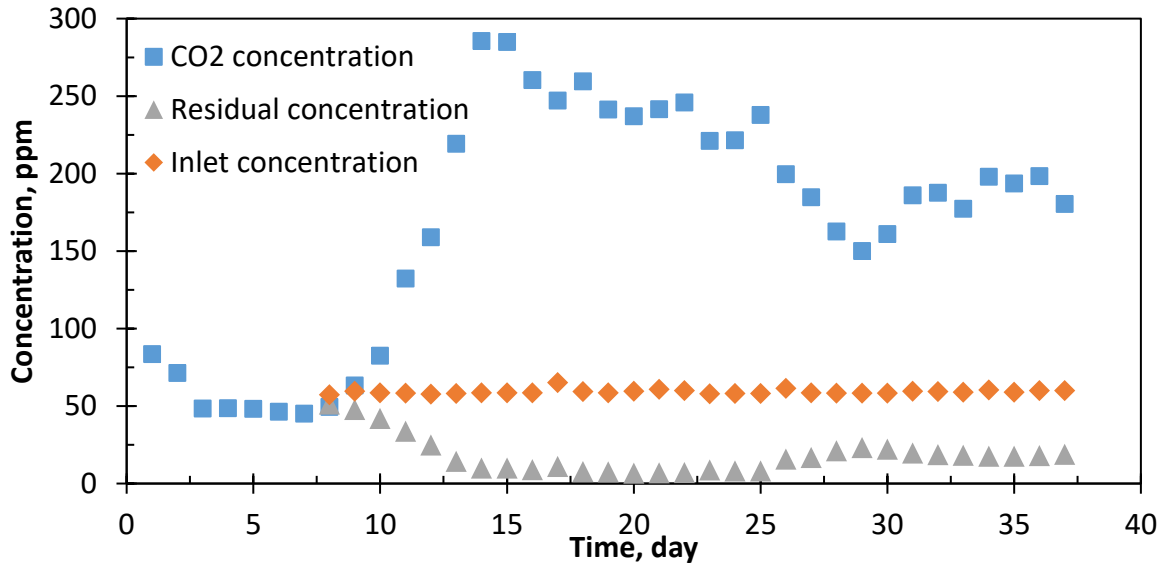


Figure 4.2: Gas concentration profile of Soil 2 at a toluene inlet loading rate of 78 $g \cdot m^{-3} \cdot h^{-1}$ and -10 $cm_{H_2O}$ at 40 $^oC$.

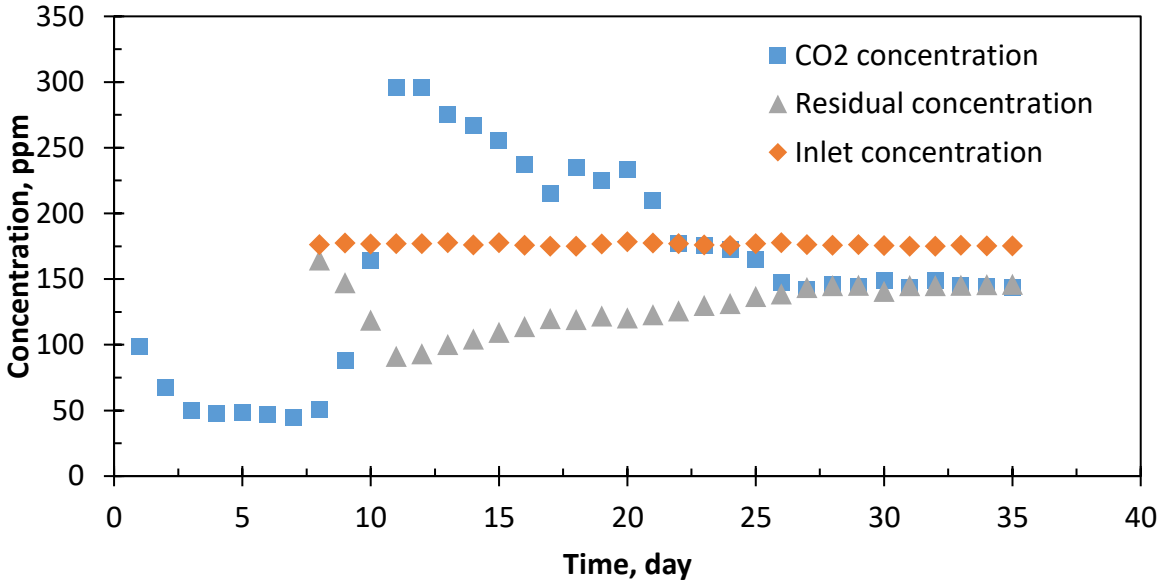


Figure 4.3: Gas concentration profile of Soil 2 at a toluene inlet loading rate of 137 $g \cdot m^{-3} \cdot h^{-1}$ and -100 $cm_{H_2O}$ at 40 $^oC$.

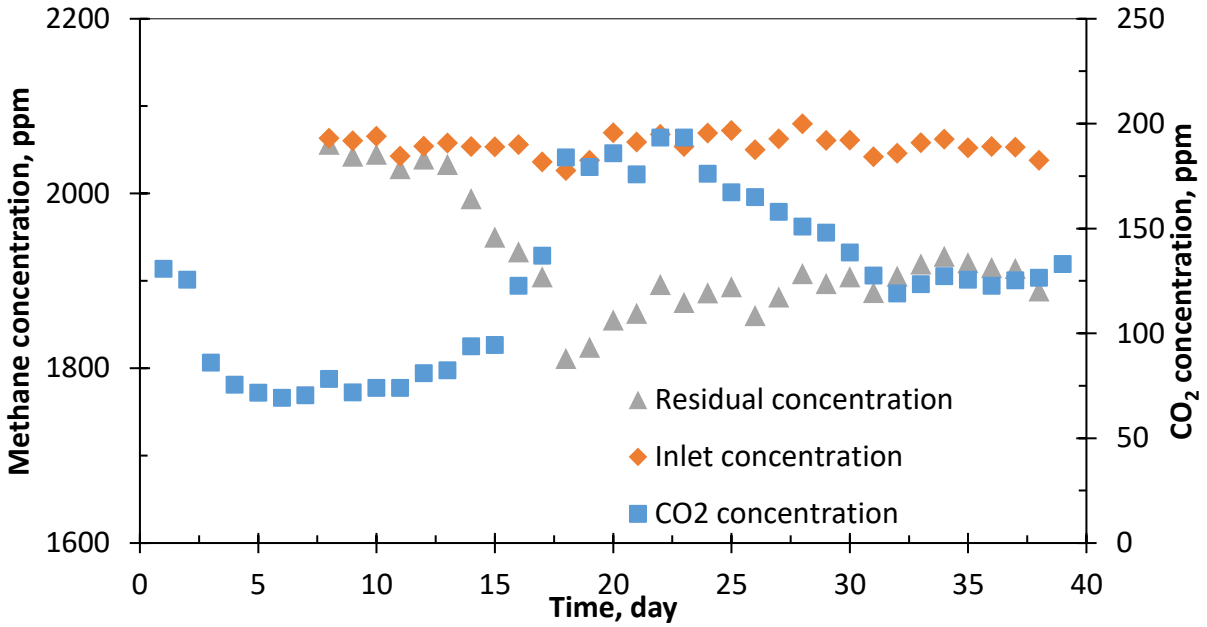


Figure 4.4: Gas concentration profile of Soil 2 at a methane inlet loading rate of 280 $g \cdot m^{-3} \cdot h^{-1}$ and -10 $cm_{H_2O}$ at 40 °C.

#### 4.5.1.2 Endogenous respiration quantification

The endogenous $CO_2$ production rate was used to identify the net $CO_2$ concentration for all three soil types at -10 $cm_{H_2O}$ and -100 $cm_{H_2O}$ and 40 °C (Figure 4.5). The analysis of variance (ANOVA) results (Table 4.3) indicated that the endogenous respiration varied depending on the matric potential ($p < 0.01$). The matric potential (tension) of the soil in the reactor was varied by adjusting the height of the external reservoir relative to the membrane, with -100 $cm_{H_2O}$ being drier than -10 $cm_{H_2O}$ (the matric potential was negative as the soil water content was below saturation).

The respiration rates at the wetter condition (-10 $cm_{H_2O}$) was significantly higher than the drier condition (-100 $cm_{H_2O}$), for three soil samples. The mean respiration rate at the wetter condition (25 $g \cdot m^{-3} \cdot h^{-1}$) was twice the rate at the drier condition (12 $g \cdot m^{-3} \cdot h^{-1}$) (Figure 4.5). This trend was consistent with the results reported by Schimel et al. (1999) and Bordoloi (2016).

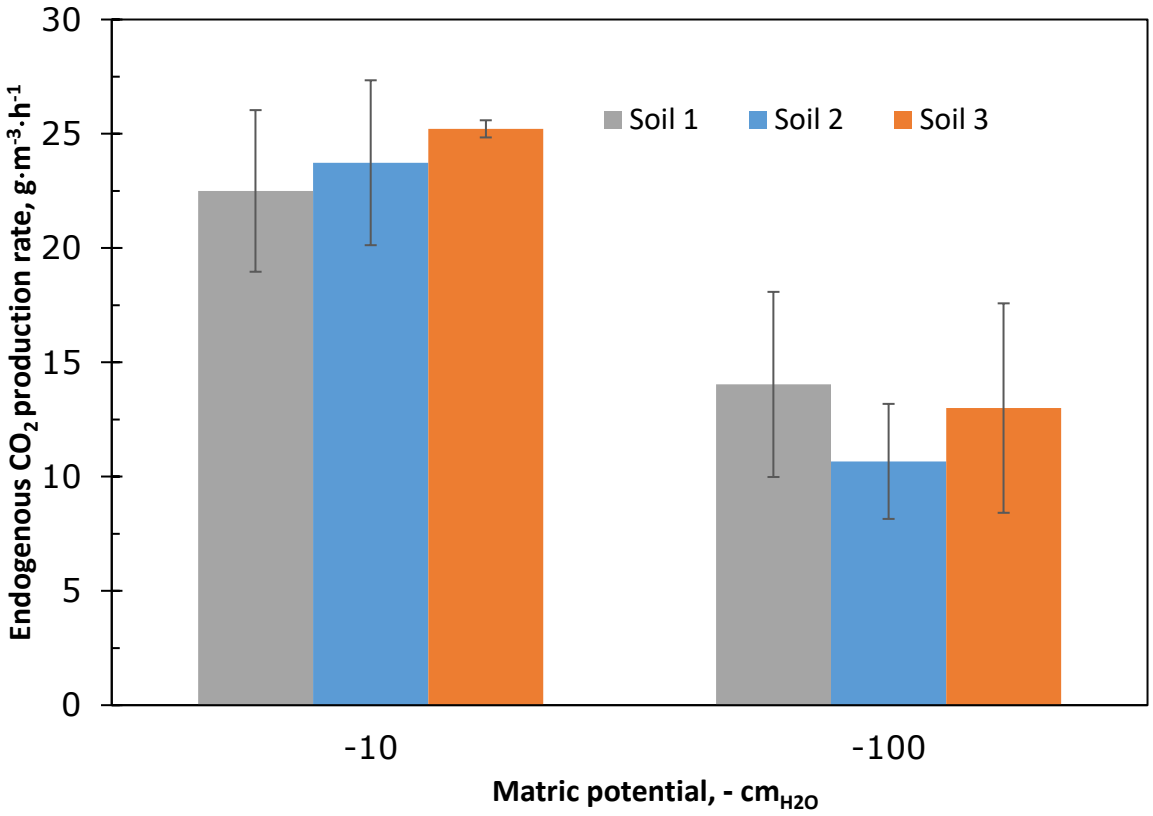


Figure 4.5: Endogenous respiration of three soil types at 40 °C at -10 and -100 $cm_{H_2O}$ matric potential after 7 – 10 days of operation. The error bars reported are the standard deviation from triplicate experiments.

Table 4.3: An ANOVA evaluation of the influence of moisture content and soil type on respiration rates in Soil 1, 2 and 3.

| | DF | Sum of Squares | Mean of Squares | F value | *p* value | $\eta^2$ |
|---|---|---|---|---|---|---|
| **Soil** | 2 | 11.1 | 5.5 | 0.53 | 0.53 | 0.02 |
| **Condition** | 1 | 575.2 | 575.2 | 54.58 | <0.01 | 0.79 |
| **Soil x Condition** | 5 | 16.6 | 8.3 | 0.79 | 0.48 | 0.02 |
| **Residuals** | 12 | 126.4 | 10.5 | | | |

### 4.5.2 Quantifying carbon end-points in the solid and liquid phase

Studies related to soil organic carbon commonly use data gathered on air-dried samples at 15 $^{o}$C to 25 $^{o}$C (Meney et al., 1998, Adhya et al., 2000) or oven dried at 105 $^{o}$C (Hofmann et al., 2016). Measurement of soil organic carbon using the air-drying method can lead to an underestimation of the mass fraction per unit dry soil since the residual water was still present (Poeplau et al., 2015). However, removal of all free water present in the soil samples can lead to the volatilisation of organic compounds which may account for some mass loss (Samuelsson et al., 2006). Experiments were carried out on soil samples to evaluate the reliability, repeatability and reproducibility of two drying methods.

Total inorganic carbon (TIC) was not detected in any of the three soil. Therefore, the total organic carbon (TC) equalled the total carbon (TOC) (Table 4.4). The highest TOC concentration was found in Soil 1 (144.9 ± 9.0 mg C·g$^{-1}$ soil in dry weight basis), which was eight times higher than Soil 2 (18.8 ± 1.8 mg C·g$^{-1}$ soil in dry weight basis). Based on the t-test results (assuming unequal variances), the drying method did not have a significant effect on TOC ($p > 0.05$) (Table 4.5). However, oven drying of soil samples to a constant weight required less drying time (24 – 48 hours) than air drying (48 – 120 hours).

Table 4.4: Results of total organic carbon (TOC) and total inorganic carbon (TIC) analysis of fresh soils subjected to oven drying and air drying. Values are the mean and standard deviation of five measurements of soil from one experiment.

| **Soil type** | **Oven drying** | | **Air drying** | |
|---|---|---|---|---|
| | **TOC** ($mgC \cdot g^{-1}$ dry wt) | **TIC** ($mgC \cdot g^{-1}$ dry wt) | **TOC** ($mgC \cdot g^{-1}$ dry wt) | **TIC** ($mgC \cdot g^{-1}$ dry wt) |
| Soil 1 | 144.9 ± 10.6 | 0 | 141.2 ± 11.3 | 0 |
| Soil 2 | 18.8 ± 1.8 | 0 | 18.7 ± 2.4 | 0 |
| Soil 3 | 91.7 ± 8.9 | 0 | 87.3 ± 13.4 | 0 |

Table 4.5: Paired t-test comparing the TOC in each fresh soil subjected to oven drying and air drying.

| **Soil type** | **oven drying vs air drying, *p* value** |
|---|---|
| Soil 1 | 0.55 |
| Soil 2 | 0.96 |
| Soil 3 | 0.34 |

Similarly, the bioreactor soils were tested at the conclusion of the experiments using similar methods with the fresh soils. The biofilter were operated at 40 $^{o}C$; a matric potential of -10 $cm_{H_2O}$ and exposed to a toluene concentration of 50 ppm. The bioreactor soil samples were kept moist to support microbial activity during the experiments and were wetter than the fresh soil samples. In addition, the development of biofilm after exposure to the pollutant could have changed the drying rate of the bioreactor soil samples (Lennon and Lehmkuhl, 2016).

After exposure to toluene, both TOC and TIC concentrations in the bioreactor soils increased (Table 4.6). The increase in organic carbon content in soils was due to the biomass production and EPS produced by toluene-degrading bacterial communities (Section 4.3.3). The highest increases in TOC was Soil 1 (~23.1 $mgC \cdot g^{-1}$ soil on a dry weight basis) followed by Soil 2 (~21.2 $mgC \cdot g^{-1}$ soil on a dry weight basis) while the lowest increase in TOC was Soil 3 (14.1 $mgC \cdot g^{-1}$ soil on a dry weight basis).This might be more carbon accumulated in biofilters packed with Soil 1 after runs rather than exiting out of the reactors (i.e. $CO_2$) like those biofilters packed with Soil 2 and Soil 3.

The TIC in the bioreactor soils ranged 1 – 1.5 $mgC \cdot g^{-1}$ soil on a dry weight basis). The presence of inorganic carbon in soils could have been due to carbonate formation resulting from $CO_2$ infiltrating the soil, which was described by Zhao et al. (2017). No statistically significant difference in the TOC concentrations between the two drying methods was detected ($p > 0.05$) (Table 4.7). However, the TOC values of fresh and bioreactor soils subjected to air drying were more variable than the oven drying, especially for Soil 3 with coefficient of variations of 15.3% for fresh soil and of 11% for bioreactor soils (Table 4.8). This was due to the residual moisture content in the air-dried soil samples, which ranged between 3 – 6%.

Table 4.6: Results of total organic carbon (TOC) and total inorganic carbon (TIC) analysis of bioreactor soils at the conclusion of toluene degradation experiments subjected to oven drying and air drying. Values are the mean and standard deviation of five measurements of soil from one experiment.

| **Soil type** | **Oven drying** | | **Air drying** | |
|---|---|---|---|---|
| | **TOC** ($mgC \cdot g^{-1}$ dry wt) | **TIC** ($mgC \cdot g^{-1}$ dry wt) | **TOC** ($mgC \cdot g^{-1}$ dry wt) | **TIC** ($mgC \cdot g^{-1}$ dry wt) |
| Soil 1 | 168 ± 9.5 | 1.5 ± 0.3 | 162 ± 11.2 | 1.3 ± 0.6 |
| Soil 2 | 40 ± 3.4 | 1.1 ± 0.1 | 36.8 ± 3.7 | 1.0 ± 0.1 |
| Soil 3 | 106.4 ± 3.5 | 1.3 ± 0.5 | 104.2 ± 11.6 | 1.2 ± 0.9 |

Table 4.7: Paired t-test comparing the TOC in each bioreactor soil at the conclusion of toluene degradation experiment subjected to oven drying and air drying.

| **Soil type** | **oven drying vs air drying, *p* value** |
|---|---|
| Soil 1 | 0.34 |
| Soil 2 | 0.13 |
| Soil 3 | 0.94 |

Table 4.8: Variation (%) in TOC of fresh and bioreactor of three soil types between oven drying and air drying.

| Soil | | Oven drying | Air drying |
|---|---|---|---|
| Fresh soil | 1 | 7.3 | 8.0 |
| | 2 | 9.7 | 12.9 |
| | 3 | 9.7 | 15.3 |
| Bioreactor soil | 1 | 5.6 | 6.9 |
| | 2 | 8.5 | 9.7 |
| | 3 | 7.8 | 11.0 |

The comparison of oven-drying and air-drying for soil samples prior to determining the TOC showed no significant differences in the water content. The oven drying method provided shorter drying times and less variability than air-drying. Therefore, oven drying was subsequently used to dry the soil samples prior to TOC analysis.

The PBS solution was tested for carbon content before operating the bioreactor. The TOC and the TIC of the autoclaved PBS were 0.29 ± 0.03 $mg \cdot l^{-1}$ and 0.05 ± 0.01 $mg \cdot l^{-1}$. The results were the mean of five independent measurements. House dust, carbon originating from bodies and gloves were potential sources of contamination which could contribute to the TOC and TIC in the PBS solution.

The liquid samples in the reactor reservoir and in the external PBS solution were analyzed after the experiments (Table 4.9). The TOC and TIC concentrations in the external PBS solution were unchanged compared to initial concentrations in PBS solution and thus were treated as negligible in the analysis ($C_{final\text{-}external\ PBS\ solution} \sim 0$).

Table 4.9: Results of total organic carbon (TOC) and total inorganic carbon (TIC) analysis of liquid samples in the reactor reservoir and in the external PBS solution at the conclusion of the toluene degradation experiments. Values are the mean and standard deviation of each measurements of liquid samples in subsequent experiments.

| **Samples** | **External PBS solution** | | **Reactor reservoir** | |
|---|---|---|---|---|
| | **TOC** ($mg \cdot l^{-1}$) | **TIC** ($mg \cdot l^{-1}$) | **TOC** ($mg \cdot l^{-1}$) | **TIC** ($mg \cdot l^{-1}$) |
| Soil 1 biofilter | 0.29 ± 0.01 | 0.05 ± 0.02 | 69.1 ± 1.5 | 12.4 ± 1.3 |
| Soil 2 biofilter | 0.30 ± 0.03 | 0.05 ± 0.01 | 31.5 ± 1.3 | 9.6 ± 0.8 |
| Soil 3 biofilter | 0.31 ± 0.03 | 0.05 ± 0.02 | 40.4 ± 1.7 | 10.8 ± 1.2 |

TOC and TIC concentrations of the liquid sample in the reactor reservoir increased. The TIC concentrations in the reactor reservoirs were: 12.4 ± 1.3 $mg \cdot l^{-1}$; 9.6 ± 1.3 $mg \cdot l^{-1}$ and 10.8 ± 1.2 $mg \cdot l^{-1}$ for Soil 1 biofilter, Soil 2 biofilter and Soil 3 biofilter, respectively. The increase in the TIC concentrations in the reactor reservoirs was probably due to the dissolved $CO_2$ forming bicarbonate ($HCO_3^-$) and carbonate ($CO_3^{2-}$) and carbonic acid depending on environmental conditions such as the pH, temperature and ionic strength of the solution (Jarvie et al., 2017). Comparing to the initial pH of 7.0 ± 0.1, the pH of the reactor reservoirs at the end of the experiments remained unchanged. Thus, the produced $CO_2$ did not form excessive amounts of dissolved $CO_2$.

The TOC concentrations in the reactor reservoirs were: 69.1 ± 1.5 $mg \cdot l^{-1}$; 31.5 ± 1.3 $mg \cdot l^{-1}$ and 40.4 ± 1.7 $mg \cdot l^{-1}$ for Soil 1 biofilter, Soil 2 biofilter and Soil 3 biofilter, respectively. The increase with time of the TC concentrations in the reactor reservoirs was most likely linked to soluble products being produced during the transformation of the pollutant (Jarvie et al., 2017). In

addition, organic material such as humic substances in the soil may have leached through into the liquid thus contributing to the increase of the TC concentrations (Aizpuru et al., 2001, Gerke, 2018) and causing the change in colour of the reactor reservoir from transparent to yellowish-brown colour (Figure 4.6). No further experiment was conducted to differentiate the humic substances and soluble products being produced during the transformation of the pollutant in the reactor reservoirs as it was beyond the scope of the study.

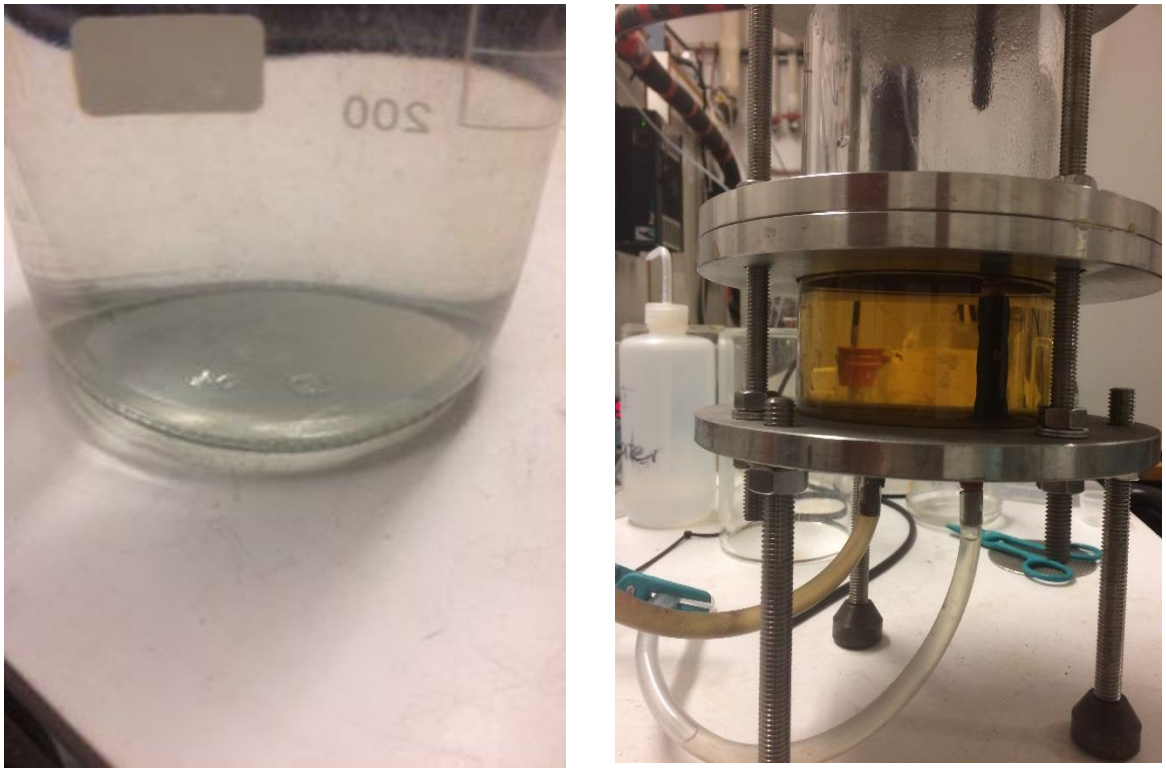

(a) (b)

Figure 4.6: The change in the colour of the liquid in the reactor reservoir: (a) fresh PBS solution; (b) 40 days after toluene treatment in Soil 3 biofilter.

Different TOC and TIC concentrations between the liquid samples in the external PBS solution and the reactor reservoir was observed. It could be accounted to two possible reasons. The first reason was no liquid water movement between the external PBS solution and the reactor

reservoir as equilibrium was reached between the reactor reservoir and the soil. The second reason was negligible amounts of carbon-containing products (i.e. soluble products, humic substances and carbonate) in the reactor reservoir diffuse into the external PBS solution therefore remaining in the reactor reservoir.

### 4.6 Overall carbon balance

All the carbon exiting the reactor in the gas or deposited in the solid and liquid phase was compared with the carbon entering the reactor for each experimental run. Equation 4.19 was used to calculate the carbon recovery in each experiment at various operating conditions. The carbon recovery for the degraded pollutants (methane and toluene) over 37 experiments operating under different environmental conditions was 96.1 ± 5.3% (Figure 4.7). In 11 out of 37 experiments, the carbon balance approached 100% or higher. Since these experiments were operated longer (40 – 55 days) than typical runs (25 – 35 days) (data not shown), more carbon accumulated in the system which might improve the uncertainty of soil organic carbon analysis as suggested by Bordoloi et al. (2019).

Previous reports on closing the carbon balance were uneven, with 10 – 50% of the degraded carbon unaccounted/missing (Table 4.2). Thus, this work represented an improvement over previous reports, providing confidence that all the pollutant's (toluene and methane) degradation products across multiple soil types (Soil 1, 2 and 3) were being tracked on a carbon basis.

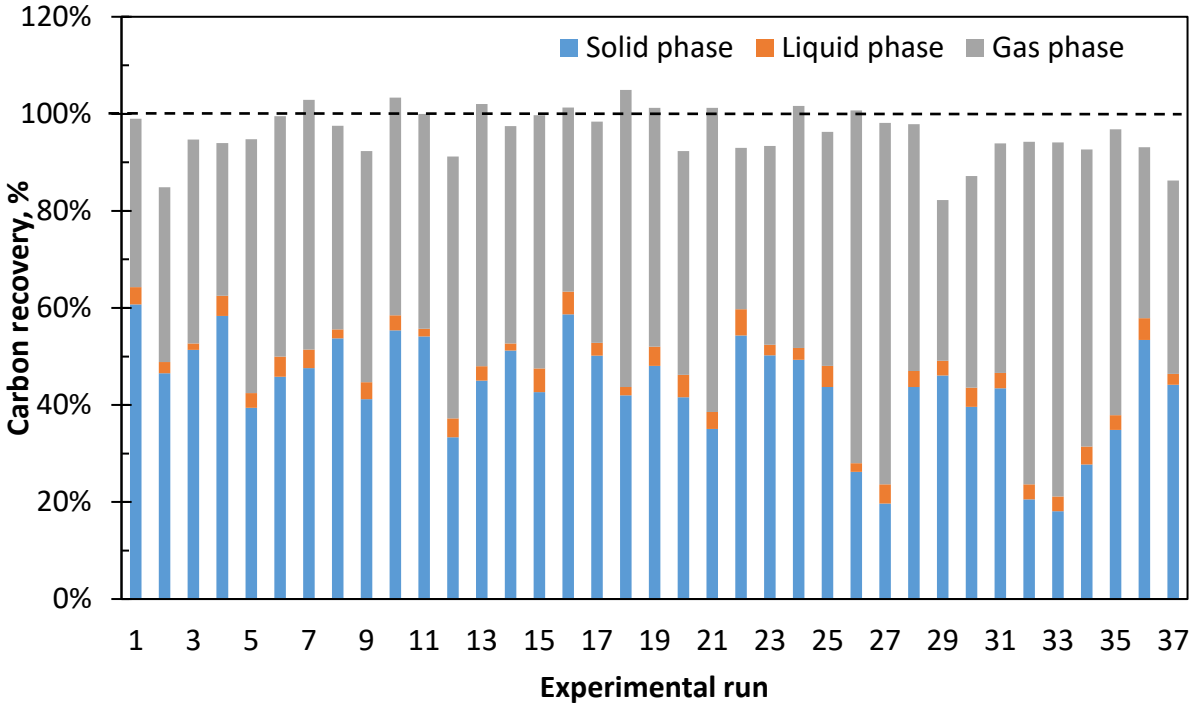


Figure 4.7: Carbon recovery for the degraded pollutants (toluene and methane) over 37 experimental biofilter runs using different soils at various operating conditions.

The carbon fraction found in the liquid phase was always less than 5% of the total carbon. The identification of the soluble carbon compounds has not yet been determined. The cumulative amount of $CO_2$ evolved ranged from 30% to 70% of the degraded carbon while 20% to 60% of the carbon accumulated in the biofilm phase. The results indicated the mineralized fraction ($CO_2$) and non-mineralized fraction varied depending on the environmental parameters. Subsequent chapters will focus on the metabolic responses of the biofilm and the %$CO_2$ recovery to changes in toluene/methane residual concentration and matric potential.

**References**

ADHYA, T. K., BHARATI, K., MOHANTY, S. R., RAMAKRISHNAN, B., RAO, V. R., SETHUNATHAN, N. & WASSMANN, R. 2000. Methane emission from rice fields at Cuttack, India. *Nutrient Cycling in Agroecosystems,* 58**,** 95-105.

AHO, T., KIVINEN, V., KOSKINEN, P., PUHAKKA, J. & YLI-HARJA, O. Exploring the interrelationship between bioreactor stability and carbon balance. Proceedings of the Fifth IEEE International Workshop on Genomic Signal Processing and Statistics, GENSIPS'07, Tuusula, Finland, 10-12 June 2007, 2007.

AIZPURU, A., MALHAUTIER, L., ROUX, J. C. & FANLO, J. L. 2001. Biofiltration of a mixture of volatile organic emissions. *Journal of the Air & Waste Management Association,* 51**,** 1662-1670.

BESTER, E., KROUKAMP, O., HAUSNER, M., EDWARDS, E. A. & WOLFAARDT, G. M. 2011. Biofilm form and function: carbon availability affects biofilm architecture, metabolic activity and planktonic cell yield. *Journal of Applied Microbiology,* 110**,** 387-398.

BORDOLOI, A. 2016. *Toluene degradation by an unsaturated biofilm: The impact of environmental parameters on the carbon end-points in biofiltration.* Doctor of Philosophy, University of Canterbury.

BORDOLOI, A., GAPES, D. J. & GOSTOMSKI, P. A. 2019. The impact of environmental parameters on the conversion of toluene to CO2 and extracellular polymeric substances in a differential soil biofilter. *Chemosphere,* 232**,** 304-314.

BORDOLOI, A. & GOSTOMSKI, P. A. 2019. Carbon recovery and the impact of start-up conditions on the performance of an unsaturated *Pseudomonas putida* biofilm compared with soil under controlled environmental parameters in a differential biofilter. *Journal of Chemical Technology and Biotechnology,* 94**,** 600-610.

CHANG, K. & LU, C. Y. 2003. Biofiltration of isopropyl alcohol and acetone mixtures by a trickle-bed air biofilter. *Process Biochemistry,* 39**,** 415-423.

CHEN, W. H. & WANGERSKY, P. J. 1993. A high-temperature catalytic-oxidation method for the determination of marine dissolved organic-carbon and its comparison with the UV photo-oxidation method. *Marine Chemistry,* 42**,** 95-106.

CHEN, W. H. & WANGERSKY, P. J. 1996. Production of dissolved organic carbon in phytoplankton cultures as measured by high-temperature catalytic oxidation and ultraviolet photo-oxidation methods. *Journal of Plankton Research,* 18**,** 1201-1211.

CHOU, M. S. & WU, F. L. 1999. Treatment of toluene in an air stream by a biotrickling filter packed with slags. *Journal of the Air & Waste Management Association,* 49**,** 386-398.

COX, H. H., NGUYEN, T. T. & DESHUSSES, M. A. Elimination of toluene vapors in biotrickling filters: performance and carbon balances. Proceedings Annual Meeting & Exhibition of the Air & Waste Management Association, June, 1998. 14-18.

COX, H. H. J. & DESHUSSES, M. A. 1999. Biomass control in waste air biotrickling filters by protozoan predation. *Biotechnology and Bioengineering,* 62**,** 216-224.

DE SILVA, D. G. V. & RITTMANN, B. E. 2000. Nonsteady-state modeling of multispecies activated-sludge processes. *Water Environment Research,* 72**,** 554-565.

DEFOER, N., DE BO, I., VAN LANGENHOVE, H., DEWULF, J. & VAN ELST, T. 2002. Gas chromatography–mass spectrometry as a tool for estimating odour concentrations of biofilter effluents at aerobic composting and rendering plants. *Journal of Chromatography A,* 970**,** 259-273.

DESHUSSES, M. A. 1997a. Biological waste air treatment in biofilters. *Current Opinion in Biotechnology,* 8**,** 335-339.

DESHUSSES, M. A. 1997b. Transient behavior of biofilters: Start-up, carbon balances, and interactions between pollutants. *Journal of Environmental Engineering-Asce,* 123**,** 563-568.

DEVINNY, J. S., DESHUSSES, M. A. & WEBSTER, T. S. 1999. *Biofiltration for air pollution control,* United States of America, CRC press.

DORADO, A. D., BAEZA, J. A., LAFUENTE, J., GABRIEL, D. & GAMISANS, X. 2012. Biomass accumulation in a biofilter treating toluene at high loads - Part 1: Experimental performance from inoculation to clogging. *Chemical Engineering Journal,* 209**,** 661-669.

ELMRINI, H., BREDIN, N., SHAREEFDEEN, Z. & HEITZ, M. 2004. Biofiltration of xylene emissions: bioreactor response to variations in the pollutant inlet concentration and gas flow rate. *Chemical Engineering Journal,* 100**,** 149-158.

ESTRADA, J. M., LEBRERO, R., QUIJANO, G., PÉREZ, R., FIGUEROA-GONZÁLEZ, I., GARCÍA-ENCINA, P. A. & MUÑOZ, R. 2014. Methane abatement in a gas-recycling biotrickling filter: Evaluating innovative operational strategies to overcome mass transfer limitations. *Chemical Engineering Journal,* 253**,** 385-393.

FIERER, N. & SCHIMEL, J. P. 2003. A proposed mechanism for the pulse in carbon dioxide production commonly observed following the rapid rewetting of a dry soil. *Soil Science Society of America Journal,* 67**,** 798-805.

FLEMMING, H. C. 2000. Biofilms in biofiltration. *Biotechnology Set, Second Edition***,** 445-455.

FÜRER, C. & DESHUSSES, M. A. Biodegradation in biofilters: Did the microbe inhale the VOC. Proceedings of the Annual Meeting & Exhibition of the Air & Waste Management Association, 2000. 18-22.

GALLASTEGUI, G., RAMIREZ, A. A., ELIAS, A., JONES, J. P. & HEITZ, M. 2011. Performance and macrokinetic analysis of biofiltration of toluene and p-xylene mixtures in a conventional biofilter packed with inert material. *Bioresource Technology,* 102**,** 7657-7665.

GARCIA-PENA, I., HERNANDEZ, S., AURIA, R. & REVAH, S. 2005. Correlation of biological activity and reactor performance in biofiltration of toluene with the fungus *Paecilomyces variotii* CBS115145. *Applied and Environmental Microbiology,* 71**,** 4280-4285.

GERKE, J. 2018. Concepts and misconceptions of humic substances as the stable part of soil organic matter: A review. *Agronomy,* 8**,** 76.

GIENTKA, I., BZDUCHA-WRÓBEL, A., STASIAK-RÓŻAŃSKA, L., BEDNARSKA, A. A. & BŁAŻEJAK, S. 2016. The exopolysaccharides biosynthesis by *Candida* yeast depends on carbon sources. *Electronic Journal of Biotechnology,* 22**,** 31-37.

GIRARD, M., RAMIREZ, A. A., BUELNA, G. & HEITZ, M. 2011. Biofiltration of methane at low concentrations representative of the piggery industry-Influence of the methane and nitrogen concentrations. *Chemical Engineering Journal,* 168**,** 151-158.

HAARSTAD, K., BERGERSEN, O. & SORHEIM, R. 2006. Occurrence of carbon monoxide during organic waste degradation. *Journal of the Air & Waste Management Association,* 56**,** 575-580.

HELLEBRAND, H. J. & SCHADE, G. W. 2008. Carbon monoxide from composting due to thermal oxidation of biomass. *Journal of Environmental Quality,* 37**,** 592-598.

HILGER, H. A., CRANFORD, D. F. & BARLAZ, M. A. 2000. Methane oxidation and microbial exopolymer production in landfill cover soil. *Soil Biology & Biochemistry,* 32**,** 457-467.

HOFMANN, K., PAULI, H., PRAEG, N., WAGNER, A. O. & ILLMER, P. 2016. Methane-cycling microorganisms in soils of a high-alpine altitudinal gradient. *Fems Microbiology Ecology,* 92**,** 10.

HU, Q. Y., WANG, C. & HUANG, K. X. 2015. Biofiltration performance and characteristics of high-temperature gaseous benzene, hexane and toluene. *Chemical Engineering Journal,* 279**,** 689-695.

HWANG, Y., MATSUO, T., HANAKI, K. & SUZUKI, N. 1994. Removal of odorous compounds in waste-water by using activated carbon, ozonation and aerated biofilter. *Water Research,* 28**,** 2309-2319.

JARVIE, H. P., KING, S. M. & NEAL, C. 2017. Inorganic carbon dominates total dissolved carbon concentrations and fluxes in British rivers: Application of the THINCARB model – Thermodynamic modelling of inorganic carbon in freshwaters. *Science of The Total Environment,* 575**,** 496-512.

JIMENEZ, L., ARRIAGA, S. & AIZPURU, A. 2016. Assessing biofiltration repeatability: statistical comparison of two identical toluene removal systems. *Environmental Technology,* 37**,** 681-693.

JORIO, H., BIBEAU, L. & HEITZ, M. 2000. Biofiltration of air contaminated by styrene: Effect of nitrogen supply, gas flow rate, and inlet concentration. *Environmental Science & Technology,* 34**,** 1764-1771.

KIM, B. J., SUIDAN, M. T., ZHU, X. & ALONSO, C. 2001. A fundamental study of biofiltration processes for VOC removal from waste gas streams. ENGINEER RESEARCH AND DEVELOPMENT CENTER CHAMPAIGN IL CONSTRUCTION ENGINEERING RESEARCH LAB.

KIM, D., CAI, Z. G. & SORIAL, G. A. 2005a. Behavior of trickle-bed air biofilter for toluene removal: Effect of non-use periods. *Environmental Progress,* 24**,** 155-161.

KIM, D., CAI, Z. L. & SORIAL, G. A. 2005b. Impact of interchanging VOCs on the performance of trickle bed air biofilter. *Chemical Engineering Journal,* 113**,** 153-160.

KIM, T. G., LEE, E. H. & CHO, K. S. 2013. Effects of nonmethane volatile organic compounds on microbial community of methanotrophic biofilter. *Applied Microbiology and Biotechnology,* 97**,** 6549-6559.

KOLLING, K., MULLER, A., FLUTSCH, P. & ZEEMAN, S. C. 2013. A device for single leaf labelling with CO2 isotopes to study carbon allocation and partitioning in *Arabidopsis thaliana*. *Plant Methods,* 9.

KRISHNAKUMAR, B., HIMA, A. M. & HARIDAS, A. 2007. Biofiltration of toluene-contaminated air using an agro by-product-based filter bed. *Applied Microbiology and Biotechnology,* 74**,** 215-220.

LEBRERO, R., LOPEZ, J. C., LEHTINEN, I., PEREZ, R., QUIJANO, G. & MUNOZ, R. 2016. Exploring the potential of fungi for methane abatement: Performance evaluation of a fungal-bacterial biofilter. *Chemosphere,* 144**,** 97-106.

LEILI, M., FARJADFARD, S., SORIAL, G. A. & RAMAVANDI, B. 2017. Simultaneous biofiltration of BTEX and Hg° from a petrochemical waste stream. *Journal of Environmental Management,* 204**,** 531-539.

LENNON, J. T. & LEHMKUHL, B. K. 2016. A trait-based approach to bacterial biofilms in soil. *Environmental Microbiology,* 18**,** 2732-2742.

LI, G. W., HU, H. Y., HAO, J. M. & FUJIE, K. 2002. Use of biological activated carbon to treat mixed gas of toluene and benzene in biofilter. *Environmental Technology,* 23**,** 467-477.

LIMBRI, H., GUNAWAN, C., THOMAS, T., SMITH, A., SCOTT, J. & ROSCHE, B. 2014. Coal-packed methane biofilter for mitigation of green house gas emissions from coal mine ventilation air. *Plos One,* 9.

LUO, J. & AGNEW, M. P. 2001. Gas characteristics before and after biofiltration treating odorous emissions from animal rendering processes. *Environmental Technology,* 22**,** 1091-1103.

MAUCLAIRE, L., SCHURMANN, A., THULLNER, M., GAMMETER, S. & ZEYER, J. 2004. Sand filtration in a water treatment plant: biological parameters responsible for clogging. *Journal of Water Supply Research and Technology-Aqua,* 53**,** 93-108.

MENARD, C., RAMIREZ, A. A. & HEITZ, M. 2014. Kinetics of simultaneous methane and toluene biofiltration in an inert packed bed. *Journal of Chemical Technology and Biotechnology,* 89**,** 597-602.

MENEY, K. M., DAVIDSON, C. M. & LITTLEJOHN, D. 1998. Use of solid-phase extraction in the determination of benzene, toluene, ethylbenzene, xylene and cumene in spiked soil and investigation of soil spiking methods. *Analyst,* 123**,** 195-200.

METRIS, A., GERRARD, A. M., CUMMING, R. H., WEIGNER, P. & PACA, J. 2001. Modelling shock loadings and starvation in the biofiltration of toluene and xylene. *Journal of Chemical Technology and Biotechnology,* 76**,** 565-572.

MILNE, G. L. & MORROW, J. D. 2009. Chapter 5 - Measurement of Biological Materials. *Clinical and Translational Science.* San Diego: Academic Press.

MORALES, M., REVAH, S. & AURIA, R. 1998. Start-up and the effect of gaseous ammonia additions on a biofilter for the elimination of toluene vapors. *Biotechnology and Bioengineering,* 60**,** 483-491.

NIKIEMA, J. & HEITZ, M. 2010. The use of inorganic packing materials during methane biofiltration. *International Journal of Chemical Engineering,* 2010.

OZIS, F., BINA, A. & DEVINNY, J. S. 2007. Biofilm growth-percolation models and channeling in biofilter clogging. *Journal of the Air & Waste Management Association,* 57**,** 882-892.

POEPLAU, C., ERIKSSON, J. & KÄTTERER, T. 2015. Estimating residual water content in air-dried soil from organic carbon and clay content. *Soil and Tillage Research,* 145**,** 181-183.

SAMUELSSON, R., BURVALL, J. & JIRJIS, R. 2006. Comparison of different methods for the determination of moisture content in biomass. *Biomass & Bioenergy,* 30**,** 929-934.

SCHIMEL, J. P., GULLEDGE, J. M., CLEIN-CURLEY, J. S., LINDSTROM, J. E. & BRADDOCK, J. F. 1999. Moisture effects on microbial activity and community structure in decomposing birch litter in the Alaskan taiga. *Soil Biology and Biochemistry,* 31**,** 831-838.

SONG, J. H. & KINNEY, K. A. 2000. Effect of vapor-phase bioreactor operation on biomass accumulation, distribution, and activity: Linking biofilm properties to bioreactor performance. *Biotechnology and Bioengineering,* 68**,** 508-516.

STANGELAND, K., KALAI, D., LI, H. L. & YU, Z. X. 2017. CO2 methanation: the effect of catalysts and reaction conditions. *In:* YAN, J., SUN, F., CHOU, S. K., DESIDERI, U., LI, H., CAMPANA, P. & XIONG, R. (eds.) *8th International Conference on Applied Energy.* Amsterdam: Elsevier Science Bv.

SUMMERFELT, S. T. & SHARRER, M. J. 2004. Design implication of carbon dioxide production within biofilters contained in recirculating salmonid culture systems. *Aquacultural Engineering,* 32**,** 171-182.

SUTHERLAND, I. W. 2001. The biofilm matrix – an immobilized but dynamic microbial environment. *Trends in Microbiology,* 9**,** 222-227.

SYED, R., SAGGAR, S., TATE, K. & REHM, B. H. A. 2016. Does acidification of a soil biofilter compromise its methane-oxidising capacity? *Biology and Fertility of Soils,* 52**,** 573-583.

TORKIAN, A., DEHGHANZADEH, R. & HAKIMJAVADI, M. 2003. Biodegradation of aromatic hydrocarbons in a compost biofilter. *Journal of Chemical Technology and Biotechnology,* 78**,** 795-801.

WAKELIN, S. A., PAGE, D. W., PAVELIC, P., GREGG, A. L. & DILLON, P. J. 2010. Rich microbial communities inhabit water treatment biofilters and are differentially affected by filter type and sampling depth. *Water Science and Technology: Water Supply,* 10**,** 145-156.

WANG, C., KONG, X. & ZHANG, X. Y. 2012. Mesophilic and thermophilic biofiltration of gaseous toluene in a long-term operation: performance evaluation, biomass accumulation, mass balance analysis and isolation identification. *Journal of Hazard Mater,* 229-230**,** 94-9.

WIECZOREK, A. 2005. Pilot-scale biofiltration of waste gases containing aliphatic and aromatic hydrocarbons, phenol, cresols, and other volatile organic compounds. *Environmental Progress,* 24**,** 60-66.

XI, J., HU, H.-Y. & QIAN, Y. 2006. Effect of operating conditions on long-term performance of a biofilter treating gaseous toluene: Biomass accumulation and stable-run time estimation. *Biochemical Engineering Journal,* 31**,** 165-172.

XI, J. Y., SAINGAM, P., GU, F., HU, H. Y. & ZHAO, X. F. 2016. Effect of continuous ozone injection on performance and biomass accumulation of biofilters treating gaseous toluene *Applied Microbiology and Biotechnology,* 100**,** 3385-3385.

ZHAO, X. H., DENG, H. Z., WANG, W. K., HAN, F., LI, C. R., ZHANG, H. & DAI, Z. X. 2017. Impact of naturally leaking carbon dioxide on soil properties and ecosystems in the Qinghai-Tibet plateau. *Scientific Reports,* 7.

ZHU, Y. Z., LI, S. Y., LUO, Y. M., MA, H. Y. & WANG, Y. 2016. A biofilter for treating toluene vapors: performance evaluation and microbial counts behavior. *Peerj,* 4.

# Chapter 5: The biodegradation of toluene in a soil biofilter

## 5.1 Introduction

Bordoloi et al. (2019) used a differential reactor which allowed rigorous control of environmental parameters on toluene degradation. Their study focused on the interactions between: temperature (20 $^{o}$C, 30 $^{o}$C, 40 $^{o}$C), matric potential (-10 $cm_{H_2O}$, -100 $cm_{H_2O}$) and residual toluene concentration (the toluene concentration in the headspace of the gas chamber) (18 – 180 ppm) on the removal rates and $CO_2$ mineralization in a soil-based biofilter. Their results showed that highest %$CO_2$ mineralization (91%) was found at lowest residual concentration (18 ppm) and wet condition (-10 $cm_{H_2O}$) whereas only 50% $CO_2$ mineralization was recorded at higher residual concentration of 100 ppm and drier condition (-100 $cm_{H_2O}$). The temperature had no influence on the %$CO_2$ recovery but had 5 and 10 times more influence than the matric potential and residual concentration on the EC, respectively.

Based on the findings of Bordoloi et al. (2019), two hypotheses were developed. The first hypothesis was that starting the biofilter at higher temperatures would result in a higher EC but make no difference to %$CO_2$ mineralization than when starting at lower temperatures. The second hypothesis was operating the biofilter at a lower residual concentration and wetter conditions would result in a higher %$CO_2$ mineralization than operating at higher residual concentration and drier conditions. The aim of this study was to conduct experiments with multiple bed material and various operational parameters so that these hypotheses could be explored. In testing hypothesis 1, the biofilters were operated at temperatures of 30 $^{o}$C and 40 $^{o}$C. Meanwhile, testing hypothesis 2 involved operating the biofilters at two different conditions: Condition A (a low residual concentration generated by an inlet load of 78 $g \cdot m^{-3} \cdot h^{-1}$, -10 $cm_{H_2O}$) and Condition B (a high residual concentration generated by an inlet load

of 137 $g \cdot m^{-3} \cdot h^{-1}$, -100 $cm_{H_2O}$). In addition, preliminary results of microbial community analysis from 10 soil samples were presented in order to link the performance of the biofilter with the prevalent microorganisms in the system.

## 5.2 Experimental design

### 5.2.1 Impact of temperature and soil type

Initially, operating temperature (30 ± 0.1 $^oC$ and 40 ± 0.1 $^oC$) and soil type (Soil 1, Soil 2 and Soil 3 as described in Section 3.1) were chosen as the factors. The soil biofilters were fed with a toluene loading rate of 157 $g \cdot m^{-3} \cdot h^{-1}$ at 25 ± 0.1 $ml \cdot min^{-1}$ and the soil was maintained at -10 $cm_{H_2O}$ matric potential. The system was operated at an initial pH of 7 ± 0.1. Each treatment was performed in duplicate.

### 5.2.2 Impact of operating conditions and soil type

In the second part of the study, matric potential and residual concentration (i.e. a function of inlet load) were combined thereby constituting the operating conditions of the biofilter. Matric potential had two levels: -10 $cm_{H_2O}$ (wet condition) and -100 $cm_{H_2O}$ (dry condition). The toluene inlet load had two levels: 78 $g \cdot m^{-3} \cdot h^{-1}$ and 137 $g \cdot m^{-3} \cdot h^{-1}$ generated by an inlet concentration of 50 ± 3 ppm & a gas flow rate of 50 ± 0.1 $ml \cdot min^{-1}$ and an inlet concentration of 175 ± 5 ppm & a gas flow rate of 25 ± 0.1 $ml \cdot min^{-1}$, respectively. These values of inlet concentration were close to the lowest (75 ppm) and highest inlet concentration (200 ppm) selected by Bordoloi et al. (2019). These inlet loads resulted in two levels of residual concentration: low and high.

Combining the inlet load with the matric potential resulted to two sets of condition: Condition A (a low residual concentration generated by an inlet load of 78 $g \cdot m^{-3} \cdot h^{-1}$, -10 $cm_{H_2O}$) and Condition B (a high residual concentration generated by an inlet load of 137 $g \cdot m^{-3} \cdot h^{-1}$, -100

$cm_{H_2O}$). These conditions were then crossed with soil type (Soil 1, Soil 2 and Soil 3) giving a total of six treatment combinations (2 x 3). Each treatment combination was performed in triplicate while maintaining the temperature of the reactor box at 40 ± 0.1 $^oC$ and the pH of the buffer solution at 7.0 ± 0.1 in all the experiments.

## 5.3 Results and discussions

### 5.3.1 Characteristics of the different soil types

The physico-chemical characteristics of the different types of soil used in this study were determined as additional information to help understand the performance of the biofilter. Three parameters were examined: pH, gravimetric water content and C/N ratio (Table 5.1). In general, the pH of the soil samples was relatively neutral, ranging from 6.8 to 7.2 which is a suitable condition for most bacterial activity (Maier and Pepper, 2009).

Regarding the elementary composition, Soil 1 has the highest content of carbon and nitrogen (14.4% and 1.08%, respectively). However, the C/N ratio (13.33) of Soil 1 was relatively lower than that of the Soil 3 (14). Soil 2 has the lowest content of carbon and nitrogen (1.87% and 0.17%, respectively).

Table 5.1: Physical properties and C/N ratios of soil types.

| Soil type | pH | C (%, dry weight basis) | N (%, dry weight basis) | C/N mass ratio |
|---|---|---|---|---|
| Soil 1 | 7.11 ± 0.06 | 14.4 | 1.08 | 13.33 |
| Soil 2 | 6.95 ± 0.09 | 1.87 | 0.17 | 11 |
| Soil 3 | 7.03 ± 0.04 | 9.1 | 0.65 | 14 |

The gravimetric water content was not directly measured in this study. The gravimetric water content was determined using its relationship with matric potential, commonly referred to soil moisture release curve. Literature revealed that the soil moisture release curve depends

on the soil types, i.e. soil texture, pore size distribution and structure (Madi et al., 2018, Ghezzehei et al., 2019). In this study, the soil moisture release curves were determined for all three soil types (Figure 5.1).

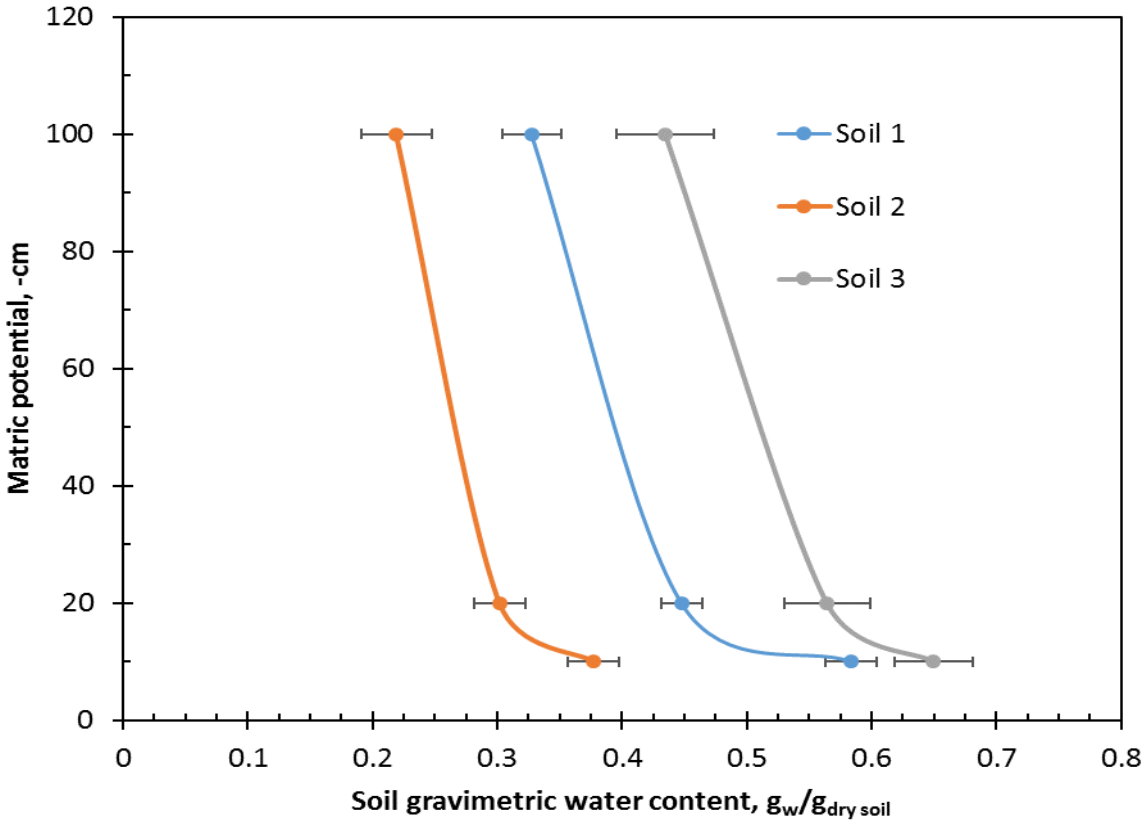


Figure 5.1: The relationship between gravimetric water content and water potential for all three fresh soil samples. The values are the mean under equilibrium conditions. The error bars are the standard deviation from triplicate soil samples.

The results clearly indicate the differences in the water availability in three soil samples. The results demonstrated that at the same levels of matric potential, Soil 3 had the highest gravimetric water content (0.65 ± 0.03 $g_w/g_{dry\ soil}$ at -10 $cm_{H_2O}$ and 0.43 ± 0.04 $g_w/g_{dry\ soil}$ at -100 $cm_{H_2O}$) whereas Soil 2 had the lowest gravimetric water content (0.37 ± 0.02 $g_w/g_{dry\ soil}$ at -10 $cm_{H_2O}$ and 0.22 ± 0.03 $g_w/g_{dry\ soil}$ at -100 $cm_{H_2O}$). Notably for each soil sample, the

gravimetric water content was shown to be significantly higher in -10 $cm_{H_2O}$ than in -100 $cm_{H_2O}$ (Table 5.2).

Table 5.2: t-test results (two tailed, $\alpha = 0.05$) comparing the mean of gravimetric water content at -10 $cm_{H_2O}$ and -100 $cm_{H_2O}$ for each soil sample.

| **Soil** | **-10 $cm_{H_2O}$ vs -100 $cm_{H_2O}$, *p* value** |
|---|---|
| Soil 1 | 0.009 |
| Soil 2 | 0.03 |
| Soil 3 | 0.006 |

### 5.3.2 Impact of temperature and soil type on $\%CO_2$ recovery

The impact of temperature and soil type on $\%CO_2$ recovery was studied by comparing the mean $\%CO_2$ recovery of reactors packed with different soil types (Soil 1, Soil 2 and Soil 3) and operated at different temperatures (30 $^oC$ and 40 $^oC$) (Figure 5.2). The highest mean $\%CO_2$ recovery of 54 ± 4% was observed in Soil 1 at 40 $^oC$. At 30 $^oC$, a similar mean $\%CO_2$ recovery of 41 ± 2% was recorded in all three soil samples.

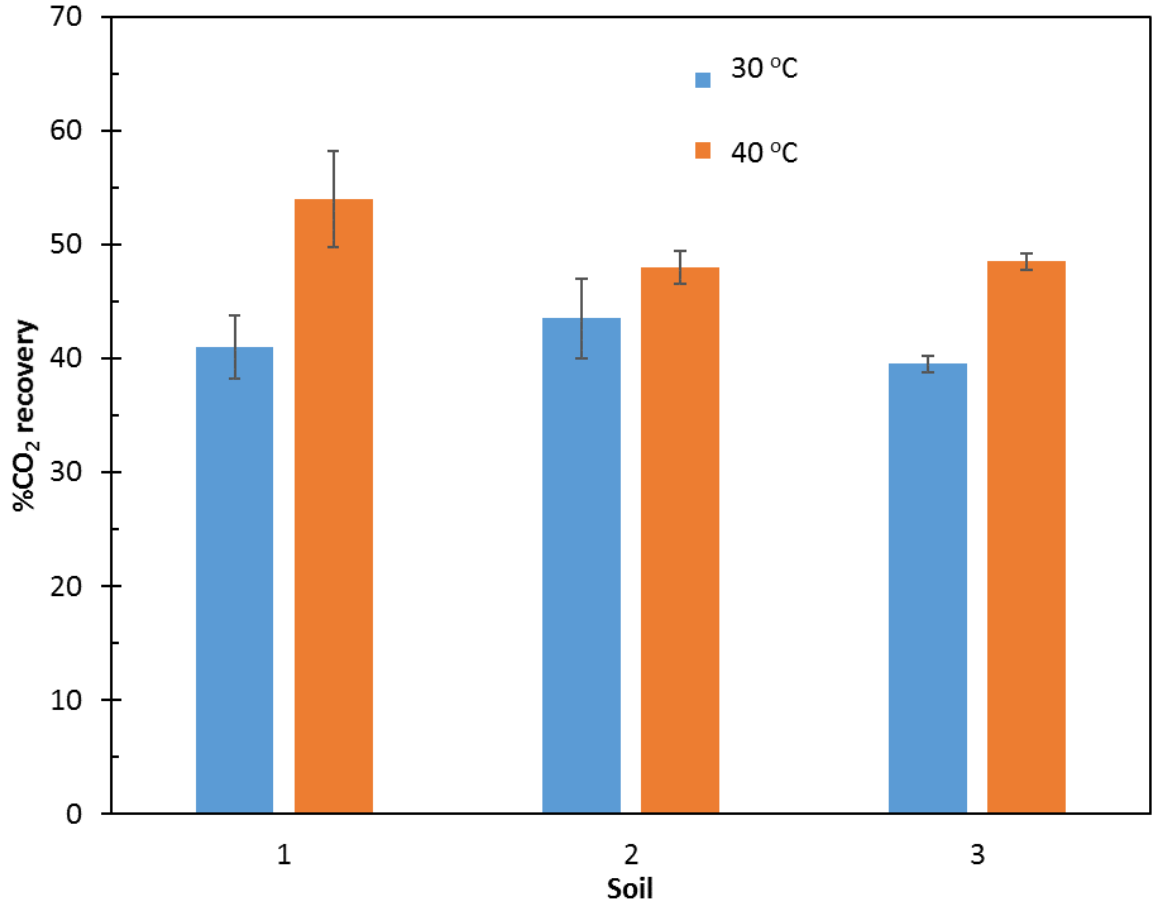


Figure 5.2: $\%CO_2$ recovery of soil samples operating at 30 °C and 40 °C. Values are the mean at steady state at a given set of conditions. The error bars reported the standard deviation from duplicate experiments with toluene as the pollutant.

ANOVA test results shows that there was a significant difference in $\%CO_2$ recovery between the biofilters operated at two different temperatures ($\rho < 0.01$) but no significant difference observed among the soil types used as packing materials ($\rho = 0.25$) (Table 5.3). The temperature had the strongest effect ($\eta^2 = 0.7$) on the $\%CO_2$ recovery. The interaction between soil type and operating temperature did not have a significant effect on $\%CO_2$ recovery ($\rho = 0.15$).

Post-hoc Tukey Honest Significant (HSD) ($\alpha = 0.05$) was carried out to evaluate the effect of the operating temperature. The test revealed a significant difference ($p_{adj} = 0.001$) between

the $\%CO_2$ recovery of biofilters operated at 30 $^oC$ and 40 $^oC$. This difference was shown as the 20% increase in $\%CO_2$ recovery from 41 ± 3% (at 30 $^oC$) to 50 ± 4% (at 40 $^oC$).

Table 5.3: Summary of ANOVA results for $\%CO_2$ recovery as a function of temperature and soil types.

| | **DF** | **Sum of Squares** | **Mean of Squares** | **F value** | ***p* value** | **$\eta^2$** |
|---|---|---|---|---|---|---|
| **Soil** | 2 | 24.5 | 12.25 | 1.771 | 0.25 | 0.07 |
| **Temperature** | 1 | 234.08 | 234.08 | 33.843 | < 0.01 | 0.70 |
| **Soil x Condition** | 2 | 36.17 | 18.08 | 2.614 | 0.15 | 0.47 |
| **Residuals** | 6 | 41.5 | 6.92 | | | |

These results agreed with previously reported $\%CO_2$ trends in the literature where $\%CO_2$ recovery increased at higher operating temperatures. The amount of toluene converted to $CO_2$ tripled when temperature increased from 11 $^oC$ to 25 $^oC$ (Armstrong et al., 1991). Lu et al. (1999) found that $\%CO_2$ from BTEX degradation increased 20% as the operating temperature increased from 15 $^oC$ to 30 $^oC$. Cox et al. (2001) found that the biotrickling filter operated at 53 $^oC$ had higher mineralization of ethanol (60%) than when operated at ambient temperature (20 – 30 $^oC$) (46%). Wang et al. (2012) observed a decrease in $\%CO_2$ recovery from 69% to 53% after the temperature dropped from 55 $^oC$ to ambient (20 – 25 $^oC$) in the degradation of toluene.

A similar trend was observed by Bordoloi et al. (2019) for Soil 1. They found the $\%CO_2$ recovery significantly dropped from 80% to 60% as the operating temperature decreased from 40 $^oC$ to 30 $^oC$. In the current work, Soil 1 had slightly lower values (39% – 57%) for $\%CO_2$ recovery than that of Bordoloi et al. (2019). The operating conditions were similar in both studies except the

residual concentration in current study (120 ppm) was twice that of Bordoloi et al. (2019) (50 ppm). It suggested that exposure to the high toluene concentration (> 100 ppm) led to a lower fraction of toluene mineralized to $CO_2$, which was in agreement with the findings of Bordoloi and Gostomski (2019). These results indicated that at high temperature, the degraded carbon was converted to $CO_2$ rather than being incorporated to cells as biomass.

### 5.3.3 Impact of temperature and soil type on biofilter elimination capacity

The EC for the biofilters was shown as a function of operating temperature (30 $^oC$, 40 $^oC$) and soil type (Soil 1, Soil 2 and Soil 3) (Figure 5.3). At 40 $^oC$, Soil 1 had the highest mean EC of 73.5 ± 4.9 $g \cdot m^{-3} \cdot h^{-1}$ whereas the lowest mean EC of 35.5 ± 4.9 $g \cdot m^{-3} \cdot h^{-1}$ was found in Soil 2. At 30 $^oC$, Soil 1 showed the best performance among of the soil samples, with the EC of 59.5 ± 3.5 $g \cdot m^{-3} \cdot h^{-1}$.

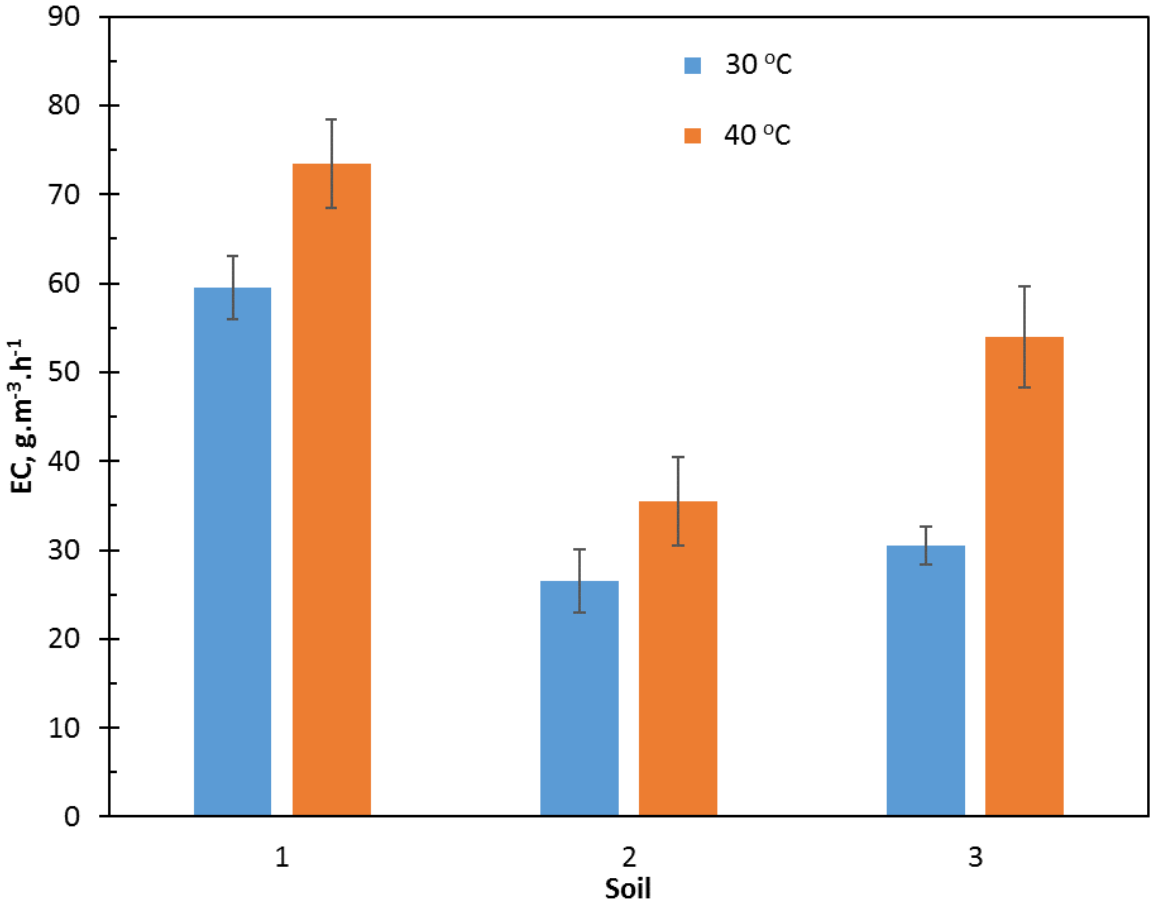


Figure 5.3: Toluene elimination capacity of soil samples operating at 30 °C and 40 °C. Values are the mean at steady state at a given set of conditions. The error bars are the standard deviation from duplicate experiments.

ANOVA analysis indicated that that there was a significant difference in EC of the biofilters operated at different temperatures ($\rho < 0.01$) and with different soil types ($\rho < 0.01$). The temperature had the stronger effect ($\eta^2 = 0.74$) on the EC than the soil type ($\eta^2 = 0.20$) (Table 5.4). However, the interaction between soil type and operating conditions was not significant with $\rho = 0.13$.

Table 5.4: Summary of ANOVA results for EC ($g \cdot m^{-3} \cdot h^{-1}$) as a function of temperature and soil types.

| | DF | Sum of Squares | Mean of Squares | F value | *p* value | $\eta^2$ |
|---|---|---|---|---|---|---|
| **Soil** | 2 | 2633.2 | 1316.6 | 71.49 | <0.01 | 0.74 |
| **Temperature** | 1 | 720.7 | 720.7 | 39.14 | < 0.01 | 0.20 |
| **Soil x Condition** | 2 | 108.5 | 54.3 | 2.95 | 0.13 | 0.03 |
| **Residuals** | 6 | 110.5 | 18.4 | | | |

Tukey HSD mean EC values showed significant differences ($p_{adj} < 0.05$) between 30 $^oC$ and 40 $^oC$. The mean EC increased with increasing the operating temperature from 30 $^oC$ to 40 $^oC$. The greatest change of EC in the experiments was observed in Soil 3, from 30.5 ± 2.1 to 54 ± 5.7 $g \cdot m^{-3} \cdot h^{-1}$ (40% increase). The EC of Soil 1 and Soil 2 increased 25%, from 59.5 ± 3.5 to 73.5 ± 4.9 $g \cdot m^{-3} \cdot h^{-1}$ and 26.5 ± 3.5 $g \cdot m^{-3} \cdot h^{-1}$ to 35.5 ± 4.9 $g \cdot m^{-3} \cdot h^{-1}$ respectively.

Pairwise comparisons of mean EC showed that there was significant difference between the three soil samples, $p_{adj} < 0.05$ (Table 5.5). The highest mean EC of 66.5 ± 8.8 $g \cdot m^{-3} \cdot h^{-1}$ was recorded in Soil 1 whereas lowest mean EC of 31 ± 6.3 $g \cdot m^{-3} \cdot h^{-1}$ was observed in Soil 2, when averaged across temperatures.

Table 5.5: Summary of pairwise results comparing mean EC between temperature and between soil samples.

| Main effect | $p_{adj}$ value |
|---|---|
| **Conditions** | |
| 30 °C – 40 °C | < 0.01 |
| **Soil** | |
| Soil 2 – Soil 1 | < 0.01 |
| Soil 3 – Soil 1 | < 0.01 |
| Soil 3 – Soil 2 | 0.02 |

The results were similar with other biofilter studies where the EC increased with increase in operating temperature. Kiared et al. (1997) reported a range of bed temperatures between 25 °C and 40 °C, with a maximum toluene EC at 40 °C. At 30 °C, the toluene elimination capacity was half that observed at 40 °C. At a toluene inlet concentration of 1000 ppm, Park et al. (2002) obtained a reduction of 50% in toluene removal, from EC of 80 $g \cdot m^{-3} \cdot h^{-1}$ at 35 °C to EC of 40 $g \cdot m^{-3} \cdot h^{-1}$ at 25 °C. Though experiments were conducted in variable operating parameters (flowrate, inlet load) and temperature was not controlled, Vergara-Fernández et al. (2007) observed the similar trend of increasing the temperature of the bed medium resulted in the increasing the EC. Likewise, increasing the temperature from 30.5 °C to 34 °C produced a two-fold increase in the EC.

The optimum temperature range for toluene degraders is 20 – 35 °C (Mohammad et al., 2007, Alvarez-Hornos et al., 2008, Vergara-Fernández et al., 2007). Deeb and Alvarez-Cohen (1999) found the toluene degradation rate peaked at 35 °C, dropped sharply at 40 °C and was almost inhibited above 45 °C. Lee et al. (2002) observed the degradation rate of toluene at 40 °C was

83% of the maximum rate which was obtained at 30 °C (2.38 µmol·$g^{-1}$-DCW·$h^{-1}$). Beuger and Gostomski (2009) investigated a range between 14 and 60 °C, with an optimum at 35 °C. At 60 °C, they did see a 15-fold reduction in the toluene degradation rate, from 75 g·$m^{-3}$·$h^{-1}$ (at 35 °C) to 5 g·$m^{-3}$·$h^{-1}$.

In this study, a higher EC was observed at 40 °C than at 30 °C for all soil samples, suggesting that the optimum temperature might fall outside of the common range. It can be attributed to the combined effect of other parameters interacting in driving the performance. This study used soil (mixed cultures) as the bed medium with no nutrient addition (non-growth) while all the other toluene biofilter studies provided a growth system by providing nutrients (Mohammad et al., 2007, Vergara-Fernández et al., 2007, Alvarez-Hornos et al., 2008) and/or pure culture (Deeb and Alvarez-Cohen, 1999, Lee et al., 2002), which could have caused the difference.

### 5.3.4 Impact of operating conditions and soil type on %$CO_2$ recovery

The impact of environmental conditions and soil type on %$CO_2$ recovery were studied by comparing the mean %$CO_2$ recovery of reactors packed with different soil types (Soil 1, Soil 2 and Soil 3) and operated at different conditions: Condition A (a low residual concentration generated by an inlet load of 78 g·$m^{-3}$·$h^{-1}$, -10 $cm_{H_2O}$) and Condition B (a high residual concentration generated by an inlet load of 137 g·$m^{-3}$·$h^{-1}$, -100 $cm_{H_2O}$) (Figure 5.4). The lowest mean %$CO_2$ recovery of 33 ± 4.4% was recorded for Soil 2 at Condition B. At Condition A, %$CO_2$ recovery of 48 ± 3.8% was observed in three soil samples.

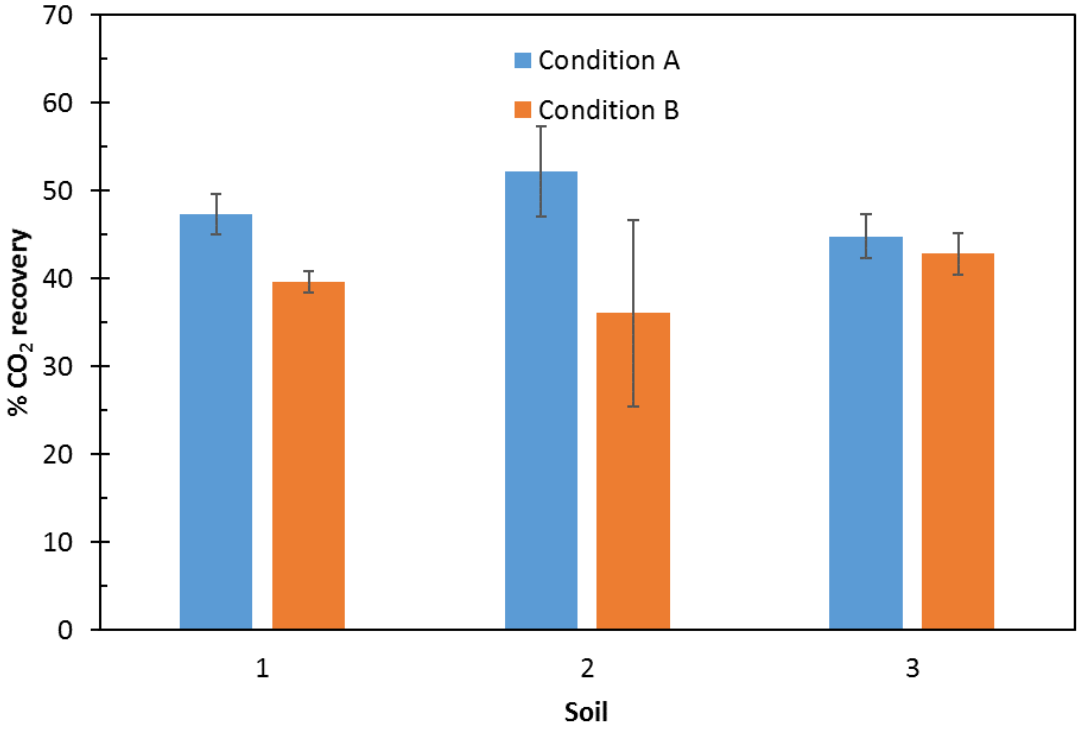


Figure 5.4: $\%CO_2$ recovery of soil samples operating at Condition A and Condition B. Values are the mean at steady state period at a given set of conditions. The error bars are the standard deviation from triplicate experiments.

Mean $CO_2$ recoveries were compared using the ANOVA test between three soils and two conditions (Table 5.6). The results showed that there was a significant difference in $\%CO_2$ recovery between operating conditions ($\rho < 0.01$) but no significant difference among the soil types ($\rho = 0.98$). The interaction between soil type and conditions was not significant ($p = 0.1$). When comparing $\eta^2$ values, conditions ($\eta^2 = 0.41$) had the strongest effect on the $\%CO_2$ recovery. Tukey HSD mean $\%CO_2$ values showed significant differences ($\rho < 0.01$) between Condition A and Condition B.

The mean $\%CO_2$ recorded at Condition A was 20% higher than at Condition B. The lower $\%CO_2$ recovery at Condition B demonstrated that a higher amount of carbon source was incorporated into biomass instead of oxidising toluene to $CO_2$. Probably the residual toluene

concentrations and moisture content maintained during the steady state operation were less favourable for the development of toluene degraders that required lower residual concentrations (< 40 ppm) and wetter conditions (-10 cm $cm_{H_2O}$) for biomass maintenance.

Table 5.6: Summary of ANOVA results for $\%CO_2$ recovery as a function of operating conditions and soil type.

| | **DF** | **Sum of Squares** | **Mean of Squares** | **F value** | ***p* value** | **$\eta^2$** |
|---|---|---|---|---|---|---|
| **Soil** | 2 | 1 | 0.5 | 0.02 | 0.98 | <0.01 |
| **Condition** | 1 | 329.4 | 329.4 | 12.54 | < 0.01 | 0.41 |
| **Soil x Condition** | 2 | 148.8 | 74.4 | 2.83 | 0.1 | 0.19 |
| **Residuals** | 12 | 315.3 | 26.3 | | | |

There was a lack of studies investigating the impact of both water potential/water content and residual concentration on $\%CO_2$ recovery in biofilters. When separating the environmental parameters, there was no clear trend between water content and $\%CO_2$ recovery. Auria et al. (1998) observed a threefold decrease in $\%CO_2$ recovery (70% to 20%) when reducing the water content of the filter bed from 70% w/w to 49% w/w. The water content restoration from 26% w/w (wet weight basis) to approximately 65% w/w by adding water and homogenization of the filter bed resulted in an increase of the $\%CO_2$ recovery, from 48% to 64%. Contradictory findings were reported by Sakuma et al. (2009) where there was no statistical differences in $\%CO_2$ recovery between a control biofilter and a biofilter with additional irrigation system (wetter conditions).

Studies published in the literature rarely mentioned the impact of residual concentration/outlet concentration to $\%CO_2$ recovery as they were often implicit in the inlet

concentration/inlet loading. The most relevant comprehensive study was Bordoloi and Gostomski (2019). They found that a soil biofilter exposed to a lower residual concentration resulted in a higher $CO_2$ recovery. The highest $\%CO_2$ recovery of 92% was recorded at the residual concentration of 20 ppm whereas at the residual concentration of 140 ppm, the percentage $CO_2$ recovery was only 60%.

Literature revealed that $\%CO_2$ recovery varied depending on operating mode, filter materials, operating parameters and the presence of suitable microorganisms (Table 4.2). In the current work, the $\%CO_2$ conversion (29 – 58%) was slightly lower than the range usually observed in the literature (40 – 90%) (Table 4.2). The $\%CO_2$ recovery results at conditions similar to Condition A (43 – 58 %) were reported in a few studies (Morales et al., 1998, Song and Kinney, 2000, Krishnakumar et al., 2007, Leili et al., 2017). However, there was a lack of studies at conditions similar to Condition B at drier soil and higher residual concentration, which had the lowest $\%CO_2$ (30 – 40%).

Bordoloi et al. (2019) used Soil 1 as a bed medium in their study. They observed a 50% conversion of toluene to $CO_2$ under Condition B, which was slightly higher than the current study (40%). However, the $\%CO_2$ conversion at Condition A (80 – 90%) was almost double the current study (47.6 ± 2%). The operating conditions were similar in both studies (residual concentration of 20 ppm, water potential of -10 $cm_{H_2O}$, operating temperature of 40 $^oC$) except the initial pH in Bordoloi et al. (2019) study was at 7.4 while in current study was at 7.0 ± 0.1. A reactor was operated under similar operating conditions (pH = 7.4) to Bordoloi et al. (2019) to confirm whether the pH values during operation affected the $\%CO_2$ formation. The $\%CO_2$ formation for this experiment was 60%, which was higher than the 48% at Condition A (pH = 7.0 ± 0.1) but still lower than the earlier work (80 – 90%). The possibility of dissolved $CO_2$ affecting the pH was eliminated since the pH remained constant (7.0 ± 0.1). This implied that

the pH values in the examined range (pH = 7.0 vs pH = 7.4) could be one reason for the different $\%CO_2$ recovery. Further study is required to determine the impact of the pH to the $CO_2$ mineralization rate in the differential biofilter.

### 5.3.5 Impact of operating conditions and soil type on biofilter elimination capacity

In this study, operating conditions were the combination of matric potential and residual concentration. Since the residual concentration in this study is the function of the inlet feed, the desired low and high values of residual concentration were achieved by using two levels of inlet load: 78 $g \cdot m^{-3} \cdot h^{-1}$ and 137 $g \cdot m^{-3} \cdot h^{-1}$, respectively. At inlet load of 78 $g \cdot m^{-3} \cdot h^{-1}$ and at -10 $cm_{H_2O}$, the residual concentrations generated were: 12 ± 6.6 ppm; 34 ± 14.9 ppm and 15 ± 1.5 ppm for Soil 1, Soil 2 and Soil 3, respectively (Figure 5.5). At high inlet load of 137 $g \cdot m^{-3} \cdot h^{-1}$ and at -100 $cm_{H_2O}$, the residual concentrations generated were: 120 ± 3.6 ppm; 141 ± 5.1 ppm and 124 ± 8.8 ppm for Soil 1, Soil 2 and Soil 3, respectively.

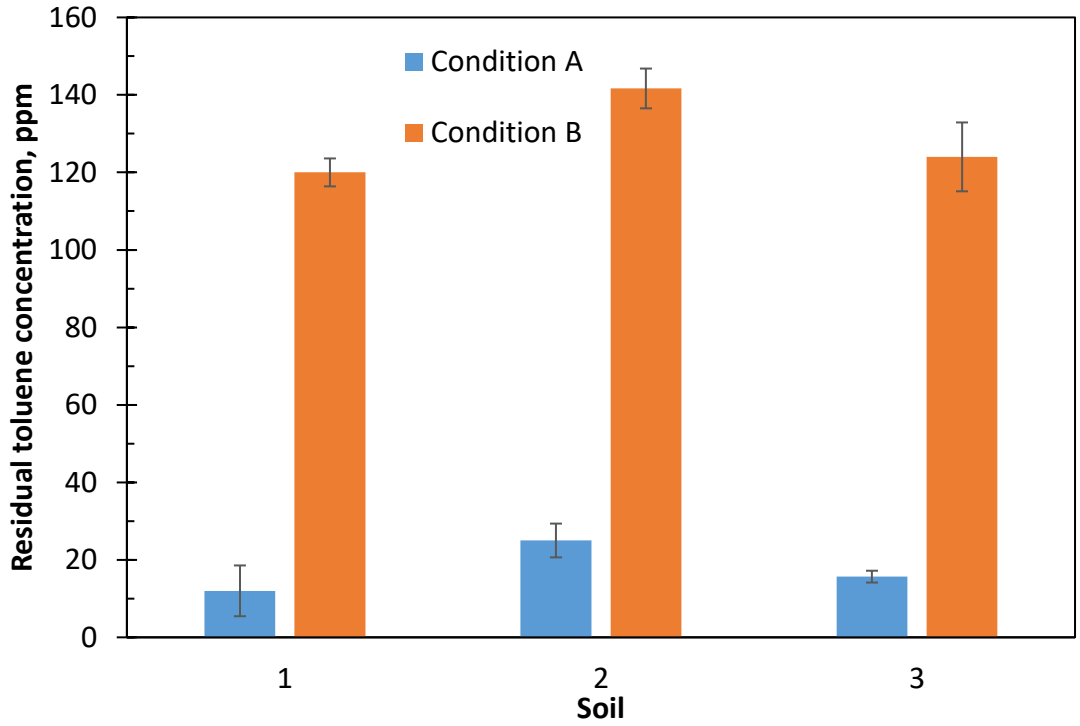


Figure 5.5: Residual toluene concentration of soil samples operating at Condition A and Condition B. Values are the mean at steady state at a given set of conditions. The error bars are the standard deviation from triplicate experiments.

Given these residual concentrations at varying inlet loads and matric potential, the resulting EC values were calculated. The EC for the biofilters was shown as a function of operating conditions (Condition A and Condition B) and soil type (Figure 5.6). The lowest mean EC of 37.3 ± 6.5 $g \cdot m^{-3} \cdot h^{-1}$ was recorded in Soil 2 at Condition A. It was similar with the average mean EC of three soil samples at Condition B (37 ± 5.3 $g \cdot m^{-3} \cdot h^{-1}$).

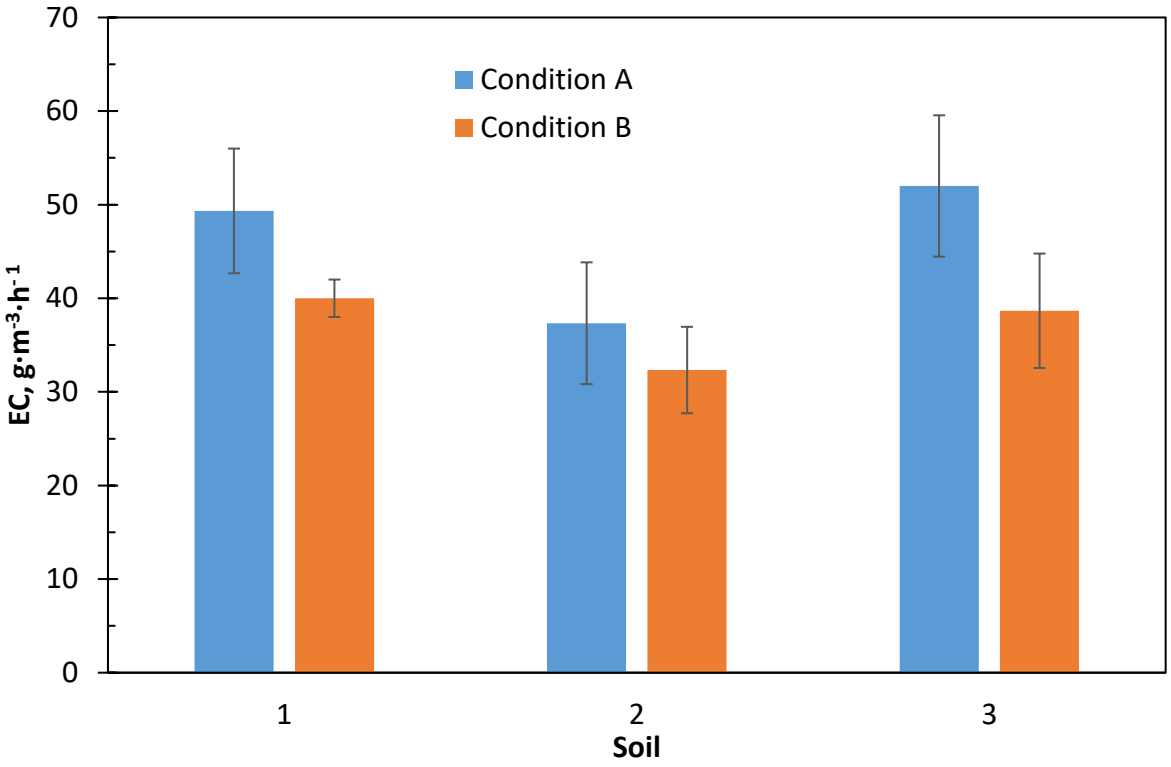


Figure 5.6: Toluene elimination capacity of soil samples operating at Condition A and Condition B. Values are the mean at steady state at a given set of conditions. The error bars reported are standard deviation from triplicate experiments.

The soil type ($p$ = 0.02) and operating conditions ($p$ < 0.01) had a significant impact on the EC (Table 5.7). The interaction between soil type and conditions was not significantly different with $p$ = 0.49 > 0.05. When comparing the $\eta^2$ value of the main effects, it was observed that the type of soils and conditions had similar effect on the EC ($\eta^2$ = 0.3).

Table 5.7: Summary of ANOVA results for EC as a function of operating conditions and soil type.

| | DF | Sum of Squares | Mean of Squares | F value | *p* value | $\eta^2$ |
|---|---|---|---|---|---|---|
| **Soil** | 2 | 414.8 | 207.4 | 6.03 | 0.02 | 0.33 |
| **Condition** | 1 | 382.7 | 382.7 | 11.13 | <0.01 | 0.30 |
| **Soil x Condition** | 2 | 52.1 | 26.1 | 0.76 | 0.49 | 0.04 |
| **Residuals** | 12 | 414.7 | 34.4 | | | |

Post-hoc Tukey Honest Significant (HSD) ($\alpha = 0.05$) was carried out to further evaluate the main effects (Table 5.8). Tukey HSD mean EC comparison showed significant differences ($p_{adj} < 0.01$) between the two conditions. The mean EC dropped ~20% by changing the operation from Condition A to Condition B. Pairwise comparisons were applied to determine the significant correlations between any two-soil samples. No significant difference was found between mean EC of Soil 1 and Soil 3 ($p_{adj} = 0.98 > 0.05$). The mean EC was significantly higher in Soil 1 and Soil 3 than in Soil 2 ($45 \pm 8$ g·m$^{-3}$·h$^{-1}$ vs $35 \pm 5.7$ g·m$^{-3}$·h$^{-1}$, $p_{adj} < 0.05$).

Table 5.8: Summary of pairwise results comparing mean EC between conditions and between soil samples.

| Main effect | $p_{adj}$ value |
|---|---|
| **Conditions** | |
| A – B | <0.01 |
| **Soil** | |
| Soil 2 – Soil 1 | 0.03 |
| Soil 3 – Soil 1 | 0.98 |
| Soil 3 – Soil 2 | 0.02 |

Based on the ANOVA and Tukey HSD analysis, it can be concluded that both type of soil and operating conditions had significant impact on the elimination of toluene. Soil 2 had the lowest mean EC in both conditions, which was less than 30% of the average mean EC in Soil 1 and Soil 3.

The mean EC increased 20% when operating the biofilters at high residual toluene concentrations and drier conditions (Condition D) as compared to the biofilters at lower residual concentrations and wetter conditions (Condition C). This could be due to the active microorganisms reduced their activity at dry conditions (lower matric potential) (Chowdhury et al., 2011, Manzoni et al., 2012) and/or the toxicity of toluene at high concentrations caused cell damage and eventually death (Alagappan and Cowan, 2003). It was unlikely the substrate inhibition occurred in the current residual toluene concentration range (120 – 150 ppm) as higher toluene concentrations (150 – 250 ppm) was fed to Soil 1 biofilters in previous studies (Detchanamurthy and Gostomski, 2015, Bordoloi et al., 2019) and Soil 2 biofilters in current study (Section 7.3.4) without substrate inhibition.

The ECs that contributed to Figure 5.6 varied between 27 $g \cdot m^{-3} \cdot h^{-1}$ and 60 $g \cdot m^{-3} \cdot h^{-1}$. Comparing the values with the $EC_{max}$ reported in the literature (Table 5.9) was difficult as the EC was dependent on the reactor configuration, packing material and operating conditions. Comprehensive studies by Detchanamurthy (2013) and Bordoloi et al. (2019) both used the differential biofilter packed with Soil 1. At residual toluene concentrations of 10 – 25 ppm and -10 $cm_{H_2O}$, Detchanamurthy (2013) obtained the EC values of 30 – 40 $g \cdot m^{-3} \cdot h^{-1}$. These were slightly lower than ECs of 45 – 57 $g \cdot m^{-3} \cdot h^{-1}$ obtained in this study at residual concentrations of 6 – 20 ppm and -10 $cm_{H_2O}$. Similar ECs of 45 – 50 $g \cdot m^{-3} \cdot h^{-1}$ were recorded by Bordoloi et al. (2019) at residual concentrations of 20 – 60 ppm. When exposed to residual concentrations of 80 – 100 ppm and -100 $cm_{H_2O}$, Bordoloi et al. (2019) found the ECs to be 20 – 30 $g \cdot m^{-3} \cdot h^{-1}$ which were lower than ECs (38 – 42 $g \cdot m^{-3} \cdot h^{-1}$) obtained at residual concentration of 117 – 124 ppm and -100 $cm_{H_2O}$.

Table 5.9: EC in toluene biofiltration systems reported in the literature.

| **Inlet load ($g \cdot m^{-3} \cdot h^{-1}$)** | **$EC_{max}$ ($g \cdot m^{-3} \cdot h^{-1}$)** | **References** |
|---|---|---|
| 1000 | 242 | Zilli et al. (2000) |
| 75 | 50 | Liu et al. (2002) |
| 65 | 55 | Delhoménie et al. (2002) |
| 90 | 85 | Moe and Li (2005) |
| 90 | 77 | Estevez et al. (2005) |
| 268 | 128 | Rene et al. (2005) |
| 328 | 342 | Singh et al. (2006) |
| 130 | 95 | Maestre et al. (2007) |
| 745 | 360 | Alvarez-Hornos et al. (2008) |
| 91 | 50 | Vigueras et al. (2008) |

| | | |
|---|---|---|
| 115 | 101 | Oh et al. (2009) |
| 1104 | 872 | Singh et al. (2010) |
| 100 | 85 | Palau et al. (2012) |
| 1280 | 595 | Dorado et al. (2012) |
| 272 | 114 | Chen et al. (2015) |
| 144 | 99 | Jimenez et al. (2016) |
| 114 | 93 | Rajamanickam and Baskaran (2017) |
| 160 | 78 | Mohammad et al. (2017) |
| 54 | 29 | Rene et al. (2018) |
| 99 | 96 | Malakar et al. (2018) |

The current findings were consistent with the trend observed in some previous studies. Sun et al. (2002) found that a reactor operated with drier packing materials (30% moisture content on a dry weight basis) and high pollutant concentration (~ 110 ppm) had poor capacity to degrade toluene in comparison with wetter packing materials (50% moisture content on a dry weight basis) and low pollutant concentration (~ 80 ppm). They recorded a two-fold decrease in toluene degradation rate, from 40 $g \cdot m^{-3} \cdot h^{-1}$ to 21 $g \cdot m^{-3} \cdot h^{-1}$.

Namkoong et al. (2004) used a compost biofilter (50% moisture content on a dry weight basis) to degrade gasoline vapor. At a gasoline total petroleum hydrocarbon (TPH) concentration of 2000 $mg \cdot m^{-3}$, 75% of the TPH was removed. When increasing the TPH concentration to above 3000 $mg \cdot m^{-3}$ and decreasing the compost moisture level to 37 – 47% (on a dry weight basis), the removal rate decreased dramatically, from 75% to 20%.

Alvarez-Hornos et al. (2008) found a higher fraction of dead bacterial (80 – 90%) in the first 25 cm of the bed height than in the rest of the 75 cm (60 – 75%) after 43 days continuously

feeding toluene at 145 ppm. Their explanation was that the upper zones were exposed to higher toluene concentrations and lower moisture content than the lower zones. However, no data was presented to support this explanation.

Contradictory trends were reported by Elmrini et al. (2004) and Znad et al. (2007). Elmrini et al. (2004) found that at a xylene loading rate of 12.8 $g \cdot m^{-3} \cdot h^{-1}$, the removal efficiency in the first section near the inlet feed (71.7%) was triple the second section (23.2%). Znad et al. (2007) reported the bottom section nearest to the inlet in the column reactor (exposure to higher pollutant concentrations and drier conditions) resulted in a higher steady EC (>100 $g \cdot m^{-3} \cdot h^{-1}$) than the top section (<50 $g \cdot m^{-3} \cdot h^{-1}$) (lower pollutant concentrations and wetter conditions).

The soil type had a the strong effect on the EC and was seen in all the experiments i.e. experiments testing the impact of operating temperature (30 $^{o}C$ and 40 $^{o}C$) as well as experiments testing the impact of operating conditions (Condition A and Condition B). This is consistent with what has been reported in the literature that packing materials had a vital role in attaining high pollutant removal rate and in maintaining the performance over a prolonged period of time (Devinny et al., 1999, Sakuma et al., 2006). Overall, Soil 1 and Soil 3 exhibited a better toluene elimination performance than Soil 2. At 40 $^{o}C$, loading rate of 157 $g \cdot m^{-3} \cdot h^{-1}$ and a matric potential of -10 $cm_{H_2O}$, Soil 1 demonstrated the highest mean EC of 73.5 ± 4.9 $g \cdot m^{-3} \cdot h^{-1}$ whereas the lowest mean EC of 35.5 ± 4.9 $g \cdot m^{-3} \cdot h^{-1}$ was observed in Soil 2. In both operating conditions A and B, Soil 2 also had lowest mean EC (34.8 ± 5.7 $g \cdot m^{-3} \cdot h^{-1}$), less than 30% of the average mean EC in Soil 1 and Soil 3 (45 ± 7.9 $g \cdot m^{-3} \cdot h^{-1}$). The possible reasons for the difference in biofilter performance are the water and nitrogen availability in the soil samples, which are needed for biomass growth (Sakuma et al., 2009). Among the three soil types, Soil 2 had the least nitrogen content (0.17 $g_N/g_{dry\ soil}$) (Table 5.1) and lowest gravimetric

water content (Figure 5.1) at the same levels of matric potential. Another reason could be due to the differences in the bacterial community composition, which will be discussed further in Section 5.3.6.

Other potential factors related to packing materials such as surface area, porosity, air permeability, water retention capability and adsorptive capacity could have contributed to the difference in the performance (Sakuma et al., 2009, Dorado et al., 2010). However, this was not explored as it was beyond the scope of this study.

### 5.3.6 Microbial community analysis

**Overall microbial community diversity**

Overall, the microbial diversity was consistently higher for fresh soil samples than for bioreactor soil samples (Table 5.10). Soil 2 had the highest microbial diversity (H' = 5.46, D = 0.99) whereas Soil 3 had the lowest microbial diversity (H' = 5.02, D = 0.97) of the fresh soil samples. For bioreactor soil samples operated at Condition A (a low residual concentration generated by an inlet load of 78 $g \cdot m^{-3} \cdot h^{-1}$, -10 $cm_{H_2O}$), Soil 1 had the highest microbial diversity (H' = 4.99, D = 0.98). At Condition B (a high residual concentration generated by an inlet load of 137 $g \cdot m^{-3} \cdot h^{-1}$, -100 $cm_{H_2O}$), the highest microbial diversity (H' = 5.14, D = 0.99) was recorded in Soil 2.

Table 5.10: Bacterial community diversity based on the ASVs from the V3-V4 region of DNA from soil samples pre- and post- toluene reactor operation.

| Sample (*) | Shannon Entropy diversity index (H') | Simpson diversity index (D) |
|---|---|---|
| S1 | 5.13 | 0.98 |
| S2 | 5.46 | 0.99 |
| S3 | 5.02 | 0.97 |
| S1 – A/1 | 4.99 | 0.98 |
| S1 – B/1 | 4.86 | 0.97 |
| S1 – B/2 | 5.01 | 0.98 |
| S2 – A/1 | 4.64 | 0.97 |
| S2 – A/2 | 4.84 | 0.98 |
| S2 – B/1 | 5.26 | 0.99 |
| S2 – B/2 | 5.02 | 0.99 |
| S3 – A/1 | 4.65 | 0.97 |
| S3 – B/1 | 5.02 | 0.98 |
| S3 – B/2 | 4.56 | 0.96 |

*S1 to S3 = Soil type 1 to 3; 1 and /2 = Run 1 and Run 2; A and B = Condition A and Condition B

**Impact of operating conditions and soil type on microbial community structure**

Non-metric multidimensional scaling (NMDS) was used to visualize variation in community structure with distance. NMDS was calculated using the Bray-Curtis dissimilarity and was created in R v3.5.0 (R Core Team, 2015). In NMDS analysis, the samples that had a similar community structure group together and samples with different communities would be further apart.

Non-metric multidimensional scaling (NMDS) analysis at ASV level showed notable changes in the community structure for all three soils type before and after experiments (especially for Soil 2) (Figure 5.7). These observed differences are mainly attributed to the soil type rather than the operating conditions during acclimation. Soil 1 pre- and post- toluene exposure at Condition A and Condition B had similar community structure. Soil 2 post toluene exposure at Condition A and Condition B also had a similar community structure. Soil 2 pre- toluene exposure appeared different from the post-toluene exposure. Soil 3 pre- and post-toluene exposure at Condition A and Condition B/1 had similar community structure except operating at Condition B/2 seemed to be closer to Soil 1 communities and may be an outlier in regard to the community analysis.

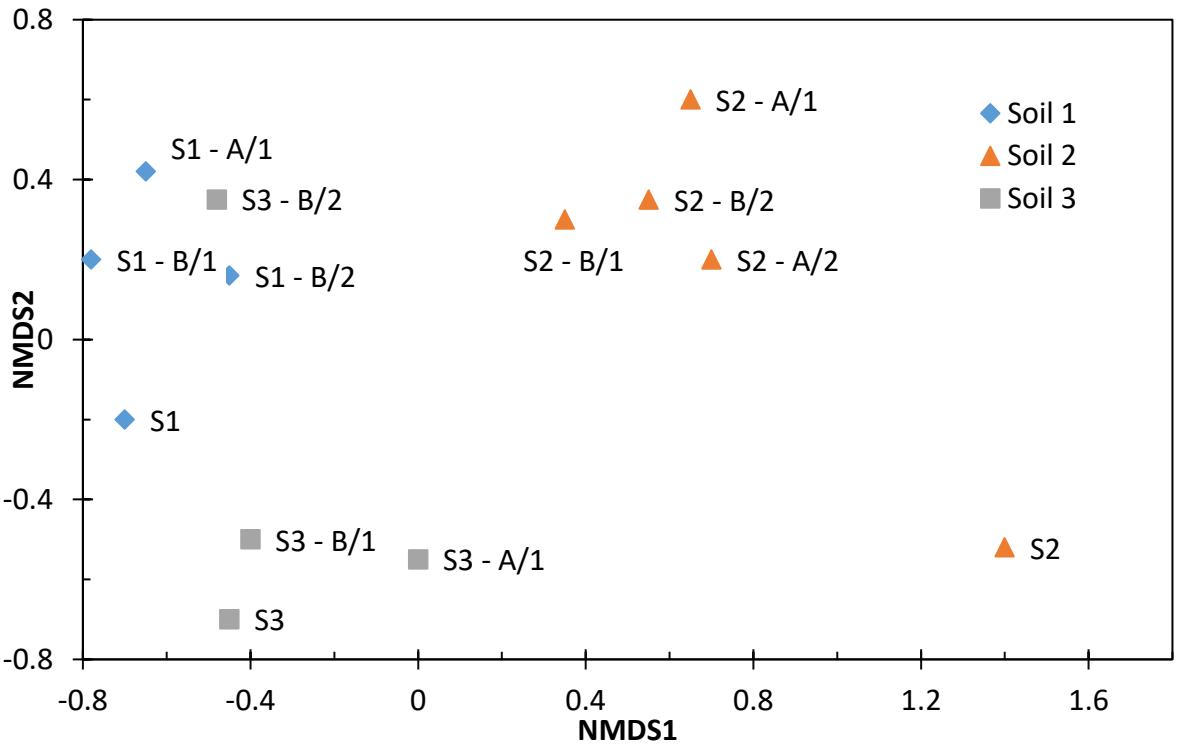


Figure 5.7: NMDS plot showing the community structure of different soil types pre- and post- toluene exposure at different environmental conditions based on the sequencing of the V3-V4 region of the extracted DNA.

**Microbial community composition**

Eleven phyla were found in all soil samples and their relative abundance was quantified (Figure 5.8). Three phyla: *Actinobacteria, Proteobacteria* and *Chloroflexi* were the most common, with a total of ~ 70% relative abundance. For fresh soil samples, *Actinobacteria* were the most dominant (35%) bacterial community in Soil 2 whereas *Chloroflexi* were the most dominant (38%) in Soil 3. The dominant phyla evenly distributed in Soil 1 (*Actinobacteria* – 28%, *Chloroflexi* – 25% and *Proteobacteria* – 22%).

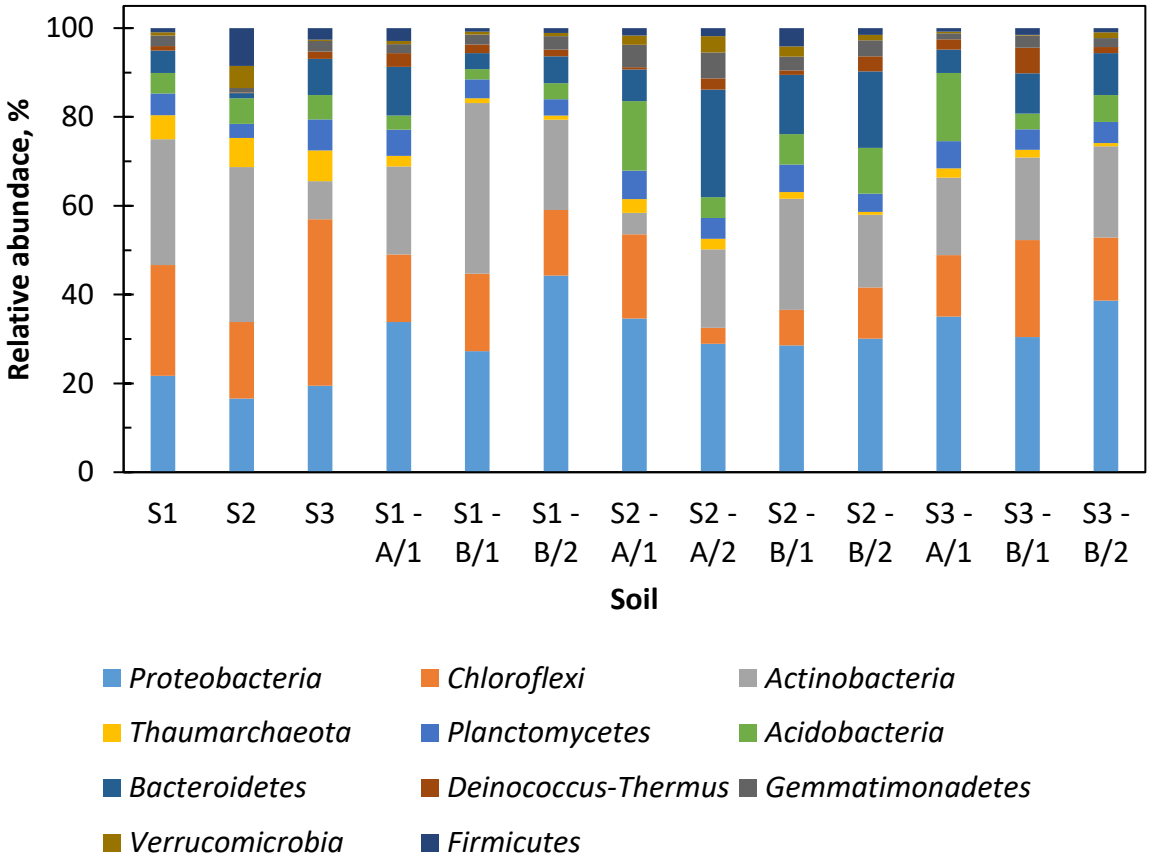


Figure 5.8: Barplot showing the relative abundances of microorganisms at the phylum level in the in the different soil types pre- and post- toluene exposure at different environmental conditions.

At the end of the experiments, the relative abundance of *Proteobacteria* in all the three soil samples increased by 6 – 23% on an absolute % basis while that of *Chloroflexi* decreased by 6 – 24%. For example, in Soil 3, the abundance of *Proteobacteria* increased in a stepwise manner from 20% to 30% (Condition B/1), 35% (Condition A) and 39% (Condition B/2), while that of *Chloroflexi* decreased from 38% to 22% (Condition B/1) and 14% (Condition A/1 and Condition B/2).

The abundance of *Actinobacteria* in Soil 3 analysed after the experiments increased from 9% to more than 15%. However, in Soil 2, this phylum showed a decreasing trend over the operating conditions (from 35% to less than 25%). The abundance of *Actinobacteria* in Soil 1 was found to fluctuate from 19% (Condition A, Condition B/2) to 38% (Condition B/1).

The relative abundance of *Acidobacteria and Bacteroidetes* made some significant increases. For example, the abundance of *Bacteroidetes* in Soil 2 increased from 1.2% to 7% (Condition A/1), 24% (Condition A/2), 13% (Condition B/1) and 17% (Condition B/2). The abundance of *Acidobacteria* increased from 6% to above 10% in Soil 2 (Condition A/1 and Condition B/2), from 5.5% to 15.5% in Soil 3 (Condition A/1).

In summary, a general increase of four phyla: *Actinobacteria, Proteobacteria, Acidobacteria and Bacteroidetes* was observed after the experiments. The majority of the known hydrocarbon degrading bacteria belongs to the phylum *Proteobacteria* (Prince et al., 2010). The phyla *Actinobacteria* and *Bacteroidetes* contain hydrocarbon degraders and all of them are aerobes (Hubert et al., 1999, Margesin et al., 2003, Maneerat et al., 2006, Al-Saleh et al., 2009). However, there is lack of information about the role of *Acidobacteria* in hydrocarbon degradation. Mukherjee et al. (2014) hypothesized that the phylum *Acidobacteria* was not affected by hydrocarbon contamination levels and behaved as generalists in contaminated

soils. Contradictory findings were reported by Xie et al. (2011) and Ren et al. (2015). Xie et al. (2011) identified a member of *Acidobacteria* among the strains involved in benzene degradation. Ren et al. (2015) found the significant increase of relative abundance of *Acidobacteria* (0 to 24%) in soil exposed to pyrene.

Microbial community analysis at genera level were conducted to examine the role of the phyla in the system. Nine genera were identified in the fresh soil samples (Figure 5.9) at a filter threshold of 1%. Unassigned genera of Soils 1, 2 and 3 were 72%, 84% and 81%, respectively. One contributing factor to the high fraction of unknowns could be due to the large amount of unculturable microbes in the soils (more than 99%) (Vartoukian et al., 2010, Pham and Kim, 2012) did not match with the sequences in the databases.

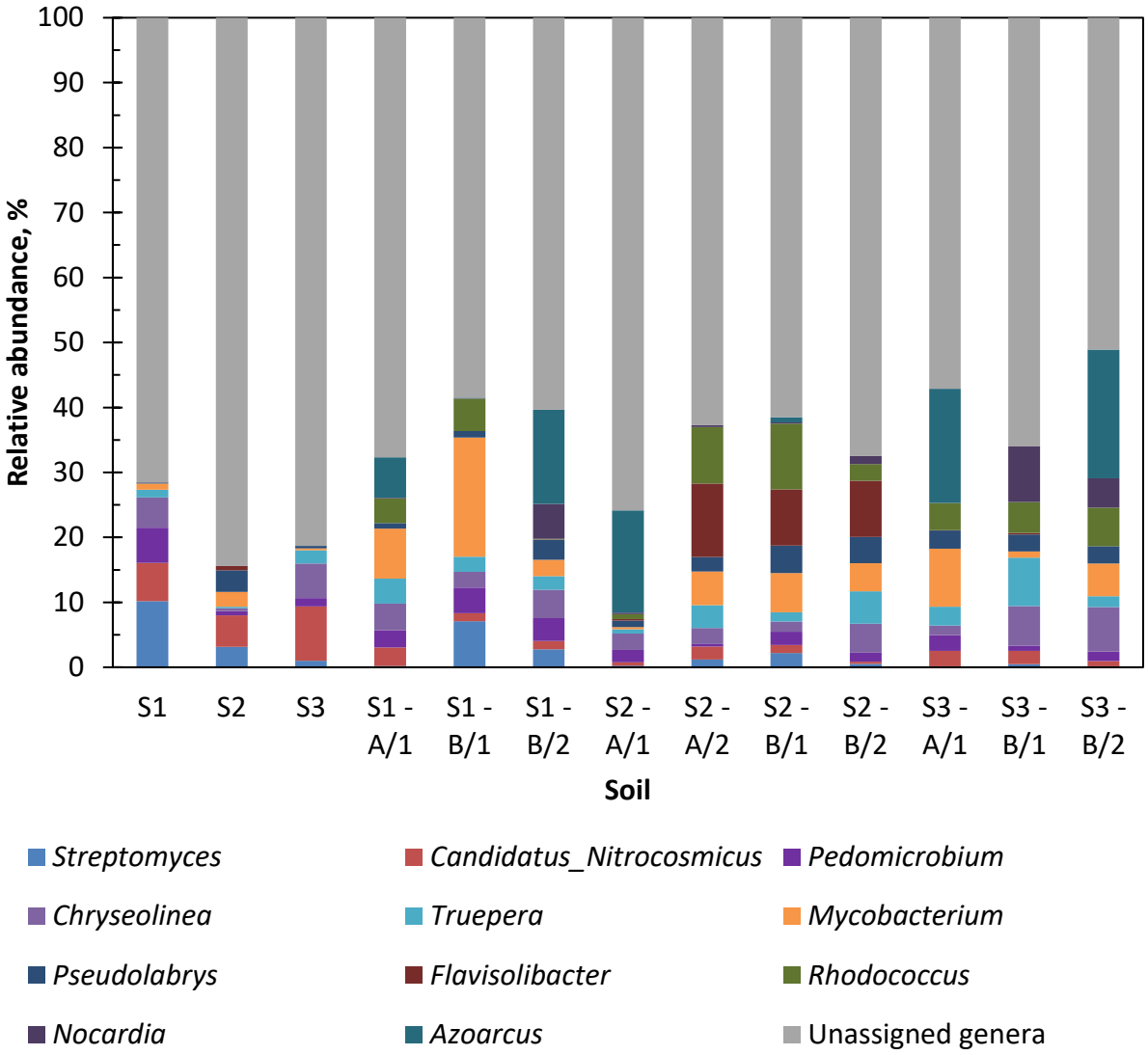


Figure 5.9: Barplot showing the relative abundances of microorganisms at the genus level in the different soil types pre- and post- toluene exposure at different environmental conditions.

Unassigned genera of ten bioreactor soil samples was more than 50% of the total DNA. The sequences clustering based on 95% similarity revealed two clusters belonging to the phylum *Chloroflexi*, which had a relative abundance of 5 – 10%. Majority of the remaining clusters had the relative abundance of 1 – 2% (Appendix D). These dominant clusters in the unassigned genera were in such low relative abundance (1 – 5%), it was assumed they had little impact in the toluene degradation.

Apart from the nine genera that existed in the fresh soil samples, two new genera: *Rhodococcus* and *Azoarcus* were found in the bioreactor soil samples. Five out of eleven genera: *Rhodococcus*, *Azoarcus*, *Streptomyces*, *Nocardia* and *Mycobacterium* in the bioreactor soil samples were present in higher abundance than the fresh soil samples. The sum of these dominant genera accounted for 25% of the total DNA or ~60% of the assigned genera.

The genus *Azoarcus* was found to fluctuate between 0% to 19% depending on the soil type and operating conditions. The abundance of *Rhodococcus* did not fluctuate to the same extent as the *Azoarcus,* ranging from 0.1% to 10%. *Nocardia* and *Mycobacterium* showed an increase in the relative abundance, from 0% to 8% and from 0% to 18% respectively, as opposed to *Streptomyces* (from 10% to 0.1%).

Many members of the genera: *Nocardia, Mycobacterium, Streptomyces, Rhodococcus* and *Azoarcus* have been shown to degrade toluene (Tay et al., 1998, Tay et al., 2001, Weelink et al., 2010, Woods et al., 2011, Rodrigues et al., 2015, Mohamed et al., 2016). Four genera: *Nocardia, Mycobacterium, Streptomyces* and *Rhodococcus* are members of the phylum *Actinobacteria* while the genus *Azoarcus* belongs to the phylum *Proteobacteria*. In this study, the abundance of the genera *Nocardia, Mycobacterium*, *Rhodococcus* and *Azoarcus* increased in the soil fed with toluene. Hence, it could be concluded that these genera played crucial roles in the toluene degradation or benefited from the environment produced (e.g. EPS production).

The abundance of the genera *Chryseolinea* and *Pseudolabrys* belong to the phylum *Bacteroidetes* were few in all of the samples (< 6% of the total DNA) while no genera belong to the phylum *Acidobacteria* was found. Looking at the phylum level, the relative abundance of *Acidobacteria and Bacteroidetes* increased by above 10% in some samples. This

inconsistency in results of the phylum and genus analyses could be due to the unassigned genera (over 40% in all samples).

The two genera that emerged after exposure to toluene were *Rhodococcus* and *Azoarcus.* *Rhodococcus* species are generally strictly aerobic bacteria (Kour et al., 2019) whereas members of the genus *Azoarcus* are capable of degrading a number of aromatic compounds under aerobic and/or anaerobic conditions (Fries et al., 1994, Fernández et al., 2014). In the current study, there was no clear trend for the abundance of these two genera. For example, in Soil 3 operated at Condition B (B/1), the abundance of the genus *Rhodococcus* increased, from 0% to 4.8% of the total biomass whereas the abundance of the genus *Azoarcus* was 0% before and after the experiment. For the replicate of Soil 3 operated under Condition B (B/2), the abundance of the genus *Rhodococcus* and genus *Azoarcus* both increased, from 0% to 5.9% and from 9% to 19.9%, respectively.

Notably, *Azoarcus* is a genus of nitrogen-fixing bacteria capable of converting nitrogen to ammonia, a form that can be used by other bacteria to grow (Hurek and Reinhold-Hurek, 1995). If this is the case, an incremental increase in EC and biomass growth would have been observed. However, in the current study, the general trend was for the EC value to gradually increase after 3 – 7 days of exposure to toluene then drifting down to its steady state value (Figure A.4: Gas concentration profile of Soil 2 at a toluene inlet loading rate of 137 $g \cdot m^{-3} \cdot h^{-1}$ and -100 $cm_{H_2O}$ at 40 $^oC$. Further investigation on the role of nitrogen-fixing bacteria on the biofilter system is required to explain why no increase in EC was observed even when nitrogen-fixers are present.

Detchanamurthy (2013) isolated *Stenotrophomonas maltophilia* and *Pseudomonas putida* from Soil 1. These two toluene degrading species are often isolated from biofilters and their

growth parameters are used for modelling studies (Lee et al., 2002, Abuhamed et al., 2004, Kim et al., 2005, Bakhshi et al., 2011). In the current study, the genus *Stenotrophomonas* was not found in any of the soil types. The genus *Pseudomonas* was found in some of the samples (data not shown) but was removed from the data because the relative abundance was < 1%. There were no reads that aligned with *P. putida*. These results indicated that not all bacteria active in the biofilter can be easily grown in pure culture in the laboratory and the ones that do may not be significant in the original mixed community, which was consistent with the findings from previous studies (Wade, 2002, Stewart, 2012). In addition, these results suggested that it is very hard to compare the performance of a *P. putida* or *S. maltophilia* biofilm with a soil biofilter, as these species may not be one of the dominant degrading microorganisms at the same set of operating conditions.

### 5.4 Conclusions

This study evaluated the impact of different combinations of soil type (Soil 1, Soil 2 and Soil 3) and operating conditions - temperature (30 $^{o}$C and 40 $^{o}$C), moisture content (-10 $cm_{H_2O}$ and -100 $cm_{H_2O}$) and toluene residual concentration (low level: 5 ppm to 49 ppm and high level: 115 ppm to 146 ppm) - on biofilter performance in terms of EC and mineralization to $CO_2$. The maximum mean EC of 73.5 ± 4.9 $g \cdot m^{-3} \cdot h^{-1}$ was found for the reactor packed with Soil 1 at 40 $^{o}$C and a loading rate of 157 $g \cdot m^{-3} \cdot h^{-1}$. The $\%CO_2$ recovery varied from 29 – 58% with the highest mean $\%CO_2$ recovery of 51.7 ± 5.5% recorded for Soil 2 exposed to toluene inlet load of 78 $g \cdot m^{-3} \cdot h^{-1}$ at -10 $cm_{H_2O}$ matric potential.

The biofilter operating at a loading rate of 157 $g \cdot m^{-3} \cdot h^{-1}$ and -10 $cm_{H_2O}$ resulted in a 30% higher EC (54.3 ± 17.4 $g \cdot m^{-3} \cdot h^{-1}$) and a 20% higher $\%CO_2$ recovery (50.1 ± 3.6%) than the biofilter starting at 30 $^{o}$C (EC = 38.8 ± 16.2 $g \cdot m^{-3} \cdot h^{-1}$; $\%CO_2$ recovery = 41.3 ± 2.7%). These results were

inconsistent with hypothesis 1 from Bordoloi et al. (2019), which was starting the biofilter at higher temperatures would result in a higher EC but no difference in $\%CO_2$ recovery compared to starting at lower temperatures.

At 40 $^oC$, operating a reactor at Condition A (residual concentrations of 5 ppm to 49 ppm, - 10 $cm_{H_2O}$) had a ~20% higher EC (46.2 ± 9 $g \cdot m^{-3} \cdot h^{-1}$) and a 20% higher $\%CO_2$ recovery (48.1 ± 4.4) than operating at Condition B (residual concentrations of 115 ppm to 146 ppm, -100 $cm_{H_2O}$), which had a EC = 37.3 ± 5.3 $g \cdot m^{-3} \cdot h^{-1}$ and $\%CO_2$ recovery = 39.5 ± 6.2%. These results were in line with Bordoloi et al. (2019) hypothesis 2 that operating the biofilter at lower residual concentrations and wetter conditions would result in a higher $\%CO_2$ recovery than operating at higher residual concentrations and drier conditions.

Except for the impact of temperature on $\%CO_2$ recovery, the results are in agreement with Bordoloi et al. (2019). They found that temperature had no influence on the $\%CO_2$ recovery but these experiments were conducted using one soil type (Soil 1) which may not be conclusive. The current study covered a wider range of soil types (Soil 1, Soil 2 and Soil 3) with duplicates of each condition, hence providing broader and more conclusive results.

Preliminary results of microbial community analysis from different soil types pre- and post-toluene exposure at different environmental conditions showed different bacterial diversity. At the phylum level, *Actinobacteria, Proteobacteria* and *Chloroflexi* were the most common (~ 70% relative abundance) of the total bacteria community in the soil samples pre-toluene exposure. Four phyla: *Actinobacteria, Proteobacteria, Acidobacteria and Bacteroidetes* constituted a major proportion (> 70% relative abundance) in the soil samples post-toluene exposure. At the genus level, five genera: *Nocardia, Mycobacterium, Streptomyces, Rhodococcus* and *Azoarcus* capable of degrading toluene were indentified. The abundance of

four genera: *Nocardia, Mycobacterium*, *Rhodococcus* and *Azoarcus* increased in the soil samples post-toluene exposure. These genera could have played crucial roles in the toluene degradation or benefited from the environment produced.

**References**

ABUHAMED, T., BAYRAKTAR, E., MEHMETOGLU, T. & MEHMETOGLU, U. 2004. Kinetics model for growth of *Pseudomonas putida* F1 during benzene, toluene and phenol biodegradation. *Process Biochemistry,* 39**,** 983-988.

AL-SALEH, E., DROBIOVA, H. & OBUEKWE, C. 2009. Predominant culturable crude oil-degrading bacteria in the coast of Kuwait. *International Biodeterioration & Biodegradation,* 63**,** 400-406.

ALAGAPPAN, G. & COWAN, R. 2003. Substrate inhibition kinetics for toluene and benzene degrading pure cultures and a method for collection and analysis of respirometric data for strongly inhibited cultures. *Biotechnology and Bioengineering,* 83**,** 798-809.

ALVAREZ-HORNOS, F. J., GABALDON, C., MARTINEZ-SORIA, V., MARZAL, P. & PENYA-ROJA, J. M. 2008. Biofiltration of toluene in the absence and the presence of ethyl acetate under continuous and intermittent loading. *Journal of Chemical Technology and Biotechnology,* 83**,** 643-653.

ARMSTRONG, A. Q., HODSON, R. E., HWANG, H. M. & LEWIS, D. L. 1991. Environmental-factors affecting toluene degradation in ground-water at a hazardous-waste site. *Environmental Toxicology and Chemistry,* 10**,** 147-158.

AURIA, R., AYCAGUER, A. C. & DEVINNY, J. S. 1998. Influence of water content on degradation rates for ethanol in biofiltration. *Journal of the Air & Waste Management Association,* 48**,** 65-70.

BAKHSHI, Z., NAJAFPOUR, G., KARIMINEZHAD, E., PISHGAR, R., MOUSAVI, N. & TAGHIZADE, T. 2011. Growth kinetic models for phenol biodegradation in a batch culture of *Pseudomonas putida*. *Environmental Technology,* 32**,** 1835-1841.

BEUGER, A. L. & GOSTOMSKI, P. A. 2009. The impact of environmental parameters on toluene degradation using a laboratory-scale biofilter with internal recycle. *International Journal of Chemical Engineering,* 2**,** 87-95.

BORDOLOI, A., GAPES, D. J. & GOSTOMSKI, P. A. 2019. The impact of environmental parameters on the conversion of toluene to CO2 and extracellular polymeric substances in a differential soil biofilter. *Chemosphere,* 232**,** 304-314.

BORDOLOI, A. & GOSTOMSKI, P. A. 2019. Carbon recovery and the impact of start-up conditions on the performance of an unsaturated *Pseudomonas putida* biofilm compared with soil under controlled environmental parameters in a differential biofilter. *Journal of Chemical Technology and Biotechnology,* 94**,** 600-610.

CHEN, X., QIAN, W., KONG, L. J., XIONG, Y. & TIAN, S. H. 2015. Performance of a suspended biofilter as a new bioreactor for removal of toluene. *Biochemical Engineering Journal,* 98**,** 56-62.

CHOWDHURY, N., MARSCHNER, P. & BURNS, R. G. 2011. Soil microbial activity and community composition: Impact of changes in matric and osmotic potential. *Soil Biology & Biochemistry,* 43**,** 1229-1236.

COX, H. H. J., SEXTON, T., SHAREEFDEEN, Z. M. & DESHUSSES, M. A. 2001. Thermophilic biotrickling filtration of ethanol vapors. *Environmental Science & Technology,* 35**,** 2612-2619.

DEEB, R. A. & ALVAREZ-COHEN, L. 1999. Temperature effects and substrate interactions during the aerobic biotransformation of BTEX mixtures by toluene-enriched consortia and *Rhodococcus rhodochrous*. *Biotechnology and Bioengineering,* 62**,** 526-536.

DELHOMÉNIE, M. C., BIBEAU, L., BREDIN, N., ROY, S., BROUSSAU, S., BRZEZINSKI, R., KUGELMASS, J. L. & HEITZ, M. 2002. Biofiltration of air contaminated with toluene on a compost-based bed. *Advances in Environmental Research,* 6**,** 239-254.

DETCHANAMURTHY, S. 2013. *Impact of different metabolic uncouplers on the specific degradation rate of toluene in a differential biofiltration reactor.* Doctor of Philosophy, University of Canterbury.

DETCHANAMURTHY, S. & GOSTOMSKI, P. A. 2015. Studies on the influence of different metabolic uncouplers on the biodegradation of toluene in a differential biofilter reactor. *Biotechnology and Bioprocess Engineering,* 20**,** 915-923.

DEVINNY, J. S., DESHUSSES, M. A. & WEBSTER, T. S. 1999. *Biofiltration for air pollution control,* United States of America, CRC press.

DORADO, A. D., BAEZA, J. A., LAFUENTE, J., GABRIEL, D. & GAMISANS, X. 2012. Biomass accumulation in a biofilter treating toluene at high loads - Part 1: Experimental performance from inoculation to clogging. *Chemical Engineering Journal,* 209**,** 661-669.

DORADO, A. D., LAFUENTE, F. J., GABRIEL, D. & GAMISANS, X. 2010. A comparative study based on physical characteristics of suitable packing materials in biofiltration. *Environ. Technol.,* 31**,** 193-204.

ELMRINI, H., BREDIN, N., SHAREEFDEEN, Z. & HEITZ, M. 2004. Biofiltration of xylene emissions: bioreactor response to variations in the pollutant inlet concentration and gas flow rate. *Chemical Engineering Journal,* 100**,** 149-158.

ESTEVEZ, E., VEIGA, M. C. & KENNES, C. 2005. Biofiltration of waste gases with the fungi *Exophiala oligosperma* and *Paecilomyces variotii*. *Applied Microbiology and Biotechnology,* 67**,** 563-568.

FERNÁNDEZ, H., PRANDONI, N., FERNÁNDEZ-PASCUAL, M., FAJARDO, S., MORCILLO, C., DÍAZ, E. & CARMONA, M. 2014. *Azoarcus* sp. CIB, an anaerobic biodegrader of aromatic compounds shows an endophytic lifestyle. *PloS one,* 9**,** e110771-e110771.

FRIES, M. R., ZHOU, J. H., CHEESANFORD, J. & TIEDJE, J. M. 1994. Isolation, characterization, and distribution of denitrifying toluene degraders from a variety of habitats. *Applied and Environmental Microbiology,* 60**,** 2802-2810.

GHEZZEHEI, T. A., SULMAN, B., ARNOLD, C. L., BOGIE, N. A. & BERHE, A. A. 2019. On the role of soil water retention characteristic on aerobic microbial respiration. *Biogeosciences,* 16**,** 1187-1209.

HUBERT, C., SHEN, Y. & VOORDOUW, G. 1999. Composition of toluene-degrading microbial communities from soil at different concentrations of toluene. *Applied and environmental microbiology,* 65**,** 3064-3070.

HUREK, T. & REINHOLD-HUREK, B. 1995. Identification of grass-associated and toluene-degrading diazotrophs, *Azoarcus* spp., by analyses of partial 16S ribosomal DNA sequences. *Applied and Environmental Microbiology,* 61**,** 2257-2261.

JIMENEZ, L., ARRIAGA, S. & AIZPURU, A. 2016. Assessing biofiltration repeatability: statistical comparison of two identical toluene removal systems. *Environmental Technology,* 37**,** 681-693.

KIARED, K., FUNDENBERGER, B., BRZEZINSKI, R., VIEL, G. & HEITZ, M. 1997. Biofiltration of air polluted with toluene under steady-state conditions: Experimental observations. *Industrial & Engineering Chemistry Research,* 36**,** 4719-4725.

KIM, D. J., CHOI, J. W., CHOI, N. C., MAHENDRAN, B. & LEE, C. E. 2005. Modeling of growth kinetics for *Pseudomonas* spp. during benzene degradation. *Applied Microbiology and Biotechnology,* 69**,** 456-462.

KOUR, D., RANA, K. L., KUMAR, R., YADAV, N., RASTEGARI, A. A., YADAV, A. N. & SINGH, K. 2019. Chapter 1 - Gene manipulation and regulation of catabolic genes for biodegradation of biphenyl compounds. *In:* SINGH, H. B., GUPTA, V. K. & JOGAIAH, S. (eds.) *New and Future Developments in Microbial Biotechnology and Bioengineering.* Amsterdam: Elsevier.

KRISHNAKUMAR, B., HIMA, A. M. & HARIDAS, A. 2007. Biofiltration of toluene-contaminated air using an agro by-product-based filter bed. *Applied Microbiology and Biotechnology,* 74**,** 215-220.

LEE, E. Y., JUN, Y. S., CHO, K. S. & RYU, H. W. 2002. Degradation characteristics of toluene, benzene, ethylbenzene, and xylene by *Stenotrophomonas maltophilia* T3-c. *Journal of the Air & Waste Management Association,* 52**,** 400-406.

LEILI, M., FARJADFARD, S., SORIAL, G. A. & RAMAVANDI, B. 2017. Simultaneous biofiltration of BTEX and Hg° from a petrochemical waste stream. *Journal of Environmental Management,* 204**,** 531-539.

LIU, Y. H., QUAN, X., SUN, Y. M., CHEN, J. W., XUE, D. M. & CHUNG, J. S. 2002. Simultaneous removal of ethyl acetate and toluene in air streams using compost-based biofilters. *Journal of Hazardous Materials,* 95**,** 199-213.

LU, C. S., LIN, M. R. & CHU, C. H. 1999. Temperature effects of trickle-bed biofilter for treating BTEX vapors. *Journal of Environmental Engineering-Asce,* 125**,** 775-779.

MADI, R., DE ROOIJ, G. H., MIELENZ, H. & MAI, J. 2018. Parametric soil water retention models: a critical evaluation of expressions for the full moisture range. *Hydrology and Earth System Sciences,* 22.

MAESTRE, J. P., GAMISANS, X., GABRIEL, D. & LAFUENTE, J. 2007. Fungal biofilters for toluene biofiltration: Evaluation of the performance with four packing materials under different operating conditions. *Chemosphere,* 67**,** 684-692.

MAIER, R. M. & PEPPER, I. L. 2009. Earth environments. *Environmental microbiology.* Elsevier.

MALAKAR, S., SAHA, P. D., BASKARAN, D. & RAJAMANICKAM, R. 2018. Microbial biofilter for toluene removal: Performance evaluation, transient operation and theoretical prediction of elimination capacity. *Sustainable Environment Research,* 28**,** 121-127.

MANEERAT, S., BAMBA, T., HARADA, K., KOBAYASHI, A., YAMADA, H. & KAWAI, F. 2006. A novel crude oil emulsifier excreted in the culture supernatant of a marine bacterium, *Myroides* sp. strain SM1. *Applied microbiology and biotechnology,* 70**,** 254-259.

MANZONI, S., SCHIMEL, J. P. & PORPORATO, A. 2012. Responses of soil microbial communities to water stress: results from a meta-analysis. *Ecology,* 93**,** 930-938.

MARGESIN, R., SPROER, C., SCHUMANN, P. & SCHINNER, F. 2003. *Pedobacter cryoconitis* sp nov., a facultative psychrophile from alpine glacier cryoconite. *International Journal of Systematic and Evolutionary Microbiology,* 53**,** 1291-1296.

MOE, W. M. & LI, C. N. 2005. A design methodology for activated carbon load equalization systems applied to biofilters treating intermittent toluene loading. *Chemical Engineering Journal,* 113**,** 175-185.

MOHAMED, E. F., AWAD, G., ANDRIANTSIFERANA, C. & EL-DIWANY, A. I. 2016. Biofiltration technology for the removal of toluene from polluted air using *Streptomyces griseus*. *Environmental Technology,* 37**,** 1197-1207.

MOHAMMAD, B. T., RENE, E. R., VEIGA, M. C. & KENNES, C. 2017. Performance of a thermophilic gas-phase biofilter treating high BTEX loads under steady- and transient-state operation. *International Biodeterioration & Biodegradation,* 119**,** 289-298.

MOHAMMAD, B. T., VEIGA, M. C. & KENNES, C. 2007. Mesophilic and thermophilic biotreatment of BTEX-polluted air in reactors. *Biotechnology and Bioengineering,* 97**,** 1423-1438.

MORALES, M., REVAH, S. & AURIA, R. 1998. Start-up and the effect of gaseous ammonia additions on a biofilter for the elimination of toluene vapors. *Biotechnology and Bioengineering,* 60**,** 483-491.

MUKHERJEE, S., JUOTTONEN, H., SIIVONEN, P., QUESADA, C. L., TUOMI, P., PULKKINEN, P. & YRJALA, K. 2014. Spatial patterns of microbial diversity and activity in an aged creosote-contaminated site. *Isme Journal,* 8**,** 2131-2142.

NAMKOONG, W., PARK, J.-S. & VANDERGHEYNST, J. S. 2004. Effect of gas velocity and influent concentration on biofiltration of gasoline off-gas from soil vapor extraction. *Chemosphere,* 57**,** 721-730.

OH, D. I., SONG, J., HWANG, S. J. & KIM, J. Y. 2009. Effects of adsorptive properties of biofilter packing materials on toluene removal. *Journal of Hazardous Materials,* 170**,** 144-150.

PALAU, J., PENYA-ROJA, J. M., GABALDON, C., ALVAREZ-HORNOS, F. J. & MARTINEZ-SORIA, V. 2012. Effect of pre-treatments based on UV photocatalysis and photo-oxidation on toluene biofiltration performance. *Journal of Chemical Technology and Biotechnology,* 87**,** 65-72.

PARK, D. W., KIM, S. S., HAAM, S., AHN, I. S., KIM, E. B. & KIM, W. S. 2002. Biodegradation of toluene by a lab-scale biofilter inoculated with *Pseudomonas putida* DK-1. *Environmental Technology,* 23**,** 309-318.

PHAM, V. H. T. & KIM, J. 2012. Cultivation of unculturable soil bacteria. *Trends in Biotechnology,* 30**,** 475-484.

PRINCE, R. C., GRAMAIN, A. & MCGENITY, T. J. 2010. Prokaryotic Hydrocarbon Degraders. *In:* TIMMIS, K. N. (ed.) *Handbook of Hydrocarbon and Lipid Microbiology.* Berlin, Heidelberg: Springer Berlin Heidelberg.

RAJAMANICKAM, R. & BASKARAN, D. 2017. Biodegradation of gaseous toluene with mixed microbial consortium in a biofilter: steady state and transient operation. *Bioprocess and Biosystems Engineering,* 40**,** 1801-1812.

REN, G., REN, W. J., TENG, Y. & LI, Z. G. 2015. Evident bacterial community changes but only slight degradation when polluted with pyrene in a red soil. *Frontiers in Microbiology,* 6**,** 11.

RENE, E. R., MURTHY, D. V. S. & SWAMINATHAN, T. 2005. Performance evaluation of a compost biofilter treating toluene vapours. *Process Biochemistry,* 40**,** 2771-2779.

RENE, E. R., SERGIENKO, N., GOSWAMI, T., LOPEZ, M. E., KUMAR, G., SARATALE, G. D., VENKATACHALAM, P., PAKSHIRAJAN, K. & SWAMINATHAN, T. 2018. Effects of concentration and gas flow rate on the removal of gas-phase toluene and xylene mixture in a compost biofilter. *Bioresource Technology,* 248**,** 28-35.

RODRIGUES, E. M., KALKS, K. H. M. & TOTOLA, M. R. 2015. Prospect, isolation, and characterization of microorganisms for potential use in cases of oil bioremediation along the coast of Trindade Island, Brazil. *Journal of Environmental Management,* 156**,** 15-22.

SAKUMA, T., HATTORI, T. & DESHUSSES, M. A. 2006. Comparison of different packing materials for the biofiltration of air toxics. *Journal of the Air & Waste Management Association,* 56**,** 1567-1575.

SAKUMA, T., HATTORI, T. & DESHUSSES, M. A. 2009. The effects of a lower irrigation system on pollutant removal and on the microflora of a biofilter. *Environmental Technology,* 30**,** 621-627.

SINGH, K., SINGH, R. S., RAI, B. N. & UPADHYAY, S. N. 2010. Biofiltration of toluene using wood charcoal as the biofilter media. *Bioresource Technology,* 101**,** 3947-3951.

SINGH, R. S., AGNIHOTRI, S. S. & UPADHYAY, S. N. 2006. Removal of toluene vapour using agro-waste as biofilter media. *Bioresource Technology,* 97**,** 2296-2301.

SONG, J. H. & KINNEY, K. A. 2000. Effect of vapor-phase bioreactor operation on biomass accumulation, distribution, and activity: Linking biofilm properties to bioreactor performance. *Biotechnology and Bioengineering,* 68**,** 508-516.

STEWART, E. J. 2012. Growing Unculturable Bacteria. *Journal of Bacteriology,* 194**,** 4151-4160.

SUN, Y. M., QUAN, X., CHEN, J. W., YANG, F. L., XUE, D. M., LIU, Y. H. & YANG, Z. H. 2002. Toluene vapour degradation and microbial community in biofilter at various moisture content. *Process Biochemistry,* 38**,** 109-113.

TAY, S. T. L., HEMOND, F. H., KRUMHOLZ, L. R., CAVANAUGH, C. M. & POLZ, M. F. 2001. Population dynamics of two toluene degrading bacterial species in a contaminated stream. *Microbial Ecology,* 41**,** 124-131.

TAY, S. T. L., HEMOND, H. F., POLZ, M. F., CAVANAUGH, C. M., DEJESUS, I. & KRUMHOLZ, L. R. 1998. Two new *Mycobacterium* strains and their role in toluene degradation in a contaminated stream. *Applied and Environmental Microbiology,* 64**,** 1715-1720.

VARTOUKIAN, S. R., PALMER, R. M. & WADE, W. G. 2010. Strategies for culture of 'unculturable' bacteria. *Fems Microbiology Letters,* 309**,** 1-7.

VERGARA-FERNÁNDEZ, A., LARA MOLINA, L., PULIDO, N. A. & AROCA, G. 2007. Effects of gas flow rate, inlet concentration and temperature on the biofiltration of toluene vapors. *Journal of Environmental Management,* 84**,** 115-122.

VIGUERAS, G., SHIRAI, K., MARTINS, D., FRANCO, T. T., FLEURI, L. F. & REVAH, S. 2008. Toluene gas phase biofiltration by *Paecilomyces lilacinus* and isolation and identification of a hydrophobin protein produced thereof. *Applied Microbiology and Biotechnology,* 80**,** 147-154.

WADE, W. 2002. Unculturable bacteria - the uncharacterized organisms that cause oral infections. *Journal of the Royal Society of Medicine,* 95**,** 81-83.

WANG, C., KONG, X. & ZHANG, X. Y. 2012. Mesophilic and thermophilic biofiltration of gaseous toluene in a long-term operation: performance evaluation, biomass accumulation, mass balance analysis and isolation identification. *Journal of Hazard Mater,* 229-230**,** 94-9.

WEELINK, S. A. B., VAN EEKERT, M. H. A. & STAMS, A. J. M. 2010. Degradation of BTEX by anaerobic bacteria: physiology and application. *Reviews in Environmental Science and Bio-Technology,* 9**,** 359-385.

WOODS, A., WATWOOD, M. & SCHWARTZ, E. 2011. Identification of a toluene-degrading bacterium from a soil sample through H(2)(18)O DNA stable isotope probing. *Applied and environmental microbiology,* 77**,** 5995-5999.

XIE, S. G., SUN, W. M., LUO, C. L. & CUPPLES, A. M. 2011. Novel aerobic benzene degrading microorganisms identified in three soils by stable isotope probing. *Biodegradation,* 22**,** 71-81.

ZILLI, M., DEL BORGHI, A. & CONVERTI, A. 2000. Toluene vapour removal in a laboratory-scale biofilter. *Applied Microbiology and Biotechnology,* 54**,** 248-254.

ZNAD, H. T., KATOH, K. & KAWASE, Y. 2007. High loading toluene treatment in a compost based biofilter using up-flow and down-flow swing operation. *Journal of Hazardous Materials,* 141**,** 745-752.

# Chapter 6: The biodegradation of methane in a soil biofilter

## 6.1 Introduction

After $CO_2$, $CH_4$ is the second most abundant anthropogenic greenhouse gas in the atmosphere and is estimated to have a global warming potential of 28 times that of $CO_2$ over a period of 100 years (Myhre et al., 2013). In 2017, $CH_4$ contributed 42% of New Zealand's national inventory of greenhouse gas emissions (MfE, 2019). New Zealand has the largest international methane emission rate (0.6 t per person per year) six times the global average. The $CH_4$ comes primarily from enteric fermentation in ruminant livestock (84%). The remainder is from manure management (2.5%), solid waste disposal (11.2%), coal mining and natural gas (2.2%) (Reisinger, 2018).

Over the past decade, biofiltration has been widely studied for its potential to reduce $CH_4$ generated during landfill, coal mine ventilation and animal husbandry operations (Nikiema et al., 2005, Nikiema et al., 2009a, Limbri et al., 2013, Syed et al., 2016, Ferdowsi et al., 2017). The $CH_4$ is oxidized by an active population of methane-oxidizing bacteria (methanotrophs) and is converted to water vapour, $CO_2$, biomass and other metabolites such as methanol and formaldehyde (Hanson and Hanson, 1996).

The studies using methane-oxidizing bacteria (methanotrophs) have revealed that the biofilter performance can be affected by a wide variety of factors, including temperature, pH, water content, packing material, inlet gas flow rate and inlet feed concentration (La et al., 2018). However, the studies of $CH_4$ oxidation in batch and column experiments have shown the difficulty to control important environmental parameters such as water content (Streese and Stegmann, 2003), pH (Hernandez et al., 2015) and oxygen (Park et al., 2009).

The differential reactor offers the ability to rigorously control the environmental conditions including pH, oxygen, water content and nutrient concentrations in biofilm matrices (Beuger, 2008, Detchanamurthy and Gostomski, 2015). The continuous flow minimises disruption to the microbial activity common in laboratory batch studies (Simoni et al., 2001).

The aim of this study was to use the differential reactor to evaluate different soils types (Soil 1, Soil 2 and Soil 3) for treating $CH_4$ in an air stream. The biofilter performance in terms of EC and $\%CO_2$ recovery/$CO_2$ production was evaluated under various operational parameters: supplemental $CO_2$ concentration of 350 – 450 ppm, Condition C (a low residual $CH_4$ concentration generated by an inlet load of 280 $g \cdot m^{-3} \cdot h^{-1}$, -10 $cm_{H_2O}$) and Condition D (a high residual $CH_4$ concentration generated by an inlet load of 1268 $g \cdot m^{-3} \cdot h^{-1}$, -100 $cm_{H_2O}$).

The results collected from Condition C and Condition D was used to test hypothesis 2 (Chapter 5): operating the biofilter at lower residual concentrations and wetter conditions would result in a higher $\%CO_2$ recovery than operating at higher residual concentrations and drier conditions. In order a better understand the role microbial diversity on the performance of the system, a microbial community analysis from the three soil types before and after methane experiments was performed.

## 6.2 Experiment design

### 6.2.1 Impact of $CO_2$

Two levels of $CO_2$ concentration were used: 0 ppm and 350 – 450 range. Soil 1 and Soil 2 were used as packing materials. To introduce 350 – 450 ppm $CO_2$ to the biofilter, the air generated from an air compressor was used to dilute the pure $CH_4$ - instead of using a dry air cylinder. The net $CO_2$ produced from the methane degradation was corrected by subtracting the $CO_2$ produced due to endogenous activity and the $CO_2$ contained in the atmospheric air from the

total $CO_2$ produced. The soil biofilters were fed with methane loading rate of 280 $g \cdot m^{-3} \cdot h^{-1}$ at -10 $cm_{H_2O}$ matric potential. The flow rate of 25 ± 0.1 $ml \cdot min^{-1}$ as kept constant during the experiment. The system was operated at the initial pH of 7.0 ± 0.1. Due to the limited time available, each treatment was performed only once.

### 6.2.2 Impact of operating conditions and soil type

Matric potential and residual concentration were combined to constitute operating conditions of the biofilter. Matric potential had two levels: -10 $cm_{H_2O}$ (wet condition) and -100 $cm_{H_2O}$ (dry condition). The methane inlet loads of 280 $g \cdot m^{-3} \cdot h^{-1}$ and 1268 $g \cdot m^{-3} \cdot h^{-1}$ were used to drive the residual methane concentrations to two levels: low and high, respectively. These inlet loads were generated by methane concentrations of 2055 ± 30 ppm and 9300 ± 70 ppm, respectively. These inlet concentrations were chosen to represent the common methane concentrations encountered in livestock, coal mine and wastewater treatment plant emissions (Melse and Van der Werf, 2005, Limbri et al., 2013).

Combining the inlet load with the matric potential resulted in two sets of condition: Condition C (a low residual concentration generated by an inlet load of 280 $g \cdot m^{-3} \cdot h^{-1}$, -10 $cm_{H_2O}$) and Condition D (a high residual concentration generated by an inlet load of 1268 $g \cdot m^{-3} \cdot h^{-1}$, -100 $cm_{H_2O}$). These operating conditions were combined with three soil types (Soil 1, Soil 2 and Soil 3) resulting in a total of six treatment combinations (2 x 3). Each treatment combination was performed in triplicate.

The temperature of the reactor box was maintained at 40 ± 0.1 $^oC$ in all the experiments. The buffer solution in contact with the soil was pH = 7.0 ± 0.1. The flow rate of methane and dry air were adjusted by the mass flow controllers to generate the desired two levels of inlet concentration. The total flow rate of methane - air was maintained at 25 ± 0.1 $ml \cdot min^{-1}$. The

aim of this study was not optimizing the operational parameters thus the temperature, pH and flow rate in methane biofilters were chosen similar with the toluene biofilters for easier comparison.

## 6.3 Results and discussions

### 6.3.1 Overall treatment performance for $CH_4$ removal

Biofilters packed with different soil types (Soil 1, Soil 2 and Soil 3) were fed with a methane inlet load of 280 $g \cdot m^{-3} \cdot h^{-1}$ based on an inlet concentration of 2055 ± 30 ppm by mixing pure $CH_4$ and $CO_2$-free air and the total flowrate of 25 $ml \cdot min^{-1}$ (Figure 6.1). At the start of the experiments, ECs of 1 – 2 $g \cdot m^{-3} \cdot h^{-1}$ were observed in all three soil biofilters. The process of adsorption of $CH_4$ on the soil (Sadasivam and Reddy, 2015) and the absorption in the water layer might be the cause of this removal. After 7 to 13 days of operation, the EC values increased to 9 – 13 $g \cdot m^{-3} \cdot h^{-1}$ and $CO_2$ production increased from 1 – 2 $g \cdot m^{-3} \cdot h^{-1}$ to above 16 $g \cdot m^{-3} \cdot h^{-1}$. This indicated that the microbial community was acclimating to $CH_4$.

EC of Soil 1 biofilter and Soil 3 biofilter peaked at 54 $g \cdot m^{-3} \cdot h^{-1}$ and 39 $g \cdot m^{-3} \cdot h^{-1}$ respectively on day 16 whereas $EC_{max}$ of Soil 2 biofilter was 28 $g \cdot m^{-3} \cdot h^{-1}$ on days 11 – 13. On day 24, the EC of Soil 1 dropped 20%, from 54 $g \cdot m^{-3} \cdot h^{-1}$ to 44 $g \cdot m^{-3} \cdot h^{-1}$ and the EC of Soil 2 dropped from 39 $g \cdot m^{-3} \cdot h^{-1}$ to 32 $g \cdot m^{-3} \cdot h^{-1}$. Subsequently, the high and stable ECs of Soil 1 and Soil 3 were maintained for the remaining period of the experiments. The EC of Soil 2 slightly decreased and reached a plateau of 19 $g \cdot m^{-3} \cdot h^{-1}$ on day 25. The $CO_2$ production followed the EC in biofilters with the highest $CO_2$ production of 81 $g \cdot m^{-3} \cdot h^{-1}$ observed in Soil 1 biofilter and the lowest $CO_2$ production of 21 $g \cdot m^{-3} \cdot h^{-1}$ in the Soil 2 biofilter.

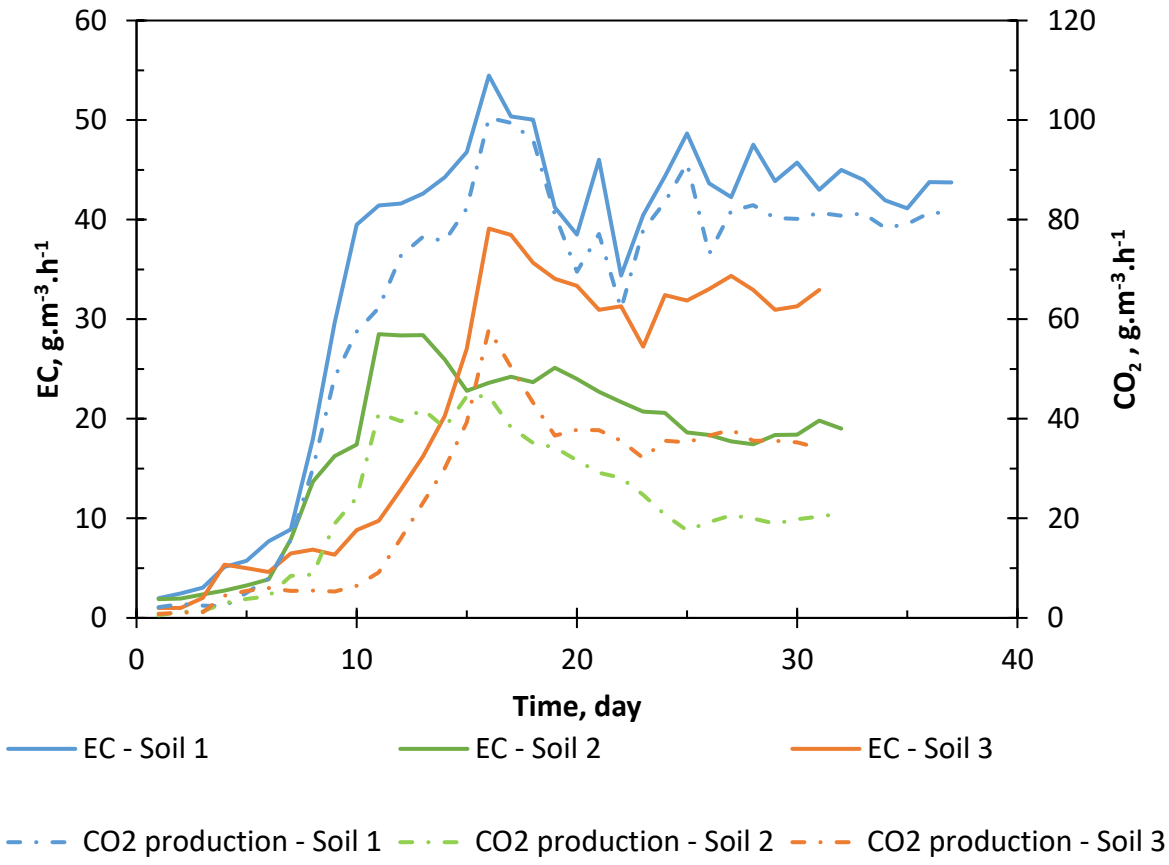


Figure 6.1: Methane elimination capacity and $CO_2$ production from soil samples operated at an inlet loading of 280 $g \cdot m^{-3} \cdot h^{-1}$ and matric potential of -10 $cm_{H_2O}$ at 40 °C.

The EC values ranged 19 – 44 $g \cdot m^{-3} \cdot h^{-1}$ depending on the soil type. These values were within the range of commonly reported EC values between 6 – 36 $g \cdot m^{-3} \cdot h^{-1}$ (Table 6.1) with similar methane concentrations (~ 2000 ppm). However, the inlet load used in the current study (280 $g \cdot m^{-3} \cdot h^{-1}$) was higher than majority of other studies (20 – 229 $g \cdot m^{-3} \cdot h^{-1}$). Meanwhile, the time taken for the biofilters to achieve steady state (2 – 3 weeks) was also within the range of the common values reported in the literature (1 – 3 weeks) (Nikiema et al., 2010, Kim et al., 2013). Both the EC and acclimation time values indicated that the three soil types were suitable as a packing material for $CH_4$ removal.

Table 6.1: EC values for methane biofiltration systems reported in the literature.

| **Type of biofilter and operation** | **Packing material** | **Inlet concentration (ppm)** | **Inlet load ($g \cdot m^{-3} \cdot h^{-1}$)** | **$EC_{max}$ ($g \cdot m^{-3} \cdot h^{-1}$)** | **References** |
|---|---|---|---|---|---|
| Biofilter - growth | Inorganic material, mature compost | 7000 – 7500 | 65 - 70 | 29.2 | Nikiema et al. (2005) |
| Biofilter – growth | Compost/perlite (40 : 60) | 760 – 8400 | 25 | 5 | Melse and Van der Werf (2005) |
| Biofilter - growth | Gravel | 300 – 2420 | 95 | 36 | Nikiema et al. (2009a) |
| Biofilter - growth | Rock particles | 1500 – 9500 | N/A | 43 | Nikiema et al. (2009b) |
| Biofilter - growth | Expanded Clay Rock | 750 – 9600 | 90 | 50 | Nikiema and Heitz (2010) |
| Biofilter - growth | Stone | 8000 | 75 | 45 | Nikiema et al. (2010) |
| Biofilter - growth | Inorganic material | 7000 – 7500 | 75 - 85 | 30 | Menard et al. (2011) |
| Biofilter – growth | Gravel | 250 – 4300 | 38 | 14 | Girard et al. (2011) |
| Biotrickingfilter - growth | Clay Spheres, Polypropylene Stones | 6800 – 7500 | 62 | 21 | Ramirez et al. (2012) |
| Biofilter – growth | Inorganic material | 9700 – 58200 | 31 | 23 | Kim et al. (2013) |
| Biotricklingfilter - growth | Polyurethane Foam | 5000 – 15000 | 229 | 30 | Estrada et al. (2014) |

| | | | | | |
|---|---|---|---|---|---|
| Biofilter – growth | Coal | 10000 | 139 | 45 | Limbri et al. (2014) |
| Biotrickingfilter - growth | Concrete | 960 | 33 | 6 | Ganendra et al. (2015) |
| Biofilter – growth | Compost | 20000 | 41 | 38 | Lebrero et al. (2016) |
| Biofilter – growth | Inorganic material | 1700 – 36300 | 20 | 6 | Brandt et al. (2016) |
| Biotrickling filter - growth | Polyethylene rings | 5000 – 39000 | 23 | 6 | Caceres et al. (2017) |
| Biofilter – growth | Stones | 1000 – 15000 | 33 | 10 | Ferdowsi et al. (2017) |
| Biofilter – growth | Polyurethane | 2000 | 40 | 8 | Gomez-Cuervo et al. (2017) |
| Biofilter – non growth | Leaf Compost | 1000 | 37 | 13 | Gunasekera et al. (2018) |
| Biofilter – growth | Inorganic material | 100 – 5000 | 30 | 15 | Ferdowsi et al. (2019) |
| Biofilter – non growth | Soil | 2050 ± 30 | 280 | 44 | Current study |

* Growth: supplemental nutrient addition; Non-growth: no nutrient addition

### 6.3.2 Impact of $CO_2$ on $CH_4$ removal and $CO_2$ production

Biofilters were exposed to a methane inlet concentration of 2055 ± 30 ppm by mixing pure $CH_4$ and ambient air ($CO_2$ concentration of 350 – 450 ppm). The biofilter packed with Soil 1 reached steady state with an average EC of 42 ± 0.9 $g \cdot m^{-3} \cdot h^{-1}$ and a $CO_2$ production of 71 ± 2.8 $g \cdot m^{-3} \cdot h^{-1}$ after 29 days of operation, while the biofilter with Soil 2 reached a steady-state EC of 30 ± 1.2 $g \cdot m^{-3} \cdot h^{-1}$ and $CO_2$ production of 54 ± 1.3 $g \cdot m^{-3} \cdot h^{-1}$ on day 19 (Figure 6.2). The steady state %$CO_2$ recovery of 67% and 28% were obtained for Soil 1 and Soil 2, respectively (data not shown).

Subsequently, the ambient air was switched to $CO_2$-free air, blended with pure $CH_4$ and fed to the Soil 1 biofilter (day 29) and to the Soil 2 biofilter (day 20). On day 21, the EC of the biofilter packed with Soil 2 dropped significantly (50%) to 19 $g \cdot m^{-3} \cdot h^{-1}$ whereas on day 30, the EC of biofilter was slightly decreased (10%) to 39 $g \cdot m^{-3} \cdot h^{-1}$. The EC dropped further to 28 $g \cdot m^{-3} \cdot h^{-1}$ in Soil 1 biofilter and to 19 $g \cdot m^{-3} \cdot h^{-1}$ in Soil 2 biofilter at the end of experiment. The $CO_2$ production was correlated with the EC trend which recorded a 45% decrease in Soil 1 biofilter and a 35% decrease in Soil 2 biofilter. On the contrary, the $\%CO_2$ recovery increased 15% in both biofilters, from 67% to 77% in Soil 1 biofilter and from 28% to 32% in Soil 2 biofilter (data not shown).

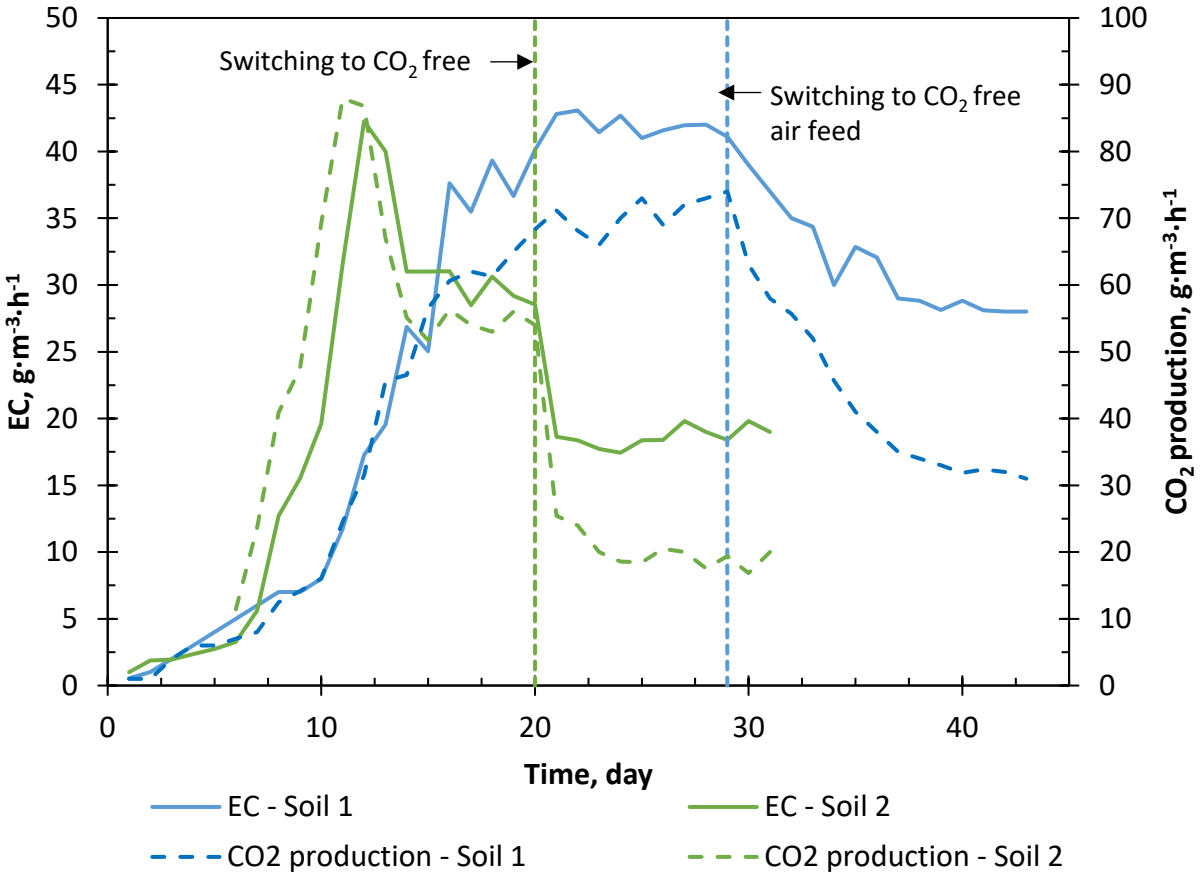


Figure 6.2: Elimination capacity and $CO_2$ production of the Soil 1 biofilter and Soil 2 biofilter as a function of time. Vertical dashed lines represent the switch from ambient air to $CO_2$-free air.

The t-test results clearly indicated a significant difference in the EC and $CO_2$ production between experiments with the presence of $CO_2$ and experiments feeding $CO_2$-free air (Table 6.2). These differences when switching from ambient air ($CO_2$ concentration of 350 – 450 ppm) to $CO_2$-free air could have been due to the change in microbial communities, from a mixture of heterotrophic and autotrophic methanotrophic consortia (utilizing $CO_2$ as the sole carbon source and $CH_4$ as the energy source) (van Bodegom et al., 2001) to a dominant heterotrophic-methanotrophic consortium (which utilized $CH_4$ as the main carbon source and energy source). The authotrophic methanotrophs (only grow with supplemental $CO_2$) could have grown in the presence of the $CO_2$, i.e. *Methylacidiphilum fumariolicum* strain SoIV (Acha et al., 2002, Khadem et al., 2011), member of the phylum *Verrucomicrobia* (Section 5.3.6). Further microbial community analysis is required to confirm the existence of autotrophic methanotrophs in the soil (Soil 1 and Soil 2).

Table 6.2: The t-test results comparing the mean of EC and $CO_2$ production for biofilters operated with and without $CO_2$ in the inlet feed with Soil 1 and Soil 2. Values are the mean of 7 days of operation at steady state at a given set of conditions.

| **Soil type** | **Mean EC ($g \cdot m^{-3} \cdot h^{-1}$)** | | | **$CO_2$ production ($g \cdot m^{-3} \cdot h^{-1}$)** | | |
|---|---|---|---|---|---|---|
| | Presence of $CO_2$ | Absence of $CO_2$ in the inlet feed | $p_{EC}$ value | Presence of $CO_2$ | Absence of $CO_2$ in the inlet feed | $p_{CO2}$ value |
| Soil 1 | 42 ± 0.9 | 28 ± 0.4 | < 0.01 | 71 ± 2.8 | 32 ± 1.0 | < 0.01 |
| Soil 2 | 30 ± 1.2 | 19 ± 0.7 | < 0.01 | 54 ± 1.4 | 19 ± 1.4 | <0.01 |

### 6.3.3 Impact of the operating conditions and soil type on $\%CO_2$ recovery

The $\%CO_2$ recovery of the biofilters varied across different soil types run at the two different operating conditions (Condition C and Condition D) (Figure 6.3). ANOVA results revealed that there was a significant difference in $\%CO_2$ recovery of the different the soil types ($p < 0.01$) (Table 6.3). Pairwise comparisons of mean $\%CO_2$ recovery further showed there was significant difference between each of the three soil samples, $p_{adj} < 0.05$ (Table 6.4). The highest mean $\%CO_2$ recovery of 66.5 ± 1.3% was recorded in Soil 1 whereas lowest mean $\%CO_2$ recovery of 39.3 ± 7.3% was observed in Soil 2. The mean $\%CO_2$ recovery of Soil 3 was 50.5 ± 6.8%. The operating conditions caused a significant difference ($p < 0.01$) in the $\%CO_2$ recovery. Condition C had a mean $\%CO_2$ recovery of 48 ± 14.8% while Condition D had 56.2 ± 14.8% mean $CO_2$ recovery. The mean $\%CO_2$ recovery of Soil 2 and Soil 3 increased 30% and 20%, respectively, for Condition D whereas no change was observed for $\%CO_2$ recovery of Soil 1. However, the interaction between soil type and operating conditions did not significantly affect the $\%CO_2$ recovery ($p = 0.13$). The soil type had the stronger effect ($\eta^2 = 0.73$) on the $\%CO_2$ recovery than the operating conditions ($\eta^2 = 0.11$) (Table 6.4).

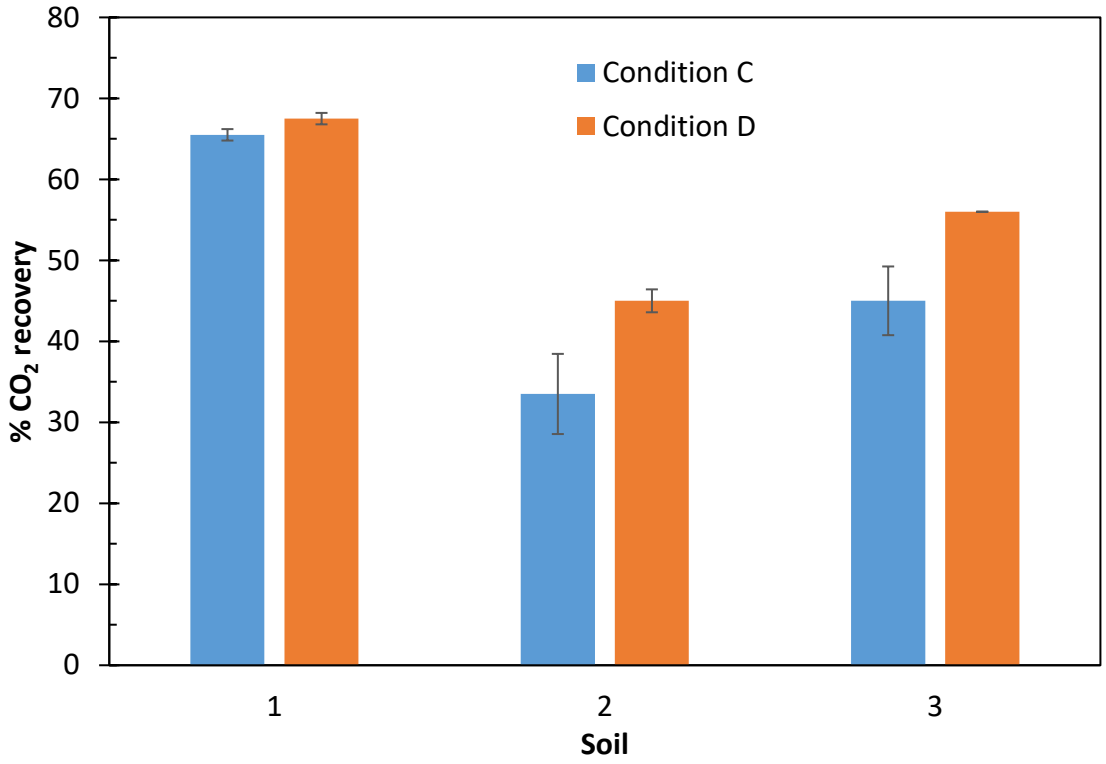


Figure 6.3: $\%CO_2$ recovery of soil samples operating at Condition C and Condition D. Values are the mean at steady state period at a given set of conditions. The error bars are the standard deviation from duplicate experiments.

Table 6.3: Summary of ANOVA results in which $\%CO_2$ recovery was modelled as a function of soil type and operating conditions.

| | **DF** | **Sum of Squares** | **Mean of Squares** | **F value** | ***p* value** | **$\eta^2$** |
|---|---|---|---|---|---|---|
| **Soil** | 2 | 1500.2 | 750.1 | 98.91 | <0.01 | 0.83 |
| **Condition** | 1 | 200.1 | 200.1 | 26.39 | < 0.01 | 0.11 |
| **Soil x Condition** | 2 | 57.2 | 28.6 | 3.77 | 0.13 | 0.03 |
| **Residuals** | 6 | 45.5 | 7.6 | | | |

Table 6.4: Summary of pairwise results comparing mean $\%CO_2$ recovery between operating conditions and between soil samples.

| Main effect | $p_{adj}$ value |
|---|---|
| **Conditions** | |
| Condition C – Condition D | <0.01 |
| **Soil** | |
| Soil 2 – Soil 1 | <0.01 |
| Soil 3 – Soil 1 | <0.01 |
| Soil 3 – Soil 2 | <0.01 |

The $\%CO_2$ recovery in the current work ranged from 37 – 68%. Comparing this range with what was typically reported (30 – 89%) (Table 4.2) was difficult due to the different operating conditions used in this study. There were no studies investigating the interaction of factors such as the water potential (water content), residual concentration and packing material on the $\%CO_2$ recovery in a methane biofilter due to the difficulty of controlling the variables that could potentially affect $\%CO_2$ recovery. For example, Syed et al. (2016) found 82% of the degraded methane was converted to $CO_2$ at day 29 with a soil moisture content of 100% (dry wt) whereas at day 90, only 32% $CO_2$ recovery was recorded with a soil moisture content of 80% (dry wt). At the same time, the pH of the soil dropped to 4.0 ± 0.3 from the initial pH of 5.1 ± 0.1 which shifted the microbial community which could have affected the $\%CO_2$ recovery. Brandt et al. (2016) observed the $CH_4$ mineralization rate of biofilters packed with mixture of composted leaves and three different non-organic materials was 100% after 182 days operation at steady state. However, these results were derived under varied environmental conditions such as methane inlet concentration (0.17% – 3.63% V/V) and operating

temperature (19 – 36 $^{o}$C) hence it was hard to evaluate the impact of packing material on the $\%CO_2$ recovery.

Limbri et al. (2014) observed a 50% increase on the $CO_2$ recovery, from 30% to 60% when increasing the inlet load from 13 $g \cdot m^{-3} \cdot h^{-1}$ to 104 $g \cdot m^{-3} \cdot h^{-1}$, respectively. In later work, Ferdowsi et al. (2016) found the similar increment (25%) in the $\%CO_2$ recovery when increasing the inlet load from 13 to 65 $g \cdot m^{-3} \cdot h^{-1}$ by changing the inlet concentration from 2000 to 10,000 ppm. The trend of these studies was similar with current study, where $\%CO_2$ recovery increased with increasing the inlet load. Results in Section 4.6 indicated that majority of the degraded carbon ended up in the form of either $CO_2$ (in the gas phase) or EPS/biomass, it is concluded that at low inlet loads and wet conditions, the degraded carbon was being incorporated to EPS/biomass rather than converted to $CO_2$. Nikiema et al. (2009a) observed the $CO_2$ production (< 20 $g \cdot m^{-3} \cdot h^{-1}$) for methane inlet loads ≤ 20 $g \cdot m^{-3} \cdot h^{-1}$ was lower than those (> 20 $g \cdot m^{-3} \cdot h^{-1}$) for inlet load ≥ 55 $g \cdot m^{-3} \cdot h^{-1}$ . Contradictory finding were reported by Caceres et al. (2017) who found the accumulated carbon increased more than doubled, from 0.1 – 0.2 $g \cdot m^{-3} \cdot h^{-1}$ to 0.4 – 0.5 $g \cdot m^{-3} \cdot h^{-1}$ when inlet loads of $CH_4$ was increased from < 10 $g \cdot m^{-3} \cdot h^{-1}$ to approximately 20 $g \cdot m^{-3} \cdot h^{-1}$. However, the moisture content of packing materials was not reported in Nikiema et al. (2009a) and Caceres et al. (2017) studies. In addition, these studies used a nutrient-supplemented biofilter which was known to affect the $\%CO_2$ recovery (Nikiema et al., 2009a) whereas the current study used a non-growth biofilter. Therefore, this hampered the comparison of results obtained in this study.

### 6.3.4 Impact of operating conditions and soil type on biofilter elimination capacity

The desired low and high values of residual methane concentration were achieved by using two levels of inlet load: 280 $g \cdot m^{-3} \cdot h^{-1}$ and 1268 $g \cdot m^{-3} \cdot h^{-1}$, respectively. At inlet load of 280 $g \cdot m^{-3} \cdot h^{-1}$ and at -10 $cm_{H_2O}$, the residual concentrations generated were: 1739 ± 43.1 ppm;

1868 ± 58 ppm and 1904 ± 53.7 ppm for Soil 1, Soil 2 and Soil 3, respectively. At the high inlet load of 1268 $g \cdot m^{-3} \cdot h^{-1}$ and at -100 $cm_{H_2O}$, the residual concentrations generated were: 8713 ± 174 ppm; 8930 ± 175 ppm and 8940 ± 102 ppm for Soil 1, Soil 2 and Soil 3, respectively (Figure 6.4).

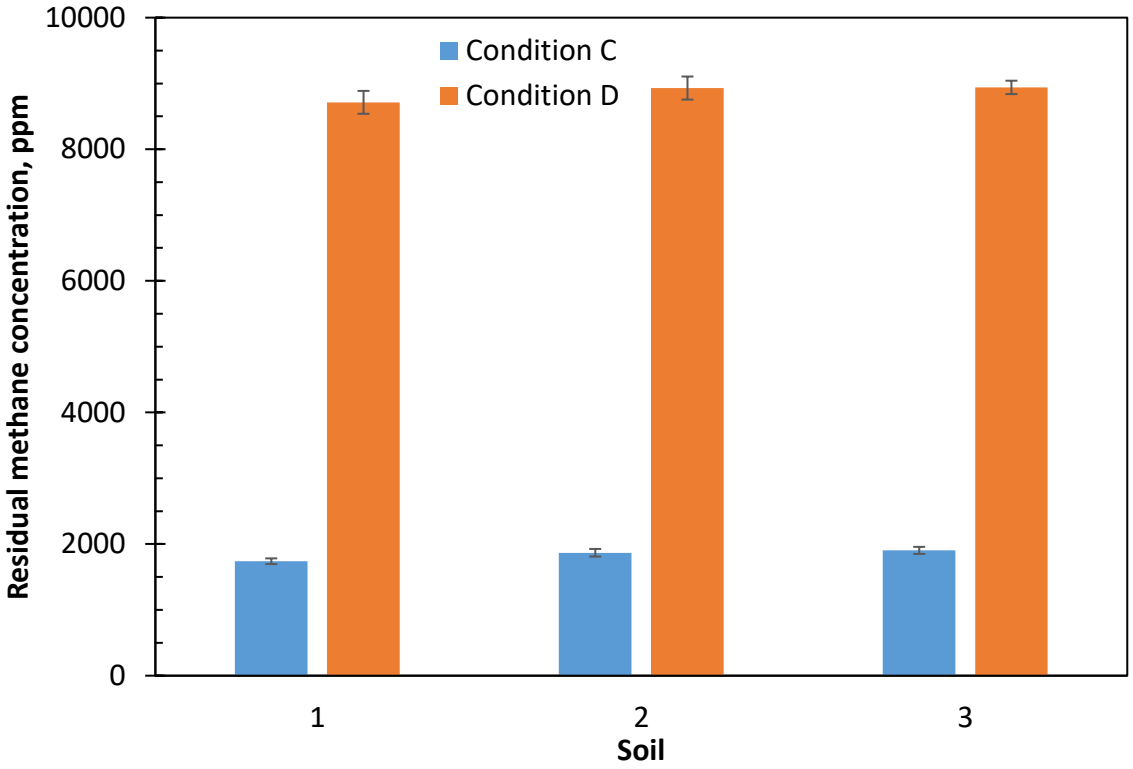


Figure 6.4: Residual methane concentration of soil samples operating at Condition C and Condition D. Values are the mean at steady state period at a given set of conditions. The error bars are the standard deviation from duplicate experiments.

The EC values were calculated based on residual concentrations obtained at varying inlet loads and matric potential. The EC for biofilters varied across different soil types and at different operating conditions (Condition C and Condition D) (Figure 6.5). Biofilters packed with different soil types exhibited significantly different methane removal rates (ANOVA, $p < 0.1$) (Table 6.5). Pairwise comparisons revealed the significant differences ($p_{adj}$ <0.05) for the EC of biofilters packed with Soil 1, 2 and 3 (Table 6.6). The highest mean EC of 46.5 ± 4.8 $g \cdot m^{-3} \cdot h^{-1}$

was observed with Soil 1 whereas lowest mean EC of 22 ± 3.5 $g \cdot m^{-3} \cdot h^{-1}$ was with Soil 2. Significant differences in the EC of biofilters run at different operating conditions (ANOVA, $p < 0.1$) were observed. The EC increased 35% when operating the biofilters at Condition D as compared to the biofilters at Condition C. When comparing the $\eta^2$ value, it showed that soil type had stronger effect ($\eta^2 = 0.72$) on the EC than the operating conditions ($\eta^2 = 0.19$). However, the interaction between soil type and conditions was not significant ($p = 0$).

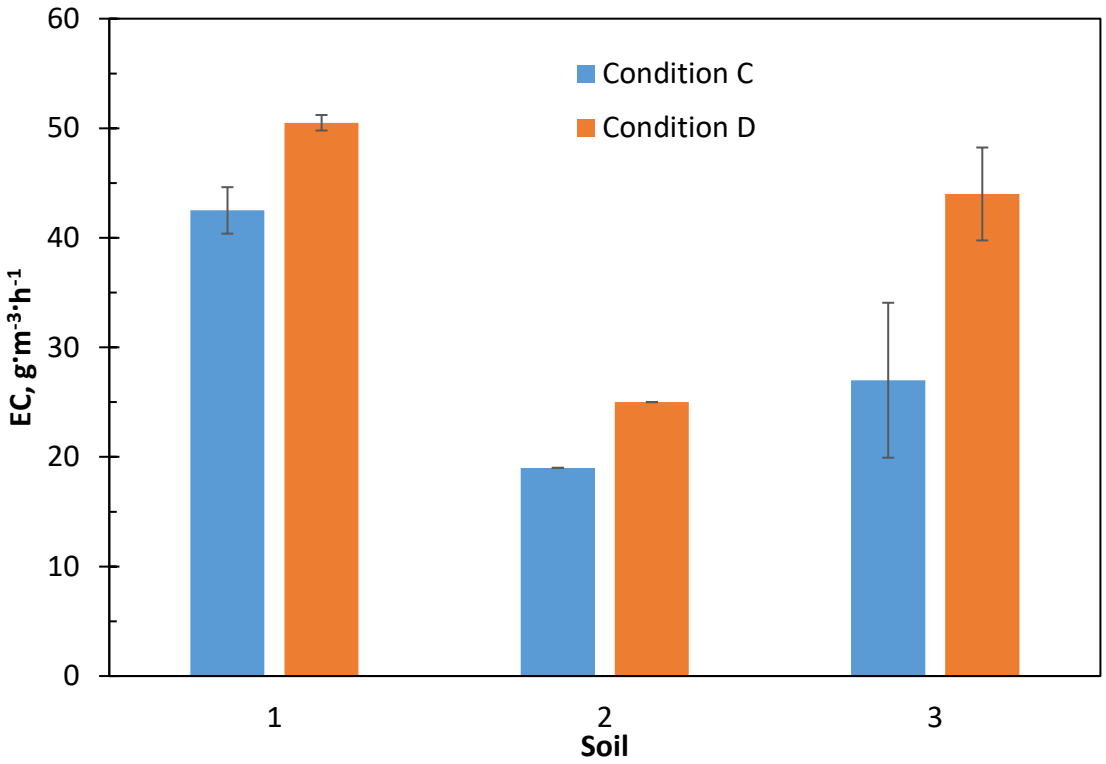


Figure 6.5: Methane elimination capacity of soil samples operating at Condition C and Condition D. Values are the mean at steady state at a given set of conditions. The error bars reported are the standard deviation from duplicate experiments.

Table 6.5: Summary of ANOVA results for methane EC as a function of operating conditions and soil type.

| | DF | Sum of Squares | Mean of Squares | F value | *p* value | $\eta^2$ |
|---|---|---|---|---|---|---|
| **Soil** | 2 | 1204.7 | 602.3 | 49.51 | < 0.01 | 0.72 |
| **Condition** | 1 | 382.7 | 382.7 | 26.33 | <0.01 | 0.19 |
| **Soil x Condition** | 2 | 52.1 | 26.1 | 2.82 | 0.13 | 0.04 |
| **Residuals** | 6 | 73 | 12.2 | | | |

Table 6.6: Summary of the pairwise results comparing mean methane EC between conditions and between soil samples.

| Main effect | $p_{adj}$ value |
|---|---|
| **Conditions** | |
| C - D | <0.01 |
| **Soil** | |
| Soil 2 – Soil 1 | <0.01 |
| Soil 3 – Soil 1 | 0.01 |
| Soil 3 – Soil 2 | <0.01 |

The EC values in this study varied between 19 – 51 $g \cdot m^{-3} \cdot h^{-1}$ depending on the soil type and operating conditions. Comparing the obtained EC values with the EC reported in the literature (5 – 50 $g \cdot m^{-3} \cdot h^{-1}$) was difficult due to the majority of other studies being performed at different operating conditions. This study used a non-growth system while other studies added nutrients intermittentlyto the biofilter (Nikiema et al., 2010) and/or were inoculated with methanotrophs (Brandt et al., 2016) or in a few cases by fungi (Lebrero et al., 2016).

The closest system to compare the operating conditions used in this study (i.e. high pollutant concentration with low moisture; low pollutant concentration with high moisture) was a soil biofilter with concurrent flow where the inlet side of the bed normally receives higher pollutant concentration (but has a lower water content) than the lower portions of the bed (with high moisture) (Alvarez-Hornos et al., 2008). Visvanathan et al. (1999) found high oxidation rates (4 x $10^{-6}$ $g_{CH4}\cdot(g_{soil})^{-1}\cdot h^{-1}$) at a depth between 10 and 40 cm below the surface (low moisture content, near the $CH_4$ feed) whereas the oxidation capacity at 80 cm depth (high moisture content, far the $CH_4$ feed) was very low (< 1x$10^{-6}$ $g_{CH4}\cdot(g_{soil})^{-1}\cdot h^{-1}$). Park et al. (2002) also found the oxidation rate followed the trend with the current study: a higher oxidation rate (4.5 – 15 $g_{CH4}\cdot m^{-2}\cdot d^{-1}$) was observed at the section near the feed port and drier treatment (5%) than the later portions with wetter conditions (13%) (2.5 – 6 $g_{CH4}\cdot m^{-2}\cdot d^{-1}$).

The mean EC increased from 29.5 ± 11.2 $g\cdot m^{-3}\cdot h^{-1}$ to 39.8 ± 13.6 $g\cdot m^{-3}\cdot h^{-1}$ when operating the biofilters at low residual methane concentrations (Condition C) as compared to the biofilters at higher residual concentrations (Condition D). This implied that the operating regime was diffusion-limited in the $CH_4$ concentrations range studied (1700 ppm – 9000 ppm) (Figure 6.4). The diffusion limitation was also observed in previous methane biofiltration studies (Nikiema et al., 2009b, Estrada et al., 2014, Gomez-Cuervo et al., 2017). Notably, Nikiema et al. (2009b) found the EC increased 6 times, from 5 to 30 $g\cdot m^{-3}\cdot h^{-1}$ after increasing the methane concentration from 1500 to 9500 ppm, which was in the similar range of residual concentrations tested with the current study. Girard et al. (2011) proposed another explanation of this phenomenon that at high methane inlet concentration the biofilter had supported of a larger microbial population as compared with lower concentration. However, no further experiment was conducted to confirm this hypothesis.

The soil type had the strong effect on the EC and the $\%CO_2$ recovery. These results show good agreement with what has been reported in the literature that packing materials play a critical role in achieving an efficient performance (Devinny et al., 1999, Baltrenas et al., 2015) and both the $\%CO_2$ recovery and EC follow similar trends during methane biofiltration (Nikiema et al., 2010, Nikiema and Heitz, 2010, Ferdowsi et al., 2016). In both conditions C and D, Soil 1 exhibited the highest performance (EC = 46 ± 4.8 $g \cdot m^{-3} \cdot h^{-1}$; $\%CO_2$ recovery = 66.5 ± 1.3%) whereas the lowest EC (22 ± 3.4 $g \cdot m^{-3} \cdot h^{-1}$) and $\%CO_2$ recovery (39.25 ± 7.2%) were observed in Soil 2. The C/N ratio is known as a possible reason for the differences in biofilter performance among three soil samples. Boeckx and VanCleemput (1996) found the methane oxidation rates of soil with high C/N ratios (> 24) was five times higher than those with low C/N ratios (< 13). Rigler and Zechmeister-Boltenstern (1999) suggested that soils with low C/N ratios could inhibit the methane oxidation due to the formation $NO_2^-$ from nitrification and denitrification processes. However, there was unlikely to have $NO_2^-$ in the system packed with Soil 1 since it was previously shown to be nitrogen-limited in regards to biomass growth (Detchanamurthy, 2013). The recommended C/N ratios for compost is from 25 – 35 (Bernal et al., 2009). However, there was a lack of studies determining the adequate C/N ratio for methane degradation in soil biofilters. In this study, the C/N ratios (11 – 14) (Section 5.3.1) between soil samples were fairly similar hence it was hard to evaluate its impact to the biofilter performance.

Another possible reason of the difference EC values was the nitrogen content. Literature revealed that the nitrogen content in the packing material could play an important role for VOC removal in general (Hwang et al., 2007) and methane removal in particular (Nikiema et al., 2007) . In the current study, Soil 1 and Soil 3 contained higher nitrogen content had better biofilter performances than Soil 2. However, there are possibilities of uncontrolled nitrogen

sources enters (i.e. nitrogen-fixing bacteria) to the Soil 2 and Soil 3 based biofilters. Further study to explore the relationship between the fate of nitrogen source and biofilter performance in more detail is suggested.

Several studies showed that methane degradation was lower in soils that had low moisture content (Park et al., 2002, Giani et al., 2002, Park et al., 2009). In the current study, this was demonstrated by Soil 2 which had the lowest water content in both conditions (0.37 ± 0.02 $g_w/g_{dry\ soil}$ at -10 $cm_{H_2O}$ and 0.22 ± 0.03 $g_w/g_{dry\ soil}$ at -100 $cm_{H_2O}$) (Section 5.3.1). However, Soil 1 (0.58 ± 0.02 $g_w/g_{dry\ soil}$ at -10 $cm_{H_2O}$ and 0.33 ± 0.02 $g_w/g_{dry\ soil}$ at -100 $cm_{H_2O}$) which had lower water content than Soil 3 (0.65 ± 0.03 $g_w/g_{dry\ soil}$ at -10 $cm_{H_2O}$ and 0.43 ± 0.04 $g_w/g_{dry\ soil}$ at -100 $cm_{H_2O}$) (Section 5.3.1) exhibited the highest degradation rate. Therefore, more tests should be done to come up with a definitive relationship between matric potential and degradation rate.

### 6.3.5 Microbial community analysis

DNA extraction was performed using the DNeasy PowerSoil Kit. After which the extracted DNA was sequenced using the Illumina Miseq high-throughput. Sequences were then analysed using the Illunmina MiSeq 2500 platform (Section 3.8).

**Overall microbial community diversity**

The Shannon Entropy's index and Simpson's index was lower for bioreactor soil samples post experiment than the fresh soil samples (Table 6.7). This trend was similar with those in toluene biofilters (as described in Section 5.3.6). The presence of the methane or toluene selected microorganisms capable of using it as theirs sole carbon source. Microorganisms capable of using metabolites from methane oxidation and toluene reduction would also appear. Certain microorganisms would die upon long-term starvation or because of predation. Thus, the microbial diversity increased for fresh soil samples than soil post-treatment samples

Among bioreactor soil samples operated at Condition C (a low residual concentration generated by an inlet load of 280 $g \cdot m^{-3} \cdot h^{-1}$, -10 $cm_{H_2O}$), Soil 3 had the highest microbial diversity (H' = 4.89, D = 0.98) whereas Soil 1 had the lowest microbial diversity (H' = 4.37, D = 0.92). The Shannon Entropy's index and Simpson's index in Soil 2 at Condition C were 4.81 and 0.98, respectively.

Table 6.7: Bacteria community diversity based on the ASVs from the V3-V4 region of DNA from soil samples pre- and post- methane exposure .

| Sample (*) | Shannon Entropy diversity index (H') | Simpson diversity index (D) |
|---|---|---|
| S1 | 5.13 | 0.98 |
| S2 | 5.46 | 0.99 |
| S3 | 5.02 | 0.97 |
| S1 – C | 4.37 | 0.92 |
| S2 – C | 4.81 | 0.98 |
| S3 – C | 4.89 | 0.98 |

* S1 to S3 = Soil type 1 to 3; C = Condition C

**Impact of operating conditions, soil type and contaminant on microbial community structure**

Soil samples pre-, post- toluene exposure and post-methane exposure was included in the NMDS analysis at ASV level to investigate the effects of contaminant on microbial

community structure (

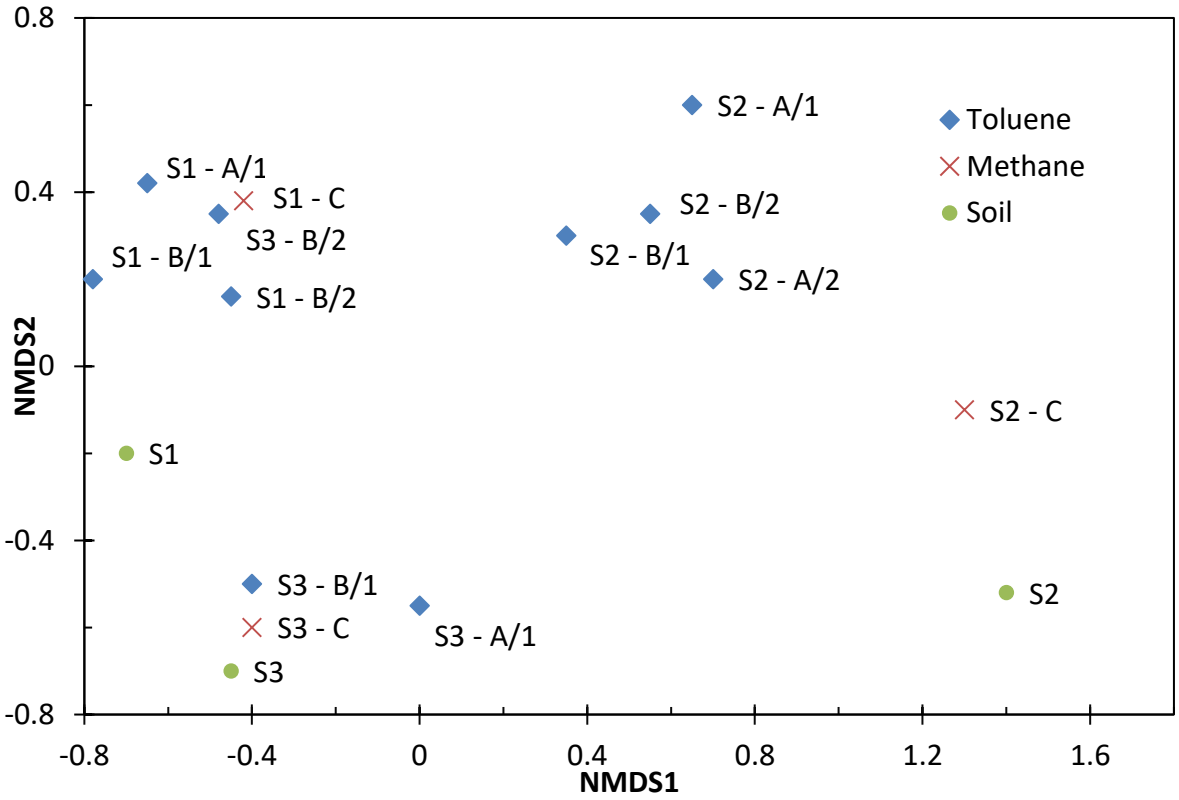


Figure 6.6). NMDS analysis at ASV level showed notable changes in the community structure for Soil 2 pre-, post- methane and post- toluene exposure. Soil 2 post-methane exposure at Condition C had a similar community structure with post-toluene exposure at Condition A and Condition B. Soil 1 pre- and post- methane exposure at Condition C had a similar community structure with Soil 1 post-toluene exposure at Condition A and Condition B. Soil 3 pre-, post-toluene and post-methane exposure at Condition A/1, Condition B/1 and Condition C had similar community structure. NMDS analysis revealed the differences in the community structure. It could be concluded that, the differences in the microbial community structure are mainly attributed to the soil type rather than the operating conditions, type of substrate during acclimation.

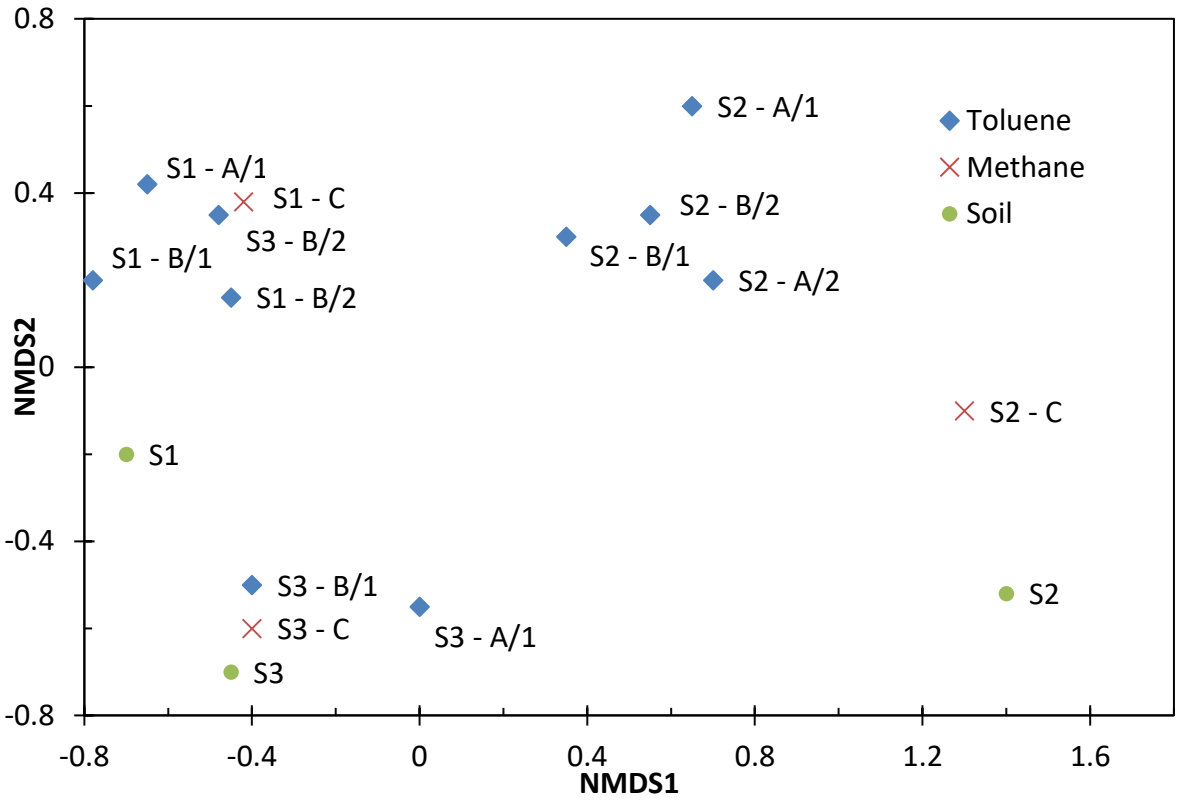


Figure 6.6: NMDS plot showing the community structure of different soil types pre- and post- methane and toluene exposure at different environmental conditions based on the sequencing of the V3-V4 region of the extracted DNA.

**Microbial community structure and composition**

At the end of the experiments, the relative abundance of *Proteobacteria* in all the three soil samples increased by 21 – 35% on an absolute % basis. A decrease in the relative abundance of other phyla was observed, for example *Chloroflex* decreased by 11 – 16%, *Actinobacteria* decreased by 3 – 25%.

*Proteobacteria* was the most abundant phyla in all three soil samples (relative abundance of 38 – 56%) (Figure 6.7). *Chloroflexi* was the second most abundant phyla (6.2 – 21%). The relative abundance of the phyla included *Actinobacteria (*5.8 – 9.5%*), Acidobacteria* (5.6 – 9.8%), *Gemmatimonadetes* (0.8 – 8.7%), *Planctomycetes* (3.8 – 8.2%), *Firmicutes* (2.3 – 7.7%)

and *Bacteroidetes* (4.2 – 6.5%) was shared at similar levels. Microorganisms in the phyla *Thaumarcheota*, *Verucomicrobia* and *Deinococcus-Thermus* were present in all soil samples, but only at lower levels < 4%.

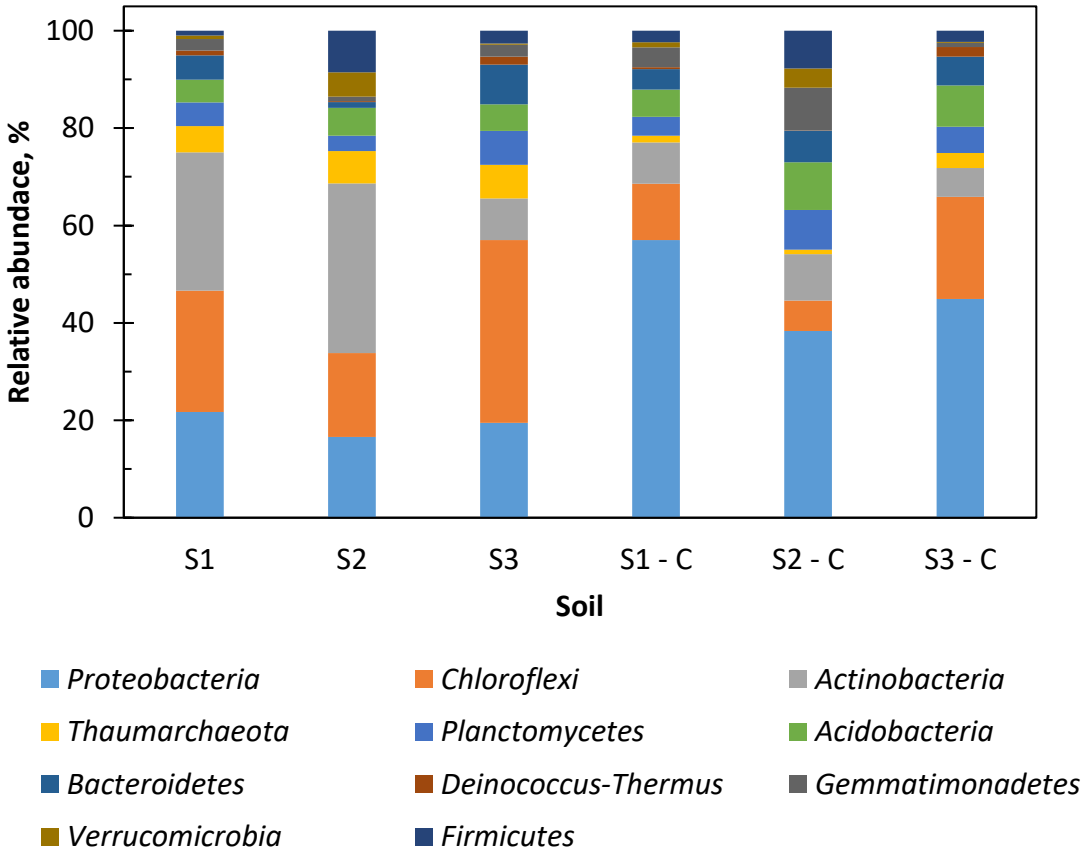


Figure 6.7: Barplot showing the relative abundances of microorganisms at the phylum level in the different soil types pre- and post- methane exposure at Condition C.

Two genera found after exposure to methane were *Methylocystis* and *Hyphomicrobium* (Figure 6.8). *Methylocystis* was the most dominant genera in the bioreactor soil samples and accounted for 20% of the total DNA or ~55% of the assigned genera. The second dominant genera was *Hyphomicrobium*, which accounted for 5% of the total DNA or 15% of the assigned genera. Both of these genera belonging to the phylum *Proteobacteria.* Conversely, the relative abundance of clustered groups in the unassigned genera made up less than 5% for individual

clusters (Table A.5 in Appendix D), which was assumed to have a negligible impact on the methane degradation.

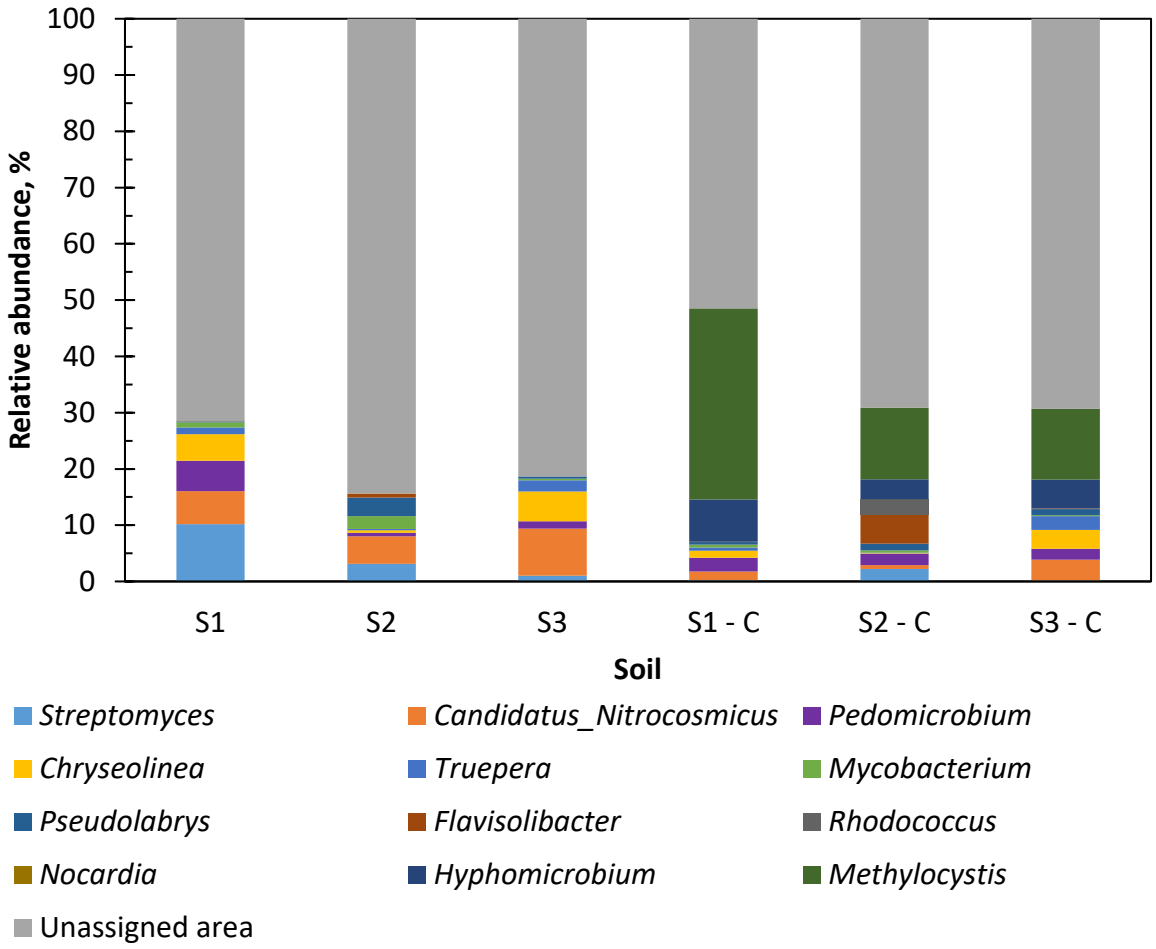


Figure 6.8: Barplot showing the relative abundances of microorganisms at the genus level in the different soil types pre- and post- methane exposure at Condition C.

The genus *Methylocystis* is a type II methanotroph which uses the serine pathway to assimilate carbon (Nikiema et al., 2005, Dam et al., 2012). Meanwhile, members of *Hyphomicrobium* are methylotrophic organisms that utilize C1 compounds via the serine pathway (Borodina et al., 2000, Borodina et al., 2002, Fujinawa et al., 2016). The co-existence of *Methylocystis* and *Hyphomicrobium* in soil samples may have been due to the cross feeding of methanotroph metabolites (i.e. methanol, formaldehyde) excreted by *Methylocystis* to *Hyphomicrobium*.

Previous studies also found a similar phenomenon that $CH_4$-C was incorporated into methylotrophs (Cebron et al., 2007, Krause et al., 2017). Krause et al. (2017) demonstrated that the methanol excreted by a methanotroph was the main carbon and energy source for the co-existing obligate methylotroph that utilized methanol exclusively. Takeuchi et al. (2019) reported organic acids such as formate and acetate produced by methanotrophs could be cross-feeding compounds to methylotrophs.

Cross-feeding on methanotrophic intermediates by *Hyphomicrobium* was shown to enhance the methanotrophic metabolic rate. Jeong and Kim (2019) observed the coexistence of *Hyphomicrobium* had a positive effect on the growth and activity of *Methylocystis* sp.M6. The methane oxidation rate increased 397%, from 3.5 ± 0.0 $mmol \cdot l^{-1} \cdot d^{-1}$ while using pure culture of *Methylocystis* to 17.4 ± 0.1 $mmol \cdot l^{-1} \cdot d^{-1}$ at *Methylocystis*: *Hyphomicrobium* mixing ratio of 1:14. In current study, the ratio of the genera *Methylocystis: Hyphomicrobium* was highest in Soil 1 (Condition C) (5:1) while in Soil 2 and Soil 3 at Condition C, the ratios were similar (3:1). However the relevant EC values at steady state of three soil types operated at a similar condition did not follow the order where Soil 1 had the highest EC of 44 $g \cdot m^{-3} \cdot h^{-1}$ followed by Soil 3 (33 $g \cdot m^{-3} \cdot h^{-1}$) then lowest EC of 19 $g \cdot m^{-3} \cdot h^{-1}$ was observed in Soil 2. The contradiction between this study and Jeong and Kim (2019) might be due to the different microbial consortium. Jeong and Kim (2019) used a synthetic microbial consortium containing only *Methylocystis* and *Hyphomicrobium* whereas mixed cultures (Soil) were used in this study. Moreover, more methylotrophs and methanotrophs could have been in the unassigned genera therefore it was difficult to say what the true methanotroph/methylotroph ratio was. Other factors such as packing materials characteristic (i.e. C/N ratio, moisture content) could have also contributed to the differences in the performance between these soil biofilters.

Therefore, it was hard to link the microbial communities of each soil samples with their biofilter performance.

### 6.4 Conclusions

This study evaluated the impact of combinations of soil type (Soil 1, Soil 2 and Soil 3) and operating conditions - moisture content (-10 $cm_{H_2O}$ and -100 $cm_{H_2O}$) and toluene residual concentration (low level: 1709 ppm to 1942 ppm and high level: 8590 ppm to 9054 ppm) - on biofilter performance in terms of EC and $\%CO_2$ recovery. The maximum mean EC of 50.5 ± 0.7 $g \cdot m^{-3} \cdot h^{-1}$ was found for the reactor packed with Soil 1 at 40 $^oC$ at the loading rate of 1268 $g \cdot m^{-3} \cdot h^{-1}$. The $\%CO_2$ recovery varied from 37 – 68%. The highest mean $\%CO_2$ recovery of 67.5 ± 0.7 % was recorded with Soil 1 exposed to methane inlet load of 1268 $g \cdot m^{-3} \cdot h^{-1}$ at -100 $cm_{H_2O}$.

The presence of $CO_2$ in the inlet feed stream showed impacts on the $CO_2$ production and biofilter performance (EC) packed with Soil 1 and Soil 2. At steady state, switching the biofilter packed with Soil 1 fed with methane-$CO_2$ free air (EC = 28 ± 0.4 $g \cdot m^{-3} \cdot h^{-1}$, $CO_2$ production = 32 ± 1.0 $g \cdot m^{-3} \cdot h^{-1}$) resulted in a 35% lower EC and a 45% lower $CO_2$ production than methane-laden air containing $CO_2$ (EC = 42 ± 0.9 $g \cdot m^{-3} \cdot h^{-1}$, $CO_2$ production = 71 ± 2.8 $g \cdot m^{-3} \cdot h^{-1}$). The same trend was observed for Soil 2 wherein the biofilter fed with methane-$CO_2$ free air (EC = 30 ± 1.2 $g \cdot m^{-3} \cdot h^{-1}$, $CO_2$ production = 54 ± 1.4 $g \cdot m^{-3} \cdot h^{-1}$) gave a 35% lower EC and a 65% lower $CO_2$ production than the one fed with methane-ambient air (EC = 19 ± 0.7 $g \cdot m^{-3} \cdot h^{-1}$, $CO_2$ production = 19 ± 1.4 $g \cdot m^{-3} \cdot h^{-1}$).

Biofilters operated at Condition C (EC = 29.5 ± 11.2 $g \cdot m^{-3} \cdot h^{-1}$, %CO2 recovery= 48 ± 14.8%) recorded a 35% lower mean of EC and 20% lower $\%CO_2$ recovery than operating at Condition D (EC = 39.8 ± 13.6 $g \cdot m^{-3} \cdot h^{-1}$, $\%CO_2$ recovery = 56.2 ± 11.9%) in all three soil types. Therefore, it was concluded that methane biofilters packed with soil performed better (EC and $\%CO_2$

recovery) when exposed to high substrate concentrations at drier conditions than low substrate concentrations at wetter conditions. These results were inconsistent with the hypothesis 2 from Bordoloi et al. (2019): operating the biofilter at lower residual concentration and wetter conditions would result in a higher $\%CO_2$ recovery than operating at higher residual concentration and drier conditions.

Preliminary results of microbial community analysis from different soil types post- methane exposure at Condition C found *Proteobacteria* was the most abundant phyla (>38%) of the total bacteria community in. Post-methane exposure, *Mythylocystis* (a type II methanotroph) and *Hyphomicrobium* (a methylotroph) were the most dominant (~ 55% of the assigned genera) and the second dominant genera (~ 15% of the assigned genera) in the soil samples post- methane exposure, respectively.

**References**

ACHA, V., ALBA, J. & THALASSO, F. 2002. The absolute requirement for carbon dioxide for aerobic methane oxidation by a methanotrophic-heterotrophic soil community of bacteria. *Biotechnology Letters,* 24**,** 675-679.

ALVAREZ-HORNOS, F. J., GABALDON, C., MARTINEZ-SORIA, V., MARZAL, P. & PENYA-ROJA, J. M. 2008. Biofiltration of toluene in the absence and the presence of ethyl acetate

under continuous and intermittent loading. *Journal of Chemical Technology and Biotechnology,* 83**,** 643-653.

BALTRENAS, P., ZAGORSKIS, A. & MISEVICIUS, A. 2015. Research into acetone removal from air by biofiltration using a biofilter with straight structure plates. *Biotechnology & Biotechnological Equipment,* 29**,** 404-413.

BERNAL, M. P., ALBURQUERQUE, J. A. & MORAL, R. 2009. Composting of animal manures and chemical criteria for compost maturity assessment. A review. *Bioresource Technology,* 100**,** 5444-5453.

BEUGER, A. L. 2008. *The impact of water content and other environmental parameters on toluene removal from air in a differential biofiltration reactor.* Doctor of Philosophy University of Canterbury

BOECKX, P. & VANCLEEMPUT, O. 1996. Methane oxidation in a neutral landfill cover soil: Influence of moisture content, temperature, and nitrogen-turnover. *Journal of Environmental Quality,* 25**,** 178-183.

BORDOLOI, A., GAPES, D. J. & GOSTOMSKI, P. A. 2019. The impact of environmental parameters on the conversion of toluene to CO2 and extracellular polymeric substances in a differential soil biofilter. *Chemosphere,* 232**,** 304-314.

BORODINA, E., KELLY, D. P., RAINEY, F. A., WARD-RAINEY, N. L. & WOOD, A. P. 2000. Dimethylsulfone as a growth substrate for novel methylotrophic species of *Hyphomicrobium* and *Arthrobacter*. *Archives of Microbiology,* 173**,** 425-437.

BORODINA, E., KELLY, D. P., SCHUMANN, P., RAINEY, F. A., WARD-RAINEY, N. L. & WOOD, A. P. 2002. Enzymes of dimethylsulfone metabolism and the phylogenetic characterization of the facultative methylotrophs *Arthrobacter sulfonivorans* sp nov.,

*Arthrobacter methylotrophus* sp nov., and *Hyphomicrobium sulfonivorans* sp. *Archives of Microbiology,* 177**,** 173-183.

BRANDT, E. M. F., DUARTE, F. V., VIEIRA, J. P. R., MELO, V. M., SOUZA, C. L., ARAUJO, J. C. & CHERNICHARO, C. A. L. 2016. The use of novel packing material for improving methane oxidation in biofilters. *Journal of Environmental Management,* 182**,** 412-420.

CACERES, M., DORADO, A. D., GENTINA, J. C. & AROCA, G. 2017. Oxidation of methane in biotrickling filters inoculated with methanotrophic bacteria. *Environmental Science and Pollution Research,* 24**,** 25702-25712.

CEBRON, A., BODROSSY, L., STRALIS-PAVESE, N., SINGER, A. C., THOMPSON, I. P., PROSSER, J. I. & MURRELL, J. C. 2007. Nutrient amendments in soil DNA stable isotope probing experiments reduce the observed methanotroph diversity. *Applied and Environmental Microbiology,* 73**,** 798-807.

DAM, B., DAM, S., KUBE, M., REINHARDT, R. & LIESACK, W. 2012. Complete genome sequence of *Methylocystis* sp strain sc2, an aerobic methanotroph with high-affinity methane oxidation potential. *Journal of Bacteriology,* 194**,** 6008-6009.

DETCHANAMURTHY, S. 2013. *Impact of different metabolic uncouplers on the specific degradation rate of toluene in a differential biofiltration reactor.* Doctor of Philosophy, University of Canterbury.

DETCHANAMURTHY, S. & GOSTOMSKI, P. A. 2015. Studies on the influence of different metabolic uncouplers on the biodegradation of toluene in a differential biofilter reactor. *Biotechnology and Bioprocess Engineering,* 20**,** 915-923.

DEVINNY, J. S., DESHUSSES, M. A. & WEBSTER, T. S. 1999. *Biofiltration for air pollution control,* United States of America, CRC press.

ESTRADA, J. M., LEBRERO, R., QUIJANO, G., PÉREZ, R., FIGUEROA-GONZÁLEZ, I., GARCÍA-ENCINA, P. A. & MUÑOZ, R. 2014. Methane abatement in a gas-recycling biotrickling filter: Evaluating innovative operational strategies to overcome mass transfer limitations. *Chemical Engineering Journal,* 253**,** 385-393.

FERDOWSI, M., DESROCHERS, M., JONES, J. P. & HEITZ, M. 2019. Moving from alcohol to methane biofilters: an experimental study on biofilter performance and carbon distribution. *Journal of Chemical Technology and Biotechnology***,** 10.

FERDOWSI, M., RAMIREZ, A. A., JONES, J. P. & HEITZ, M. 2017. Steady state and dynamic behaviors of a methane biofilter under periodic addition of ethanol vapors. *Journal of Environmental Management,* 197**,** 106-113.

FERDOWSI, M., VEILLETTE, M., RAMIREZ, A. A., JONES, J. P. & HEITZ, M. 2016. Performance Evaluation of a Methane Biofilter Under Steady State, Transient State and Starvation Conditions. *Water Air and Soil Pollution,* 227**,** 11.

FUJINAWA, K., ASAI, Y., MIYAHARA, M., KOUZUMA, A., ABE, T. & WATANABE, K. 2016. Genomic features of uncultured methylotrophs in activated-sludge microbiomes grown under different enrichment procedures. *Scientific Reports,* 6**,** 9.

GANENDRA, G., MERCADO-GARCIA, D., HERNANDEZ-SANABRIA, E., BOECKX, P., HO, A. & BOON, N. 2015. Methane biofiltration using autoclaved aerated concrete as the carrier material. *Applied Microbiology and Biotechnology,* 99**,** 7307-7320.

GIANI, L., BREDENKAMP, J. & EDEN, I. 2002. Temporal and spatial variability of the CH4 dynamics of landfill cover soils. *Journal of Plant Nutrition and Soil Science,* 165**,** 205-210.

GIRARD, M., RAMIREZ, A. A., BUELNA, G. & HEITZ, M. 2011. Biofiltration of methane at low concentrations representative of the piggery industry-Influence of the methane and nitrogen concentrations. *Chemical Engineering Journal,* 168**,** 151-158.

GOMEZ-CUERVO, S., ALFONSIN, C., HERNANDEZ, J., FEIJOO, G., MOREIRA, M. T. & OMIL, F. 2017. Diffuse methane emissions abatement by organic and inorganic packed biofilters: Assessment of operational and environmental indicators. *Journal of Cleaner Production,* 143**,** 1191-1202.

GUNASEKERA, S. S., HETTIARATCHI, J. P., BARTHOLAMEUZ, E. M., FARROKHZADEH, H. & IRVINE, E. 2018. A comparative evaluation of the performance of full-scale high-rate methane biofilter (HMBF) systems and flow-through laboratory columns. *Environmental Science and Pollution Research,* 25**,** 35845-35854.

HANSON, R. S. & HANSON, T. E. 1996. Methanotrophic bacteria. *Microbiol. Mol. Biol. Rev.,* 60**,** 439-471.

HERNANDEZ, J., GOMEZ-CUERVO, S. & OMIL, F. 2015. EPS and SMP as stability indicators during the biofiltration of diffuse methane emissions. *Water Air and Soil Pollution,* 226.

HWANG, J. W., JANG, S. J., LEE, E. Y., CHOI, C. Y. & PARK, S. 2007. Evaluation of composts as biofilter packing material for treatment of gaseous p-xylene. *Biochemical Engineering Journal,* 35**,** 142-149.

JEONG, S. Y. & KIM, T. G. 2019. Development of a novel methanotrophic process with the helper micro-organism *Hyphomicrobium* sp. NM3. *Journal of Applied Microbiology,* 126**,** 534-544.

KHADEM, A. F., POL, A., WIECZOREK, A., MOHAMMADI, S. S., FRANCOIJS, K. J., STUNNENBERG, H. G., JETTEN, M. S. M. & OP DEN CAMP, H. J. M. 2011. Autotrophic methanotrophy in

verrucomicrobia: *Methylacidiphilum fumariolicum* SolV uses the Calvin-Benson-Bassham cycle for carbon dioxide fixation. *Journal of Bacteriology,* 193**,** 4438-4446.

KIM, T. G., LEE, E. H. & CHO, K. S. 2013. Effects of nonmethane volatile organic compounds on microbial community of methanotrophic biofilter. *Applied Microbiology and Biotechnology,* 97**,** 6549-6559.

KRAUSE, S. M. B., JOHNSON, T., KARUNARATNE, Y. S., FU, Y. F., BECK, D. A. C., CHISTOSERDOVA, L. & LIDSTROM, M. E. 2017. Lanthanide-dependent cross-feeding of methane-derived carbon is linked by microbial community interactions. *Proceedings of the National Academy of Sciences of the United States of America,* 114**,** 358-363.

LA, H., HETTIARATCHI, J. P. A., ACHARI, G. & DUNFIELD, P. F. 2018. Biofiltration of methane. *Bioresource Technology,* 268**,** 759-772.

LEBRERO, R., LOPEZ, J. C., LEHTINEN, I., PEREZ, R., QUIJANO, G. & MUNOZ, R. 2016. Exploring the potential of fungi for methane abatement: Performance evaluation of a fungal-bacterial biofilter. *Chemosphere,* 144**,** 97-106.

LIMBRI, H., GUNAWAN, C., ROSCHE, B. & SCOTT, J. 2013. Challenges to developing methane biofiltration for coal mine ventilation air: A review. *Water Air and Soil Pollution,* 224.

LIMBRI, H., GUNAWAN, C., THOMAS, T., SMITH, A., SCOTT, J. & ROSCHE, B. 2014. Coal-packed methane biofilter for mitigation of green house gas emissions from coal mine ventilation air. *Plos One,* 9.

MELSE, R. W. & VAN DER WERF, A. W. 2005. Biofiltration for mitigation of methane emission from animal husbandry. *Environmental Science & Technology,* 39**,** 5460-5468.

MENARD, C., RAMIREZ, A. A., NIKIEMA, J. & HEITZ, M. 2011. Analysis of the effects of temperature, the amount of nutrient solution and the carbon dioxide concentration

on methane biofiltration. *International Journal of Sustainable Development and Planning,* 6**,** 312-324.

MFE 2019. New Zealand's greenhouse gas inventory 1990–2017.

MYHRE, G., SHINDELL, D., BRÉON, F.-M., COLLINS, W., FUGLESTVEDT, J., HUANG, J., KOCH, D., LAMARQUE, J.-F., LEE, D. & MENDOZA, B. 2013. Anthropogenic and natural radiative forcing. *Climate change,* 423**,** 658-740.

NIKIEMA, J., BIBEAU, L., LAVOIE, J., BRZEZINSKI, R., VIGNEUX, J. & HEITZ, M. 2005. Biofiltration of methane: An experimental study. *Chemical Engineering Journal,* 113**,** 111-117.

NIKIEMA, J., BRZEZINSKI, R. & HEITZ, M. 2007. Elimination of methane generated from landfills by biofiltration: a review. *Reviews in Environmental Science and Bio/Technology,* 6**,** 261-284.

NIKIEMA, J., BRZEZINSKI, R. & HEITZ, M. 2010. Influence of phosphorus, potassium, and copper on methane biofiltration performance. *Canadian Journal of Civil Engineering,* 37**,** 335-345.

NIKIEMA, J., GIRARD, M., BRZEZINSKI, R. & HEITZ, M. 2009a. Biofiltration of methane using an inorganic filter bed: Influence of inlet load and nitrogen concentration. *Canadian Journal of Civil Engineering,* 36**,** 1903-1910.

NIKIEMA, J. & HEITZ, M. 2010. The use of inorganic packing materials during methane biofiltration. *International Journal of Chemical Engineering,* 2010.

NIKIEMA, J., PAYRE, G. & HEITZ, M. 2009b. A mathematical steady state model for methane bioelimination in a closed biofilter. *Chemical Engineering Journal,* 150**,** 418-425.

PARK, S., BROWN, K. W. & THOMAS, J. C. 2002. The effect of various environmental and design parameters on methane oxidation in a model biofilter. *Waste Management & Research,* 20**,** 434-444.

PARK, S., LEE, C.-H., RYU, C.-R. & SUNG, K. 2009. Biofiltration for reducing methane emissions from modern sanitary landfills at the low methane generation stage. *Water, Air, and Soil Pollution,* 196**,** 19-27.

RAMIREZ, A. A., JONES, J. P. & HEITZ, M. 2012. Methane treatment in biotrickling filters packed with inert materials in presence of a non-ionic surfactant. *Journal of Chemical Technology and Biotechnology,* 87**,** 848-853.

REISINGER, A. 2018. The contribution of methane emission from New Zealand livestock to global warming. Palmerston North, New Zealand: New Zealand Agricultural Greenhouse Gas Research Centre (NZAGRC).

RIGLER, E. & ZECHMEISTER-BOLTENSTERN, S. 1999. Oxidation of ethylene and methane in forest soils - effect of CO2 and mineral nitrogen. *Geoderma,* 90**,** 147-159.

SADASIVAM, B. Y. & REDDY, K. R. 2015. Adsorption and transport of methane in landfill cover soil amended with waste-wood biochars. *Journal of Environmental Management,* 158**,** 11-23.

SIMONI, S. F., SCHAFER, A., HARMS, H. & ZEHNDER, A. J. B. 2001. Factors affecting mass transfer limited biodegradation in saturated porous media. *Journal of Contaminant Hydrology,* 50**,** 99-120.

STREESE, J. & STEGMANN, R. 2003. Microbial oxidation of methane from old landfills in biofilters. *Waste Management,* 23**,** 573-580.

SYED, R., SAGGAR, S., TATE, K. & REHM, B. H. A. 2016. Does acidification of a soil biofilter compromise its methane-oxidising capacity? *Biology and Fertility of Soils,* 52**,** 573-583.

TAKEUCHI, M., OZAKI, H., HIRAOKA, S., KAMAGATA, Y., SAKATA, S., YOSHIOKA, H. & IWASAKI, W. 2019. Possible cross-feeding pathway of facultative methylotroph

*Methyloceanibacter caenitepidi Gela4* on methanotroph *Methylocaldum marinum S8*. *Plos One,* 14**,** 19.

VAN BODEGOM, P., STAMS, F., MOLLEMA, L., BOEKE, S. & LEFFELAAR, P. 2001. Methane oxidation and the competition for oxygen in the rice rhizosphere. *Applied and Environmental Microbiology,* 67**,** 3586-3597.

VISVANATHAN, C., POKHREL, D., CHEIMCHAISRI, W., HETTIARATCHI, J. P. A. & WU, J. S. 1999. Methanotrophic activities in tropical landfill cover soils: effects of temperature, moisture content and methane concentration. *Waste Management and Research,* 17**,** 313-323.

# Chapter 7: The impact of toluene concentration on the performance of soil biofilters

## 7.1 Introduction

In the differential biofilter, the residual concentration referred to the contaminant concentration of the gas in the headspace (

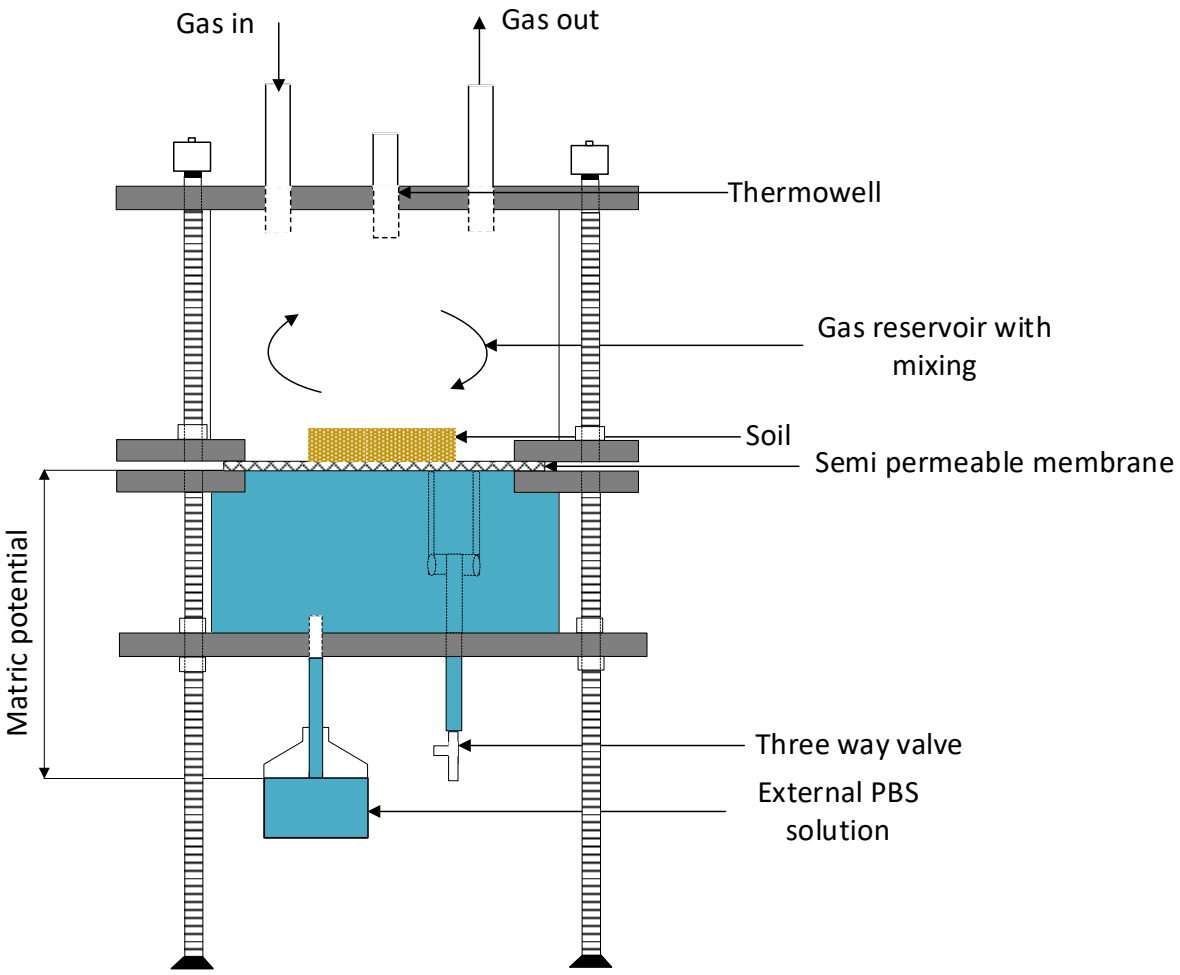


Figure 3.1). It was the concentration the biofilm was exposed to at steady state. Hence, the residual concentration rather than inlet concentration/inlet load was the crucial factor which could potentially affect the EC in the differential biofilter.

However, controlling the residual concentration was difficult. The residual toluene concentrations in Chapter 5 were varied between 9 ppm to 140 ppm depending on: operating

conditions (operating temperature, matric potential, inlet load), soil type (Soil 1, Soil 2 and Soil 3) and operating conditions. Controlling the value of the residual concentration with the use of a feedback control system would be helpful in making future experiments easier. In particular, a feedback control system enables experiments that would have the same residual concentration hence exploring the interactions between residual concentrations and other independent parameters (matric potential, temperature, inlet load etc.) easier.

The aim of this chapter is three-fold. First, it discusses the development of a feedback control system which controlled the toluene residual pollutant concentration through the online manipulation of the inlet concentration. Secondly, using this feedback control system, the relation between the residual concentrations and EC was investigated. Finally, the impact of toluene start-up concentration (residual concentration) on the EC was explored.

The impact of toluene concentration on EC for Soil 1 was explored in the Bordoloi and Gostomski (2019) study. They hypothesized that a higher EC could be attained by acclimating at a lower inlet concentration and associated residual concentration before increasing it to a higher value rather than starting the reactor at the higher inlet concentration. Specifically, EC was 100% higher in a pure culture system (*Pseudomonas putida)* and 70% higher in a mixed culture system (Soil 1) when reactors were started with an inlet feed concentration of 75 ppm and then increased to 120 ppm than when reactors were started at an inlet concentration of 120 ppm. However, their results were derived under variable residual concentrations hence this hypothesis was not explicit. With the development of the feedback control system, the impact of residual concentration on biofilter performance packed with different soil type (Soil 2) could be used to confirm and generalise their hypothesis.

## 7.2 Experimental methods

### 7.2.1 System improvement

There were two options to change the concentration of the toluene vapor generated in the diffusion system. The first option was to dilute a concentrated toluene air stream with clean air to change the inlet concentration (Nelson, 1971). The second option was to manipulate the temperature of the diffusion system which could cause a change in the vapour pressure and the diffusion coefficient and hence change the diffusion rate and subsequently the inlet toluene concentration (Appendix B). In this study, the second option was chosen as this option was more cost-effective than the first option, which would require two mass flow controllers for each reactor (Figure A.7 in Appendix F).

#### 7.2.1.1 Air bath system

An air bath system similar to water bath used to control the reactor temperature was developed (Figure 7.1). A 500 ml reagent bottle containing the diffusion flask (tube length = 0.09 m and inner diameter = 0.002 m) with toluene (HPLC grade) was placed inside a small plastic insulated box (width = 0.388 m, height = 0.305 m, depth = 0.245 m). The bottle was sealed with a plastic lid and had two fittings attached for inlet and outlet air flow. The temperature inside the box was controlled using a Love Controls temperature controller (Series 16B, Dwyer Instruments). It took an input from a temperature sensor (PT100) and controlled a silicone heater (60 W, Argus heating) and a cooling fan (16 W, Sunnon). An aluminium base was placed under the silicone heater to allow it to conduct heat out to fins exposed to the air inside the air bath. The temperature probe was positioned inside the reagent bottle to eliminate the difference of temperature between the box and inside the bottle.

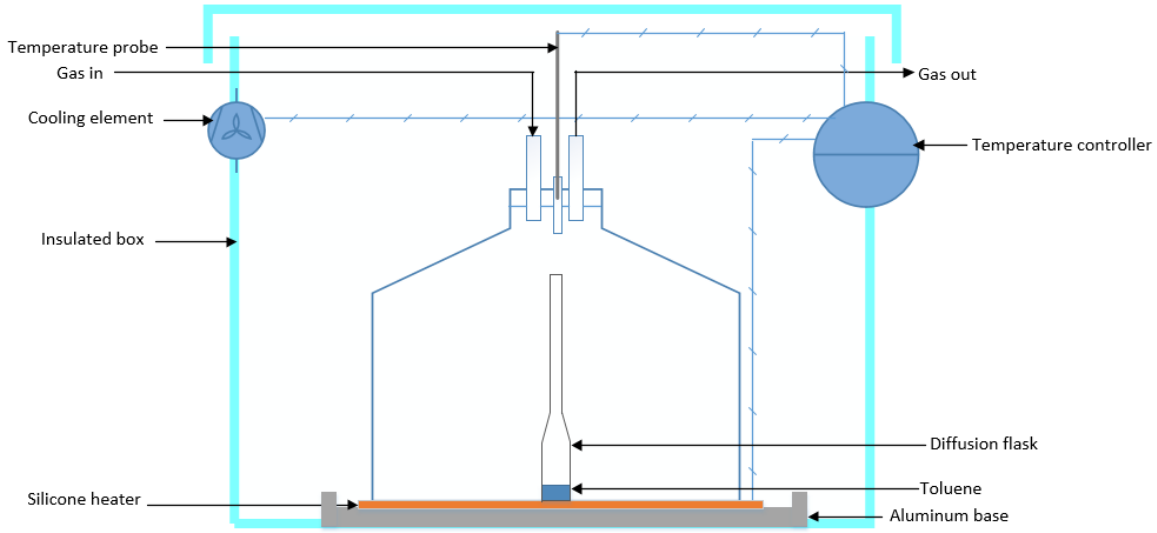


Figure 7.1: Schematic of the air bath system.

### 7.2.2 Feedback control system

#### 7.2.2.1 Feedback controller

A cascade controller was used in the current study (Figure 7.2). The primary controller was the PI controller. It was selected to regulate the residual concentration due to its ability to eliminate steady-state offset and rapidly reject disturbances. The PI controller received the residual concentration reading from the GC (Section 3.7.1) (Figure A.8 in Appendix G). LabVIEW software version 2012 (National Instruments, US) was used to deploy the PI controller and provide the signal to the PID temperature controller of the air bath (secondary controller) (Figure A.9 in Appendix G). The temperature controller was tuned by using the built-in auto tune function of the Love Controls controller. The temperature in the air bath as a result of the PID temperature control then dictated the concentration of toluene entering the reactor.

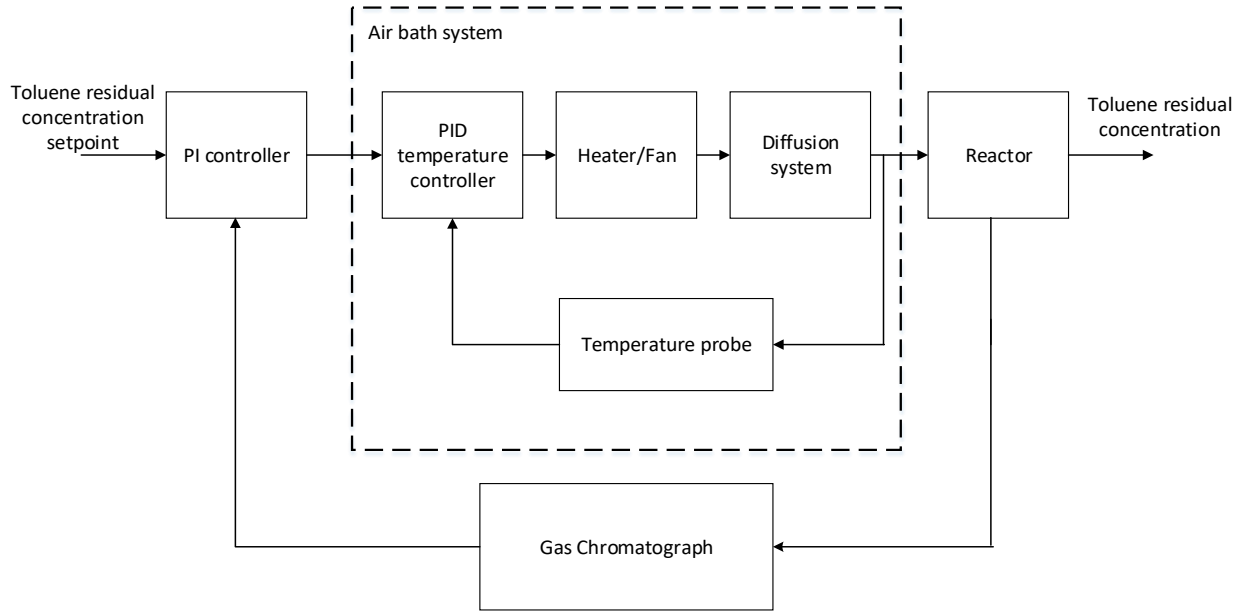


Figure 7.2: Schematic of the cascade control system.

### 7.2.2.2 Open-loop system

The parameters in the PI controller were determined using the process reaction curve proposed by Ziegler and Nichols (1942). The system's response was modelled as a first order with dead time system in the Laplace domain.

$$G_{(s)} = K_p \times \frac{e^{-\theta s}}{\tau s + 1} \qquad \text{(Equation 7.1)}$$

Where:

$G_{(s)}$ – transfer function represents the flow of signal through the PI controller

$K_p$ - the system gain, ppm/$^oC$

$\tau$ - the system time constant, hour

$\theta$ - the dead time, hour

The system was operated in open loop mode to determine the parameters from Equation 7.1. The biofilter was operated until achieving a steady state residual toluene concentration. At

this point, a disturbance was introduced by changing the setpoint temperature of the diffusion tube, which resulted in the change of the inlet toluene concentration. The residual concentration of the system was monitored as a function of time until achieving the new the steady state toluene concentration. The process reaction curve was generated based on the response of the biofilter to the change diffusion tube temperature.

#### 7.2.2.3 Closed-loop system

The closed-loop system was a fully automatic control system in which the desired residual concentration was maintained by adjusting the diffusion tube temperature to generate a new inlet toluene concentration. After reading each new residual concentration from the reactor, the controller was calculated the new diffusion tube temperature.

In this study, Ciancone correlations (Ciancone and Marlin, 1992) were used to estimate the tuning constants ($K_c$, $T_i$) according to the value of the parameters $K_p$, $\tau$ and $\theta$ estimated from the progress reaction curve (Figure 7.3). The discrete PI control algorithm was used to calculate the diffusion tube temperature at each execution (Marlin and Marlin, 1995):

$$\Delta MV_N = K_c \left( E_N - E_{N-1} + \frac{\Delta t}{T_I} E_N \right) \quad \text{(Equation 7.2)}$$

$$MV_N = MV_{N-1} + \Delta MV_N \quad \text{(Equation 7.3)}$$

$$E_N = SP_N - CV_N \quad \text{(Equation 7.4)}$$

Where:

$MV_N$ - the diffusion tube temperature at time N ($^o$C)

$MV_{N-1}$ - the diffusion tube temperature at time N-1 ($^o$C)

$E_N$ - the error between the desired value ($SP_N$) with the measured toluene concentration ($CV_N$) (ppm)

Δt - the execution period of the controller (h)

$T_i$ - integral time in the controller (h)

$K_c$ - the controller gain ($^o$ C /ppm)

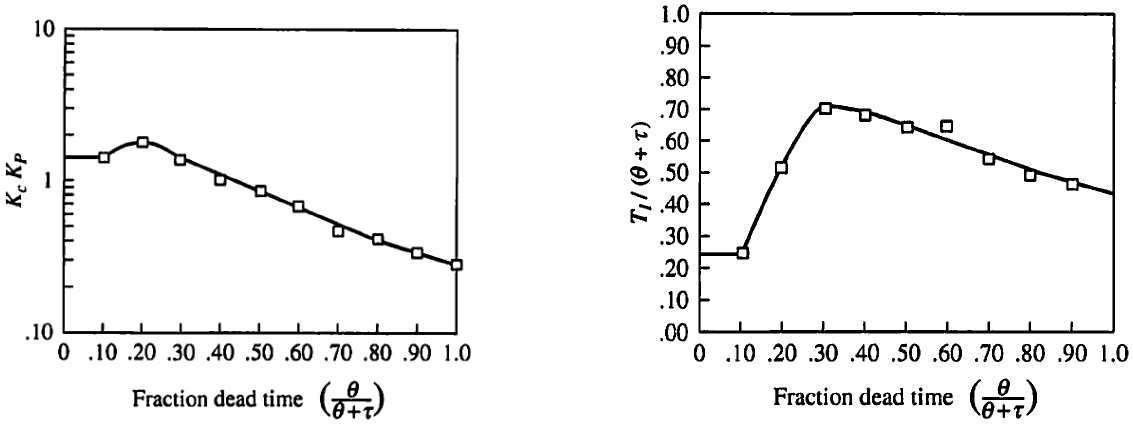


Figure 7.3: Ciancone correlations for dimensionless tuning constants developed by Ciancone and Marlin (1992).

The new inlet concentration ($C_{in\text{-}N}$, ppm) was estimated from the new diffusion tube temperature ($MV_n$, $^o$C) using the Equation 7.5 that was based on a power curve fit ($r^2$ = 0.996) (Figure A.10 in Appendix H) .A power curve fit was selected to describe the relationship between the inlet concentration and the diffusion tube temperature because of it had the higher $r^2$ value as compared to the linear ($r^2$ = 0.925) curve. Although logarithmic and other higher order curves also had $r^2$ greater than 0.99, power curve fit was chosen for simplicity.

$$C_{in\text{-}N} = \left(\frac{MV_N}{10.402}\right)^{1/0.338} \qquad \text{(Equation 7.5)}$$

## 7.3 Results and discussions

### 7.3.1 Air bath system performance

The performance of the air bath system was compared with that of a water bath at different operating temperatures (i.e. constant temperature and varying temperature conditions). Both systems were operated at the same flow rate of 25 ml·min$^{-1}$ and used a similar diffusion flask (tube length = 0.05 m and inner diameter = 0.0035 m).

At a temperature of 30 $^{o}$C and 35 $^{o}$C, the toluene concentrations generated by both systems were in good agreement with their respective theoretical estimates based on the equation stated in Figure A.2 in Appendix A.2 (Figure 7.4). The differences between the calculated and experimental concentration of toluene generated by both systems were between 6 - 10%. The generation of toluene contaminated air both systems was stable with a standard deviation less than 0.8% over 20 hours.

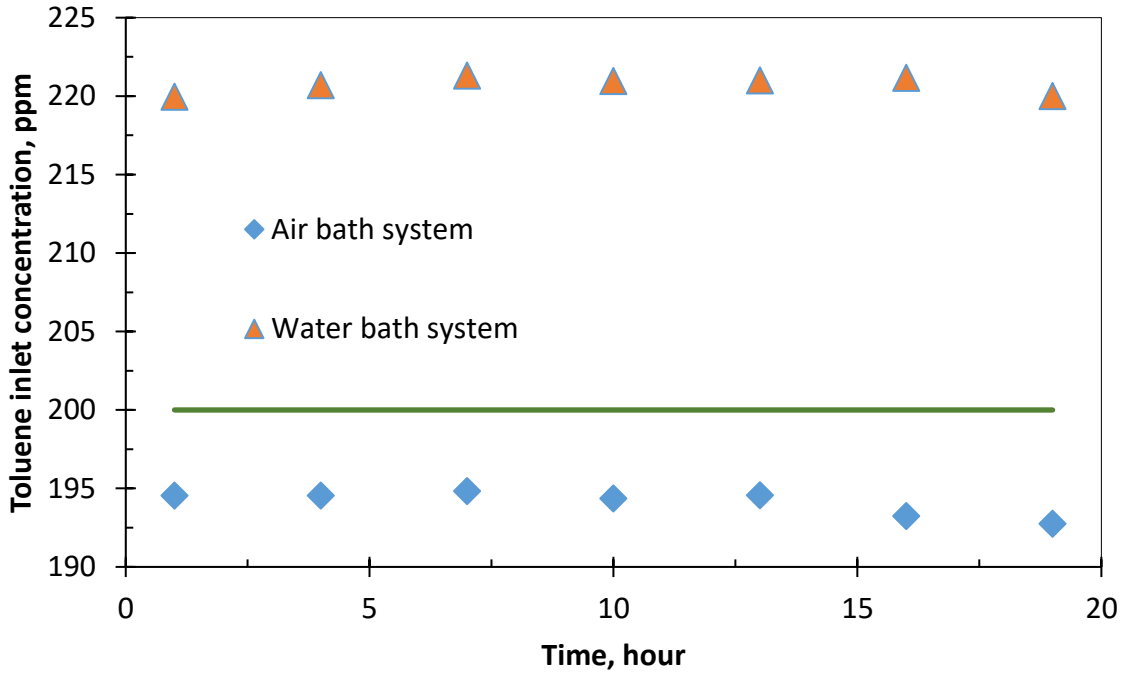


(a)

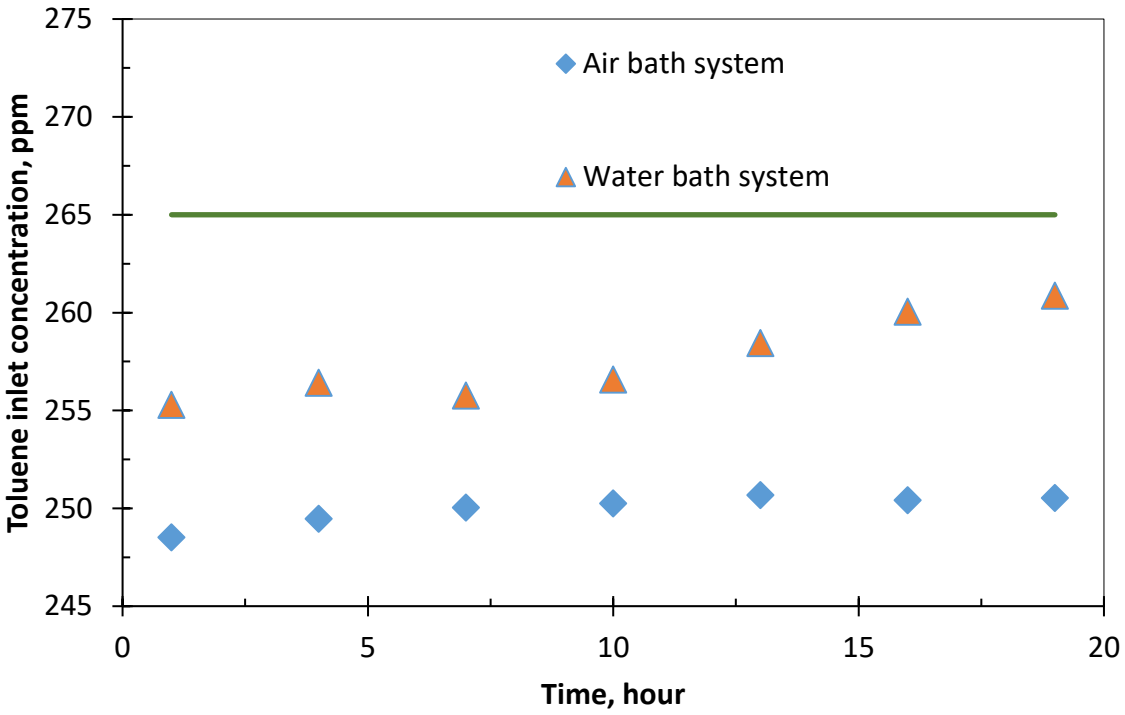


(b)

Figure 7.4: Toluene concentration generated using the air bath and water bath systems at (a) 30 °C; (b) 35 °C. The green line is the desired theoretical concentration.

The heating and cooling rate of the air bath and water bath system were explored by changing the operating temperature between 40 °C and 70 °C (Figure 7.5.). It took 0.4 hours to heat from 40 °C to 70 °C in the water bath system and 0.6 hours for the air bath system. However, the cooling process in air bath was almost nine times faster than cooling process in the water bath. As shown in the temperature time history (Figure 7.5), the air bath system took 0.6 hours to cool from 70 °C to 40 °C whereas it was approximately 6 hours in the water bath system. This difference was due to the presence of the cooling fan intergrated in the air bath system, while water bath with larger volume relied on passive heat loss to the environment.

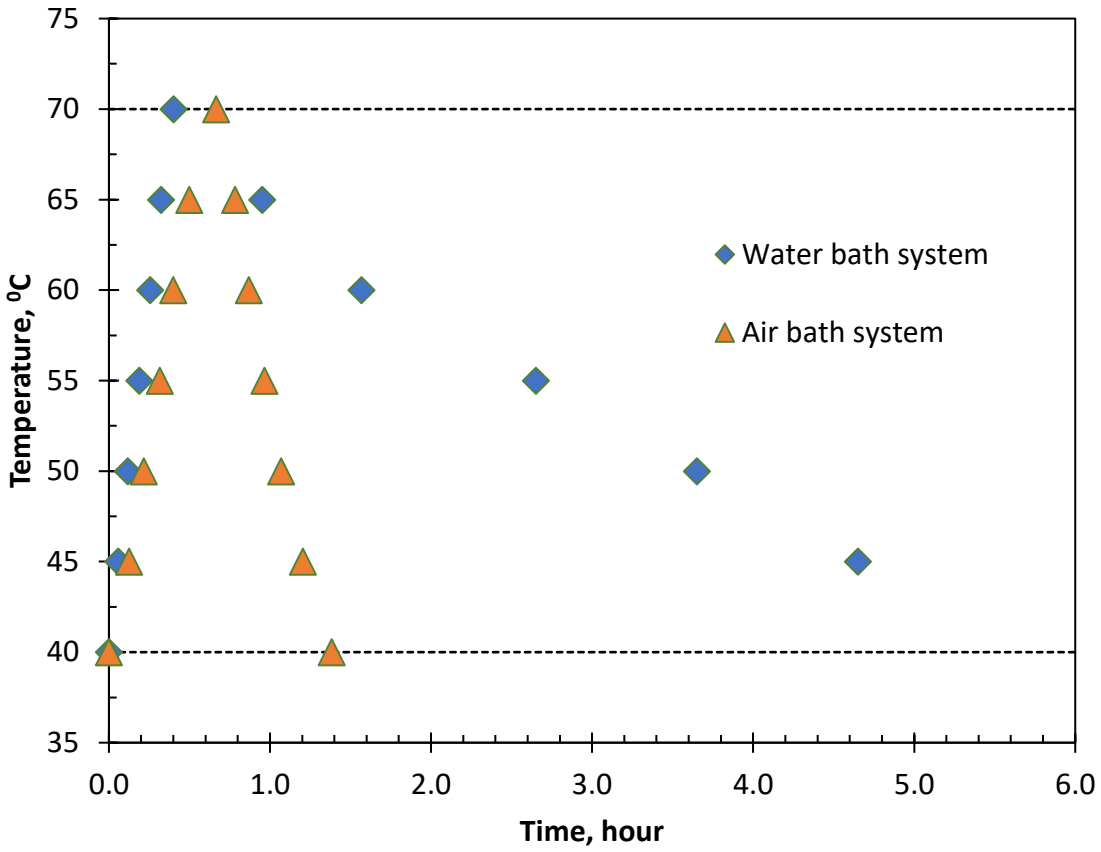


Figure 7.5: The temperature profile when changing the temperature setpoint from 40 °C – 70 °C – 40 °C in the water and air bath systems.

In conclusion, the air bath performed better than the water bath due to its faster dynamic response. The dynamic of the water bath could be improved by adding a fixed cooling load. The dynamic of the air bath could be improved by using a bigger heater, adding more fins and/or using bigger fan. However, the dynamics achieved with the present design i.e. maximum of 20 hours stabilization of inlet concentration was deemed enough for a biofilter system with at least 10 days to achieve steady state EC. Therefore, this was no longer pursued.

One of the disadvantages of the air bath over the water bath was its sensitivity to external disturbances (i.e. influent of the immediate surrounding air). However, this was minimized by

the insulation provided by the insulated box. On the other hand, the water bath provided thermal mass to minimize this kind of disturbances.

### 7.3.2 The process reaction curve

The process reaction experiment was performed on a biofilter packed with Soil 2. Instead of measuring the actual inlet concentration using the GC, its value was estimated using equation 7.5. This was done to avoid disruption in the continuous flow of inlet gas to the system which could affect reactor performance. However, the inlet concentration was measured once a day to confirm whether the actual concentration generated by the diffusion flask differed from the measured values by less than 5%. The system achieved steady state after 18 days of operation, at an EC of 27 ± 0.6 $g \cdot m^{-3} \cdot h^{-1}$ (Figure 7.6).

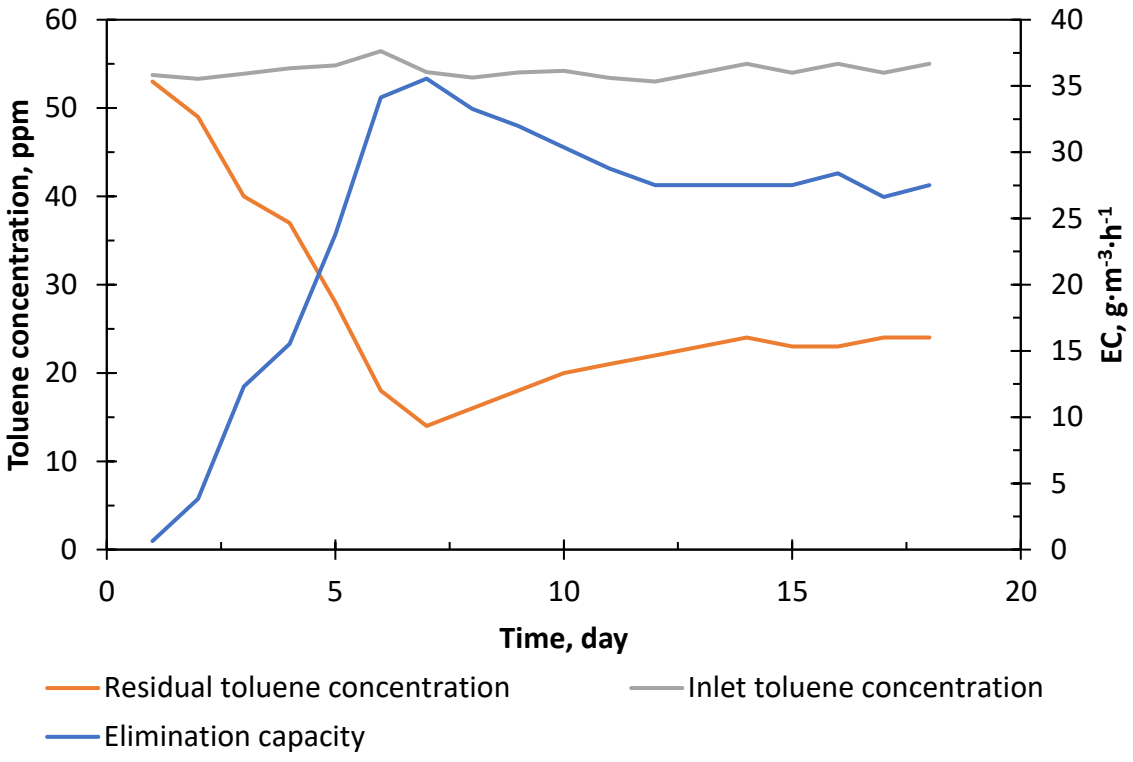


Figure 7.6: Gas concentration profile and elimination capacity of Soil 2 at an inlet concentration of 54.2 ± 0.8 ppm toluene and - 10 $cm_{H_2O}$ at 40 °C.

At day 19, the inlet concentration was increased from 53 ppm to 281 ppm by increasing the diffusion tube temperature from 40 °C to 70 °C. During this period, the toluene residual concentration increased by 98 ppm, from 9 ± 0.6 ppm to 107 ± 0.9 ppm. The residual concentration of the system and diffusion tube temperature was monitored as a function of time until reaching the new steady state (Figure 7.7).

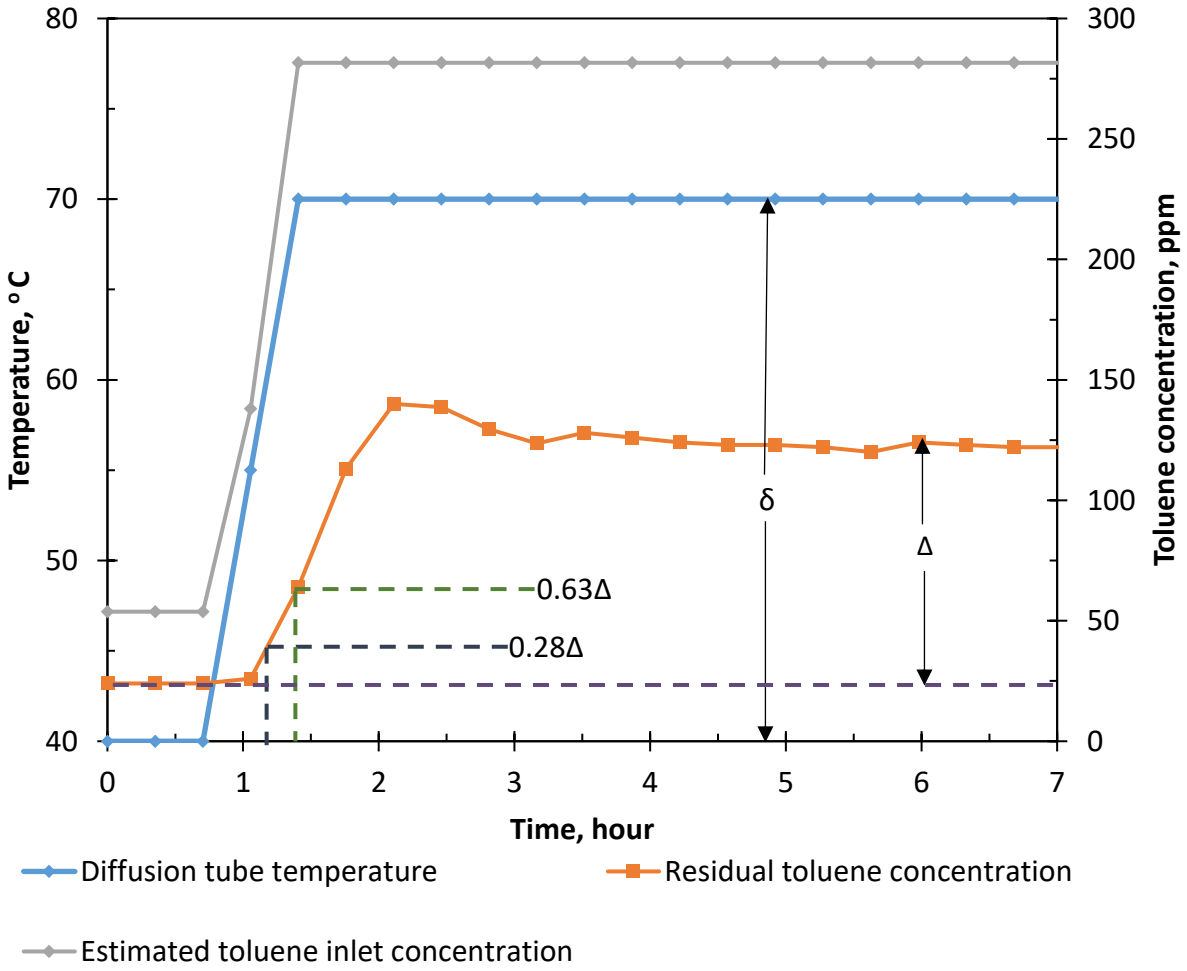


Figure 7.7: Process reaction curve in response of a change in the diffusion tube temperature.

Method II adapted from Marlin and Marlin (1995) was used to determine the steady state process gain ($K_p$), dead time (θ) and the time constant (τ) as follows:

$K_p = \Delta/\delta = 98/30 = 3.27$ (ppm/°C) (Equation 7.6)

$\tau = 1.5(t_{63\%} - t_{28\%}) = 1.5(1.4 - 1.1) = 0.45$ (hour) (Equation 7.7)

$\theta = (t_{63\%} - t_{0\%}) - \tau = (1.4 - 0.6) - 0.45 = 0.35$ (hour) (Equation 7.8)

Where:

$\Delta$ - the magnitude of the residual concentration change, ppm

$\delta$ - the magnitude of the diffusion tube temperature change, $^{o}C$

$t_{0\%}$; $t_{28\%}$ and $t_{63\%}$ - the time at which the residual concentration was 0%, 28% and 63% of its final steady state value, hour

Further experiments with multiple step changes of diffusion tube temperature were conducted to determine the linearity of the system (Figure 7.8). The magnitude of the step changes was based on the rough guideline (Marlin and Marlin, 1995) that the change of the diffusion tube temperature was large enough to cause a residual concentration change ($\Delta$) of at least five times the noise level (Marlin and Marlin, 1995) which was ± 0.6 ppm. The duration of a specific toluene concentration was at least 3.2 hours ($\theta + 4\tau$) after achieving the final steady state (Marlin and Marlin, 1995).

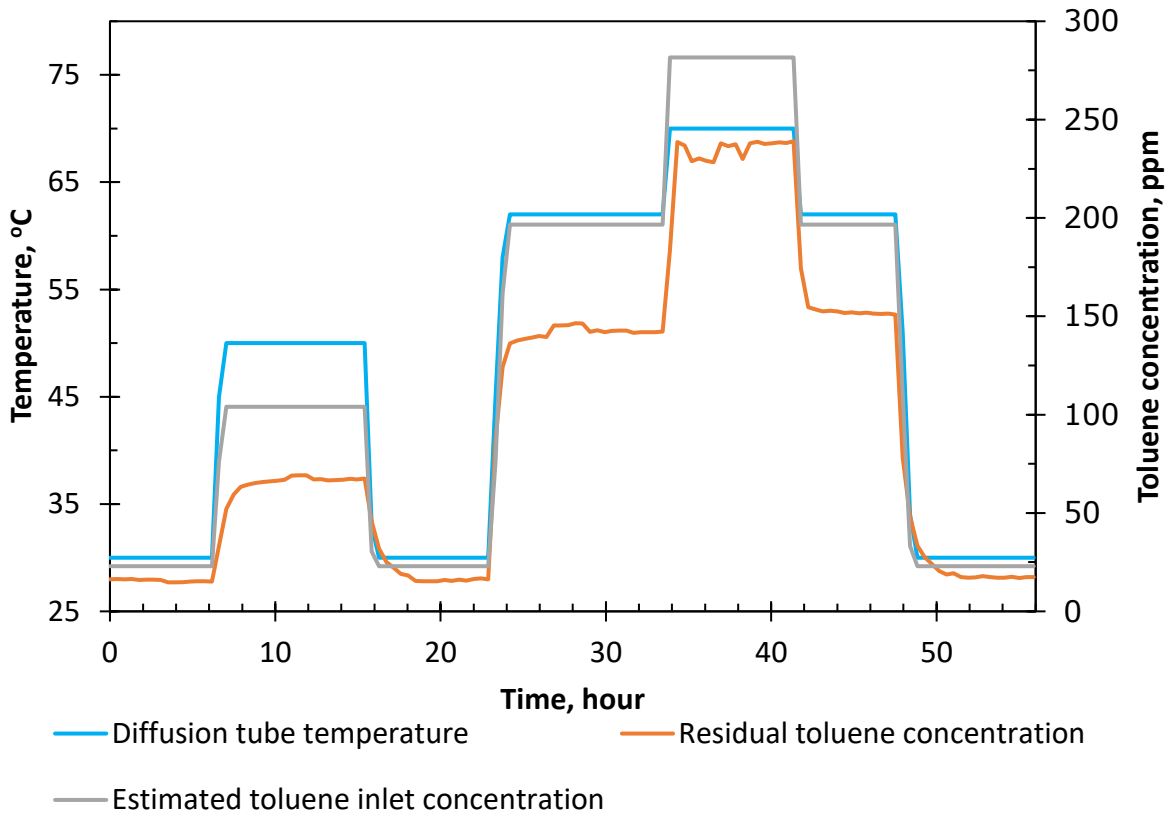


Figure 7.8: Process reaction curve in response to multiple changes in the diffusion tube temperature.

The temperature sequence was: 30 °C → 50 °C → 30 °C → 62 °C → 70 °C → 62 °C → 30 °C. The change in the inlet concentration was: 23 ppm → 104 ppm → 23 ppm → 197 ppm → 281 ppm → 197 ppm → 23 ppm. Hysteresis was observed at 62 °C, where the residual toluene concentration did not achieve the same value when the temperature was lowered (142 ppm) compared to when it was increased (151 ppm). The resulted residual concentration was: 16 ppm → 67 ppm → 16 ppm → 142 ppm → 239 ppm → 151 ppm → 17 ppm. This hysteresis may have been because the microorganisms subjected to concentration fluctuations require more time to reacclimatize or the community may have changed in some way (Cheng et al., 2016).

The difference between the controller gain, system time constant and dead time constant at higher residual concentration than those at lower residual concentration indicating that the system was non-linear (Table 7.1). The controller gain, system time constant and dead time constant changed when the residual concentration moved from a diffusion-limited (zero-order) to reaction-limited (first order) regions as describing in the operation of the biofilter in Section 7.3.4.

Table 7.1: Summary of process dynamics for the toluene biodegradation process.

| **Case** | **Estimated inlet concentration (ppm)** | **Residual concentration (ppm)** | **$K_p$ (ppm/$^oC$)** | **θ (hour)** | **τ (hour)** |
|---|---|---|---|---|---|
| A: 30 $^oC$ – 50 $^oC$ | 23 – 104 | 16 – 67 | 2.55 | 0.09 | 0.75 |
| B: 50 $^oC$ – 30 $^oC$ | 104 – 23 | 67 – 16 | 2.6 | 0.22 | 0.66 |
| C: 30 $^oC$ – 62 $^oC$ | 23 – 197 | 16 – 142 | 3.94 | 0.12 | 0.23 |
| D: 62 $^oC$ – 70 $^oC$ | 197 – 281 | 142 – 239 | 12 | 0.36 | 0.3 |
| E: 70 $^oC$ – 62 $^oC$ | 281 – 197 | 239 – 151 | 11 | 0.34 | 0.3 |
| D: 62 $^oC$ – 30 $^oC$ | 197 – 23 | 151 – 17 | 4.19 | 0.32 | 0.36 |

### 7.3.3 Feedback control system

#### 7.3.3.1 The controller tuning constants

The initial tuning constant values were calculated based on the process reaction curve in Figure 7.8 using correlations in Figure 7.3 (Table 7.2). The execution period (Δt) of 1.3 hour was selected as it was the interval time between each residual toluene measurement. The initial estimates tuning constants changed by 60% to 150% over the range of estimated inlet concentrations (23 ppm – 281 ppm).

Table 7.2: Summary of initial tuning constant values for the toluene biodegradation process.

| Case | Kc ($^oC$/ppm) | $T_i$ (hour) | Δt (hour) |
|---|---|---|---|
| A: 30 $^oC$ – 50 $^oC$ | 0.39 | 0.21 | 1.3 |
| B: 50 $^oC$ – 30 $^oC$ | 0.34 | 0.44 | |
| C: 30 $^oC$ – 62 $^oC$ | 0.24 | 0.23 | |
| D: 62 $^oC$ – 30 $^oC$ | 0.21 | 0.42 | |
| E: 62 $^oC$ – 70 $^oC$ | 0.06 | 0.34 | |
| F: 70 $^oC$ – 62 $^oC$ | 0.06 | 0.36 | |

Based on the Table 7.2, the least aggressive ($K_c$ = 0.06 °C/ppm, $T_i$ = 0.36 hour and $\Delta t$ = 1.3 hour) and the most aggressive ($K_c$ = 0.39 °C/ppm, $T_i$ = 0.21 hour, $\Delta t$ = 1.3 hour) were applied to the process to evaluate the closed-loop performance. These values were entered into Equation 7.2 for controller calculations to drive the residual concentration to the setpoint.

The results in Figure 7.9 (a) and (b) showed the dynamic responses of the closed loop system with $K_c$ = 0.39 °C/ppm, $T_i$ = 0.21 hour moving between toluene residual concentration setpoints of 10 ppm and of 110 ppm. When the setpoint was moved from 110 ppm to 10 ppm, the response was well behaved and achieved the new set-point. However, the controller dynamics when changing the setpoint back to 110 ppm was unacceptable because the system was unstable.

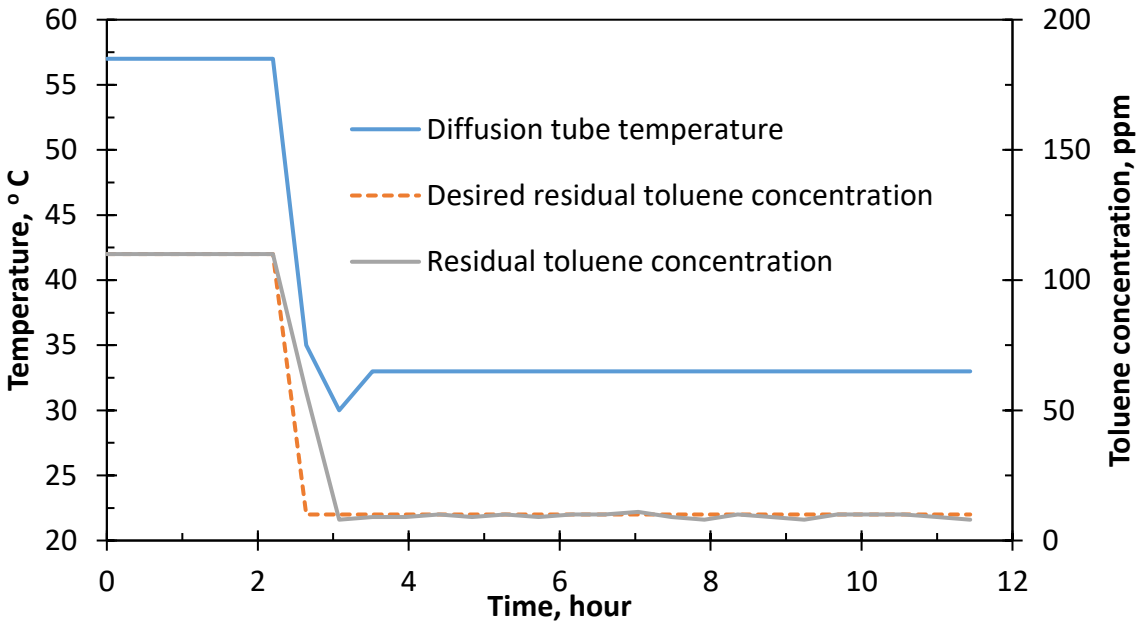


(a)

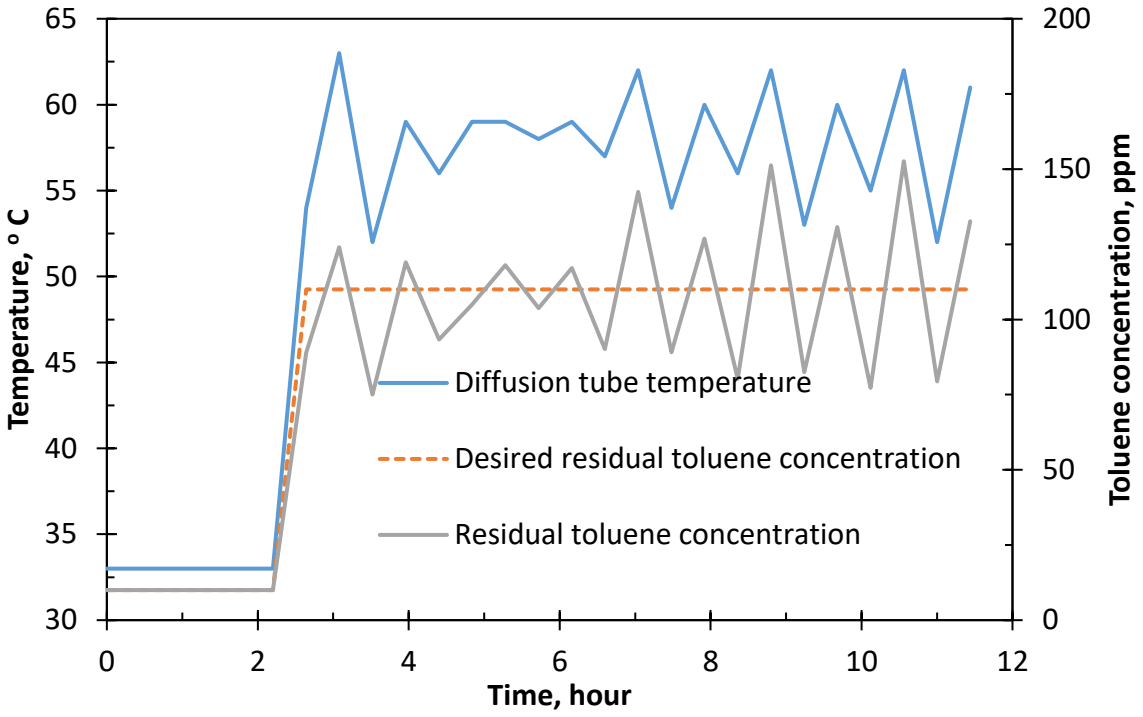


(b)

Figure 7.9: Dynamic response of feedback control system in the biofilter to a toluene residual concentration change of: (a) 10 ppm to 110 ppm; (b) 110 ppm to 10 ppm with tuning constants of $K_c$ = 0.39 $^oC$/ppm and $T_i$ = 0.21 hour.

Applying the less aggressive feedback controller parameters $K_c$ = 0.06 $^oC$/ppm, $T_i$ = 0.35 hour (Table 7.2) resulted in a good performance when changing the residual toluene setpoint from 10 ppm to 110 ppm Figure 7.10 (a). However, when moving to a 10 ppm setpoint, the performance was poorer, with a longer time (4 hours) required to achieve the desired value than the previous set of tuning constants, $K_c$ = 0.39 $^oC$/ppm, $T_i$ = 0.21 hour (2 hours) (Figure 7.10 (b)).

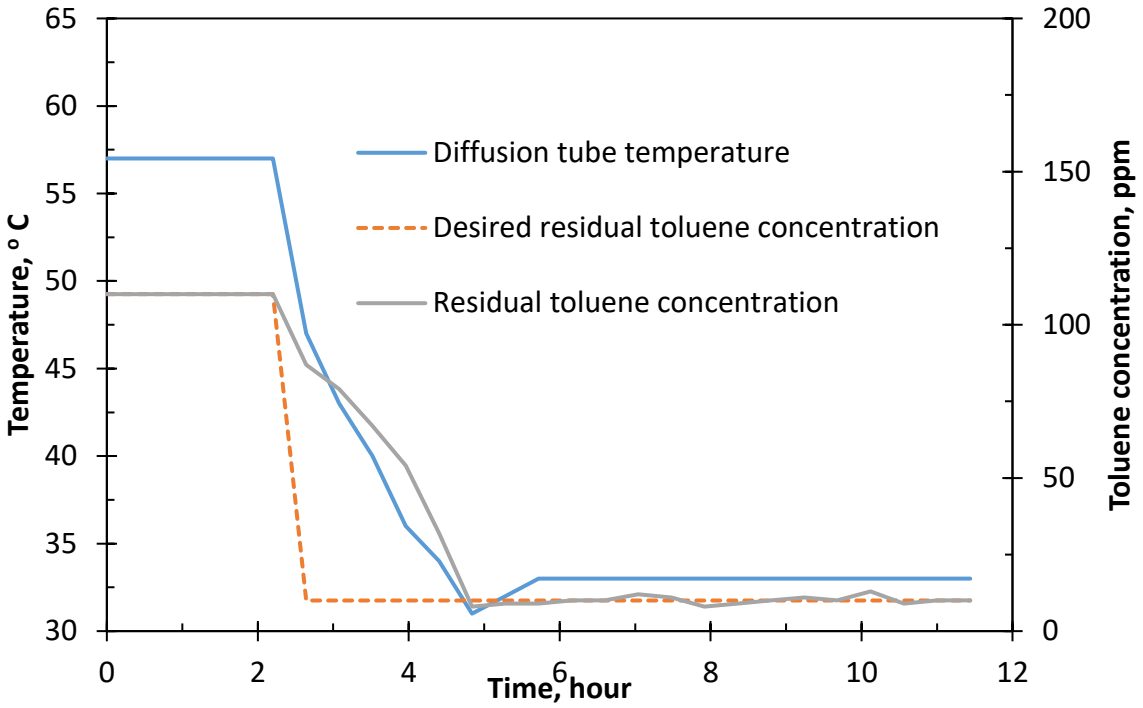


(a)

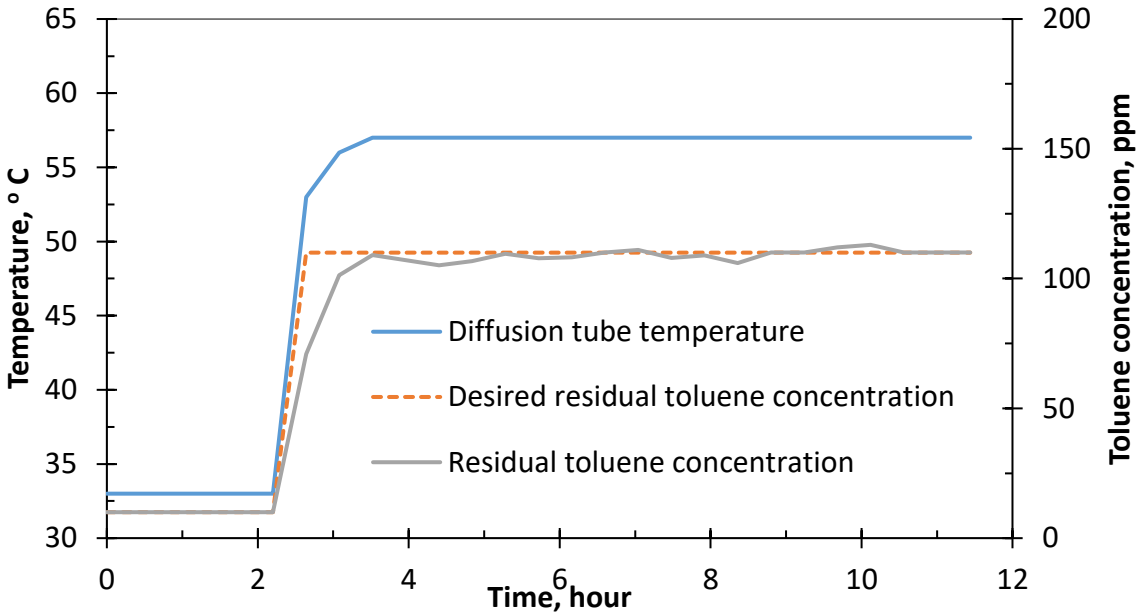


(b)

Figure 7.10: Dynamic response of the feedback control system in the biofilter to setpoint change of: (a) 10 ppm to 110 ppm; (b) 110 ppm to 10 ppm with tuning constants of $K_c$ = 0.06 $^{o}$C/ppm and $T_i$ = 0.36 hour.

These results indicated that maintaining constant controller tuning values did not provide a good control performance. The simplest control design approach started with the most aggressive set of tuning constants ($K_c$ = 0.39 $^oC$/ppm, $T_i$ = 0.21 hour, $\Delta t$=1.3 hour) and detuned by adjusting the controller gains based on the initial tuning values when the control system became highly oscillatory or unstable. The gain scheduling would be required if regularly changing setpoints between different gain settings.

#### 7.3.3.2 Disturbance rejection

The differential biofilter is subject to external disturbances that could affect the residual concentration (Bordoloi, 2016). In this study, the biofilter reactor operating temperature was changed from 20 $^oC$ to 40 $^oC$ to 20 $^oC$ (Figure 7.11). The feedback controller with tuning parameters $K_c$ = 0.39 $^oC$/ppm, $T_i$ = 0.21 hour was applied to maintain the residual toluene concentration at 80 ppm.

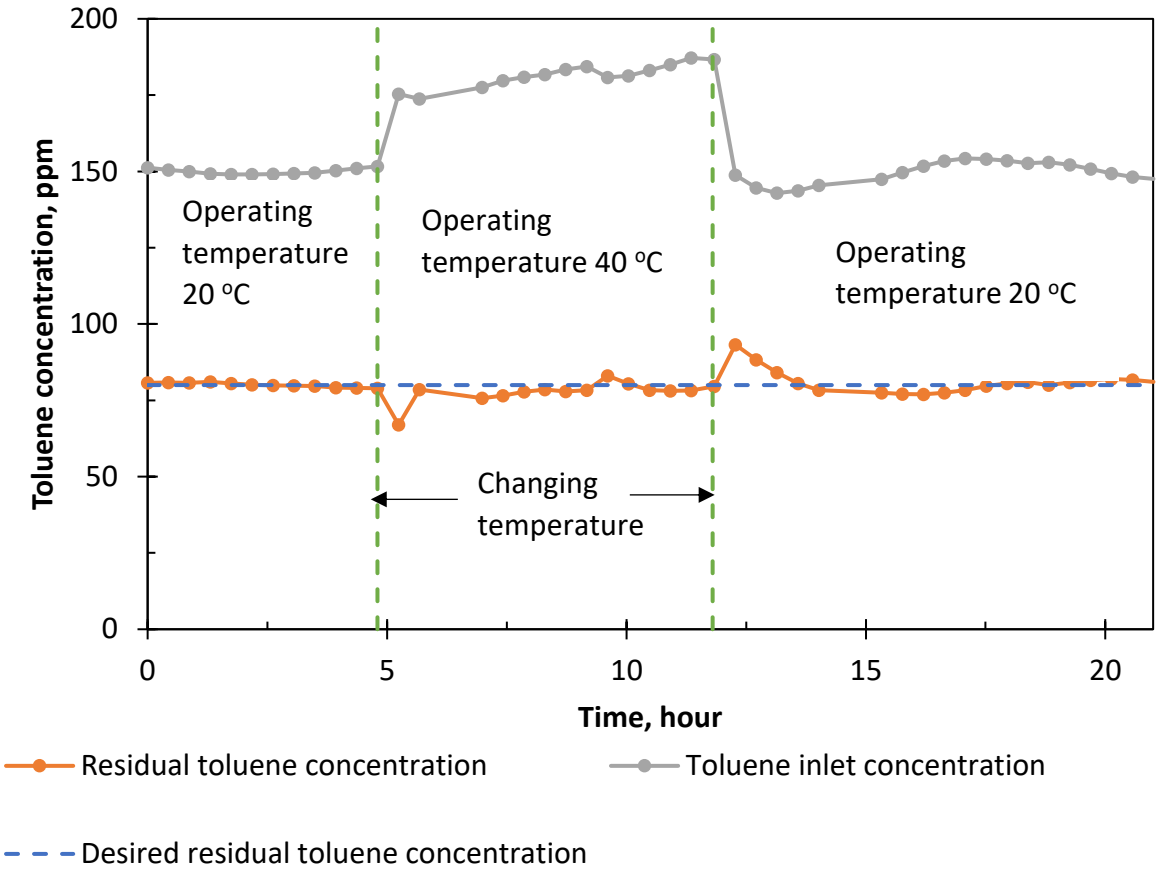


Figure 7.11: Variation of residual concentration with time with a change in the reactor operating temperature.

The results showed the feedback controller kept the residual concentration close (1 – 3 ppm) to the desired value by changing the inlet concentration. At 20 °C, the mean residual concentration and inlet concentration were 80.1 ± 0.7 ppm and 150 ± 0.9 ppm, respectively. The residual concentration dropped from 79 ppm to 67 ppm after increasing the reactor operating temperature from 20 °C to 40 °C. The mean inlet concentration increased from 150 ± 0.9 ppm to 182 ± 3.7 ppm to drive the residual concentration to the desired value (~ 80 ppm). At 40 °C, the mean residual concentration was 79 ± 1.8 ppm. Subsequently, the operating temperature was decreased from 40 °C to 20 °C. The residual concentration increased from 80 ppm to 93 ppm up-on the change of operating temperature. Consequently,

the controller took 1 hour to drive the residual concentration from 93 ppm to 81 ppm. After that, the residual concentration (80 ± 1.8 ppm) remained constant with the inlet concentration of 151 ± 2.7 ppm.

The residual concentration profiles in the open loop and closed loop systems were compared to show that latter rejected disturbances in the biofilters (Figure 7.12). This rejection of the disturbances resulted in a constant residual concentration in a closed loop system. This test was done when both systems were at a residual concentration of 50 ± 2 ppm then the operating temperature of two systems decreased from 40 °C to 20 °C.

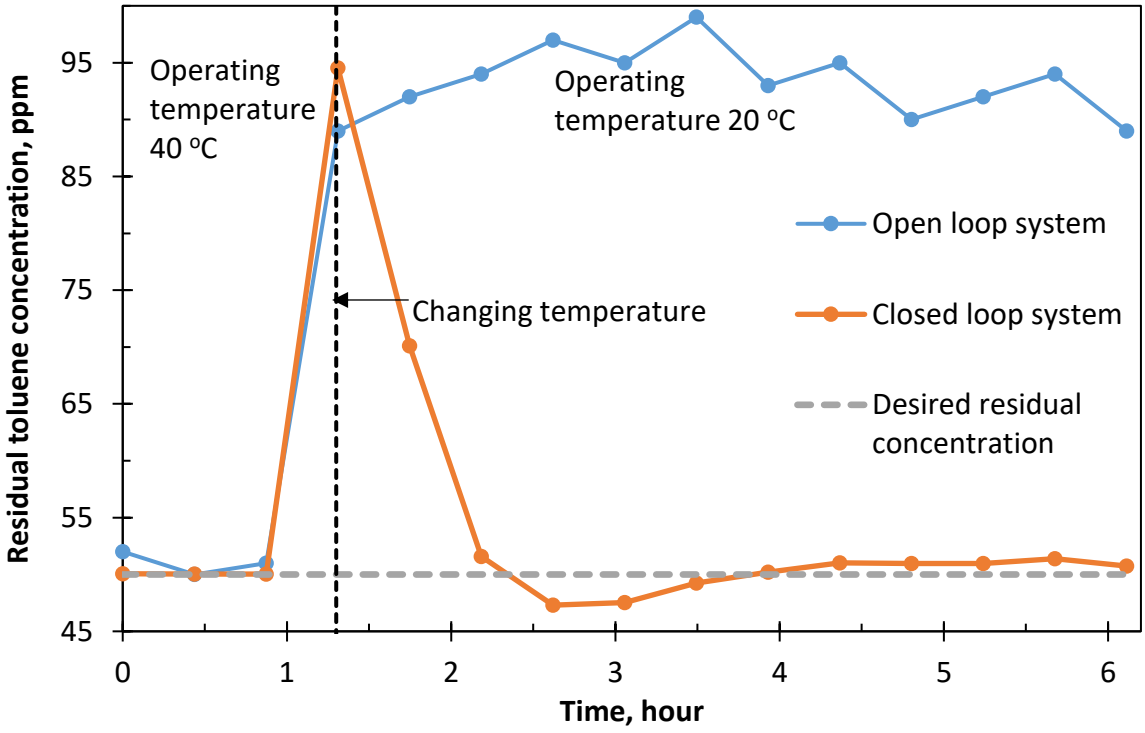


Figure 7.12: The toluene residual concentration profiles with time under closed and open loop control.

The two systems displayed a clear difference in the residual concentration response with the change in operating temperature after 6 hours of operation. The initial increase in the residual

concentration in both systems could be attributed to the reduction in the microbial activity due to the drop in the operating temperature (Bordoloi et al., 2019). The closed loop system showed good performance with an average residual concentration of 50.5 ppm, a 0.5 ppm offset from the desired concentration (50 ppm). However, the open loop showed an oscillating residual concentration at 93 ppm, 100% offset from the desired concentration. Hence, the closed loop system provided a better performance than the open loop system in response to the bed temperature disturbance. The closed loop system demonstrated an initial poor response but that possibly could have been improved with better tuning parameters.

### 7.3.4 The impact of residual toluene concentration on biofilter elimination capacity

The relationship between the residual toluene concentration and the EC was explored through the manipulation of the inlet toluene concentration with the use of the feedback control system (Set 1 and Set 2) and varying the water bath temperature in open-loop mode (Set 3 and Set 4). Due to the supply of Soil 3 ran out and Soil 1 has already been studied in the past (Baskaran et al., 2016, Bordoloi and Gostomski, 2019), Soil 2 was chosen as a packing medium. It was replaced each time when starting a new set of experiments. The operating conditions: operating temperature of 40 $^{o}$C, matric potential of -10 $cm_{H_2O}$ and flow rate of 25 $ml \cdot min^{-1}$ were kept throughout of the experiments. The biofilters were first exposed to toluene until achieving steady state. Any excess nutrients to stimulate growth were assumed depleted during this period. The experiments were then conducted with the assumption that the active biomass in the soil layer was constant. Song and Kinney (2000) found the production of active biomass affected the removal rate so a change in biomass concentration would affect the relationship between the residual concentration and the EC.

The biofilter was started at an inlet toluene concentration of 50 ± 3 ppm and operated for 14 days in open-loop mode and eventually achieved a residual toluene concentration of 21 ± 1.4

ppm with a steady state EC of 26 ± 1.1 $g \cdot m^{-3} \cdot h^{-1}$ (data not shown). After achieving steady-state EC, the biofilter system was switched from open-loop mode to the closed loop mode with the first residual concentration setpoint was 30 ppm (Figure 7.13). Each residual concentration was maintained for 8 – 10 hours via feedback control system to obtain a steady state EC. The numerical labels correspond to the order of the experiments.

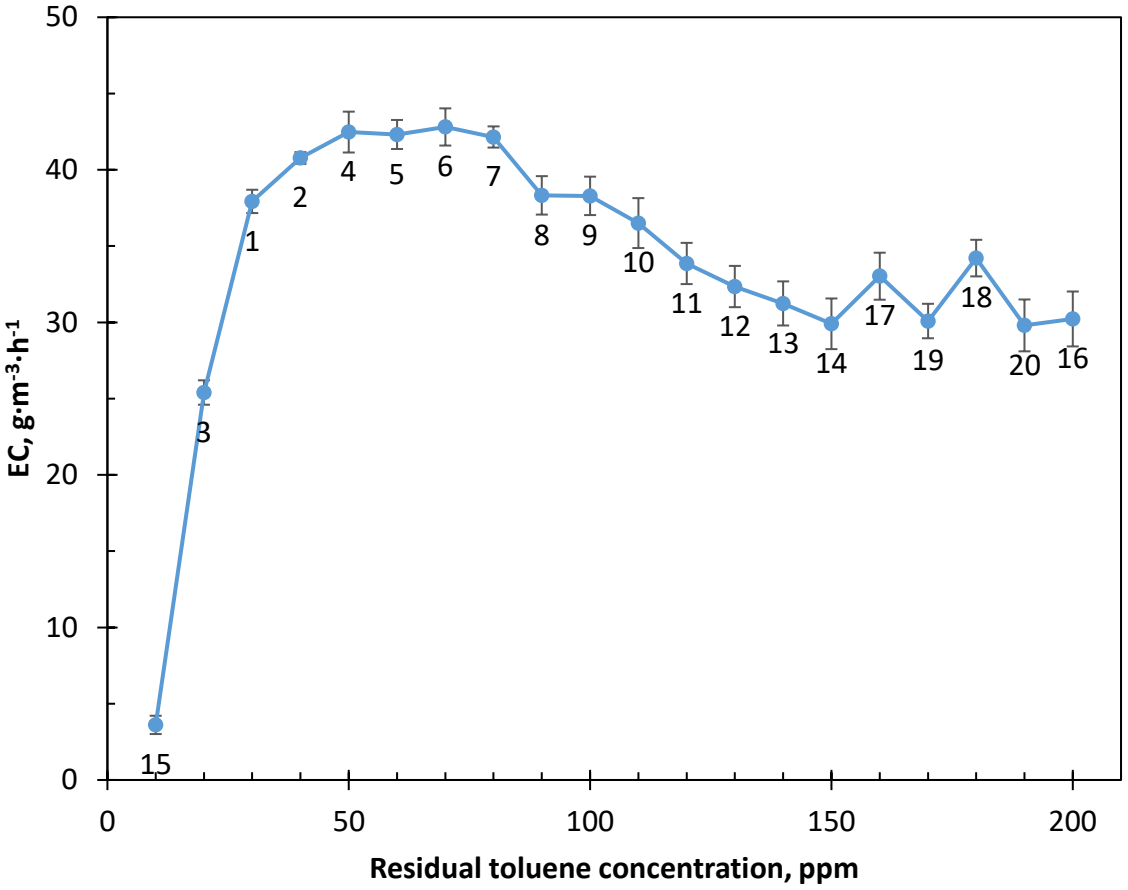


Figure 7.13.: The relationship between the residual toluene concentration and the EC. The labels represent the order in which Set 1 was generated. Values are the mean over 8 – 10 hours of steady state operation at a given residual toluene concentration setpoint. The error bars are the standard deviation.

Set 1 was started with a setpoint of 30 ppm (#1) and achieved an EC of 38 ± 0.7. The residual toluene setpoint was then increased to 40 ppm (#2) and decreased to 20 ppm (#3). The EC at

#2 (41 ± 0.6 $g \cdot m^{-3} \cdot h^{-1}$) was slightly higher than at #1 and 1.5 times higher than at #3 (25 ± 1.0 $g \cdot m^{-3} \cdot h^{-1}$). At #4 to #7, the EC (42 ± 0.28 $g \cdot m^{-3} \cdot h^{-1}$) was independent of the toluene concentration in the range of 40 – 80 ppm. The EC started to decrease at higher residual concentrations (#t 8 to #14, #16 to #20). The EC at toluene concentrations from 90 – 120 ppm (#8 to #11) was 37 ± 2.1 $g \cdot m^{-3} \cdot h^{-1}$, whereas the EC at toluene concentrations from 130 – 200 ppm (#13 to #14, #16 to #20) was 31 ± 1.7 $g \cdot m^{-3} \cdot h^{-1}$.

Following the first experiment (Set 1), the experiment was repeated (Set 2) but with a different setpoint order and operated to a higher residual concentration setpoint (300 ppm) and fresh packing medium (Soil 2) to further understand the toluene degraders' response (Figure 7.14). The biofilter was started at the residual toluene concentration of 65 ± 0.1 ppm (#1) using the feedback control system. An EC of 29 ± 1.3 $g \cdot m^{-3} \cdot h^{-1}$ was achieved during its 20 days continuous operation. The residual toluene setpoint was then decreased to 10 ppm (#2). The toluene setpoint was increased sequentially, from 10 ppm (#2) to 300 ppm (#23). Each residual concentration from #2 to #23 was maintained for 8 - 10 hours to obtain a steady state EC. The EC at #2 was 4 ± 0.2 $g \cdot m^{-3} \cdot h^{-1}$. A significant increase in EC (22 ± 1.2 $g \cdot m^{-3} \cdot h^{-1}$) was observed at residual concentration of 20 ppm (#3). The setpoints were then gradually increased and the EC reached 30 ± 0.6 $g \cdot m^{-3} \cdot h^{-1}$ at a 50 ppm setpoint (#6). From 60 ppm (#7) to 250 ppm (#22), the average EC remained nearly constant at 34.6 ± 1.6 $g \cdot m^{-3} \cdot h^{-1}$. At 300 ppm (#23), the EC decreased to 29 ± 2.5 $g \cdot m^{-3} \cdot h^{-1}$.

The response of the last setpoint (#23) of Set 2 raised a question whether the substrate inhibition and/or oxygen limitation occurred at the toluene residual concentration of 300 ppm. However, it was stated in previous reports that the oxygen limitation is unlikely to influence the EC at this concentration (Shareefdeen et al., 1993, Zilli et al., 2000, Maestre et al., 2007, Malakar et al., 2018). The inhibition effect of high residual concentrations (≥ 300

ppm) was further elucidated when the results of Set 3 and 4 were compared with the results of Set 1 and 2. The toluene inlet concentration in Set 3 and 4 was varied between 80 – 500 ppm by varying the water bath temperature 20 – 65 $^{o}$C. These experiments were open loop and did not use the feedback control.

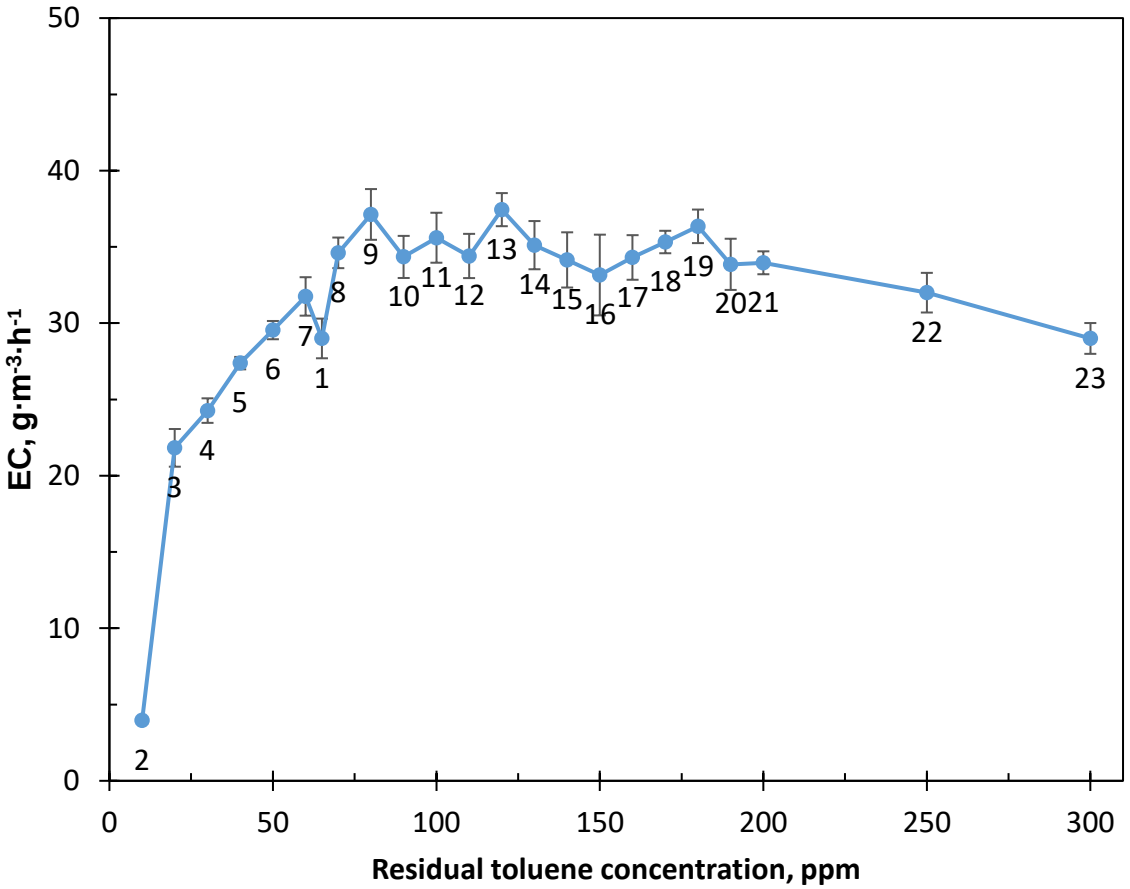


Figure 7.14: The relationship between the residual toluene concentration and the EC. The labels represent the order in which Set 2 was generated. Values are the mean over 8 – 10 hours of steady state operation at a given residual toluene concentration setpoint. The error bars are the standard deviation.

The data collected in Set 3 and Set 4 were generated in increasing order of residual concentration (Figure 7.15 and Figure 7.16). The operating parameters were similar as those used in Set 1 and Set 2. However, each residual concentration was maintained for 5 – 7 days

versus the 8 – 10 hours in Set 1 and 2 to obtain a steady state EC in the biofilters. The difference in the steady state equilibration time for Set 1 and 2 compared to Set 3 and 4 was due to time constraints during experimentation.

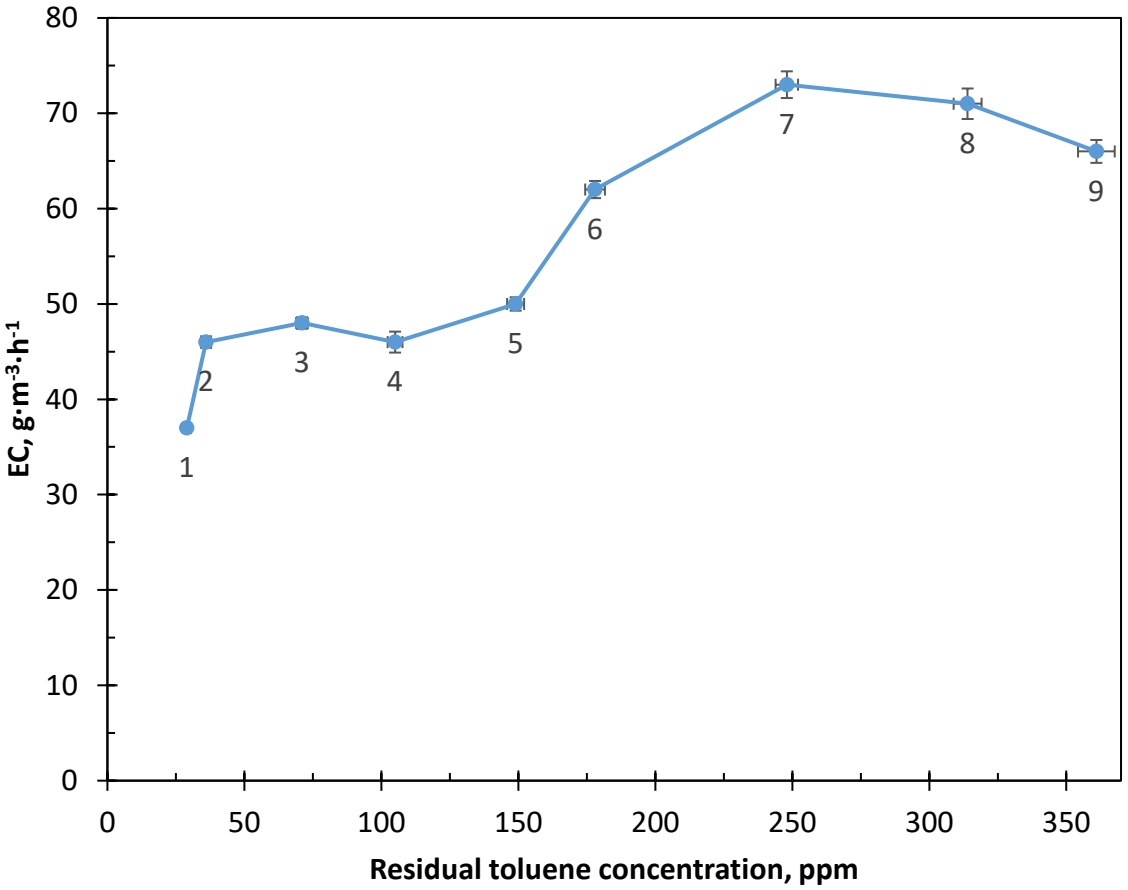


Figure 7.15: The relationship between the residual toluene concentration and the EC. The labels represent the order in which steady values were obtained in Set 3. Values are the mean over 5 – 7 days of operation at steady state at a given residual toluene concentration. The error bars are the standard deviation.

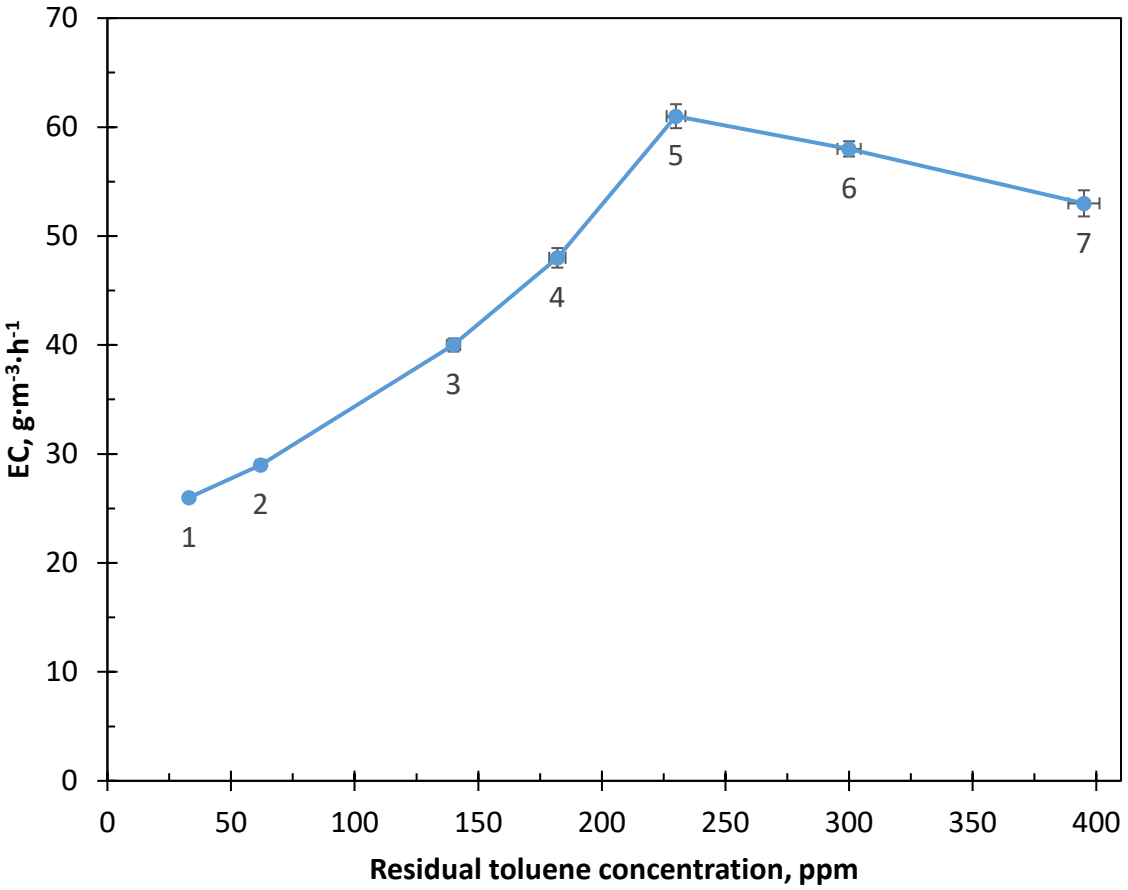


Figure 7.16: The relationship between the residual toluene concentration and the EC. The labels represent the order in which steady values were obtained in Set 4. Values are the mean over 5 – 7 days of at steady state operation at a given residual toluene concentration. The error bars are the standard deviation.

The EC values in Set 3 and Set 4 dropped when the residual concentration exceeded 250 ppm. This response was consistent with #22 in Set 2 (Figure 7.14), where the EC decreased by 20% when changing the residual concentration from 250 ppm to 300 ppm. In Set 3, the EC at residual concentration of 361 ppm (#9) was 66 ± 1.2 $g \cdot m^{-3} \cdot h^{-1}$ which was 10% lower than the EC (73 ± 1.4 $g \cdot m^{-3} \cdot h^{-1}$) at a residual concentration of 248 ppm (#7). In Set 4, the EC was decreased by 15%, from 61 ± 0.9 $g \cdot m^{-3} \cdot h^{-1}$ to 53 ± 1.1 $g \cdot m^{-3} \cdot h^{-1}$ when increasing the residual concentration from 230 ppm (#5) to 395 ppm (#7). Thus, it could be concluded that at a

residual concentration of 300 ppm and above, toluene became inhibitory for toluene degradation in Soil 2.

Similar EC values (38 – 48 $g \cdot m^{-3} \cdot h^{-1}$) were observed between Set 1 and Set 3 at toluene residual concentrations between 30 – 70 ppm. At toluene residual concentrations between 30 – 60 ppm, the EC values of Set 2 and Set 4 were between 26 – 32 $g \cdot m^{-3} \cdot h^{-1}$. However, for residual concentrations > 140 ppm, the average ECs in Set 3 and Set 4 (55.7 ± 11.9 $g \cdot m^{-3} \cdot h^{-1}$) were 45% higher compared with the average ECs in Set 1 and Set 2 (31.2 ± 1.91 $g \cdot m^{-3} \cdot h^{-1}$). These differences could possibly be attributed to the different microbial communities after the initial operations. Changing toluene concentrations can change the community structure (Estrada et al., 2012, Lu et al., 2018). Furthermore, in Set 3 and Set 4 each steady state lasted for 5 – 7 days which allowed a longer acclimation time for each residual concentration compared to Set 1 and Set 2 (8 – 10 hours). This longer acclimation time may have been the driving force in changing the community in Set 3 and Set 4 (Fowler et al., 2014). Further microbial community analysis is required to confirm this hypothesis.

Another possible explanation of the difference EC value was the depletion in nutrients over time. However, all the soil biofilters were operated at a steady EC for 14 – 20 days prior to the experiment. Therefore, the loss of nutrients through the experiments was probably not significantly different between experiments.

The pattern observed for increasing toluene concentration for Set 1 & 2 was different from Set 3 & 4. In Set 1 and Set 2, the obtained EC values for both diffusion-limited region and reaction-limited region against residual concentration ranges tested were obtained. For residual concentrations lower than 40 ppm, the EC increased with the concentration. This behaviour could be described as a diffusion limitation regime at which the EC was proportional

to the concentration (Ottengraf and Vandenoever, 1983). For higher residual concentrations (120 - 200 ppm), the EC was independent of the concentration and the process became exclusively limited by the biodegradation reaction (reaction-limited region) (Ottengraf and Vandenoever, 1983). These diffusion-limited and reaction-limited region were commonly observed in many biofilter operations (Jorio et al., 2000, Ashok Kumar et al., 2015, Malakar et al., 2018).

In Set 3 and Set 4, the EC increased with an increase in the residual concentration (diffusion-limited region) (29 – 250 ppm) before substrate inhibition occurred (for residual concentrations ≥ 300 ppm). The presence of substrate inhibition behavior was also observed by Rene et al. (2009), Shukla et al. (2011) and Zhu et al. (2017) for biofilters treating benezene, trichloroethylene and $H_2S$, respectively. Moreover, no plateau (reaction-limited) was observed in both Set 3 and 4. This could due to the residual concentration was abruptly changed to the inhibitory concentration (≥ 300 ppm) hence immediately causing inhibition.

### 7.3.5 Effect of start-up substrate toluene concentration on elimination capacity

In the differential biofilter, the microbes were exposed to the inlet concentration at time zero. This concentration decreased overtime as the microbes started to degrade the pollutants. The residual concentration was the concentration that microbes were directly exposed to. Therefore, the start-up residual concentration was a crucial factor which could potentially affect the EC.

In this study, the steady state EC recorded from experiments involving varying residual concentrations (Experiment 1) was compared with that of the EC obtained from experiments at constant residual concentration (Experiment 2). Soil 2 was chosen as the packing medium.

The temperature of the reactor box was maintained at 40 ± 0.1 $^{o}$C. The matric potential of -10 $cm_{H_2O}$ and flowrate of 25 ± 0.1 ml·min$^{-1}$ were kept constant during the experiments.

For Experiment 1, the biofilters were started at a residual toluene concentration of 20 ppm by using the feedback control system (Figure 7.17). It took 14 – 18 days to reach steady state with an average EC of 24 ± 0.8 g·m$^{-3}$·h$^{-1}$ (data not shown). The residual concentration was increased to 65 ppm. The average steady EC values approximately doubled (42 ± 0.9 g·m$^{-3}$·h$^{-1}$) after increasing the residual concentration to 65 ppm. These results were consistent with the pattern in Set 1 (Figure 7.13), where the EC doubled after changing the residual concentration from 20 ppm to 60 ppm.

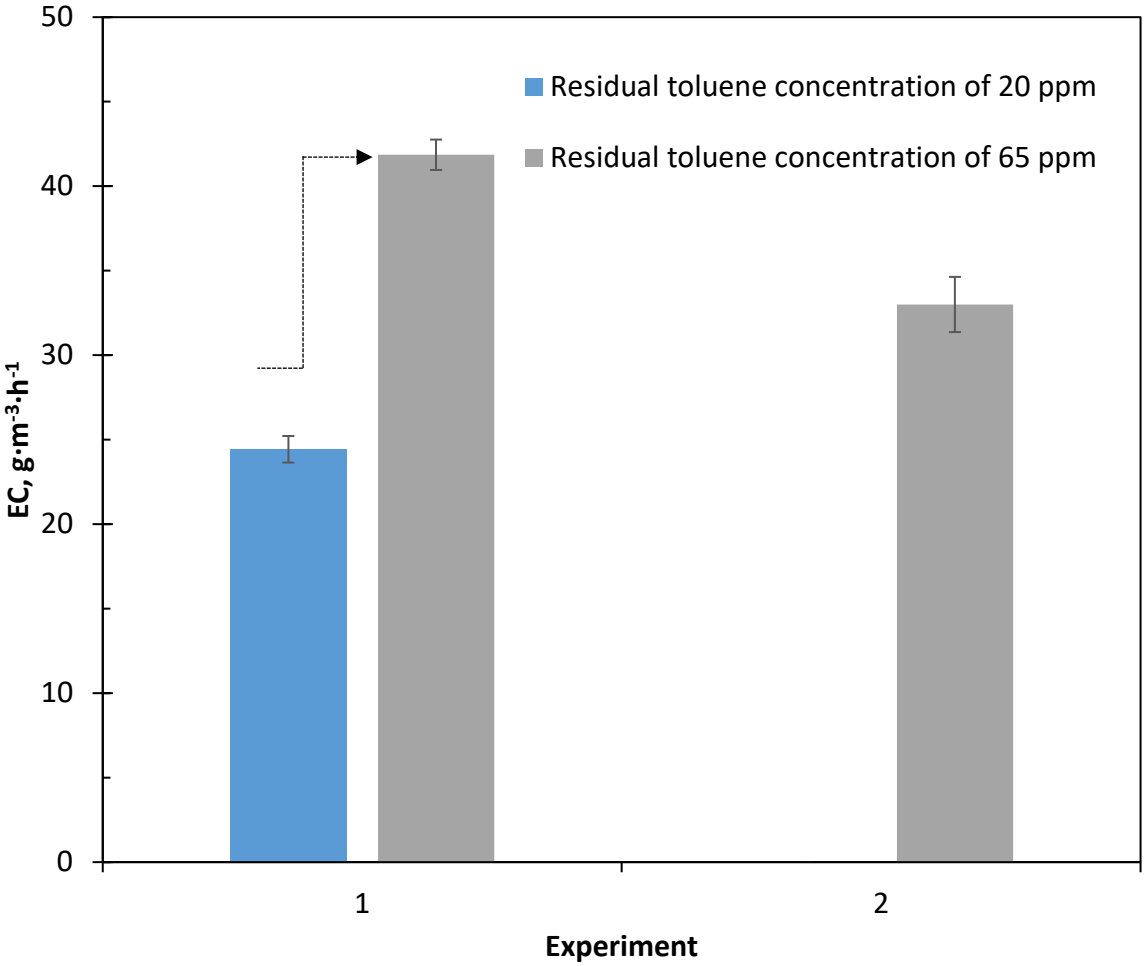


Figure 7.17: Comparison of Experiment 1: Biofilters run with varying residual concentrations in a step-wise manner and Experiment 2: Biofilters run with constant residual concentration and its effect on Soil 2 biofilter performance operated at 40 $^{o}$C. Values are the mean at steady state over replicate experiments. The error bars reported are the standard deviation.

Starting the toluene residual concentration of 20 ppm prior to increasing to 65 ppm resulted in a 22% higher EC (42 ± 0.9 g·m$^{-3}$·h$^{-1}$) than starting at a constant residual concentration of 65 ppm (33 ± 1.6 g·m$^{-3}$·h$^{-1}$) (Figure 7.17). This comparison confirmed Bordoloi and Gostomski (2019)'s hypothesis that lower start up concentrations then increasing to higher concentrations in a stepwise manner leads to a higher EC than when starting at higher concentrations. This improved performance suggested that the toluene degrading microbial

communities were more active due to the favourable start-up conditions. Exposure to low toluene concentrations/loading rates at start-up showed a higher EC and possibly maintained a healthier microbial diversity (Bayle et al., 2009, Lebrero et al., 2011). Estrada et al. (2012) found that the community adapted to low residual concentration gradually improved its biodegradation performance over time. On the other hand, previous studies found the microbial inhibition mediated by the exposure of the microbial community to high toluene concentrations and metabolites causing a loss of toluene degrading activity thus lowering the removal efficiency (Díaz et al., 2008, Baskaran et al., 2016, Bordoloi and Gostomski, 2019)

### 7.4 (Detchanamurthy, 2013, Bordoloi and Gostomski, 2019). Conclusions

The feedback control system developed in these studies performed well when controlling the residual toluene concentration (average  standard deviation less than 4.5% at the residual concentration ranges of 10 - 300 ppm) for both setpoint changes and disturbance rejection. From 4 sets of separate experiments conducted with Soil 2 when the residual toluene concentration exceeded 250 ppm, the EC started to decrease due to potential substrate inhibition. Start-up concentration studies showed that starting the reactor at a lower residual concentration (20 ppm) then increasing it to a higher value (65 ppm) increased the EC by 22% compared to starting the reactor at a high residual concentration (65 ppm). This trend for Soil 2 was consistent with the outcome from Bordoloi and Gostomski (2019) where they examined Soil 1. In conclusion, this work demonstrated feedback control was a useful tool for the differential biofilter and provided useful knowledge of residual toluene concentration in starting up a biofilter and long-term operation to achieve better process efficacy.

**References**

ASHOK KUMAR, S., NAIR, A. S., SARAVANAN, V. & RAJASIMMAN, M. 2015. Modeling of kinetics approach on the removal in methyl ethyl ketone using pressmud based biofilter systems. *Modeling Earth Systems and Environment,* 1**,** 4.

BASKARAN, S., SELVAKUMAR, S. V. P., MOHAN, R., JOHN, R. M., DETCHANAMURTHY, S., NARAYANAN, M. & GOSTOMSKI, P. A. 2016. Influence of substrate concentration, nutrients and temperature on the biodegradation of toluene in a differential biofilter reactor. *In:* B. D, P., GUMMADI, S. N. & VADLANI, P. V. (eds.) *Biotechnology and Biochemical Engineering: Select Proceedings of ICACE 2015.* Singapore: Springer Singapore.

BAYLE, S., MALHAUTIER, L., DEGRANGE, V., GODON, J. J. & FANLO, J. L. 2009. Structural and functional responses of sewage microbial communities used for the treatment of a complex mixture of volatile organic compounds (VOCs). *Journal of Applied Microbiology,* 107**,** 85-96.

BORDOLOI, A. 2016. *Toluene degradation by an unsaturated biofilm: The impact of environmental parameters on the carbon end-points in biofiltration.* Doctor of Philosophy, University of Canterbury.

BORDOLOI, A., GAPES, D. J. & GOSTOMSKI, P. A. 2019. The impact of environmental parameters on the conversion of toluene to CO2 and extracellular polymeric substances in a differential soil biofilter. *Chemosphere,* 232**,** 304-314.

BORDOLOI, A. & GOSTOMSKI, P. A. 2019. Carbon recovery and the impact of start-up conditions on the performance of an unsaturated *Pseudomonas putida* biofilm compared with soil under controlled environmental parameters in a differential biofilter. *Journal of Chemical Technology and Biotechnology,* 94**,** 600-610.

CHENG, Z., LU, L., KENNES, C., YU, J. & CHEN, J. 2016. Treatment of gaseous toluene in three biofilters inoculated with fungi/bacteria: Microbial analysis, performance and starvation response. *Journal of Hazardous Materials,* 303**,** 83-93.

CIANCONE, R. & MARLIN, T. 1992. Tune controllers to meet plant objectives. *Control,* 5**,** 50-57.

DETCHANAMURTHY, S. 2013. *Impact of different metabolic uncouplers on the specific degradation rate of toluene in a differential biofiltration reactor.* Doctor of Philosophy, University of Canterbury.

DÍAZ, L. F., MUÑOZ, R., BORDEL, S. & VILLAVERDE, S. 2008. Toluene biodegradation by *Pseudomonas putida* F1: targeting culture stability in long-term operation. *Biodegradation,* 19**,** 197-208.

ESTRADA, J. M., RODRIGUEZ, E., QUIJANO, G. & MUNOZ, R. 2012. Influence of gaseous VOC concentration on the diversity and biodegradation performance of microbial communities. *Bioprocess and Biosystems Engineering,* 35**,** 1477-1488.

FOWLER, S. J., GUTIERREZ-ZAMORA, M. L., MANEFIELD, M. & GIEG, L. M. 2014. Identification of toluene degraders in a methanogenic enrichment culture. *Fems Microbiology Ecology,* 89**,** 625-636.

JORIO, H., BIBEAU, L. & HEITZ, M. 2000. Biofiltration of air contaminated by styrene: Effect of nitrogen supply, gas flow rate, and inlet concentration. *Environmental Science & Technology,* 34**,** 1764-1771.

LEBRERO, R., RODRIGUEZ, E., GARCIA-ENCINA, P. A. & MUNOZ, R. 2011. A comparative assessment of biofiltration and activated sludge diffusion for odour abatement. *Journal of Hazardous Materials,* 190**,** 622-630.

LU, L. C., WANG, G. C., YEUNG, M., XI, J. Y. & HU, H. Y. 2018. Response of microbial community structure and metabolic profile to shifts of inlet VOCs in a gas-phase biofilter. *Amb Express,* 8**,** 8.

MAESTRE, J. P., GAMISANS, X., GABRIEL, D. & LAFUENTE, J. 2007. Fungal biofilters for toluene biofiltration: Evaluation of the performance with four packing materials under different operating conditions. *Chemosphere,* 67**,** 684-692.

MALAKAR, S., SAHA, P. D., BASKARAN, D. & RAJAMANICKAM, R. 2018. Microbial biofilter for toluene removal: Performance evaluation, transient operation and theoretical prediction of elimination capacity. *Sustainable Environment Research,* 28**,** 121-127.

MARLIN, T. E. & MARLIN, T. 1995. *Process control: designing processes and control systems for dynamic performance*, McGraw-Hill New York.

NELSON, G. O. 1971. *Controlled test atmospheres: Principles and techniques,* Michigan, United States of America, Ann Arbor Science.

OTTENGRAF, S. P. P. & VANDENOEVER, A. H. C. 1983. Kinetics of organic-compound removal from waste gases with a biological filter. *Biotechnology and Bioengineering,* 25**,** 3089-3102.

RENE, E. R., MURTHY, D. V. S. & SWAMINATHAN, T. 2009. TREATMENT OF BENZENE VAPORS FROM CONTAMINATED AIR STREAM IN A LABORATORY-SCALE COMPOST BIOFILTER. *Macedonian Journal of Chemistry and Chemical Engineering,* 28**,** 119-123.

SHAREEFDEEN, Z., BALTZIS, B. C., OH, Y. S. & BARTHA, R. 1993. Biofiltration of methanol vapor. *Biotechnology and Bioengineering,* 41**,** 512-524.

SHUKLA, A. K., SINGH, R. S., UPADHYAY, S. N. & DUBEY, S. K. 2011. Substrate inhibition during bio-filtration of TCE using diazotrophic bacterial community. *Bioresource Technology,* 102**,** 3561-3563.

SONG, J. H. & KINNEY, K. A. 2000. Effect of vapor-phase bioreactor operation on biomass accumulation, distribution, and activity: Linking biofilm properties to bioreactor performance. *Biotechnology and Bioengineering,* 68**,** 508-516.

ZHU, R., LI, S., BAO, X. & DUMONT, É. 2017. Comparison of biological H(2)S removal characteristics between a composite packing material with and without functional microorganisms. *Scientific reports,* 7**,** 42241-42241.

ZIEGLER, J. G. & NICHOLS, N. B. 1942. Optimum settings for automatic controllers. *trans. ASME,* 64.

ZILLI, M., DEL BORGHI, A. & CONVERTI, A. 2000. Toluene vapour removal in a laboratory-scale biofilter. *Applied Microbiology and Biotechnology,* 54**,** 248-254.

# Chapter 8: Summary, Conclusions and Future Work

## 8.1 Summary and conclusions

The focus of this study was to quantitatively determine the importance and potential interaction between operating conditions - combination of residual pollutant concentration and water potential and soil type on $\%CO_2$ recovery and biofilter performance (EC) for multiple pollutants (toluene and methane). Residual concentration and water potential were selected based on the results by Bordoloi et al. (2019): operating the biofilter at a lower residual pollutant concentration and wetter conditions would result in a higher $\%CO_2$ mineralization than operating at higher residual concentration and drier condition.

The differential reactor system was used to quantify and track the carbon fractions in the gas, solid and liquid phases to close the carbon balance. Experiments were performed at various operating conditions without addition of nutrient medium. Quantitative closure of the carbon balance was 96.1 ± 5.3% over 37 experiments. The carbon fraction found in the liquid phase was less than 5% of the degraded carbon. The cumulative amount of $CO_2$ evolved ranged from 30% to 70% of the degraded carbon while the carbon accumulated in the biofilm ranged from 20% to 60%. These results indicated that majority of the biodegraded carbon ends up in the form of either $CO_2$ or active biomass/EPS (Chapter 4).

The performance of toluene biofilters in terms of $\%CO_2$ recovery and EC was investigated by creating two experiments of multi-factorial operating conditions: Set 1 - temperature (30 $^oC$, 40 $^oC$) and soil type (Soil 1, Soil 2, Soil 3). Set 2 varied a combination of residual toluene concentration, water potential (residual concentrations of 5 ppm to 49 ppm, -10 $cm_{H_2O}$ and residual concentrations of 115 ppm to 146 ppm, -100 $cm_{H_2O}$) and soil type (Soil 1, Soil 2, Soil 3). ANOVA results of Set 1 showed there was a significant difference in $\%CO_2$ recovery and EC

between the biofilters operated at two different temperatures ($\rho < 0.01$). Operating the biofilter at high temperature (40 $^{o}$C) resulted in a 30% higher EC and a 20% higher $\%CO_2$ recovery than operating at 30 $^{o}$C. This was inconsistent with Bordoloi et al. (2019) who found that the temperature had no influence on the $\%CO_2$. However, this outcome was derived only from one soil (Soil 1) which may not be conclusive. The current study covered a wider range of soil types (Soil 1, Soil 2 and Soil 3) with at least a duplicate of each condition, hence providing broader and more statistically conclusive results. For Set 2, operating the biofilter at low residual concentrations (5 ppm to 49 ppm) and wet condition (-10 $cm_{H_2O}$) resulted in a 20% higher EC and a 20% higher $\%CO_2$ than operating at high residual concentrations (115 ppm to 146 ppm) and drier condition (-100 $cm_{H_2O}$). The interaction between soil type and operating conditions was not significant in both Set 1 and Set 2. Preliminary results of microbial community analysis from different soil types pre- and post- toluene exposure at different environmental conditions revealed the dominance of four genera: *Nocardia,* *Mycobacterium*, *Rhodococcus* and *Azoarcus*. These genera belong to two phyla: *Actinobacteria* and *Proteobacteria*, which could have played crucial roles in the toluene degradation or benefited from the environmental conditions (Chapter 5).

The performance of methane biofilters in terms of $\%CO_2$ recovery and EC was investigated by creating a factorial design of operating conditions: combination of residual concentration and water potential (residual concentrations of 1709 ppm to 1942 ppm, -10 $cm_{H_2O}$ and residual concentrations of 8590 ppm to 9054 ppm, -100 $cm_{H_2O}$) and soil type (Soil 1, Soil 2, Soil 3). Operating the biofilter at low residual concentrations (1709 ppm to 1942 ppm) and wet condition (-10 $cm_{H_2O}$) resulted in a 35% lower EC and a 45% lower $\%CO_2$ than operating at high residual concentrations (8590 ppm to 9054 ppm) and drier condition (-100 $cm_{H_2O}$). The interaction between soil type and operating conditions was not significant. Preliminary results

of microbial community analysis from different soil types post methane exposure at residual concentrations of 1709 ppm to 1942 ppm and at matric potential of -10 $cm_{H_2O}$ found *Mythylocystis* – a type II methanotroph belonging to the phylum *Proteobacteria* were the most dominant genera. In addition, the influence of supplemental $CO_2$ concentration of 350 – 450 ppm on the $CO_2$ production rate and biofilter performance packed with Soil 1 and Soil 2 was investigated. Switching the biofilter packed with Soil 1 and Soil 2 fed with methane-$CO_2$ free air resulted in a 35% lower EC and a 45 – 65% lower $CO_2$ production than methane-laden air containing $CO_2$ (Chapter 6).

It could be concluded that Bordoloi et al. (2019) result "operating the biofilter at a lower residual concentration and a wetter conditions would result in a higher %$CO_2$ mineralization than operating at higher residual concentration and drier conditions" was true with toluene but not with methane. Preliminary findings in this study demonstrate that soil type had a strong effect on the EC in toluene and methane biofilters and %$CO_2$ recovery in methane biofilters. Among three soil types, Soil 2 had the lowest performance (EC). This could be due to Soil 2 had the least nitrogen, carbon content and lowest gravimetric water content at the same levels of matric potential (Chapter 5 and Chapter 6). These findings suggest that environmental parameters and soil type have a significant effect on %$CO_2$ recovery, EC and community structure.

The impact of residual toluene concentration on biofilter performance packed with Soil 2 was investigated. A feedback control system was developed using on-line GC measurements to manipulate the inlet concentration and maintain residual toluene to the desired value. Substrate inhibition occurred when the residual toluene concentration exceeded 250 ppm. Start-up concentration studies showed that starting the reactor at a lower residual concentration then increasing it to higher value increased the EC by 22% compared to starting

the reactor at a high residual concentration. This trend was in agreement with the result from Bordoloi and Gostomski (2019) where they examined Soil 1. These outcomes provided useful knowledge in starting up a biofilter and long-term operation to achieve better process efficacy (Chapter 7).

## 8.2 Future work

### 8.2.1 Metagenomics study of microbial community

Future work can involve using stable isotope probing (e.g. $^{13}C$) combined with high throughput sequencing to identify the microorganisms involved in toluene or methane removal in a biofilm. Feeding the labelled genetic material to the system labels the DNA/RNA of the active degrading community with $^{13}C$. It can then be separated from the wider community's DNA/RNA and sequenced (Neufeld et al., 2007, Whiteley et al., 2007). The sequenced DNA/RNA will identify which groups of organisms are active in degrading the pollutant in the microbial community.

Identifying how the active microorganisms change with operating conditions and correlating them with the product distribution between carbon end-points (e.g. $CO_2$ and EPS) and removal rate of the biofilter will improve the fundamental understanding of methane or toluene removal biofilters. This information could be used to increase the ability to operate successful full-scale biofilter systems for toluene or methane degradation.

### 8.2.2 Characterisation of the EPS

In this study, the carbon accumulated in the biofilm ranged 20 – 60% depending on the operating conditions. Future work can be followed by differentiating the formation of extracellular polymeric substance (EPS) or internal storage polymers (e.g. polyhydroxyalkanoate-PHA, or glycogen) from the cell mass by using standard extractive

methodologies (Denkhaus et al., 2007, Kim and Sorial, 2007). Characterising the biofilm productions, such as EPS and PHA will be helpful in understand the overflow metabolism.

Experiments using biofilters with a pure culture of active communities pertaining to degradation of toluene or methane are suggested. The use of pure culture will allow more definitive analysis of the carbon end-points. The EPS from pure culture are more easily extractable than that from soil which has complex structures and microbial communities (Redmile-Gordon et al., 2014). In addition, the impact of operating conditions on the carbon end-points and performance of the pure culture can be explored and compared to the mixed cultures results collected in this study. This will provide a good framework to determine the influence of critical operational parameters on the microbe(s) which eventually affects the elimination rate of the substrate.

### 8.2.3 The impact of $N_2$ on the biofiltration performance

Nitrogen-fixing microbes are found on the biofilter system (Section 5.3.6). Nitrogen-fixing microbes are able to fix nitrogen in both aerobic and anaerobic environments (Klawonn et al., 2015). The current reactor system is aerobic but there is the possibility that the biofilm could become oxygen limited (anaerobic conditions) as previously observed in Yang et al. (2002). However, the results showed no increase in EC and no significant biomass growth. The role of nitrogen-fixing could be investigated by changing the carrier inert gas from $N_2$ to Argon while also observing their impact to metabolism and carbon end-points of this change.

### 8.2.4 The impact of $CO_2$ on the biofiltration performance

In this study, $CO_2$-free air was mixed with the pollutants (toluene, methane) prior entering the biofiltration system. However, in industrial emissions, $CO_2$ is often present in the inlet stream. Future experiments can therefore include investigating the impact of supplemental $CO_2$ to the

carbon end-points and biofilter performance. This can be done by supplementing inlet feeds with a mixture of pollutants and different $CO_2$ concentrations (i.e. 350 – 450 ppm). Along with investigating carbon end-points and biofilter performance is examining the potential shift in microbial community over time (i.e. mixture of heterotrophic and autotrophic methanotrophic consortia to a dominant heterotrophic-methanotrophic consortium) after switching from $CO_2$ free to supplemented inlet feed and vice versa.

### 8.2.5 Optimization of methane biofilters operation

This study examined the performance of the methane biofilters packed with different soil type. Further works determining the optimum operating parameters in the methane biofilters can be done. The parameters to test include: temperature, pH, residual concentration and matric potential. The feedback control system similar to the developed toluene system needs to be developed in order to control the residual methane concentration. This empirical information gathered from this study will contribute valuable information when choosing operational parameters in full-scale biofilters.

**References**

BORDOLOI, A., GAPES, D. J. & GOSTOMSKI, P. A. 2019. The impact of environmental parameters on the conversion of toluene to CO2 and extracellular polymeric substances in a differential soil biofilter. *Chemosphere,* 232**,** 304-314.

BORDOLOI, A. & GOSTOMSKI, P. A. 2019. Carbon recovery and the impact of start-up conditions on the performance of an unsaturated *Pseudomonas putida* biofilm compared with soil under controlled environmental parameters in a differential biofilter. *Journal of Chemical Technology and Biotechnology,* 94**,** 600-610.

DENKHAUS, E., MEISEN, S., TELGHEDER, U. & WINGENDER, J. 2007. Chemical and physical methods for characterisation of biofilms. *Microchimica Acta,* 158**,** 1-27.

KIM, D. & SORIAL, G. A. 2007. Role of biological activity and biomass distribution in air biofilter performance. *Chemosphere,* 66**,** 1758-1764.

KLAWONN, I., BONAGLIA, S., BRUCHERT, V. & PLOUG, H. 2015. Aerobic and anaerobic nitrogen transformation processes in N2-fixing cyanobacterial aggregates. *Isme Journal,* 9**,** 1456-1466.

NEUFELD, J. D., VOHRA, J., DUMONT, M. G., LUEDERS, T., MANEFIELD, M., FRIEDRICH, M. W. & MURRELL, J. C. 2007. DNA stable-isotope probing. *Nature Protocols,* 2**,** 860-866.

REDMILE-GORDON, M. A., BROOKES, P. C., EVERSHED, R. P., GOULDING, K. W. T. & HIRSCH, P. R. 2014. Measuring the soil-microbial interface: Extraction of extracellular polymeric substances (EPS) from soil biofilms. *Soil Biology and Biochemistry,* 72**,** 163-171.

WHITELEY, A. S., THOMSON, B., LUEDERS, T. & MANEFIELD, M. 2007. RNA stable-isotope probing. *Nature Protocols,* 2**,** 838-844.

YANG, H., MINUTH, B. & ALLEN, D. G. 2002. Effects of nitrogen and oxygen on biofilter performance. *Journal of the Air & Waste Management Association,* 52**,** 279-286.

# Appendix A: Methane and toluene calibration data

## A.1 Methane calibration data

The methane was calibrated against a bottle dry air cylinder and a pure methane cylinder (99.995% V/Vpurity). The dry air cylinder was used for calibrating the zero value. An accurate mixture of methane and dry air was produced using a gas mixing unit. The methane concentration generated ranges from 400 to 20,000 ppm by adjusting the methane flow rate of 0.01 to 0.5 ml·min$^{-1}$.

Table A.1: GC calibration data for methane.

| Methane flow rate (ml) | Air flow rate (ml) | Concentration (ppm) | Average peak area |
|---|---|---|---|
| 0 | 25 | 0 | 0 |
| 0.01 | 24.99 | 399.98 | 2224 ± 56 |
| 0.01 | 20 | 499.7 | 3014 ± 23 |
| 0.05 | 50 | 998.9 | 3803 ± 8 |
| 0.1 | 50 | 1995.9 | 8734 ± 49 |
| 0.1 | 20 | 4974.8 | 16287 ± 190 |
| 0.25 | 24.75 | 9999.5 | 41627 ± 212 |
| 0.5 | 24.5 | 19999 | 83255 ± 437 |

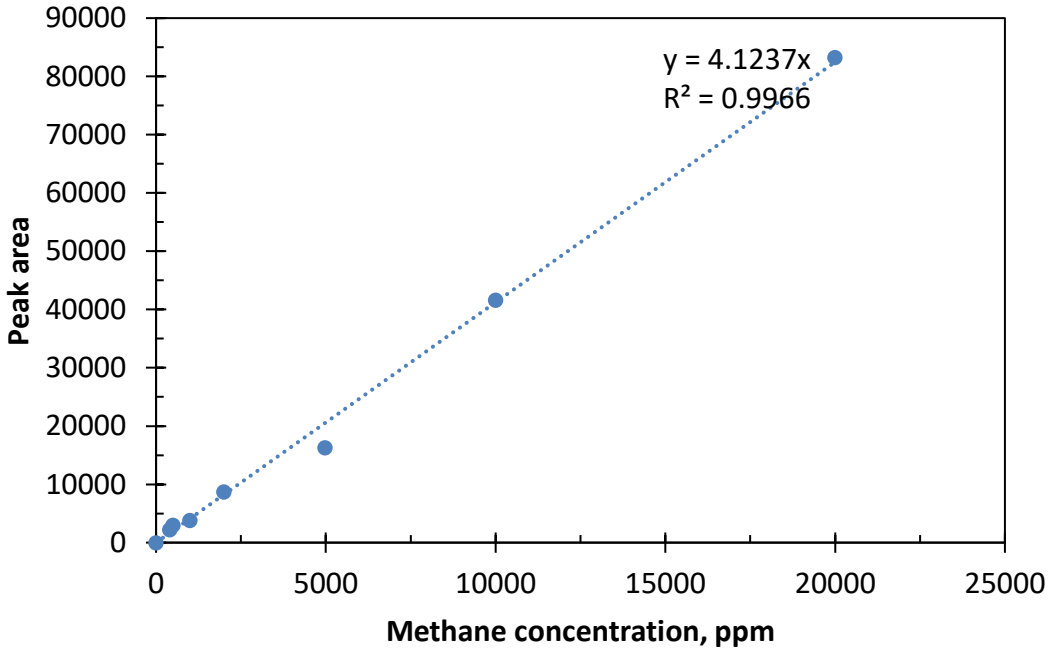


Figure A.1: GC calibration curve for methane.

## A.2 Toluene calibration data

A calibration curve was generated using known volume of liquid toluene in known volume of air in tedlar bags. Five different concentrations of toluene were calculated based on below example calculation.

For 1 µl of liquid toluene mixing with 1l of air in standard condition (25°C and atmospheric pressure)

The density of liquid toluene in ambient temperature is: 867 ($kg \cdot m^{-3}$) = 867 ($g \cdot l^{-1}$)

The mass of 1 µl of liquid toluene is equivalent with: $1\times 10^{-6} \times 867 = 867 \times 10^{-6}$(g)

The moles of 1 µl of liquid toluene is: $867 \times 10^{-6}$: 92.14=$9.41 \times 10^{-6}$ (moles)

The moles of 1l of air is: $n= \frac{P\times V}{R\times T} = \frac{1.013 \times 1}{0.083 \times (25 + 273.15)}$ =0.04 (moles)

Hence, the concentration of the toluene in the air would be:

$$9.41 \times 10^{-6} \times 0.04 \times 10^{6} = 230 \text{ (ppm)}$$

Same principle was used with different volume of liquid toluene and air. The results of these concentration were shown in Table A.2. Figure A.2 showed the generated calibration curve. This calibration curve was used to correct all toluene concentration throughout the study.

Table A.2: GC calibration data for toluene.

| Liquid toluene (µl) | Air (l) | Concentration (ppm) | Average peak area |
|---|---|---|---|
| 1 | 0.5 | 461 | 7259 ± 255 |
| 1 | 1 | 230 | 4333 ± 247 |
| 1 | 2 | 115 | 2351 ± 186 |
| 1 | 3 | 77 | 1523 ± 52 |
| 1 | 5 | 46 | 775 ± 29 |

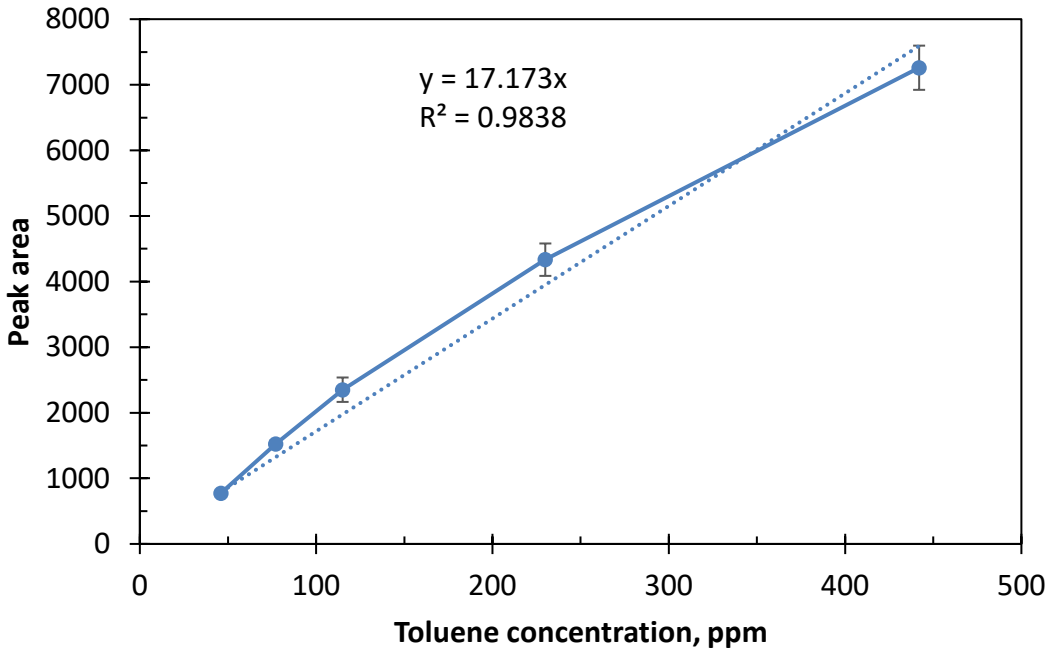


Figure A.2: GC calibration curve for toluene.

# Appendix B: Relevance equation for diffusion system

Diffusion coefficient at current experimental values at 25°C and 1 atm can be found in the *International Critical Tables* (Washburn, 1929). Diffusion coefficients at other temperatures and pressures can be expressed by the following equation (Lugg, 1968):

$$D = D_{298} \left(\frac{T}{298}\right)^{n} \frac{760}{P} \qquad \text{(Equation A.1)}$$

Where:

D - experimental diffusion coefficient at a pressure P and temperature T ($cm^2 \cdot s^{-1}$)

$D_{298}$ - the diffusion coefficient at 25°C and 1 atm ($cm^2 \cdot s^{-1}$)

n - number of moles

The value of constant n varies between 1.5 to 2.0 (Chen and Othmer, 1962, Altshuller and Cohen, 1960). A coefficient of 1.81 is used according on Jacek studies (Jacek, 1984).

Assuming the concentration of the vapour at the tube exit is maintained at nearly zero by the dilution air; the vapor in the tube is saturated and the volumetric flow rate ($q_d$) can be calculated by (Nelson, 1971):

$$q_d = \frac{D \times A}{L} \ln \frac{P}{P - P_V} \qquad \text{(Equation A.2)}$$

Where:

$q_d$ - Diffusion rate ($ml \cdot s^{-1}$)

D - experimental diffusion coefficient at a pressure P and temperature T ($cm^2 \cdot s^{-1}$)

A - Diffusion tube cross sectional area ($cm^2$)

L - Length of the diffusion tube (cm)

P - Pressure in the diffusion cell (mmHg)

$P_v$ - Partial pressure of the diffusion vapor (mmHg)

The concentration of the dynamic diffusion system can be controlled by varying the gas flow rate (Nelson, 1971):

$$C_{dif} = \frac{q_d 10^6}{F_g} \quad \text{(Equation A.3)}$$

Where:

$C_{dif}$ - Concentration of the diffusion system (ppm)

$F_g$ - Gas flow rate ($ml \cdot s^{-1}$)

In addition, the change in temperature will also lead to the change in the vapour pressure ($p_V$) by using Antoine's equation: (Perry and Green, 2008)

$$\log p_v = A - \frac{B}{T+C} \quad \text{(Equation A.4)}$$

Where:

$p_v$ - Vapour pressure of the component (mmHg) at the temperature T ($^oC$)

A,B and C are regression constants for the specific compound. For toluene substrate, the constant values are 6.946; 1344.8;219.5 respectively (Beneke et al., 2012)

Table A.3: Experimental and calculated toluene concentrations generated by the diffusion system at different temperatures at 25 $ml \cdot min^{-1}$ using the diffusion tube: tube length = 0.05 m and inner diameter = 0.0035 m.

| Temperature ($^o$ C) | Temperature ($^o$ K) | Toluene concentration theoretical (ppm) | Toluene concentration experimental (ppm) |
|---|---|---|---|
| 20 | 293 | 111 | 102 ± 3 |
| 25 | 298 | 150 | 172 ± 4 |
| 30 | 303 | 200 | 222 ± 3 |
| 35 | 308 | 265 | 284 ± 2 |
| 40 | 313 | 348 | 361 ± 4 |
| 45 | 318 | 453 | 445 ± 3 |
| 50 | 323 | 587 | 581 ± 2 |
| 55 | 328 | 755 | 761 ± 3 |
| 60 | 333 | 969 | 940 ± 4 |

# Appendix C: $CO_2$ calibration data

The carbon dioxide probe was calibrated against bottled dry air and carbon dioxide gas concentration (3100 ppm). The dry air was used for calibrating the zero value of the probe. For the $CO_2$ calibration, an accurate mixture of dry air and carbon dioxide was used. The operating temperature was 25.0 ± 1 $^oC$, which was measured by the built-in temperature sensor of probe. The pressure compensation was made by adjusting the regulator of the cylinder, which was 100 kPa.

Table A.4: $CO_2$ calibration data for the $CO_2$ analyser.

| Carbon dioxide flow rate (ml) | Air gas flow rate (ml) | Concentration (ppm) | Observed concentration (ppm) |
|---|---|---|---|
| 0 | 25 | -12.5 | 0 |
| 10 | 40 | 620 | 578 |
| 10 | 30 | 775 | 722 |
| 20 | 40 | 1033 | 985 |
| 25 | 25 | 1550 | 1479 |
| 40 | 20 | 2067 | 1978 |
| 30 | 10 | 2325 | 2246 |
| 40 | 10 | 2480 | 2390 |
| 50 | 0 | 3100 | 2970 |

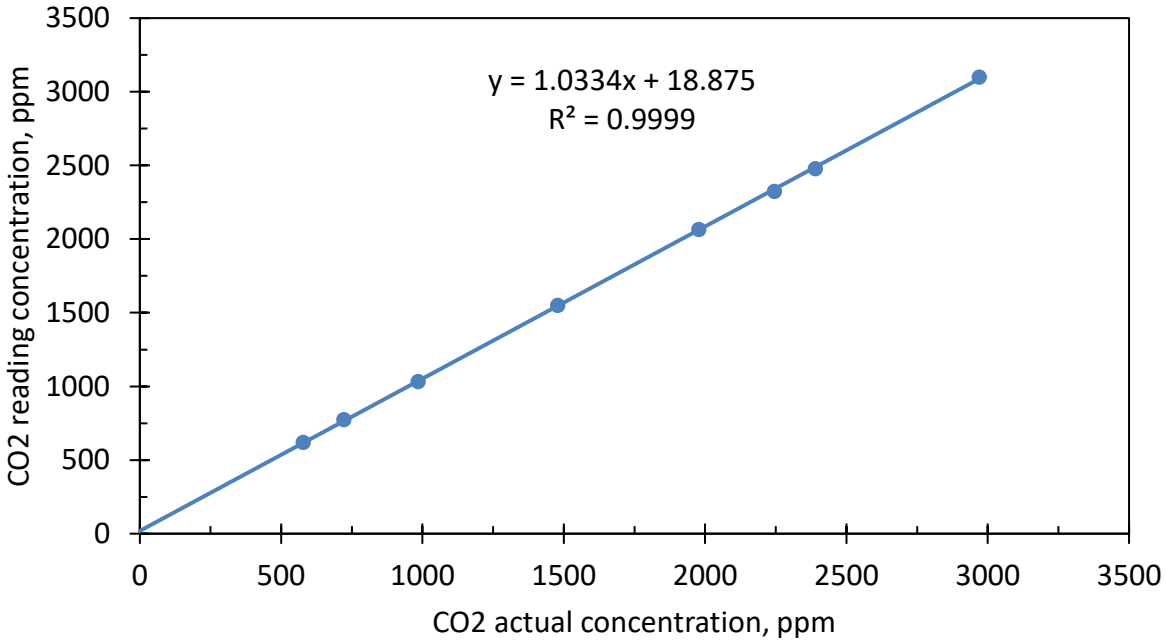


Figure A.3: $CO_2$ calibration curve for $CO_2$ analyzer.

# Appendix D: Unknown cluster data

Clustering of sequences was done based on 95% similarity. After clustering:

- The relative abundance of each cluster was calculated.

- The sequences with known genera filtered out.

- The clusters with unknown genera and a relative abundance of less than 1% were filtered out.

Table A.5: Unknown clusters data.

| Cluster | Sample | R.Abundance (%) | Phylum | Genus |
|---|---|---|---|---|
| Cluster.4163 | S1 | 7.070273365 | *Actinobacteria* | NA |
| Cluster.4148 | S1 | 5.176279758 | *Chloroflexi* | NA |
| Cluster.4185 | S1 | 3.112924002 | *Chloroflexi* | NA |
| Cluster.4243 | S1 | 2.456943848 | *Chloroflexi* | NA |
| Cluster.1258 | S1 | 2.452173083 | *Actinobacteria* | NA |
| Cluster.4184 | S1 | 1.424073279 | *Proteobacteria* | NA |
| Cluster.4296 | S1 | 1.419302514 | *Acidobacteria* | NA |
| Cluster.1281 | S1 | 1.383521779 | *Actinobacteria* | NA |
| Cluster.1287 | S1 | 1.144983541 | *Acidobacteria* | NA |
| Cluster.4228 | S1 | 1.116358952 | *Proteobacteria* | NA |
| Cluster.4110 | S2 | 6.749405862 | *Chloroflexi* | NA |
| Cluster.4248 | S2 | 1.357274888 | *Thaumarchaeota* | NA |
| Cluster.4163 | S2 | 1.330868762 | *Actinobacteria* | NA |
| Cluster.4148 | S2 | 1.254290996 | *Chloroflexi* | NA |

| | | | | |
|---|---|---|---|---|
| Cluster.1089 | S2 | 1.02719831 | *Acidobacteria* | NA |
| Cluster.4026 | S3 | 16.45270908 | *Chloroflexi* | NA |
| Cluster.1287 | S3 | 3.728525581 | *Acidobacteria* | NA |
| Cluster.4163 | S3 | 2.598955384 | *Actinobacteria* | NA |
| Cluster.4148 | S3 | 2.001132717 | *Chloroflexi* | NA |
| Cluster.4243 | S3 | 1.503995973 | *Chloroflexi* | NA |
| Cluster.4083 | S3 | 1.255427601 | *Gemmatimonadetes* | NA |
| Cluster.1258 | S3 | 1.132716632 | *Actinobacteria* | NA |
| Cluster.4184 | S3 | 1.088666541 | *Proteobacteria* | NA |
| Cluster.4584 | S3 | 1.05090932 | *Proteobacteria* | NA |
| Cluster.4133 | S2 - C | 4.625202766 | *Gemmatimonadetes* | NA |
| Cluster.4110 | S2 - C | 2.044736617 | *Chloroflexi* | NA |
| Cluster.1089 | S2 - C | 1.131221719 | *Acidobacteria* | NA |
| Cluster.4110 | S2 - C | 1.243720299 | *Chloroflexi* | NA |
| Cluster.1089 | S2 - C | 1.107942974 | *Acidobacteria* | NA |
| Cluster.4148 | S1 - B/1 | 3.059927657 | *Chloroflexi* | NA |
| Cluster.4185 | S1 - B/1 | 2.052986607 | *Chloroflexi* | NA |
| Cluster.4163 | S1 - B/1 | 1.710822172 | *Actinobacteria* | NA |
| Cluster.4083 | S1 - B/1 | 1.466419005 | *Gemmatimonadetes* | NA |
| Cluster.4184 | S1 - B/1 | 1.261120344 | *Proteobacteria* | NA |
| Cluster.4083 | S1 - B/2 | 2.24192311 | *Gemmatimonadetes* | NA |
| Cluster.4148 | S1 - B/2 | 2.033074759 | *Chloroflexi* | NA |
| Cluster.4185 | S1 - B/2 | 1.538658256 | *Chloroflexi* | NA |
| Cluster.4163 | S1 - B/2 | 1.039979541 | *Actinobacteria* | NA |
| Cluster.1258 | S1 - B/2 | 1.027192908 | *Actinobacteria* | NA |
| Cluster.4148 | S1 - A/1 | 1.377777778 | *Chloroflexi* | NA |

| | | | | |
|---|---|---|---|---|
| Cluster.4185 | S1 - A/1 | 1.348148148 | *Chloroflexi* | NA |
| Cluster.1258 | S1 - A/1 | 1.185185185 | *Actinobacteria* | NA |
| Cluster.4083 | S1 - A/1 | 1.111111111 | *Gemmatimonadetes* | NA |
| Cluster.4163 | S1 - A/1 | 1.007407407 | *Actinobacteria* | NA |
| Cluster.4163 | S3 - A/1 | 1.693363844 | *Actinobacteria* | NA |
| Cluster.1287 | S3 - A/1 | 1.647597254 | *Acidobacteria* | NA |
| Cluster.1287 | S3 - B/1 | 2.360380666 | *Acidobacteria* | NA |
| Cluster.4163 | S3 - B/1 | 1.959679439 | *Actinobacteria* | NA |
| Cluster.4026 | S3 - B/1 | 1.890808916 | *Chloroflexi* | NA |
| Cluster.4148 | S3 - B/1 | 1.715502129 | *Chloroflexi* | NA |
| Cluster.4083 | S3 - B/1 | 1.471324818 | *Gemmatimonadetes* | NA |
| Cluster.4184 | S3 - B/1 | 1.233408465 | *Proteobacteria* | NA |
| Cluster.4249 | S3 - B/2 | 2.961378953 | *Acidobacteria* | NA |
| Cluster.1089 | S3 - B/2 | 1.639450492 | *Acidobacteria* | NA |
| Cluster.4083 | S3 - B/2 | 1.179367548 | *Gemmatimonadetes* | NA |
| Cluster.4328 | S3 - B/2 | 1.114567133 | *Acidobacteria* | NA |
| Cluster.4110 | S2 - B/1 | 2.441216115 | *Chloroflexi* | NA |
| Cluster.1089 | S2 - B/1 | 1.490190205 | *Acidobacteria* | NA |
| Cluster.4083 | S2 - B/1 | 1.228096451 | *Gemmatimonadetes* | NA |
| Cluster.4105 | S2 - B/2 | 6.065110748 | *Chloroflexi* | NA |
| Cluster.1089 | S2 - B/2 | 1.085179129 | *Acidobacteria* | NA |
| Cluster.4105 | S2 - A/1 | 10.54072989 | *Chloroflexi* | NA |
| Cluster.4249 | S2 - A/1 | 3.744984396 | *Acidobacteria* | NA |
| Cluster.1287 | S2 - A/1 | 3.222724667 | *Acidobacteria* | NA |
| Cluster.4328 | S2 - A/1 | 2.796000255 | *Acidobacteria* | NA |
| Cluster.4133 | S2 - A/1 | 2.776893192 | *Gemmatimonadetes* | NA |

| | | | | |
|---|---|---|---|---|
| Cluster.4459 | S2 - A/1 | 2.254633463 | *Chloroflexi* | NA |
| Cluster.4110 | S2 - A/1 | 1.216483027 | *Chloroflexi* | NA |
| Cluster.4083 | S2 - A/2 | 3.762376238 | *Gemmatimonadetes* | NA |
| Cluster.1287 | S2 - A/2 | 2.538253825 | *Acidobacteria* | NA |
| Cluster.4110 | S2 - A/2 | 1.410141014 | *Chloroflexi* | NA |
| Cluster.1089 | S2 - A/2 | 1.332133213 | *Acidobacteria* | NA |
| Cluster.4605 | S2 - A/2 | 1.152115212 | *Verrucomicrobia* | NA |
| Cluster.1287 | S1 - C | 1.649250913 | *Acidobacteria* | NA |
| Cluster.4115 | S3 - C | 7.571953571 | *Proteobacteria* | NA |
| Cluster.4163 | S3 - C | 2.066732162 | *Actinobacteria* | NA |
| Cluster.4243 | S3 - C | 1.30262344 | *Chloroflexi* | NA |
| Cluster.1089 | S3 - C | 1.182549212 | *Acidobacteria* | NA |
| Cluster.1287 | S3 - C | 1.14252447 | *Acidobacteria* | NA |

# Appendix E: Examples of biofilter performance monitoring throughout the experimental run

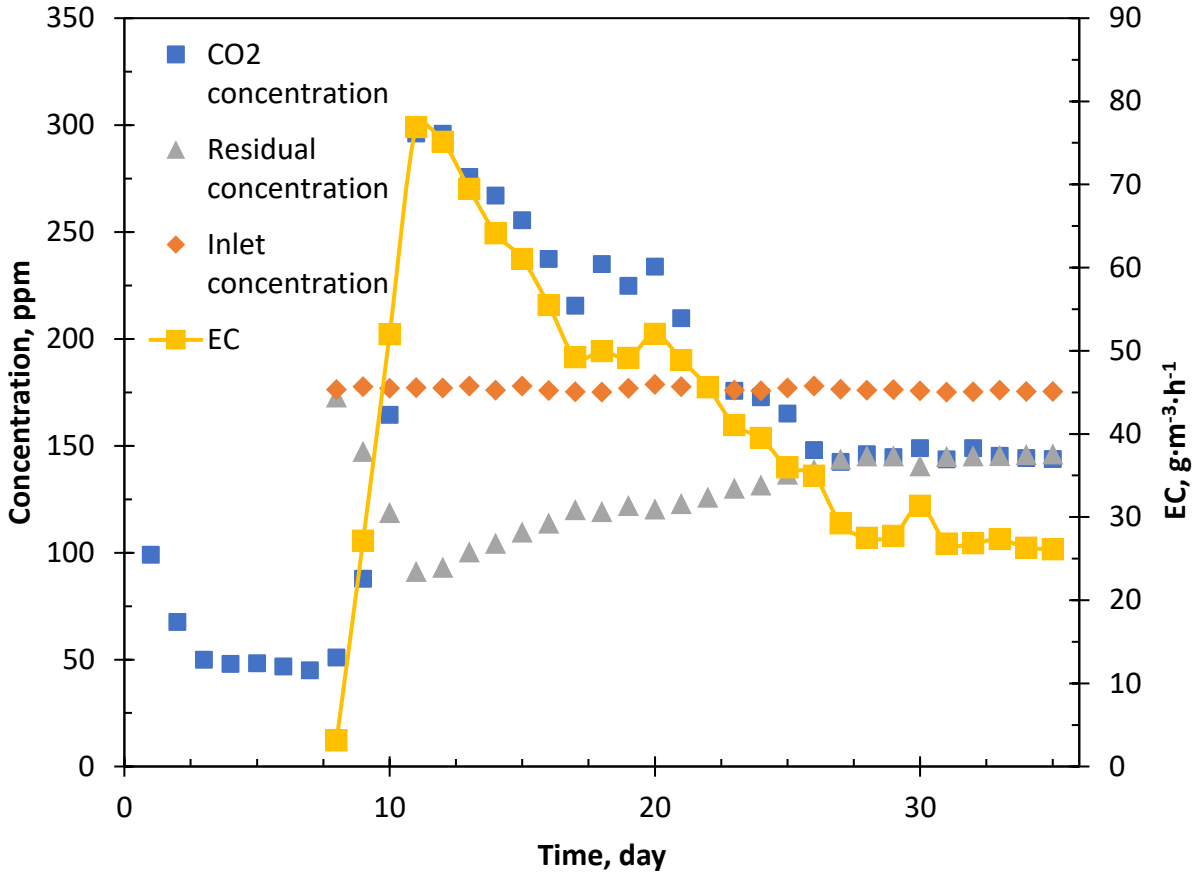


Figure A.4: Gas concentration profile of Soil 2 at a toluene inlet loading rate of 137 $g \cdot m^{-3} \cdot h^{-1}$ and -100 $cm_{H_2O}$ at 40 °C.

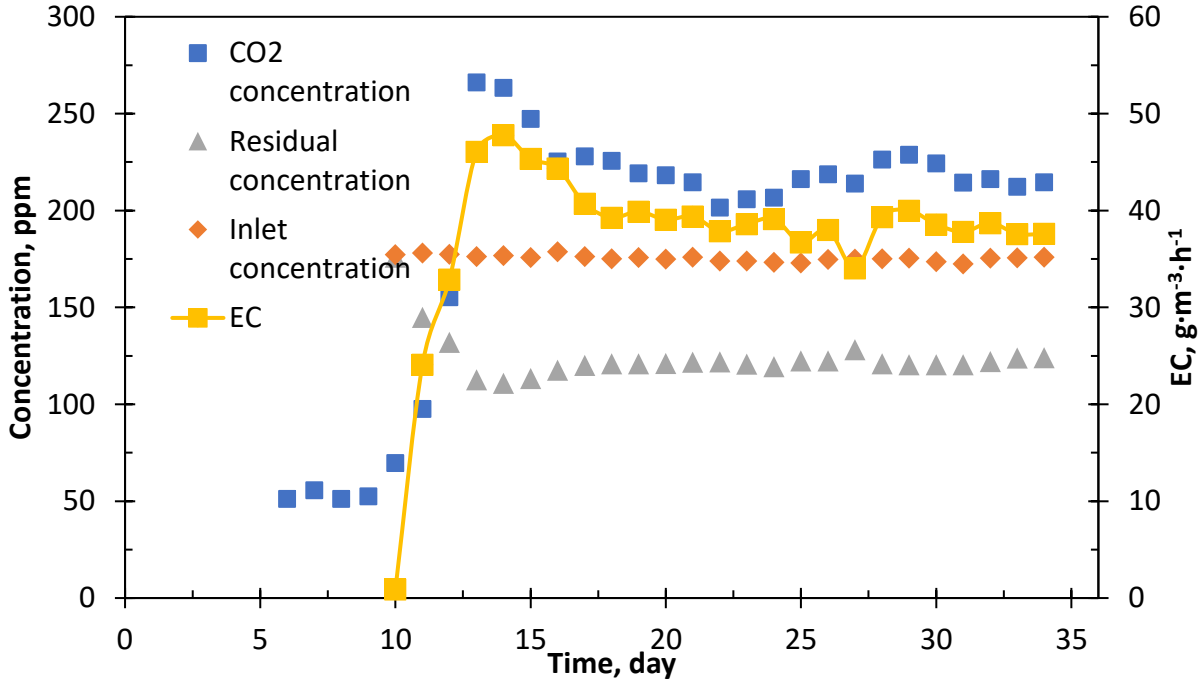


Figure A.5: Gas concentration profile of Soil 1 at a toluene inlet loading rate of 137 $g \cdot m^{-3} \cdot h^{-1}$ and -100 $cm_{H_2O}$ at 40 °C.

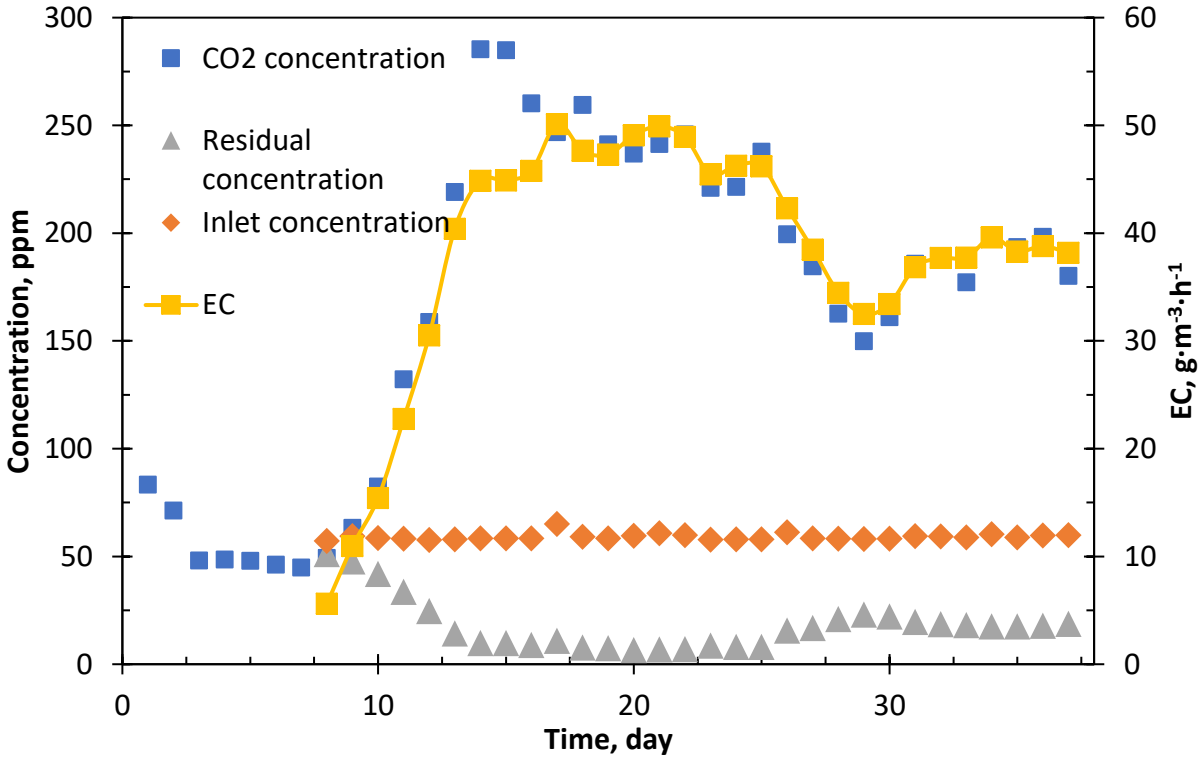


Figure A.6: Gas concentration profile of Soil 2 at a toluene inlet loading rate of 67 $g \cdot m^{-3} \cdot h^{-1}$ and -10 $cm_{H_2O}$ at 40 °C.

# Appendix F: Feedback control system using mass flow controllers

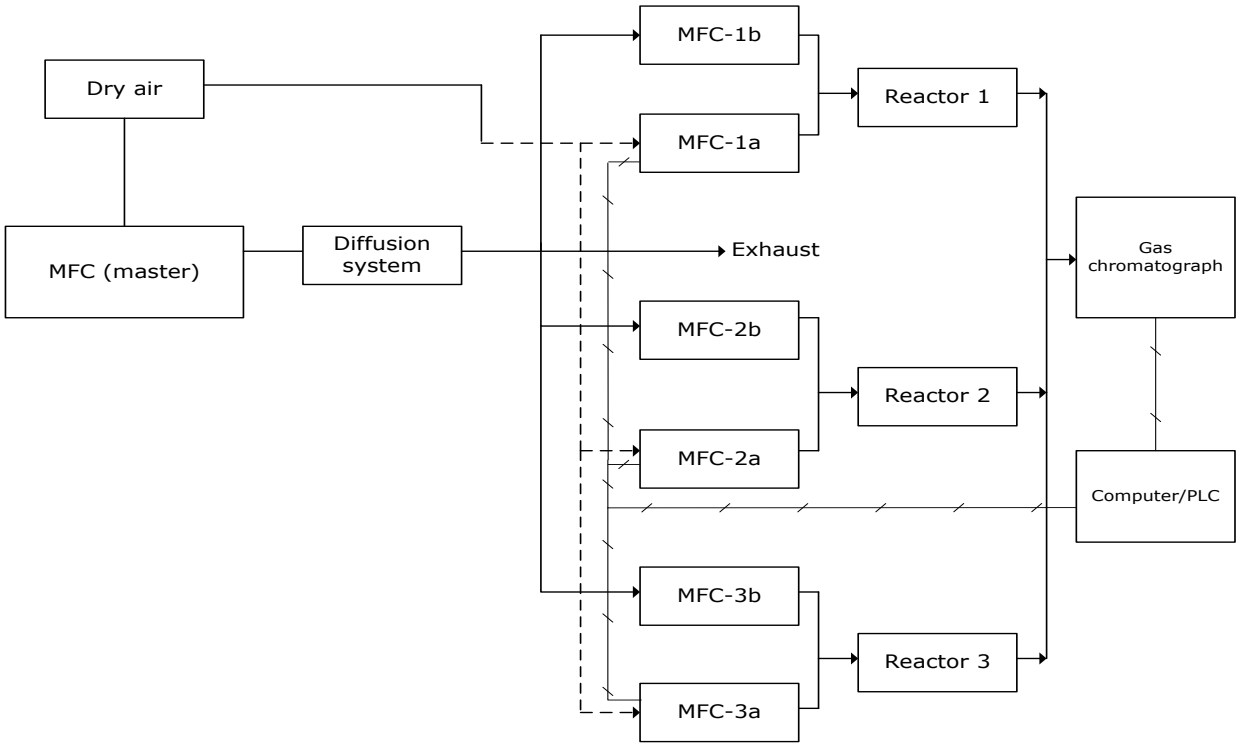


Figure A.7: Schematic of the feedback control system using mass flow controllers.

# Appendix G: LabView programming for feedback control system

LabView programming had two main sections integrating in a continuous loop. The first section used to read the peak area from the GC log file and convert to toluene concentration using the GC calibration equation in Appendix A.2. The second section used to apply the discrete PI control algorithm and transfer the signal to the air bath system.

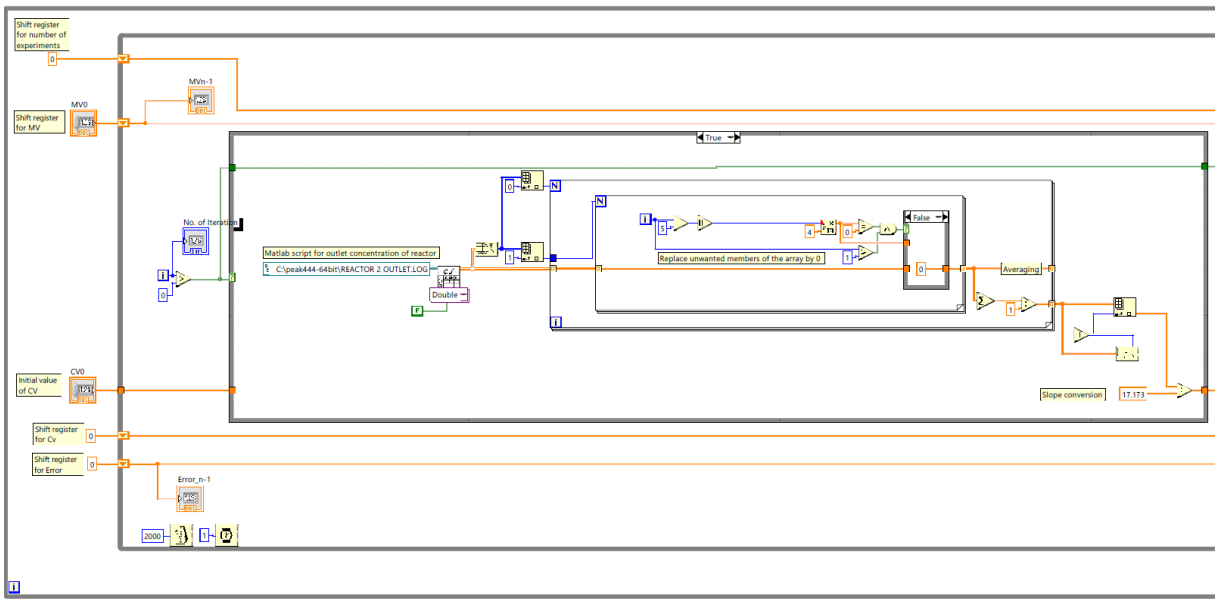


Figure A.8: LabView programming section to process data from the GC log file.

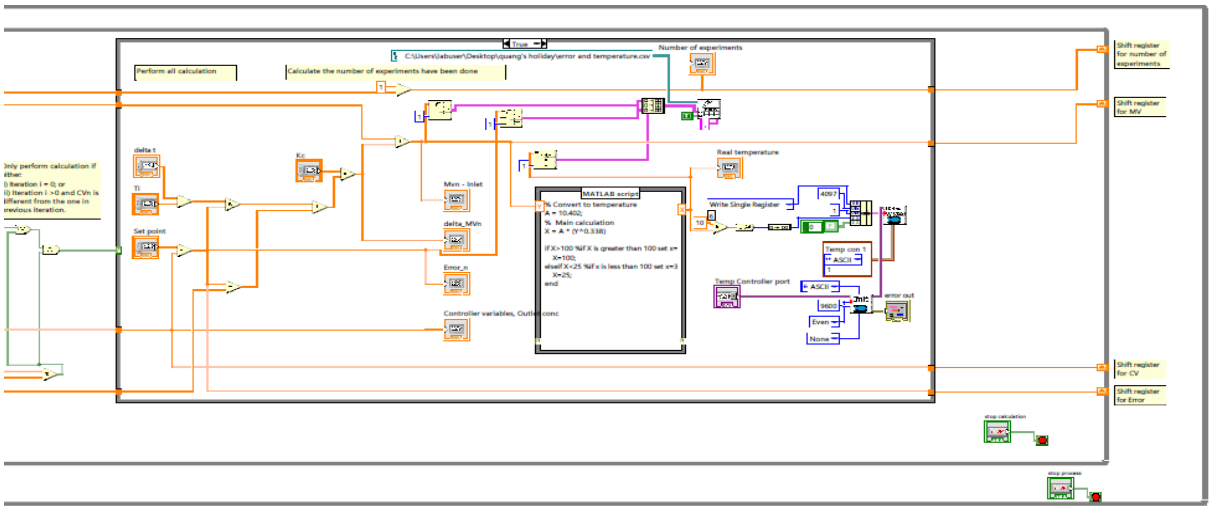


Figure A.9: LabView programming section to apply the discrete PI control algorithm and transfer the signal to the air bath system.

# Appendix H: Relation between the diffusion tube temperature and toluene concentration

The relation between the diffusion tube temperature and the generated toluene inlet concentration was determined by varying the temperature and measuring the generated toluene concentration. Table A.6 shows the different diffusion tube temperatures used in the study and Figure A.10 shows the generated curve.

Table A.6 The relation between the diffusion tube temperature and the generated toluene inlet concentration.

| Diffusion tube temperature ($^{o}$C) | Toluene inlet concentration (ppm) |
|---|---|
| 30 | 24.7 ± 1.3 |
| 40 | 50.4 ± 0.7 |
| 50 | 98.1 ± 3.1 |
| 60 | 176.4 ± 1 |
| 70 | 299.3 ± 3.1 |

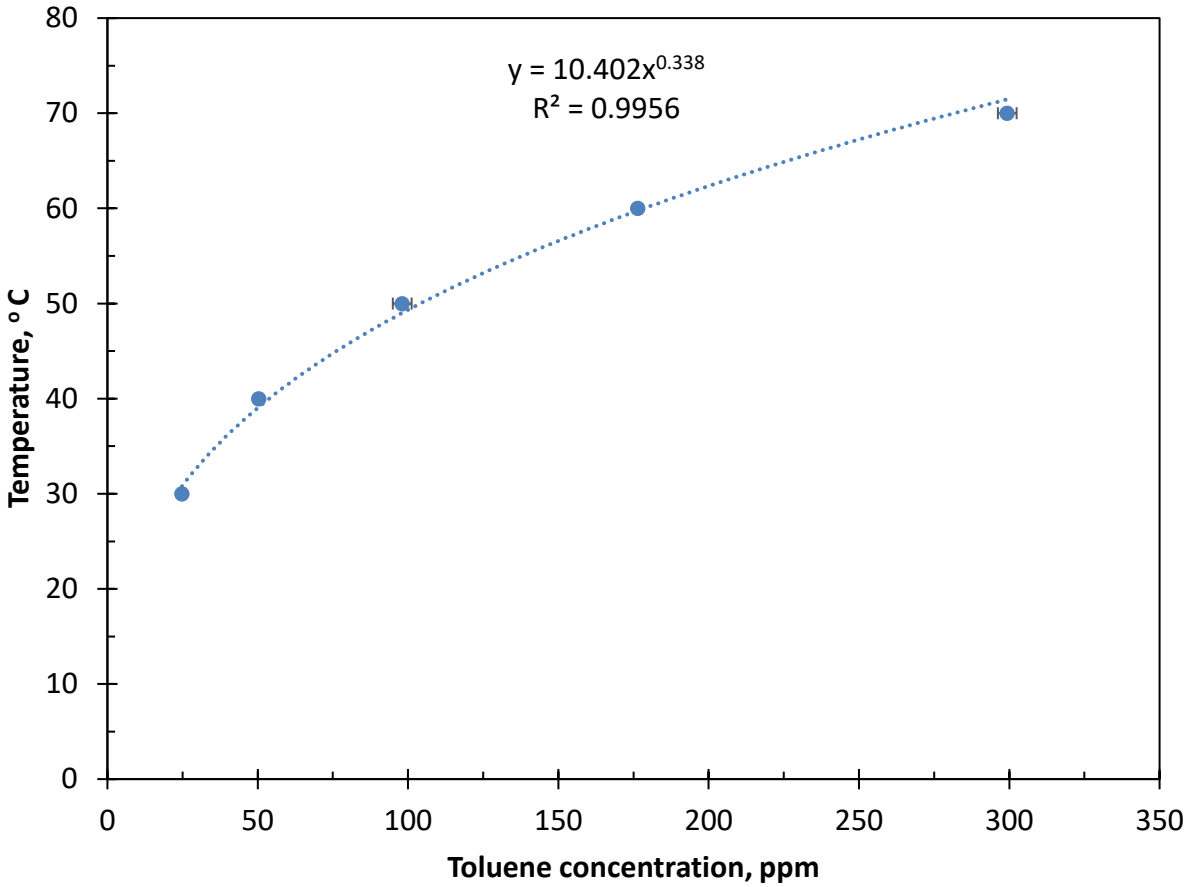


Figure A.10: The relation between the diffusion tube temperature and generated toluene inlet concentration. The equation is based on a power fit through the origin. Error bars are the standard deviations.

**References**

ALTSHULLER, A. P. & COHEN, I. R. 1960. Determination of primary nitroparaffins by the nitrous acid reaction. *Analytical Chemistry,* 32**,** 881-882.

BENEKE, D., PETERS, M., GLASSER, D. & HILDEBRANDT, D. 2012. *Understanding distillation using column profile maps*, John Wiley & Sons.

CHEN, N. H. & OTHMER, D. F. 1962. New generalized equation for gas diffusion coefficient. *Chemical and Engineering Data,* 7**,** 37-41.

JACEK, N. 1984. Generation of standard gaseous mixtures. *Chromatography A,* 300**,** 79-108.

LUGG, G. A. 1968. DIFFUSION COEFFICIENTS OF SOME ORGANIC AND OTHER VAPORS IN AIR. *Analytical Chemistry,* 40**,** 1072-&.

NELSON, G. O. 1971. *Controlled test atmospheres: Principles and techniques,* Michigan, United States of America, Ann Arbor Science.

PERRY, R. H. & GREEN, D. W. 2008. *Perry's chemical engineers' handbook,* New York, McGraw-Hill.

WASHBURN, E. W. 1929. *International critical tables of numerical data, physics, chemistry and technology,* New York, McGraw-Hill Book Company.